Characterisation of the Involvement of Angiotensin-Signalling Pathway in Anthracycline-Induced Cardiotoxicity

Ray Alsuhaibani

A thesis submitted for the degree of Doctor of Philosophy

Institute of Translational and Clinical Research

Faculty of Medical Sciences

Newcastle University

May 2025

Abstract

Delayed cardiotoxicity is a major clinical issue with anthracyclines and cancer treatment, associated with development of life-threatening heart failure. Clinically, drugs interfering with the angiotensin-signalling pathway have shown promise for mitigation of anthracycline-induced cardiotoxicity (AIC). However, the mechanistic basis for this response remains unclear. In this study, both angiotensin II stimulation and exposure to sub-therapeutic concentrations of the anthracycline doxorubicin have been shown to induce cellular hypertrophy in human cardiomyocyte cells, an effect associated with a significant upregulation of expression of the angiotensin receptor (AT1R). In contrast, no such morphological changes were observed in primary human cardiac fibroblasts (HCF). Surprisingly, despite no observable structural change being detected in HCF, exposure to doxorubicin did cause an increase in AT1R expression. Such an observation indicating a potential interplay between these two cell types of the myocardium in AIC, involving crosstalk of the angiotensin-signalling pathway. The importance for AT1R in the cardiomyocyte response to doxorubicin was confirmed by knockdown of AT1R using small interfering RNA (siRNA), which mitigated the hypertrophic response. From a therapeutic perspective, the hypertrophic response of cardiomyocytes was mitigated by pre-exposure to the angiotensin-receptor blocking drug telmisartan, offering an explanation for the cardioprotective effects of blocking angiotensin-signalling in AIC. Together these findings support an involvement for angiotensin signalling in drug-induced hypertrophy and subsequent cardiotoxicity, with scope for interaction of this pathway for mitigation of chronic cardiotoxicity in the clinic.

Acknowledgements

With the grace of Allah, I am honoured to present this thesis as a significant milestone in my academic journey.

I would like to express my deepest gratitude to my supervisors, Dr Jason Gill and Professor Gavin Richardson, for their invaluable guidance, support, and constructive feedback throughout my research. Their expertise has been instrumental in shaping the direction and completion of this work.

I am sincerely grateful to the Government of Saudi Arabia for their generous sponsorship and financial support, which enabled me to pursue this academic endeavour.

My heartfelt appreciation goes to my beloved parents, whose unconditional love, sacrifices, and prayers have always been the foundation of my success. I am also deeply appreciative of my brothers and sisters for their continuous encouragement, support, and belief in me throughout this journey.

Finally, I would like to thank my friends and colleagues for their valuable input, motivation, and companionship during this research.

Declaration

I declare that this thesis entitled 'Characterisation of the Involvement of Angiotensin-Signalling Pathways in Anthracycline-Induced Cardiotoxicity' is original research, which I have undertaken for the award of Doctor of Philosophy. I hereby confirm that this thesis has not been submitted for a higher degree to any other University or Institution, and that there is no plagiarism contained within, with all sources of information cited and appropriately referenced.

Ray Alsuhaibani

Table of contents

List of figures

List of tables

List of abbreviations

ATP	Adenosine triphosphate
ACEi	Angiotensin converting enzyme inhibitor
AT1R	Angiotensin II type 1 receptor
AT2R	Angiotensin II type 2 receptor
ARB	Angiotensin receptor blocker
ACE	Angiotensin-converting enzyme
ACE2	Angiotensin-converting enzyme 2
AIC	Anthracycline-induced cardiotoxicity
AT1KO	AT1R knockout
ABCB8	ATP-binding cassette sub-family B member 8
ANP	Atrial natriuretic peptide
β-blockers	Beta adrenoceptor blockers
Ca^{2+}	Calcium
CICR	Calcium-induced calcium release
CO_2	Carbon dioxide
CFs	Cardiac fibroblasts
CPCs	Cardiac progenitor cells
CI	Cell index
CHF	Congestive heart failure
r^2	Correlation coefficients
Cq	Cycle quantification
cGMP	cyclic guanosine monophosphate
DNA	Deoxyribonucleic acid
DAG	Diacylglycerol
DMSO	Dimethyl sulfoxide
dsRNA	Double strand RNA
DMEM/F12	Dulbecco's Modified Eagle Medium/ Ham's F-12 medium (1:1 ratio)
ECG	Electrocardiogram
E-plate	Electrode plate
EDTA	Ethylenediaminetetraacetic acid
ECM	Extracellular matrix
Fe^{3+}	Ferric cation
Ft	Ferritin
Fe^{2+}	Ferrous cation
FBS	Foetal Bovine Serum
GPCR	G-protein coupled receptors
GLS	Global longitudinal strain
GPX	Glutathione peroxidase
GAPDH	Glyceraldehyde-3-phosphate dehydrogenase
HBSS	Hank's Balanced Salt Solution
HSF	Heat shock factors
hiPSC-CMs	Human-induced pluripotent stem cell derived cardiomyocytes
H_2O_2	Hydrogen peroxide
OH^-	Hydroxyl radical
HPRT1	Hypoxanthine-guanine phosphoribosyl transferase 1

IC_{50}	Inhibitory concentration, 50%
IP3	Inositol trisphosphate
LVEF	Left ventricle ejection fraction
LV	Left ventricular
LVD	Left ventricular dysfunction
LOOH	Lipid hydroperoxide
LOO•	Lipid radicals
MasR	Mas G-protein coupled receptor
MMP	Matrix metalloproteinases
C_{max}	Maximum serum concentration
Ct	Mean threshold cycles
FtMt	Mitochondria-specific ferritin protein
mtDNA	Mitochondrial DNA
MAPK	Mitogen-activated protein kinase
NO	Nitric oxide
NOS	Nitric oxide synthase
NTC	No template controls
O_2	Oxygen
PFA	Paraformaldehyde
pen/strep	Penicillin/streptomycin
PMS	Phenazine methosulfate
PBS	Phosphate-buffered saline
K^+	Potassium
ROS	Reactive oxygen species
RTCA	Real-time cell analyser
RT-qPCR	Real-time quantitative polymerase chain reaction
RAAS	Renin-angiotensin aldosterone system
RPL13A	Ribosomal protein L13a
RISC	RNA-induced silencing complex
RyRs	Ryanodine receptors
SERCA	Sarcoplasmic reticulum Ca^{2+} ATPase
SASP	Senescence-associated secretory phenotype
SAN	Sinoatrial node
siRNA	Small interfering RNA
Na^+	Sodium
SDS	Sodium Dodecyl Sulphate
NCX	Sodium-calcium exchanger
SEM	Standard error of mean
O_2^-	Superoxide
SOD	Superoxide dismutase
TopII	Topoisomerase II
TopIIα	Topoisomerase IIα
TopIIβ	Topoisomerase IIβ
TGF-β	Transforming growth factor-beta
TBS	Tris-Buffered Saline
TNF-α	Tumour necrosis factor α
VEGF	Vascular endothelial growth factor
VSMCs	Vascular smooth muscle cells
WT	Wild type

α-SMA	α-smooth muscle actin
β-actin	Beta-actin

Chapter 1. Introduction

1.1 Cancer and its management

Cancer represents a significant global health concern; it is a broad and complex family of diseases that involve uncontrolled cell proliferation, invasion of surrounding tissues, and dissemination to other organs in the body (1). The number of cancer cases diagnosed each day is over 55,500, and the number of cancer-related deaths is over 26,900 every day globally (2). It is expected to be 28 million new cancer diagnoses and 16.2 million cancer-related deaths worldwide by 2040 (3). Effective cancer treatment requires multidisciplinary approaches to treat cancer and control its spread to enhance cancer patient quality of life. This is a complex process often involving single or combinations of approaches, such as surgical resection, radiotherapy, chemotherapy, and more recently targeted therapies such as immunotherapy (4).

In recent years, the field of oncology has brought extensive changes and advancements in cancer treatment with new targeted drugs and chemotherapy. Despite these advancements, cytotoxic chemotherapeutic agents remain as the cornerstone therapy in various oncological settings (5). Conventional cytotoxic chemotherapy aims to disrupt cell proliferation and therefore prevent the growth of rapidly dividing cancer cells, with these therapeutics being categorised based on their primary mode of action, such as perturbation of nucleotide synthesis, DNA alkylation, disruption of microtubule dynamics, and DNA intercalation (6). One of the most commonly used classes of cytotoxic chemotherapy are the anthracyclines, such as daunorubicin, doxorubicin, idarubicin and epirubicin (7). However, the clinical success of these agents is now known to be affected by cumulative and dose-dependent cardiotoxicity, leading to progressive and often delayed heart damage (8, 9).

1.2 Anthracyclines in cancer treatment

Anthracyclines have been used in the clinic for over 50 years with a broad spectrum of clinical activities against many haematological malignancies as well as solid tumours, such as cancers of the breast, stomach and lung, amongst others (10). The antineoplastic effects of anthracyclines are mediated by several mechanisms that disrupt cellular processes critical to cancer cell survival. These include intercalation between base pairs in the DNA double helix

that leads to prevention of replication and transcription in rapidly dividing cancer cells and inhibition of the topoisomerase IIα (TopIIα) enzyme, responsible for resolving DNA supercoiling during replication and transcription, leading to DNA breaks which induce cell cycle arrest and apoptosis in rapidly dividing cancer cells (Figure 1.1) (11, 12). Additionally, anthracyclines also undergo redox cycling, producing reactive oxygen species (ROS) that cause induction of oxidative damage and mitochondrial dysfunction causing a multitude of molecular disturbances, and ultimately cessation of DNA replication and induction of cell death (Figure 1.2) (11-13).

However, despite anthracyclines being widely used cancer therapeutics, with significant evidence for treatment success and improvements in cancer survivorship, their use is strongly associated with significant adverse effects upon the cardiovascular system (8, 9). These detrimental effects present many months or years after cessation of chemotherapeutic treatment, often as life-threatening cardiac failure (14). Unlike the acute cardiotoxicity associated with other cancer chemotherapeutics, such as cyclophosphamide, anthracyclines are now known for their cumulative and dose-dependent cardiotoxicity, leading to progressive and often delayed heart damage (8, 9). It is now believed that 9% of adult and 7% of paediatric cancer patients, receiving anthracycline-based chemotherapy, present with delayed cardiotoxicity within the clinic (15, 16). Consequently, the balance between maximizing therapeutic efficacy and minimising these serious side effects, through improved understanding of the mechanism of cardiotoxicity caused by anthracycline is crucial to improving patient outcomes and the quality of cancer management.

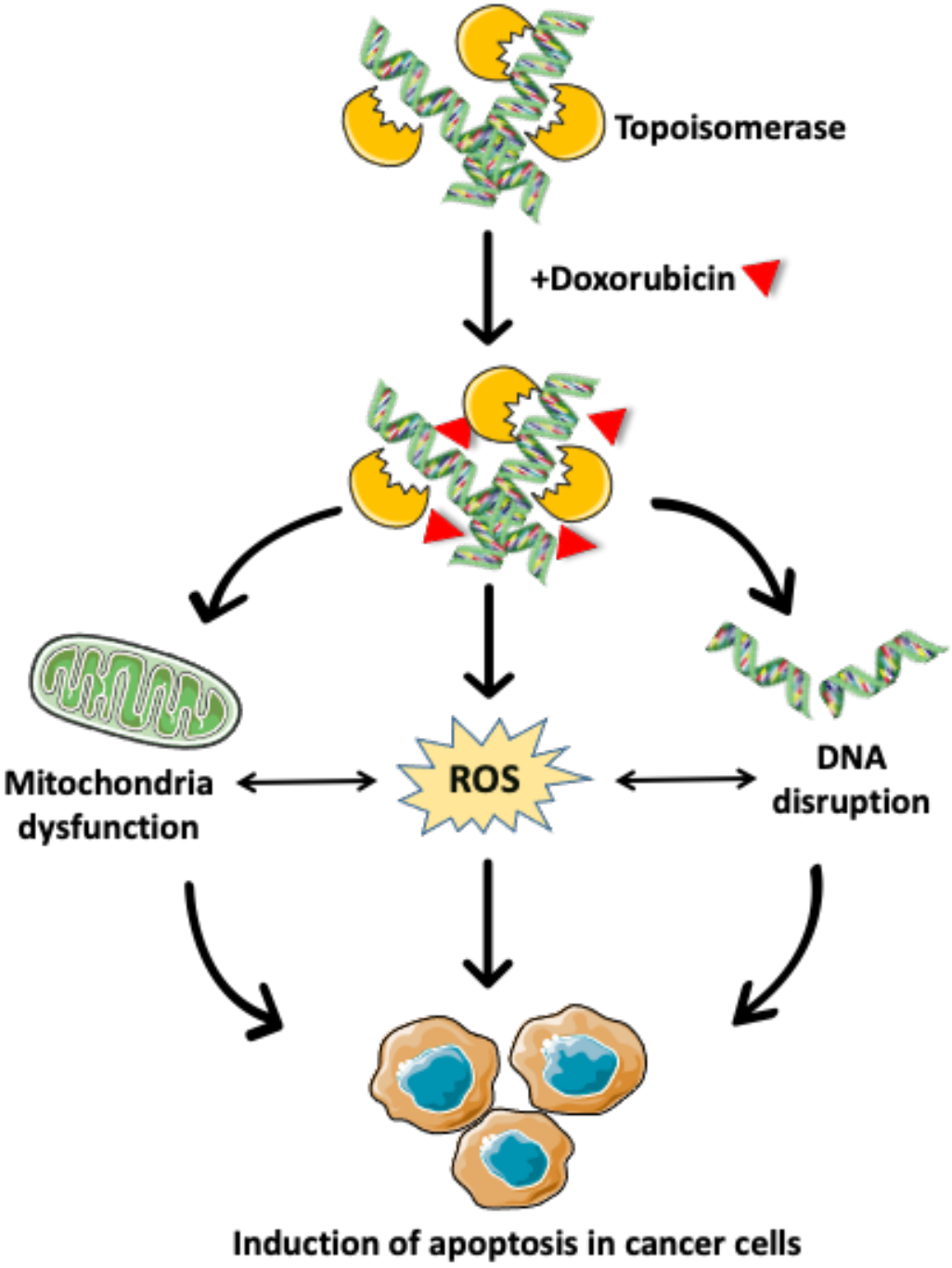

Figure 1.1 Mechanism of action of anthracycline. Anthracycline induces cell death in cancer cells by different mechanisms, including intercalation of DNA, inhibition of the topoisomerase II, induction of free radicals, and mitochondrial dysfunction. Made by SERVIER Medical Art.

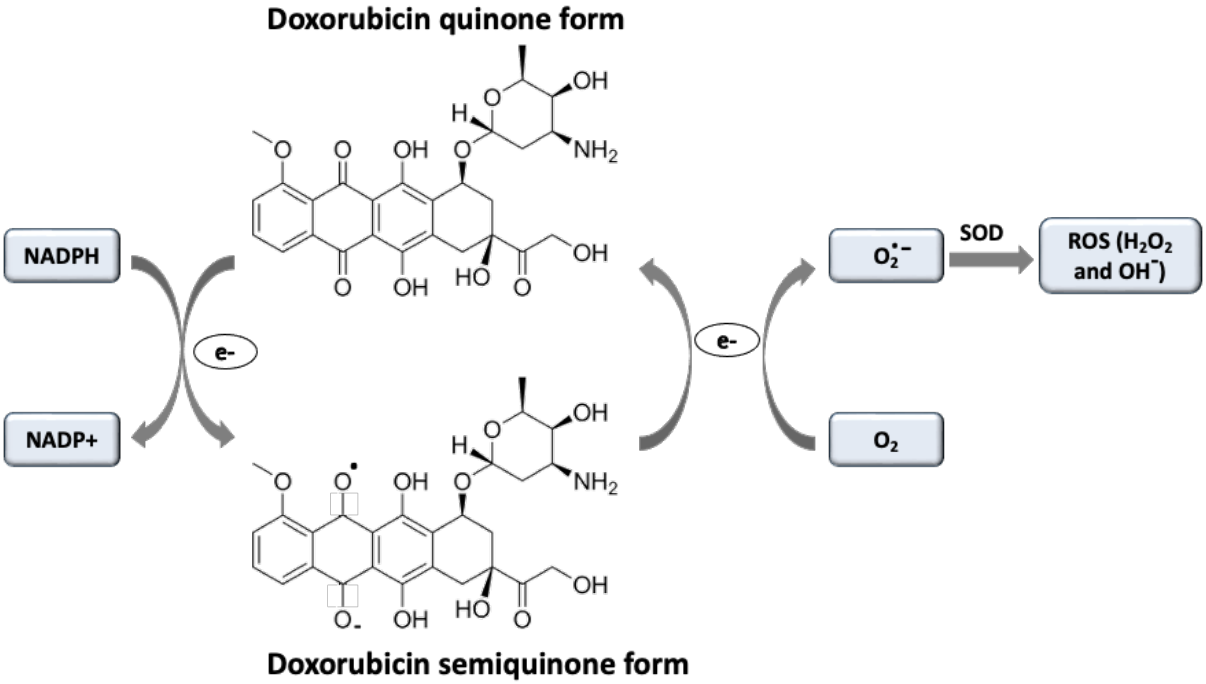

Figure 1.2 Redox cycling of doxorubicin in mitochondria. It starts when doxorubicin binds to cardiolipin and redox cycling initiates with the reduction of one-electron of the quinone moiety through cellular oxidoreductases, resulting in forming of semiquinone radical. In the presence of intracellular oxygen (O_2), the parent compound is regenerated, and O_2 is reduced to superoxide (O_2^-). O_2^- is converted to hydrogen peroxide (H_2O_2) through superoxide dismutase (SOD), resulting in generation of ROS, including hydroxyl radical (OH^-). Adapted from reference (17).

1.3 Clinical perspectives of anthracycline-induced cardiotoxicity (AIC)

Anthracycline-induced cardiotoxicity (AIC) is adverse cardiac effects as a result of using anthracycline-based chemotherapy. The first documented report of anthracyclines cardiotoxicity was by Lefrak et al. in 1973, who found that 11% of patients receiving doxorubicin developed transient electrocardiographic abnormalities, independent of cumulative dose, while 3% of patients receiving doxorubicin doses exceeding 500 mg/m^2 experienced severe congestive heart failure (CHF) (18). A retrospective analysis by Von Hoff et al. reported that cumulative dose played a key role in heart failure development among over 4,000 patients treated with anthracyclines (8). Consequently, it is now accepted that there is an exponential increase in heart failure incidence in adults treated with anthracycline from 5% to 48% with a cumulative dose of 400 mg/m^2 and 700 mg/m^2, respectively (8, 19). Although it has been observed that limiting total cumulative doxorubicin exposure to 450 mg/m^2 leads to a reduction of acute cardiovascular toxicity events, late-onset complications (as described in section 1.3.1) are not significantly reduced (20, 21). In addition, studies have now found that doxorubicin doses below 300 mg/m^2 are associated with a higher risk of cardiotoxicity (20). This suggests that no anthracycline dosage is safe for the cardiovascular system (22). To address this significant issue, many infusion rates (bolus, short infusions of ≤1 hour, or extended continuous infusions of up to 96-hours) and newer formulations (analogues, pegylation, liposomes and other nanodelivery systems) of anthracyclines have been trialled, aimed at reducing cardiac exposure whilst maintaining tumour exposure and therapeutic efficacy (23). However, cardiotoxicity with these agents is not abated and further clinical strategies are still required for management of the cardiac effects (22). Therefore, in addition to cumulative dose, several other factors may play a role in the development of cardiovascular toxicity. Consequently, strategies for clinical management and potential mitigation of AIC remain a high priority.

1.3.1 Clinical presentation of AIC

In the clinic, presentations of acute AIC within hours or days post-treatment, is somewhat rare, with its management largely handled by cessation of treatment or administration of medicines focused on stabilising cardiac electrophysiology or contractile disturbances (24, 25). The more concerning presentation of AIC is that occurring several months or even years after cancer chemotherapy (14). The adverse effects associated with this chronic cardiotoxicity are

believed to be irreversible and are largely asymptomatic in the early stages but are associated with left ventricular dysfunction (LVD), and symptomatic heart failure due to chronic cardiomyopathy in the latter stages (14, 25). Therefore, compared to the general population, many cancer patients who already have a higher baseline risk of cardiovascular disease, AIC threatens to limit long-term cancer patient survival.

1.3.2 Clinical risk factors of AIC

In addition to cumulative dose, which still remains the most significant factor, several other risk factors have now also been associated with AIC, including age, patient gender, presence of other cardiovascular diseases such as hypertension, concomitant treatment with other chemotherapeutic agents, and the dosing rate and schedule for anthracyclines (8, 27). In this context, a retrospective analysis showed that older patients treated with doxorubicin had a higher incidence of cardiotoxicity within 2-years of receiving treatment (28). Similarly, it is estimated that over 50% of paediatric cancer survivors experience cardiotoxicity following treatment with doxorubicin (29). Interestingly, sex is also a crucial risk factor in younger patients, with females experiencing cardiac events more frequently than males following anthracycline exposure (30). Additionally, concomitant treatment of anthracyclines with other chemotherapeutic agents further increases the cardiotoxicity risk. For example, cardiovascular complications are significantly increased when anthracyclines are combined with trastuzumab in breast cancer patients (31). Patients with pre-existing hypertension have an increased susceptibility to doxorubicin cardiotoxicity. The increase in blood pressure leads to an increase in cardiac wall stress, preload, and afterload, which increase the risk of heart damage and the progress to heart failure after doxorubicin exposure (32).

1.4 Molecular mechanisms of AIC

Although AIC remains the most noted chemotherapy-induced cardiotoxicity to date, it remains unclear as to the mechanistic basis of this toxicity and how acute exposure relates to a delayed presentation of AIC (33). Doxorubicin-induced cardiomyopathy is widely recognised as a progressive and multi-factorial process (33, 34). Furthermore, AIC is a complex process, targeting many cell types within the myocardium and activating several other pathways (33). Importantly, cardiotoxicity against cardiac tissue appears to be separate from the primary anticancer mechanism of anthracyclines, since cardiomyocytes are non-proliferative and

express significantly lower levels of TopIIα, the main target of anthracyclines, compared to rapidly dividing cells (35). Potential mechanisms underlying doxorubicin-induced cardiomyopathy involve disrupted calcium regulation, inhibition of the enzyme topoisomerase IIβ (TopIIβ) as opposed to TopIIα, the formation of oxygen free radicals within cardiac cells, disruption of mitochondrial dynamics, activation of cellular stress pathways, and initiation of cellular senescence (36-40). Together, disruption of the cardiac cellular phenotype and cellular responses ultimately contributes to cardiac cellular dysfunction and tissue remodelling, with a subsequent asymptomatic decline in cardiac function. This thereafter progresses to symptomatic cardiomyopathy and heart failure (27).

1.4.1 Inhibition of topoisomerase II enzyme activity hypothesis

A primary mechanism for the therapeutic mechanism of anthracyclines is the inhibition of the topoisomerase II (TopII) enzyme complex, involved with changing the conformation of DNA prior to cellular division (see section 1.2) (11). Doxorubicin binds with the DNA and TopII to form a complex namely, TopII-doxorubicin-DNA cleavage complex, which results in disruption of DNA replication kinetics and promotion of cell death (11). In cancer cells, this mechanism is mediated via inhibition of TopIIα, which is overexpressed in cancer cells but expressed at very low levels or is undetectable in non-malignant tissues (11, 35).

With respective to cardiac tissue, expression of TopIIα is negligible, however the beta isoform of the enzyme (TopIIβ) is expressed (35). In this context, several studies have now shown that anthracyclines can also bind to TopIIβ, forming a ternary TopIIβ-anthracycline-DNA complex, with the outcome being similar to its primary mechanism against TopIIα, in that DNA becomes damaged and the cell ultimately undergoes cell death (41). In this context, a role for TopIIβ inhibition in AIC is supported by a murine model in which deletion of the TopIIβ type enzyme from cardiomyocytes mitigated the cardiotoxicity of anthracyclines (36). Consequently, due to the limited generation capacity of cardiomyocytes, the chronic TopII-inhibition-mediated loss of these cells through apoptosis and necrosis offers an explanation in support of progressive development of heart failure, as the functional cellular structure of cardiac tissue is compromised much earlier than experienced through natural cellular deterioration and loss (42).

Interestingly, an *in vitro* study utilising immature and matured human-induced pluripotent stem cell-derived cardiomyocytes (hiPSC-CMs) has shown that the matured hiPSC-CMs predominantly expressed TopIIβ whereas the immature cells expressed TopIIα, with the

latter correlating with a greater degree of DNA damage (43). This observation thus implies that susceptibility to AIC may be more pronounced in paediatric cancer patients than adult cancer patients, a hypothesis supporting the differential prevalence of AIC observed in clinical studies (29).

1.4.2 Impaired calcium handling hypothesis

Disruption of calcium (Ca^{2+}) ions is one of the most important mechanisms of AIC. During the excitation-contraction coupling of cardiomyocytes, the primary metabolite of doxorubicin, doxorubicinol, accumulates in cardiomyocytes and disrupts Ca^{2+} ions homeostasis by inhibiting sarcoplasmic reticulum Ca^{2+}ATPase (SERCA) that responsible of pumping Ca^{2+} ions into sarcoplasmic reticulum to reduce the Ca^{2+} ions concentration in the cytoplasm (44). The content of Ca^{2+} ions in the sarcoplasmic reticulum is critically important for cardiac electrical activity, since cardiac muscle contraction and relaxation depend on efficient Ca^{2+} ions uptake and release (44). Doxorubicin can also affect the membrane permeability and activate sarcoplasmic reticulum channels, which results in an increase in the Ca^{2+} ions in the cytoplasm. This excessive intracellular free Ca^{2+} ions concentration leads to impaired cardiomyocyte contractility and therefore, contributes to arrhythmias (45).

1.4.3 Disruption of mitochondrial structure and function hypothesis

Effects upon cellular mitochondria are a major component of AIC, with concentrations of anthracyclines being highest within these subcellular organelles (46). These effects involve direct damage to mitochondrial DNA (mtDNA) through DNA intercalation and/or TopII inhibition, culminating in loss of mitochondrial replicative capacity and depletion of cellular bioenergetics (37, 38, 45). This then results in reduced functional capacity of cardiomyocytes and tissue function, due to cardiomyocyte death and loss of cellular mass alongside reduced contractile capacity of the remaining cardiomyocytes (9).

In addition to mtDNA-mediated effects, due to the role of mitochondria in cellular oxidative respiration, these organelles are also the primary site for oxidative damage mediated by anthracyclines, a primary mechanism involved in their cardiotoxic action (37).

1.4.3.1 Anthracycline-induced oxidative damage in cardiac cells

It has long been believed that oxidative stress due to anthracycline metabolism is a major mechanism behind the toxicity of cardiomyocytes. Analogous to that observed within cancer cells, anthracyclines have also been shown to generate ROS within cardiac cells, through redox cycling mechanisms involving mitochondria (40).

As shown in Figure 1.2, the anthracycline moiety is readily reduced from quinone to semiquinone when it encounters reductants, culminating in doxorubicin acquiring electrons and the resultant generation of free radicals (47). Within the mitochondria, this can be through pathways involving NADPH, nitric oxide synthase (NOSs) and essentially several components of the electron transport chain involved in cellular respiration (48). This mechanism is especially pertinent to cardiomyocytes since they are rich in mitochondria (49). Importantly, when compared to other tissues such as the liver and kidneys, expression of 'protective' enzymes such as superoxide dismutase (SOD), glutathione peroxidase (GPX) and catalase are reportedly much lower in cardiac tissue, meaning that the level of defence against oxidant damage is particularly low (50). This provides further support for the damage of cardiomyocytes by anthracyclines, where mitochondria are particularly damaged due to their higher abundance and the strong affinity of anthracyclines towards the phospholipid cardiolipin, the latter of which arises as a consequence of oxidative stress in these cells (40, 51, 52). The evidence for an involvement of oxidative stress, centred around mitochondria, in AIC is increasing. Several studies have demonstrated that genetic variations in enzymes responsible for regulating oxidative stress can significantly influence susceptibility to cardiac injury following doxorubicin exposure. In particular, polymorphisms in genes encoding NADPH oxidase have been associated with an increased risk of developing anthracycline-related cardiomyopathy (53, 54). Mitochondria further amplify ROS production, exacerbating oxidative damage within cardiac cells (55). Excessive ROS generation can impair Ca^{2+} ions handling in cardiomyocytes, leading to calcium overload and altered excitation-contraction coupling. This disruption of calcium homeostasis, in turn, contributes to impaired cardiac contractility (56). Consequently, ROS-mediated damage affects mitochondrial function, inhibits adenosine triphosphate (ATP) generation and increases inflammation which all promoting apoptosis and cardiac remodelling (57).

Oxidative stress also promotes lipid peroxidation, forming lipid radicals (58). These lipid radicals (LOO•) react with a hydrogen molecule from another lipid, producing lipid

hydroperoxide (LOOH), which destabilises membrane integrity and increases membrane permeability (59). Several studies have confirmed an upregulation of these factors after doxorubicin treatment (60, 61).

Increased ROS production and oxidative stress have been implicated in development of heart failure through several pathological processes, including cardiomyocyte apoptosis, fibrosis, inflammation and cardiac hypertrophy, amongst others (62). There is now also evidence to support a direct involvement of ROS in development of heart failure, evidenced by the increased levels of myocardial ROS in the progression of hypertension-induced cardiac hypertrophy towards heart failure in rats, and by increased levels of oxidative stress in cardiac tissue of individuals with dilated cardiomyopathies and heart failure (62). However, although the potential is compelling, the role of oxidative stress in AIC has yet to be confirmed.

1.4.3.2 Iron dysregulation and ferroptosis

An involvement for iron in the development of AIC has also been proposed (63). Within cells, including cardiomyocytes, iron localisation and metabolism are tightly controlled to restrict free involvement of the ferrous cation (Fe^{2+}) in the Fenton reaction and the subsequent production of hydroxyl radicals (OH^-) and oxidative stress (27, 64).

Cellular uptake of iron is mediated by the plasma glycoprotein transferrin which binds the ferric cation (Fe^{3+}) and transports it into the cell (65). Inside the cell, the Fe^{3+} is converted to the Fe^{2+}, with excess iron stored in the cytoplasmic protein ferritin (Ft) (65). The primary site for utilisation of iron within cells is the mitochondria, where uptake of iron is mediated by specialised ferritin receptors and any excess iron is thereafter stored in the mitochondria-specific ferritin protein (FtMt) (66). Maintenance of mitochondrial iron levels is facilitated by ATP-binding cassette sub-family B member 8 (ABCB8) through coordination of mitochondrial iron export (67).

In the presence of anthracyclines, a direct reaction occurs with the Fe^{3+}, leading to generation of OH^- (64). As a result of anthracycline treatment, mitochondrial iron is accumulated, and iron homeostasis is disrupted (64). Subsequently, this results in sulfhydryl oxidation of key proteins, mitochondrial dysfunction, and mtDNA damage (68). This mechanism is supported by an *in vivo* study using mice genetically overexpressing ABCB8, which exhibits decreased mitochondrial iron content and oxidative stress (51). These mice were shown to be protected against doxorubicin-induced cardiomyopathy (51). Furthermore,

changes in ABCB8 expression have been shown to regulate doxorubicin retention and cellular toxicity (51).

Another process in the context of an involvement for iron in AIC is ferroptosis, a form of programmed cell death reliant upon iron accumulation and concomitant lipid peroxide formation (33). Anthracyclines have been demonstrated to chelate the Fe^{3+}, with the anthracycline-Fe^{3+} complex reduced to the anthracycline-Fe^{2+} complex in the presence of oxygen (69). This ferrous-containing complex subsequently enters the Fenton reaction, resulting in production of OH^{-}, increased levels of lipid peroxidation, and exacerbation of ferroptosis (33).

1.4.4 Induction of cellular senescent hypothesis

Although many mechanisms of AIC have been proposed, there is still a deficit in understanding the relationship of short-term acute drug exposure to delayed and late-onset cardiac failure. One proposed mechanism in this regard is anthracycline-induced cellular senescence, a state of irreversible growth arrest in cells constituting the cardiac tissue (39, 70, 71).

Mature cardiomyocytes are terminally differentiated and post-mitotic, having lost their ability to proliferate and regenerate early in development (42). As defined above, anthracyclines induce oxidative stress within cardiomyocytes, with associated mitochondrial dysfunction, leading to cellular senescence (72). After receiving doxorubicin, it has been demonstrated that cardiomyocytes express cellular senescence biomarkers such as β-galactosidase, p16INK4a, and p53, which results in physiological effects that are consistent with an accelerated ageing process of the cardiomyocytes (73, 74). Additionally, these cells develop a senescence-associated secretory phenotype (SASP) which create a chronic inflammatory environment in the heart (71). As a result, the heart continues to be inflamed even after the chemotherapy regimen is completed.

The specific trigger for senescence within cardiac tissue is as yet undefined (72). One contributory mechanism to promotion of cellular senescence is the persistence of low levels of anthracycline-induced DNA damage within cardiac cells, which is not sufficient to trigger p53-mediated apoptosis but rather leads to activation of persistent cell cycle arrest and subsequent senescence (71). Subsequently, the damage to these cells is often below the threshold for elimination meaning that they persist within the tissue (71).

Importantly, recent evidence suggests that post-mitotic cardiomyocytes can undergo senescence in the absence of cell division through a mechanism involving telomere-associated

DNA damage that does not require telomere shortening. Anderson et al. (2019) demonstrated that this type of damage, independent of telomere length, is sufficient to trigger senescence in cardiomyocytes, supporting the idea that persistent DNA damage, such as those caused by doxorubicin, can promote senescence independently of replication (75). This provides a mechanistic explanation for how terminally differentiated non-dividing cardiomyocytes can still transition into senescence following anthracycline exposure.

The limited capacity of cardiomyocytes to regenerate and compensate the loss of the functional cellular architecture leads to impaired contractility of the heart and other cardiac dysfunctions (42). In addition, senescence in non-cardiomyocyte support cells within cardiac tissue leads to generation of extracellular matrix (ECM) proteins, cardiac fibrosis and exacerbation of impaired cardiac contractility (76). The permeant cardiomyocyte changes, inflammatory response, impaired compensatory responses and accelerated cellular ageing profile offer one explanation for the delayed onset of AIC (70). While the actual mechanisms responsible for anthracycline-induced cellular senescence remain undefined (39), evidence supports a causal role for senescent cells in cardiac dysfunction. Demaria et al. (2017) revealed that selective clearance of senescent cells in a murine model after doxorubicin administration led to significant improvements in cardiac function (77). This study demonstrated that senescence is not merely a consequence of cardiotoxic injury but actively contributes to the deterioration of cardiac performance.

1.5 Cellular structure of cardiac tissue

The heart is the earliest organ to become functional during embryonic development, beginning to beat spontaneously by the fourth week of gestation (78). As the central component of the cardiovascular system, the heart functions within a closed circulatory circuit in conjunction with the peripheral vasculature (79). Structurally, it comprises four chambers and is primarily composed of specialised striated cardiac muscle. This muscle tissue is densely perfused by a complex coronary microvascular network, ensuring the delivery of oxygen and nutrients necessary to meet the high metabolic demands of the myocardium (80).

The heart is composed of several types of cells, including cardiomyocytes, CFs, endothelial cells, inflammatory cells, and smooth muscle cells, all with distinct roles in cardiac function (Figure 1.3) (81). All functions of the heart rely on the coordination between these cells to generate electrical impulses for contracting rhythmically and maintaining structural support of the heart to pump blood to the body. Understanding the role of each cell is

important to provide insights into cardiac health and the mechanisms underlying heart diseases (82).

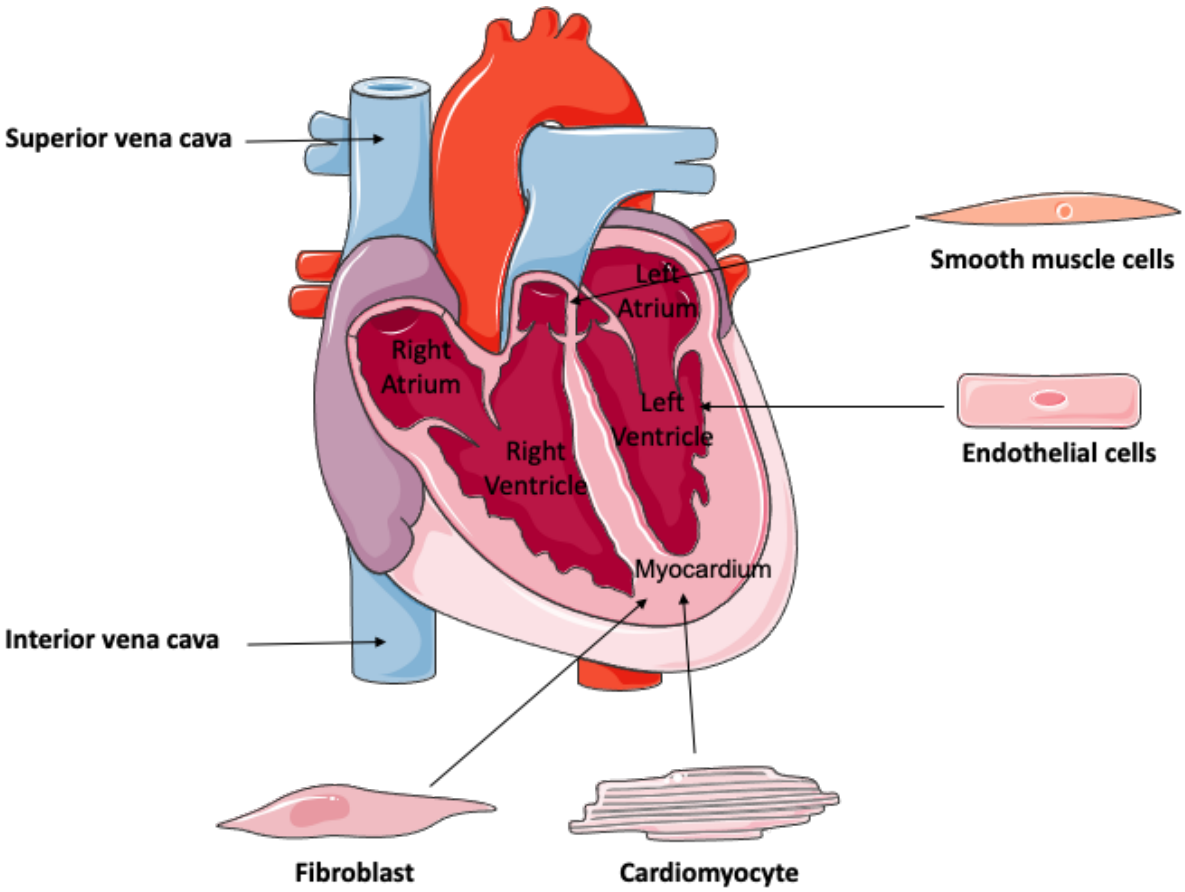

Figure 1.3 Anatomical structure and cellular composition of the human heart. The diagram shows the four cardiac chambers, heart valves, and major cell types present in cardiac tissue. Image adapted from SERVIER Medical Art.

1.5.1 Cardiomyocytes

Cardiomyocytes are the contractile unit that simultaneously contract to maintain coordinated pump function, to adequately supply organs and tissues, through a well-defined contraction–relaxation cycle (79). Although cardiomyocytes represent only about 30% of the total cardiac cell types, they are estimated to occupy nearly 85% of the myocardial volume due to their relatively large size (81). These cells have a high density of mitochondria to meet the energy demand of the heart, with organised arrangements of contractile myofilaments called sarcomeres (49). The sarcomeres are composed of thin actin and thick myosin filaments, which glide past one another in an energy-dependent process thereby shortening the sarcomere, resulting in cardiomyocyte contraction (and subsequent relaxation) (49). These synchronised contractions lead to efficient atrial and thereafter ventricular systole, pumping blood throughout the body (82).

The development and proliferation of mammalian cardiomyocytes start in foetal stages and continue after birth in the neonatal period (83). However, with development progresses, the ability of cardiomyocytes to proliferate declines but cardiomyocytes undergo physiological hypertrophy to support cardiac growth (84). The shift to a fully matured state is defined by the cessation of both mitosis and cytokinesis (84). Once this transition is complete, the total number of cardiomyocytes stays relatively constant into adulthood and a slow but constant rate of cardiomyocyte turnover is enough to maintain the heart's structural integrity, even when some are gradually lost as a result of apoptosis and minor cardiac damage (42).

Cardiomyocytes undergo hypertrophic response as a compensation mechanism in response to physiological stress or minor cardiac injury, allowing functioning myocytes to counteract cell loss and sustain cardiac output (85). However, due to limited proliferative capacity, cardiomyocyte loss resulting from apoptosis or necrosis is largely irreversible (84). Cellular renewal occurs predominantly in endothelial and mesenchymal cell types, particularly fibroblasts, during processes such as cardiac repair and remodelling (86). This process promotes fibroblast proliferation which in severe cardiac damage increases cardiac fibrosis, a phenomenon often linked with ageing hearts, which stabilizes the injured myocardium but compromises contractility and eventually leads to irreversible myocardial scarring (86). This fibrosis lowers the heart's contractile efficiency, which contributes considerably to the progression of heart failure (87).

1.5.1.1 Cardiomyocyte excitation-contraction coupling

Cardiac excitation-contraction coupling refers to the physiological process required to translate an electrical impulse into mechanical contraction in myocardium. This energy-dependent process is ultimately regulated by sequential activity of cellular ion channels, with Ca^{2+} ion being the driving force of cardiomyocyte contraction (88).

This process is initiated in the sinoatrial node (SAN), where pacemaker cells generate an action potential that propagate through the myocardium, triggering cardiomyocyte contraction. During the action potential, atrial and ventricular cardiomyocytes progress through distinct phases, with each marked by activation of specific ions channels and the movement of defined ions, which subsequently leads to coordinated cellular depolarization/repolarization and myocardial, contraction, and relaxation (Figure 1.4) (89, 90).

The ventricular action potential begins with Phase 0, activation of fast voltage-gated sodium (Na^+) channels permitting influx of Na^+ ions into the cell. This Na^+ influx results in a sharp rise in membrane potential, eventually leading to inactivation of Na^+ channels as membrane charge equilibrates which initiates Phase 1 of the action potential (89). During this phase, potassium (K^+) channels remain open, leading to efflux of K^+ ions that initiates partial cardiomyocyte repolarization. This is followed by Phase 2, known as the plateau phase, which is unique to cardiac myocytes and is the major driver in excitation-contraction coupling (89). During this phase, L-type Ca^{2+} channels open, allowing Ca^{2+} to influx into the cardiomyocyte (89). The sarcoplasmic reticulum, a specialised organelle acting as the main intracellular Ca^{2+} reservoir, has ryanodine receptors (RyRs), which are subsequently activated by the external Ca^{2+} influx (88). This causes the sarcoplasmic reticulum to release a significantly higher amount of Ca^{2+} into the cytoplasm, a process known as calcium-induced calcium release (CICR). Through its interaction with myofilaments, the subsequent increase in free cytosolic Ca^{2+} triggers cardiac contraction. In particular, Ca^{2+} binds to troponin C, causing a conformational shift that displaces troponin I and exposes myosin-binding sites on actin filaments. The sarcomeres shorten as the thick and thin filaments pass one another, generating cardiomyocyte contraction propelling blood from the heart. At the end of the contraction, Ca^{2+} dissociates from troponin C, which inhibits the production of cross-bridges. Either through sodium-calcium exchanger (NCX) activation and Ca^{2+} ion to leave cell, or sarcoplasmic reticulum SERCA pump excess cytosolic Ca^{2+} back into the sarcoplasmic reticulum. The

repolarisation of cardiomyocytes is defined by phase 3 of the action potential, characterised by the closure of Ca^{2+} channels and increased permeability to K^+ efflux, restoring the resting membrane potential. Phase 4 (resting phase) starts, during this phase, K^+ channels remain open while Na^+ and Ca^{2+} channels remain closed. This phase is to ensure that cardiomyocyte is ready to the next action potential cycle (88-90). Normal cardiomyocyte contraction and heart rhythm depend on the exact synchronisation of ion fluxes, Ca^{2+} release, and myofilament interactions. Any disruptions in this mechanism result in abnormal contractility, arrhythmias, and reduced cardiac output (89).

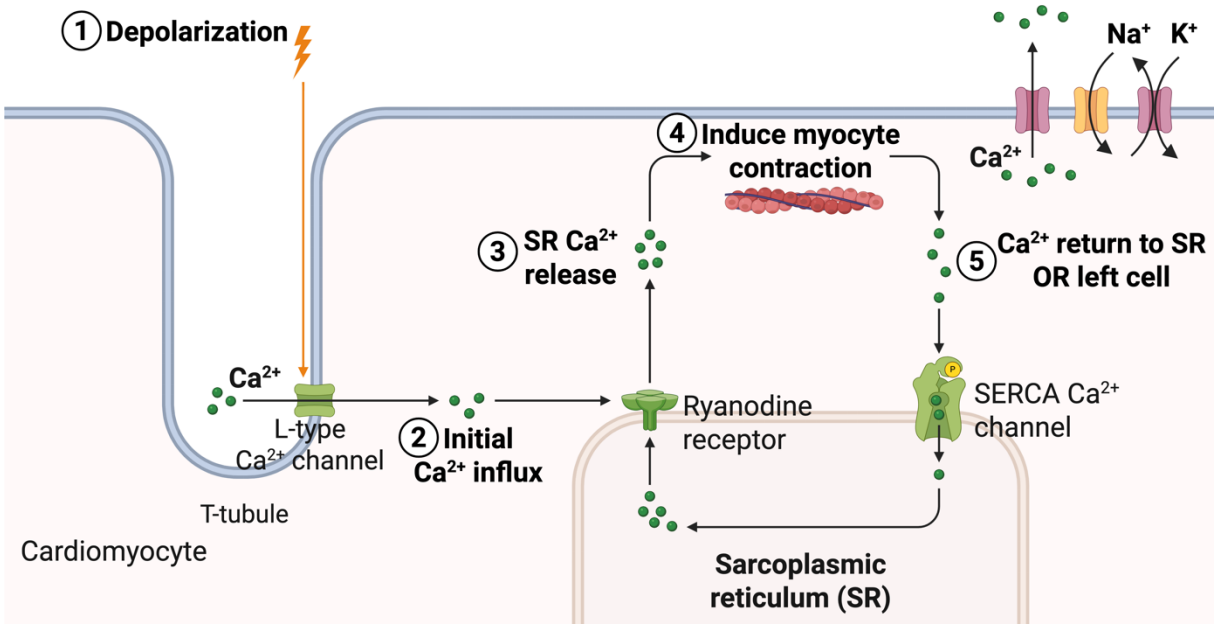

Figure 1.4 Cardiomyocyte excitation-contraction coupling. 1) Action potential initiates the opening of L-type Ca^{2+} channel. 2) Ca^{2+} influx into cytoplasm and activation of RyRs on sarcoplasmic reticulum. 3) Increase Ca^{2+} release from sarcoplasmic reticulum into cytoplasm. 4) High intracellular Ca^{2+} concentration induces cardiomyocyte contraction. 5) In the diastolic phase, following contraction, intracellular Ca^{2+} levels are restored to baseline primarily by SERCA Ca^{2+} channel which pumps excess cytosolic Ca^{2+} back into sarcoplasmic reticulum. In addition, excess Ca^{2+} is extruded from the cell by activating NCX. Adapted from BioRender.

1.5.2 Cardiac fibroblast

Cardiac fibroblasts (CFs) are from mesenchymal origin and constitute around 15% of cardiac cell volume, with key roles in responding to cardiac injury by providing structural support to cardiomyocytes, maintaining myocardial integrity and production of the supportive ECM proteins (91). They provide mechanical stability to cardiomyocytes by arranging collagen networks around cardiomyocytes (92). In addition, CFs play a role in electrical support by maintaining the fibrous structure that separates the atrial and ventricular myocardium, ensuring the heart's electrical impulses go along a synchronised course (93). Furthermore, paracrine factors released by CFs, such as transforming growth factor-beta (TGF-β) and vascular endothelial growth factor (VEGF), are crucial in maintaining cardiac haemostasis and driving the physiological and pathological cellular responses of cardiac tissue (94).

During pathological cardiac conditions including myocardial infarction, heart failure, and cardiac hypertrophy, CFs are responsive to injury by differentiation into myofibroblasts to promote cardiac repair and maintain optimal cardiac health (92). Myofibroblasts are characterised by a spindle-like shape, excessive proliferation, increased synthesis of α-smooth muscle actin (α-SMA), and increased production of collagen which all contribute to tissue remodelling and fibrosis (92). Pro-inflammatory cytokines such as tumour necrosis factor α (TNF-α) and interleukin-6 (IL-6) are also triggered to increase cells proliferation and promote cellular repair (94). However, fibrotic remodelling results in increased stiffness of heart and reduced systolic and diastolic function which all contribute to arrhythmias (91).

In case of AIC, cardiomyocytes have been considered the classic target of AIC and not much research has been done on other types of cells in relation to structural cardiotoxicity, including CFs (22). However, in recent years, there has been a clear shift in attention toward CFs and their involvement in structural toxicities, which may thus lead to impairment of cardiac function and contractility without direct damage to cardiomyocytes (95). However, the mechanism of the toxic effects of anthracyclines on non-myocytes is still unclear.

1.5.3 Vasculature cells: Endothelial cells and pericytes

Cardiac tissue, in addition to cardiomyocytes and CFs, also contains several other cell types to support and contribute to heart functions. Endothelial cells line the heart chambers and are the main cell type composition of intramyocardial capillaries (96). These cells are responsible for transferring nutrients and oxygen to cardiomyocytes to maintain the energy requirement

for the highly demanding organ (96). Consequently, any drug that adversely affects cardiac endothelial function would cause a reduction in oxygen, nutrients and cellular signalling factors to cardiomyocytes. Furthermore, continual and progressive damage to the endothelial population within cardiac tissue would also increase permeability of the aforementioned microvasculature and contribute to development of cardiac ischaemia, as reported in survivors of paediatric cancer following chemotherapy (97).

Stability of vasculature, including the vasculature and microvasculature present in cardiac tissue, is maintained by pericytes (98). These specialised cells that wrap around the endothelial cells of capillaries and small blood vessels, regulating blood flow, coagulation, and maintaining heart tissue integrity (98). The highly vascularized myocardium relies on these cells to regulate blood flow, making them potential targets in cardiotoxicity. When damaged, they could impair proper blood supply to the heart, compromising its function (99).

1.5.4 Cardiac progenitor cells

Cardiac progenitor cells (CPCs) are those from which other cells of the cardiac tissue can be derived, embryonic CPCs and adult CPCs (100). This class of cells is involved in both maintaining tissue homeostasis and promoting cardiac tissue regeneration (100). The mechanical and/or hormonal stimulation of this cell population is central to preserving cardiac function following cardiac injury and damage (101). However, depletion of this cell population and thus the tissues' ability to regenerate, results in increased potential for vulnerability to toxicological insult, including drug-induced cardiotoxicity (22, 101). In this context, anthracyclines have been reported to inhibit CPCs proliferation and subsequently lead to a depletion in these cardiac stem cells through both cytotoxic action and induction of cellular senescence (22, 102). Co-treatment with senolytic agents effectively eliminated senescent CPCs, thereby suppressing the SASP and mitigating its deleterious effects on surrounding healthy CPCs (102). Ultimately, in the clinic, this would manifest in accelerated progression of cardiac failure following exposure of already damaged cardiac tissue to further toxicological and/or physiological insult, such as is the case with initial anthracycline-induced tissue damage and latter subsequent stressors such as hypertension, myocardial injury, and ageing (103).

1.6 Cellular communication within cardiac tissue

Cell-cell communication is important for cardiac tissue to ensure coordination among the various cell types and maintain physiological cardiac functions (104). These multifaceted communications include both electrical and chemical signalling pathways, to maintain integrity and synchronicity of the cardiac syncytium, including gap junctions, neurohumoral factors, and paracrine and autocrine signalling.

1.6.1 Cell-cell communications

Cardiac contractility, structural integrity, and functionality are driven through the interactions between cells of the same type and across cell types. Cardiomyocytes and support cells use gap junctions to facilitate intercellular connections, both homotypic (between similar types of cells) and heterotypic (between different types of cells) (105). These channels direct communication between cells to transfer ions, metabolites, and intracellular signalling molecules, to facilitate the heart to rhythmically contract in a coordinated manner (104, 106). In addition, they support the transfer of nutrients and oxygen to the myocardium to provide energy to the high demand organ (105). Gap junctions are composed of connexons that are formed from connexin proteins, with the most abundant being connexin-43 in cardiomyocytes, which align to create continuous channels between neighbouring cells (106). Consequently, dysfunction of gap junctions can cause disturbances to action potential in the heart, leading to cardiac arrhythmias and cardiac failure. Anthracycline reduces connexin-43 phosphorylation and expression and affects gap junction functions which facilitate Ca^{2+} overload, amplifying cardiotoxic effects across the myocardium (107).

1.6.2 Intercellular chemical communication and signalling

In cardiac cells, gap junctions not only allow the passage of ions and electrical impulses but also enable the autocrine and paracrine exchange of chemical signalling molecules, a process essential for maintaining coordinated tissue function (108). These pathways are important for coordinated cell functions, especially in the heart, where paracrine signalling is responsible for regulating process of angiogenesis, fibrosis, and tissue repair after myocardial injury (108). As an example, nitric oxide (NO) is produced by endothelial cells to regulate contractility of cardiomyocytes, vascular tone, and assist in cardiac remodelling (109). However, dysregulated

paracrine signalling is often characterised by excessive cytokine release during chronic inflammation of the heart, contributing to fibrosis and heart failure (94).

1.6.3 Intracellular signalling and communication

Along with direct communication between cells, cardiac function is also dependent upon communication between the cellular environment and the individual cells of the myocardium, mediated by cell surface receptors. This forms a complex network of signalling cues to maintain the physiological responses and the functional outputs of the cardiac tissue, with dysfunctions in these pathways being a major driver for cardiac pathologies and dysregulation (110).

These cell surface receptors belong mainly to the G-protein coupled receptors (GPCR) family. In cardiac tissue, amongst several others, these include the α- and β-adrenergic receptors, which drive cardiac inotropy and chronotropy, and the angiotensin receptor family, responsible for controlling cellular tone and cardiac outputs (111). Expression and activity of these GPCRs are associated with both cardiomyocytes, CFs and other cell types associated with the vasculature network (111). As such, aberrant or dysregulated activation of these receptors leads to cardiac conditions such as hypertension, dysrhythmias, cardiac ischaemia and cardiac hypertrophy (110).

1.7 Renin-Angiotensin-Aldosterone System (RAAS)

The renin-angiotensin-aldosterone system (RAAS) plays a crucial role in regulating multiple physiological functions in the renal and cardiovascular systems. The dysregulation of RAAS is implicated in several pathological conditions, particularly hypertension and heart failure (112, 113). The dysregulation of RAAS has also been reported to increase ROS production and oxidative stress, contributing to cardiac remodelling and hypertrophy (114, 115). Angiotensin II-induced oxidative stress can cause mitochondrial damage, cardiac hypertrophy, apoptosis, and fibrosis, as well as play a role in angiotensin II-dependent inflammation and cardiomyocyte contractile dysfunction (62). However, although the potential is compelling, the role of oxidative stress in several pathological cardiac conditions has yet to be confirmed.

Decreases in blood pressure or systemic sodium chloride levels trigger the release of renin, a proteolytic enzyme produced by the juxtaglomerular apparatus in the kidneys (116). This enzyme thereafter functions upon the pre-hormone angiotensinogen, an alpha-2 globulin

protein, synthesised in the liver and released systemically (116). The action of renin is to convert angiotensinogen into the inactive hormone, angiotensin I (116, 117). This hormone is then further converted into its active octapeptide form, angiotensin II, through enzymatic action of an enzyme termed angiotensin-converting enzyme (ACE), an enzyme primarily localised to pulmonary tissue (117). Angiotensin II is the key effector of the RAAS, exerting potent effects on blood pressure regulation and fluid balance. This is achieved through a complex receptor signalling pathway that affects its actions upon the cardiovascular, adrenal and renal systems (Figure 1.5) (113).

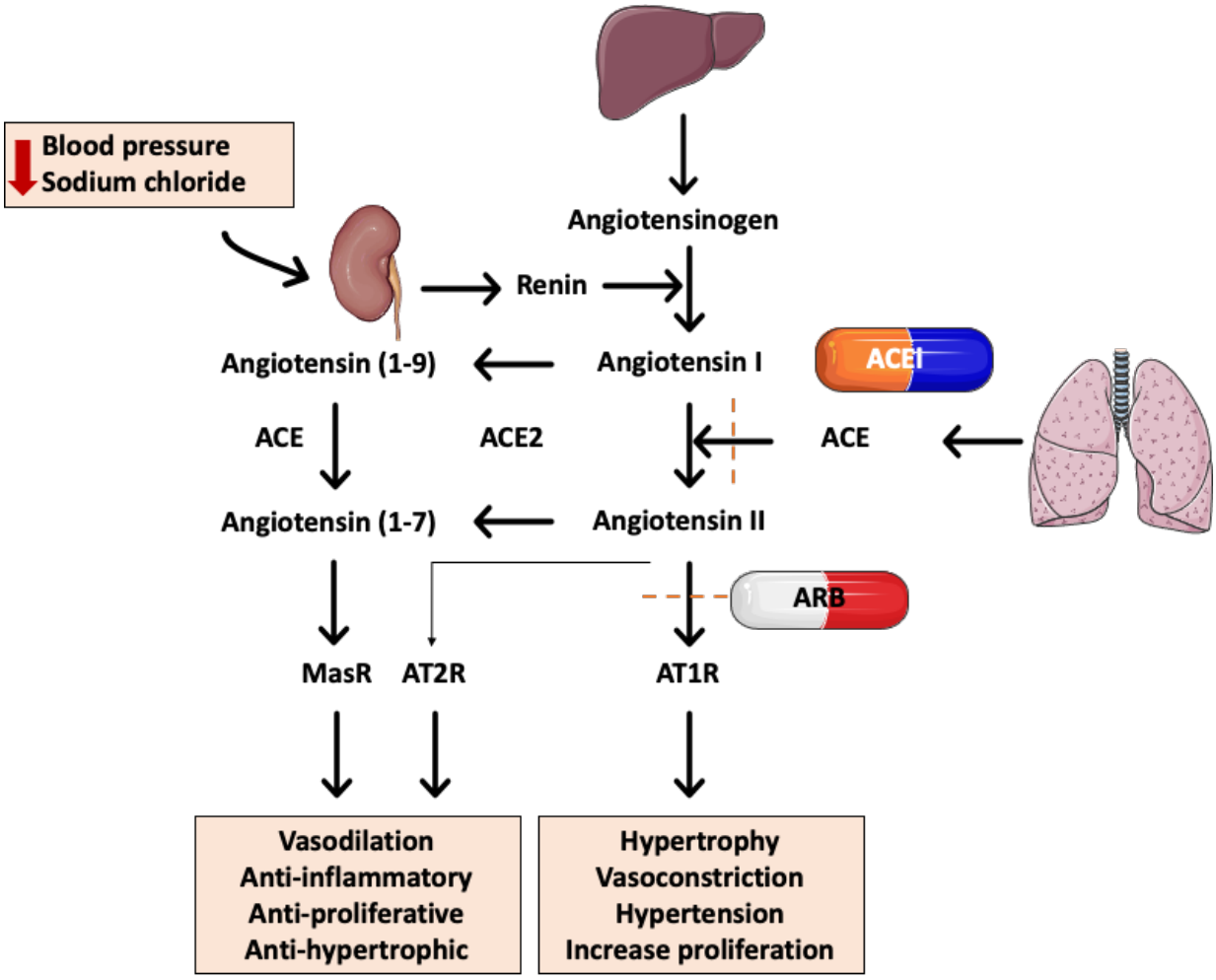

Figure 1.5 Illustration of the renin-angiotensin-aldosterone system (RAAS) and where the drugs that perturb angiotensin II signalling work. Angiotensin converting enzyme inhibitor (ACEi) prevent the conversion of angiotensin I into angiotensin II, by preventing ACE activity. Angiotensin receptor blockers (ARB) prevent angiotensin II binding with AT1R. Made by SERVIER Medical Art.

1.7.1 Angiotensin receptor signalling

Angiotensin II interacts with two different GPCR, namely the angiotensin II type 1 receptor (AT1R) and the angiotensin II type 2 receptor (AT2R) (118). Activated by angiotensin II through reversible binding, angiotensin receptor activation regulates several elements of cardiovascular and renal physiology, including blood pressure regulation, cellular growth and tissue remodelling (Figure 1.6) (112, 113).

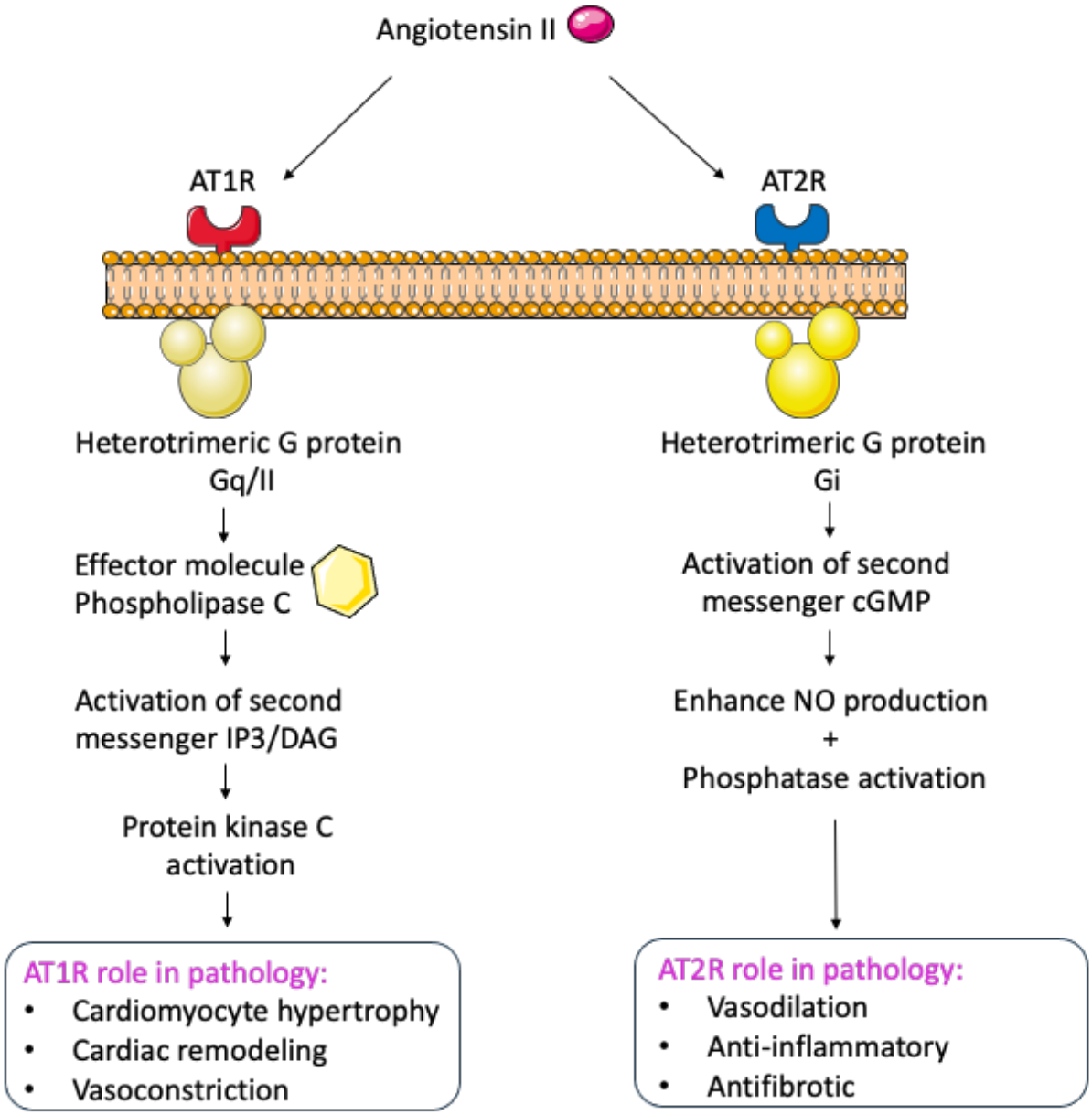

Figure 1.6. The schematic represents the signalling cascades activated by the binding of angiotensin II to AT1R and AT2R and cellular responses. Angiotensin type-1 receptor (AT1R), Angiotensin type-2 receptor (AT2R), inositol trisphosphate (IP3), Diacylglycerol (DAG), cyclic guanosine monophosphate (cGMP), Nitric Oxide (NO). Made by SERVIER Medical Art.

1.7.1.1 Angiotensin type 1 receptor (AT1R) signalling

Among the two types of receptors, AT1R is the most prevalent type of angiotensin II receptor in the cardiovascular system and primarily responsible for mediating the well-known effects of angiotensin II (115). AT1R is expressed in many tissues such as adrenal gland, kidney, heart, blood vessels, and brain (119). Two subtypes of AT1R have been identified: type-A (AT1RA) and type-B (AT1RB) receptors. AT1RA is necessary for cardiomyocyte growth and blood pressure regulation, whilst AT1RB is important to control vascular tone in the absence of AT1RA stimulation (120). The specific role and crosstalk of each of these sub-types in the cardiac system has yet to be fully defined.

Physiologically, angiotensin II plays a critical role in blood pressure through triggering of AT1R which is highly expressed in vascular smooth muscle cells (VSMCs) (121). AT1R is present in the proximal tubules of the kidney and AT1R stimulation in the kidneys promotes sodium and water retention, contributing to increased blood pressure (122). In addition, AT1R activation also increases systemic vascular resistance, primarily through activation of phospholipase C, which increases intracellular Ca^{2+} levels, resulting in enhancement of smooth muscle contraction, reducing vessel diameter and increasing resistance (121, 123). Under normal physiological conditions, these changes are transient and function to assist in the regulation of blood pressure and cardiac output. Conversely, chronic activation of AT1R, leads to prolonged vasoconstriction, promotion of endothelial dysfunction, and decreased NO bioavailability, all which are major characteristics of hypertension and atherosclerosis (114).

With respect to cardiac tissue, AT1R expression is believed to play a role in promotion of cardiac inotropy and chronotropy to maintain cardiac output (124). Activation of cardiac AT1R initiates a multitude of signalling pathways, resulting in both promotion of cellular growth and pathological remodelling of cardiac tissue (115, 124). Consequently, AT1R activation in cardiac tissue facilitates adaptive responses of cardiac cells towards optimisation of cardiac contractility and cardioprotection (114). In this context, chronic AT1R activation leads to cardiomyocyte hypertrophy and fibroblast activation (114). Additionally, activation of AT1R within cardiomyocytes has also been reported to increase oxidative stress and promote pro-inflammatory pathways, contributing to cardiac remodelling and hypertrophy (114, 115). Together, these pathophysiological and structural changes lead to cardiac stiffening and subsequent reduction in the cardiac ejection fraction, independently of effects upon systemic blood pressure (125).

1.7.1.2 Angiotensin type 2 receptor (AT2R) signalling

The primary pathophysiological actions of angiotensin II action are attributed to binding to AT1R. The interaction of angiotensin II with the AT2R receptor mediates the opposite effects to those of AT1R activation. AT2R activation promotes vasodilatation and prevents cellular proliferation (118). Despite this, AT2R activation has a limited physiological role in adults since it is present and expressed during development with its presence significantly declining after birth (126). However, AT2R expression is elevated in pathological conditions such as vascular injury and heart failure (127, 128). The preclinical studies widely showed the protective effect of AT2R agonist through inducing vascular relaxation and decreasing blood pressure (129). However, the role of AT2R in decreasing blood pressure in hypertensive patients is still elusive (129).

1.7.1.3 Alternative angiotensin pathway: angiotensin-converting enzyme 2 (ACE2) and angiotensin (1-7)

The regulation of blood pressure and other pathophysiological conditions mediated by angiotensin II is primarily regulated by conversion of angiotensin I to angiotensin II by ACE, as defined above (117). However, a homologue of ACE, termed angiotensin-converting enzyme 2 (ACE2), which has 40% sequence similarity to ACE, has been identified and shown to play a role in several pathophysiological processes, involving different metabolites of angiotensin I and II (130). ACE2 is shown to convert angiotensin I into angiotensin (1–9), which can be converted to angiotensin (1–7) by ACE (130). Furthermore, ACE2 can then degrade angiotensin II to angiotensin (1–7) (130). This specific angiotensin metabolite has been shown to lower blood pressure due to vasodilation of blood vessels, induction of the synthesis of anti-inflammatory prostaglandins, and increases in the release of NO (130). With respect to cardiac tissue, angiotensin (1–7) exhibits a positive effect by limiting the proliferative and hypertrophic responses to angiotensin II (131). Furthermore, this has been postulated to counter the activity of ACE and function as a mechanism for clearance of angiotensin II from the circulation (132).

ACE2 demonstrates a different expression profile to that of ACE, with it being generally ubiquitous and exhibiting highest levels in the cardiovascular system and lungs (130). In cardiac tissue, ACE2 is expressed in cardiomyocytes, CFs, as well as VSMC and endothelial cells (133, 134). The product of ACE2, angiotensin (1-7), binds to the Mas G-protein coupled

receptor (MasR) on the cell surface and counterbalances the potential detrimental effects of angiotensin II (135). In this regard, ACE2 is believed to be protective by the fact that it acts to degrade angiotensin II to limit its availability and generates angiotensin (1-7) to stimulate the protective nature of the ACE2/angiotensin (1-7)/MasR axis (136). Furthermore, ACE2 overexpression significantly prevents myocardial fibrosis, reduces the development of cardiac hypertrophy and improves cardiac function (135).

1.8 Management of cardiotoxicity caused by anthracyclines

Management of AIC has primarily focused on elucidating the underlying mechanism of anthracycline and identifying targeted interventions to prevent cardiotoxic effects. However, a major challenge in this approach is how to preserve the antitumor effect of anthracycline, decrease the risk of incomplete tumour eradication or cancer recurrence, and lower the incidence of adverse cardiac events induced by anthracyclines (137). While acute cardiotoxicity can be reversible with timely intervention, the chronic cardiotoxicity of anthracyclines is the most concerning and prevalent form of cardiotoxicity because of its progressive and irreversible nature (14, 24, 25). As a result, there is an urgent need for cardioprotective strategies that effectively prevent long-term cardiac complications of anthracycline without compromising the therapeutic benefits of anthracycline chemotherapy.

The demonstration that anthracycline chemotherapy is associated with a high risk of long-term progressive cardiotoxicity emphasises the importance of implementing effective management strategies to treat chemotherapy-induced cardiotoxicity. Many strategies have been studied for management of AIC including differential infusion rates (bolus, short infusions of ≤ 1 hour, or extended continuous infusions of up to 96-hours) and newer formulations (pegylation, liposomes and other nano-delivery systems) of anthracyclines, aimed at reducing cardiac exposure whilst maintaining therapeutic efficacy (23). In parallel to this, strategies have also focused on administration of therapeutics to either mitigate the detrimental effects of anthracyclines by tackling proposed mechanisms of toxicity or reinforce the cardioprotective pathways present within cardiac tissue (137).

1.8.1 Iron Chelation to reduce cellular oxidative stress

One of the proposed mechanisms of AIC involves iron dysregulation (see section 1.4.3.2). Anthracyclines have a high affinity for iron, forming an anthracycline-iron complex that

increases the generation of ROS which contributes to mitochondria dysfunction and cardiomyocyte damage (27, 64). Given the important role of iron in mediating AIC pathogenesis, one strategy employed and evaluated clinically is the iron chelators, such as dexrazoxane (138).

Dexrazoxane, an iron chelator agent, which is one of the FDA-recommended cardioprotective agents for preventing AIC has been evaluated regarding their ability to mitigate this cardiotoxicity in many preclinical studies and clinical trials (138). Dexrazoxane contains the ethylenediaminetetraacetic acid (EDTA) moiety, which is known to chelate metal ions such as Ca^{2+}, Mg^{2+}, and Fe^{2+}, reducing their activity (139). When dexrazoxane binds to iron, it exerts its effect by inhibiting the formation of an anthracycline-iron complex, which, therefore, inhibits free radical formation and results in the prevention of cardiac injury (137). Unfortunately, due to some concerns about the result from clinical trials on the effect of dexrazoxane on antitumor efficacy and developing of secondary malignancy after treatment with dexrazoxane, particularly in paediatric patients, there is a reluctance from oncologists to use dexrazoxane (138).

1.8.2 Blockade of beta-adrenergic signalling within cardiac tissue

Beta adrenoceptor blockers (β-blockers) are widely used for treatment of hypertension and heart failure (140). β-adrenergic receptors consist of three subtypes: β1, expressed in the heart, where it controls cardiac automaticity and conduction velocity; β2, expressed in many organs and responsible for mediating smooth muscle relaxation; and β3, which plays a role in lipolysis (140). The cardioprotective effect of β-blockers for preventing AIC has been evaluated regarding an ability to mitigate this cardiotoxicity in many preclinical studies and clinical trials (141). Administration of the beta-blocker carvedilol has demonstrated a significant decreasing in ROS generation and prevention of apoptosis in cardiomyocytes in both in *in vitro* and *in vivo* models, due to antioxidant properties of this agent (142, 143). A network meta-analysis comparing the effectiveness of β-blockers in mitigation of AIC reported that carvedilol was effective in lower the incidence of left ventricle ejection fraction (LVEF) decline during anthracycline therapy compared to other β-blockers (141). This suggest that cardioprotective effect of carvedilol may be attributed to its antioxidant effects.

1.8.3 Interference in angiotensin signalling pathways

The clinical presentation of delayed cardiotoxicity associated with anthracyclines is noted as being similar to that observed with other cardiac conditions, such as cardiac hypertrophy and heart failure (144, 145). In these latter conditions, therapeutic approaches are primarily focused upon preventing further progression of cardiac impairments, limiting cardiac remodelling and restoration of cardiac function (27). One such strategy is centred around perturbation of the RAAS axis and re-engagement of normal cardiac physiological action alongside restoring of haemodynamic functions (27).

Drugs targeting RAAS, such as angiotensin-converting enzyme inhibitors (ACEi) and angiotensin receptor blockers (ARBs), are widely used in clinical practice to treat cardiovascular disorders in non-cancer patients (146, 147). These drugs are commonly prescribed to manage many cardiovascular disorders, including hypertension and heart failure, and they have demonstrated effectiveness in preventing the progression of LVD (148, 149). Despite targeting the same system, ACEi and ARBs work through distinct mechanisms within the RAAS. ACEi exert their effect by inhibiting the ACE activity, which is responsible for converting angiotensin I into its active form, angiotensin II (Figure 1.5) (146). By inhibiting this conversion, ACEi reduces the levels of angiotensin II, a potent vasoconstrictor, this leads to a decrease in vascular resistance and, ultimately, a reduction in blood pressure (150). However, ARBs work by selectively blocking the AT1R, which mediates many of the harmful effects of angiotensin II, such as vasoconstriction, sodium retention, and adverse cardiac remodelling (115). By inhibiting the AT1R signalling pathway, ARBs effectively reduce the physiological impact of angiotensin II, leading to improved cardiovascular outcomes without affecting the production of angiotensin II itself (151).

1.8.3.1 Clinical studies supporting perturbation of angiotensin signalling pathway for mitigation of AIC

Clinical studies have unequivocally demonstrated success of ACEi as a management strategy for heart failure (148, 149). This, in combination with the confirmation that AIC is linked to progressive development of cardiac failure has led to several studies to evaluate the potential of ACEi and ARBs for mitigation of AIC (34). These studies are summarised in Table 1.1, with notable findings highlighted. One such observation is the implication that earlier administration of ACEi appears to have greater effects. However, inconsistencies are evident

between these trials, attributed largely to differences in study population age, specific therapeutic agent employed, time-periods of study analyses and variability in assessment methodology, amongst others (152-161). In terms of the ACEi as a therapeutic, a limitation of many of these studies is the use of sub-optimal doses compared to cardiology clinical guidelines (162). This subsequently led to the PROACT clinical trial, which involves prophylactic administration of enalapril prior to starting, and throughout treatment period, for anthracycline-based therapy in breast cancer and lymphoma patients (163). Preliminary observations for this trial indicate that ACEi did not provide any advantages in the short-term acute period, as determined by troponin biomarkers and cardiac-imaging modalities (161). However, the effect of inclusion of ACEi on longer-term development of AIC, reflective of the major clinical issue, has yet to be established with this trial, with such outcomes expected over the next decade or so.

From the perspective of ARBs and their slightly different approach to modulation of the angiotensin response, similar to ACEi, studies have also evaluated ARBs for the management of AIC (164-169). Murine studies have shown that blocking, or deletion, of AT1R provides a cardioprotective effect against anthracyclines (170). In clinical studies, administration of the ARB telmisartan prior to anthracycline chemotherapy associated with a preservation of cardiac function as determined by electrocardiogram (ECG) (165).

Clinical trials have shown that drugs which perturb the RAAS are effective to some extent in the prevention of AIC. However, the limitations of these studies include the small number of patients involved in the study, as well as the short period of observation, single-centre randomized clinical trials, and the limited number of clinical trials that were conducted which evaluate the role of ACEi alone in the prevention of AIC. Although the data from these clinical trials have shown promising protective effects by drugs that perturb the angiotensin II signalling pathway, there is a need to validate these findings in larger, randomized controlled trials.

There are several mechanisms proposed to explain how drugs perturbing angiotensin II signalling mitigate the adverse cardiac event associated with anthracyclines. These include the reduction of ROS production and oxidative stress and prevention of mitochondrial damage (171, 172). Additionally, ACEi and ARBs contribute to the preservation of cardiovascular haemodynamics by maintaining systolic and diastolic functions (155, 173). However, the mechanism of perturbing angiotensin II signalling pathway confers cardioprotection in the context of AIC remains not fully understood.

Table 1.1 Summary of key studies evaluating cardioprotective strategies (ACEi and ARBs) with anthracycline based chemotherapy.

Study	Study participants	Aim of the study	Intervention	Key findings	Reference
ACEi					
Cardinale et al., 2006	Any adult tumour type (n=114)	Evaluate cardioprotective efficacy of enalapril in patients from one-month post-chemotherapy monitored by systemic troponin I levels	Enalapril (titrated up to 20 mg/day) for 1 year	No significant change in LVEF was observed in the treatment group. No increase in end-diastolic and end-systolic volumes was noted either.	(152)
Cardinal et al., 2010	Patients with LVEF due to anthracycline chemotherapy (n=201)	Evaluate response of patient with anthracycline induced cardiomyopathy to standard of care HF therapy	Enalapril (2.5- to 5 mg/day titrated up to 20 mg/day) OR Enalapril (5 mg/day) AND carvedilol (6.25 mg/day titrated up to 50 mg/day)	Early treatment allows for complete recovery of LVEF and positively impacts cardiac outcome.	(153)
OVERCOME trial (2013)	Adult haematological malignancies (n=90)	Evaluate efficacy of enalapril and carvedilol in reducing the risk of developing LVEF after chemotherapy	Enalapril (5 mg/day titrated up to 20 mg/day) AND carvedilol (6.25 mg/day titrated up to 50 mg/day)	Low incidence of decrease in LVEF, heart failure, and death in patients in the treatment group.	(154)
Janbabai et al., 2017	Any adult tumour type (n=69)	Assess cardioprotective efficacy of enalapril against AIC	Enalapril (10–20 mg/day)	After one month of initiation of chemotherapy, enalapril was shown to protect the patient against elevations in troponin I. After 6 months, LVEF same as baseline in enalapril group. Generally, enalapril	(155)

				can inhibit anthracycline-induced systolic and diastolic heart dysfunction.	
ICOS-ONE (2018)	Any adult tumour type (n=273)	Compare the cardioprotective efficacy of initiating enalapril in all patients prior to chemotherapy versus initiating enalapril in patients with elevated troponin levels	Enalapril (10-20 mg/day)	Regardless of the time of enalapril initiation, no difference in terms of the elevation of troponin I. Moreover, the incidence of LVD was low in both groups.	(156)
Gupta et al., 2018	Paediatric leukaemia or lymphoma (n=84)	Assess cardioprotective efficacy of enalapril against AIC.	Enalapril (0.1 mg/kg/day) for 6 months	Patients receiving enalapril had lower incidence of elevation in cardiac biomarker and decline in LVEF compared to placebo.	(157)
Słowik et al., 2020	Women with breast cancer (n=96)	Assess cardioprotective efficacy of ramipril against AIC	Ramipril (2.5 mg/day titrated up to 10 mg/day) for 1 year	Patients receiving enalapril had lower incidence of decline in LVEF and no change in cardiac biomarker compared to placebo.	(158)
Wihandono et al., 2021	Adult breast cancer (n=74)	Assess cardioprotective efficacy of lisinopril and bisoprolol against AIC	Lisinopril (2.5 mg/day titrated up to 10 mg/day) AND Bisoprolol (1.25 mg/day titrated up to 10 mg/day)	Patients receiving lisinopril and bisoprolol had lower incidence of decline in LVEF	(159)
Livi et al., 2021	Women with breast cancer (n=174)	Assess cardioprotective efficacy of ramipril and bisoprolol against AIC	Ramipril (5 mg/day) OR Bisoprolol (5 mg/day)	Patients receiving ramipril and bisoprolol had lower incidence of decline in LVEF and heart remodelling	(160)

PROACT trial (2024)	Adult breast or lymphoma receiving high does [≥300 mg/m^2] anthracycline (n=111)	Assess cardioprotective effectiveness of enalapril against high dose anthracycline based regimen	Enalapril (20 mg/day), starting 2 days pre-chemotherapy	Enalapril did not significantly reduce the troponin T or troponin I levels, measured from one-month post-treatment. LVEF and global longitudinal strain (GLS) similar between groups	(161)
ARBs					
Nakamae et al., 2005	Adult, non-Hodgkin lymphoma (n=40)	Evaluate ability of valsartan to inhibit acute AIC.	Valsartan (80 mg/day)	No increase of BNP after one week in treatment group, and left ventricle (LV) dilatation is inhibited by valsartan.	(164)
Cadeddu et al., 2010	Any adult tumour type (n=49)	Evaluate cardioprotective ability of telmisartan against AIC.	Telmisartan (40 mg/day)	Reduction of LV diastolic impairment. No increase in the serum ROS level in treatment group	(165)
PRADA trial (2016)	Adult, breast cancer (n=120)	Assess cardioprotective effects of candesartan or metoprolol against AIC	Candesartan (32 mg/day)/placebo OR Metoprolol (100 mg/day)/placebo	Prevention of LVEF decline with candesartan, but no effects of metoprolol observed.	(166)
PRADA trial (2021)	Adult, breast cancer (n=120)	Assess efficacy of candesartan and/or metoprolol in the reduction of long-term cardiac damage associated with an anthracycline.	Candesartan (32 mg/day)/placebo OR Metoprolol (100 mg/day)/placebo	Candesartan associated with slight reduction in LV end-diastolic volume and preservation of GLS after two years.	(167)
Lee et al., 2021	Adult, breast cancer (n=195)	Assess cardioprotective effects of candesartan or carvedilol against AIC	Candesartan (4 mg/day) OR Carvedilol (3.125 mg/day)	Candesartan prevented the early decrease in LVEF.	(168)

Cardiac CARE Trial (2023)	Adult non-Hodgkin lymphoma or breast cancer (n=175)	Evaluate if cardiac troponin levels predictive of LVEF, and whether candesartan carvedilol co-treatment is protective of LVEF.	Candesartan (8-32 mg/day) AND Carvedilol (6.25-25 mg/day)	After 6-month, candesartan and carvedilol therapy did not protect against decline in LVEF after 6 months of completion of anthracycline treatment.	(169)

1.9 *In vitro* preclinical cardiac models

Several cellular models have been developed for the *in vitro* studies of cardiac biology and evaluation of molecule upon the cardiac system (174-176). One of the first models was the immortalised rat cardiomyoblast H9c2 cell line, which exhibits several features of cardiac cells such as some contractile proteins and an ability to fuse to a multinucleated structure but also lacks several features such as contractility and cardiomyocyte morphology (174). Another cell model used in this context is the HL-1 murine atrial cardiomyocyte cell line model (176). Unlike Hc92 cells, this cell line has contractile capacity but exhibits an unconventional action potential profile (176). However, the downside to both the Hc92 and HL-1 cell lines is their origin from rodent tissue, originating cell type which limits their ability to accurately mimic the characteristics of human cardiac cells (177). This is especially pertinent when evaluating the effects of drugs, such as anthracyclines, upon cardiac cells and thereafter translation to the clinical scenario. Such studies therefore require cell models which recapitulate human cardiac cells.

1.9.1 Immortalized human ventricular cardiomyocytes (AC10)

A cell line of immortalized human ventricular cardiomyocytes (AC1, AC10, AC12, AC16) was developed by fusing human heart ventricle cardiomyocytes with SV40-transformed human fibroblasts devoid mtDNA (175). The AC10 initiated and developed by Davidson et al., 2005, has been previously characterised and proved suitable for studying drug response on cardiomyocytes *in vitro* (175, 178). Although this cell line does not contract and remains in a pre-contractile state, it expresses different clinically relevant cardiomyocyte markers such as troponins, tropomyosin, and α-actinin and expresses many contractile proteins which make them a qualified model to study the cardiomyocyte response to anthracyclines (175). However, this cell line expresses the mesenchymal cell marker vimentin and, unlike mature cardiomyocytes, is proliferative (175). This latter action offers great utility as an unlimited source of cardiomyocytes *in vitro* (179). These differences from clinical adult cardiomyocytes are explained by the nature of these cells being a fusion between human cardiomyocytes and mitochondria-devoid human fibroblasts (175). This human derived cell line however does overcome the limitation of previous rodent cardiomyocyte models, in their ability to represent the human cardiomyocytes and their structural response to external agents (175, 178). With

their cellular growth patterns, mitochondrial function, and expression of cardiac markers, several studies used this cardiac model to detect cardiomyocyte inflammation and myocardial injury (180-182).

1.9.2 Human induced pluripotent stem cell cardiomyocytes (hiPSC-CM)

The highest profile cardiac model used for preclinical studies is now hiPSC-CM (183). These are physiologically relevant human derived cardiomyocytes expressing multiple cardiac markers, which can be cultured *in vitro*, making them an ideal model for cardiovascular research (184). This cell model has many advantages, including spontaneous contraction, sensitive to cardioactive drugs and express multiple cardiac ion channels and receptors important for cardiac functions (184). An often-reported limitation of these cells is their relative immaturity, although this has recently been addressed by strategies to stimulate their maturation *in vitro* (43). A major limitation of hiPSC-CM for *in vitro* studies and the analysis of drug effects is their cost to produce and maintain compared to other models, such as the AC cell lines described above (185).

As these cells are the closest model available to primary human cardiomyocytes, they are now central and widely recognised as essential to many *in vitro* cardiotoxicity assays and have demonstrated significant potential in reliably identifying cardiac liabilities in preclinical drug safety studies (183, 184). However, in many cases their limited growth characteristics, high cost and limited scope for evaluation of structural cellular effects has restricted their use for fundamental molecular analyses studies (185).

1.10 Thesis aims and objectives

The cardioprotective potential against AIC of therapies that act on the angiotensin signalling pathway has shown significant potential in clinical studies, implying a strong relationship exists between these two pathways. The mechanistic basis for these relationships has not yet been fully explored.

The aim of this thesis is to evaluate the relationship between development of AIC and the angiotensin-signalling pathway, in order to explain why ACEi may reduce AIC and improve clinical management of this condition.

This thesis is divided into three sections:

A) Evaluation of response of *in vitro* cardiac cells to clinically relevant exposure of doxorubicin and physiologically relevant concentrations of angiotensin II.

B) Characterisation of an involvement of the angiotensin-signalling pathway in cardiac cellular response to doxorubicin.

C) Determination of a role for the AT1R in the cardiotoxicity response of cardiomyocytes to the anthracycline doxorubicin.

Chapter 2. Materials and Methods

All reagents were obtained from Sigma-Aldrich Company Ltd (UK) unless specified otherwise. Plastic tissue culture materials were supplied by Sarstedt (UK).

2.1 Cell culture and maintenance of cells

All the cell models utilised in this study were cultured at 37°C in a humidified atmosphere of 5% carbon dioxide (CO_2). Throughout, culture medium was refreshed every two days to maintain optimal cell health and viability.

The human immortalised human ventricular AC10 cell line was graciously provided by Dr. Barbara Savoldo at Texas Children's Hospital, Texas, USA. AC10 cells were cultured in Dulbecco's Modified Eagle Medium (DMEM/F12) supplemented with 10% Foetal Bovine Serum (FBS) (Gibco; product code 10500-064), 2mM L-Glutamine, and 1% penicillin/streptomycin (pen/strep).

Primary human cardiac fibroblasts (HCF) obtained from Promocell (Heidelberg, Germany) were established in Fibroblast Growth Medium 3 (Promocell) containing 0.1 ml/ml Fetal Calf Serum, 1 ng/ml Basic Fibroblast Growth Factor (recombinant human), and 5 µg/ml Insulin (recombinant human). Once established this media was changed to DMEM/F-12 supplemented with 10% FBS, 2mM L-glutamine and 1% pen/strep.

Cells were passaged when confluency approximately 70-80% by washing the monolayer with Hank's Balanced Salt Solution (HBSS) and then addition of 0.25% trypsin/EDTA. Following detachment, the effects of trypsin were neutralised via addition of media containing FBS. Resultant cell suspensions were then either reseeded at a 1:10 ratio for onward culture, or centrifuged (400 x g for 5 minutes) and the cells re-suspended into new flasks, or cell pellets were stored at -20°C for subsequent molecular analyses.

2.2 Cell counting

Cell number was determined using a Neubauer haemocytometer. After cells trypsinisation and centrifugation, cell pellets were carefully resuspended in an appropriate volume of medium. A 10 µL of cell suspension were pipetted under the coverslip onto the haemocytometer. The number of cells in five 1mm^2 sections were counted, with cells only counted if they showed a viable appearance – bright and rounded in shape. The average

number of cells in the five sections (N) was then calculated. Due to the dimensions of the haemocytometer the average value of cells (N) in the five sections equates to N x10^4 cells/ml.

2.3 Cryopreservation of cells

Cells were cryopreserved to maintain long-term stocks at -196°C under liquid nitrogen. Confluent cells were trypsinized, centrifuged at 400 x g for 5 minutes, the supernatant discarded, and the resultant cell pellet resuspended in fresh medium. The cell suspension was transferred to a 2.0 mL cryovial, to which 10% dimethyl sulfoxide (DMSO) was added. Cryovials were placed in a Mr. Frosty™ Freezing Container (Nalgene, Thermo Scientific) filled with propan-2ol (Fisher Bioreagents) and stored at -80°C, to achieve a cooling rate of approximately 1°C per minute. The following day, the cryovials were moved to a liquid nitrogen storage for long-term storage.

2.4 Assessment of cell viability using MTS assay

Cellular viability was assessed using the well-established MTS assay ([3-(4,5-dimethylthiazol-2-yl)-5-(3-carboxymethoxyphenyl)-2-(4-sulfophenyl)-2H-tetrazolium, inner salt), using the CellTiter 96® Aqueous One Solution Cell Proliferation Assay (Promega). This assay measures the activity of mitochondrial NAD(P)H-dependent oxidoreductase within viable cells. These enzymes reduce the MTS reagent to produce soluble formazan crystals, promoted by the electron-coupling agent phenazine methosulfate (PMS). The absorbance of the soluble formazan product is measured spectrophotometrically at 490nm, with this output being directly proportional to mitochondrial activity and therefore cellular viability (186).

2.4.1 Evaluation of cell growth and proliferation characteristics by MTS assay

For optimisation of the MTS assay for assessment of cellular viability and proliferative response, cells were seeded into flat-bottomed 96-well cell culture plates at densities ranging from 1.250 x 10^3 to 2 x 10^4 cells/well for AC10 and HCF in a total volume of 100 µL/well, with cells being absent from the first lane (cell blank control). MTS assays were conducted over a 7-day period, with MTS assays conducted daily over this period from individual plates incubated in a humidified atmosphere of 5% CO_2. To each well to be evaluated, 20 µL of a 10x stock solution of MTS/PMS (2 mg/ml MTS, 0.092 mg/ml PMS, made fresh prior to addition) was added, with the plate reincubated for 4 hours at 37°C/5% CO_2. After incubation, the

absorbance of each well was determined at 490nm using a Thermoscientific Multiskan GO plate reader (Multiskan Go-Thermo Scientific®). Analysis of absorbance readings were conducted using Microsoft Excel; the mean absorbance of each treatment concentration was calculated, from which the mean absorbance of blank control was subtracted. All experiments were performed in triplicate (N) and standard error of mean (SEM) between replicate were calculated.

2.4.2 Evaluation of compound cytotoxicity by MTS assay

To determine the cytotoxicity of drugs and other compounds, MTS assays were conducted after various exposure periods. AC10 cells or HCFs were seeded at 5 x 10^3 cells per well of a 96-well plate in a total volume of 100 µL media. Cells were incubated in a humidified 5% CO_2 incubator to adhere overnight. For each plate, one column remained cell-free (media alone; blank), one column remained cells plus media (cell control), and one received cells and media in the presence of the compound vehicle (0.1% DMSO final or media, as required).

Cells were then treated for 24-96 hours with serial dilutions of test drug/compound, with each drug concentration replicated 8 times, therefore producing 8 intra-experimental replicates. The procedure outlined in section 2.4.1 was used for subsequent MTS analyses. Cell viability was expressed as a percentage relative to the vehicle control, with the mean and standard error of mean (SEM) calculated. All studies were repeated in triplicate. The half maximal inhibitory concentration (IC50) was calculated by combining the replicate values and using non-linear regression for curve fitting on GraphPad Prism (Version 10.4.0, GraphPad Software, Inc.). For comparison, un-paired t-test or One-way analysis of variance (ANOVA) test, and a post-hoc Dunnett's test were used to compare between IC_{50}. Statistically significant differences were defined as $P<0.05$.

2.5 Cellular impedance assay (xCELLigence system)

The xCELLigence Real Time Cell Analyzer (RTCA) (Agilent technologies, USA) system employs electronic sensors to measure impedance changes caused by cellular proliferation, cell morphology, and to monitor the drug response of cells in real time using a 16 well electrode plate (E-plate) (Figure 2.1) (187).

Cell index values are calculated using microelectrode sensors located in the base of the wells within the E-plate, which measure electrical impedance. The current flow between the

electrodes is impeded as cells attach to the base of the wells; with greater densities associated with cell division, growth, and adhesion increasing impedance measurements (Figure 2.2). Conversely, a lack of cells within the well removes this restriction to the current flow, completing the circuit between the electrodes. Consequently, increased cell death, decreased cell size and cell detachment are associated with a decrease in the impedance value. Changes in cellular impedance are defined as a parameter termed cell index (CI), which indicates the variation relative to a cell-free impedance value (188). The xCELLigence continuously collects data over time, allowing for real-time monitoring of cellular activities, and transforming them into graphical output for analysis and comparison (188). This allows the detection of cellular perturbations caused by tested drug/compound.

The xCELLigence RTCA software and experimental setup followed the manufacturer's instructions, as defined below.

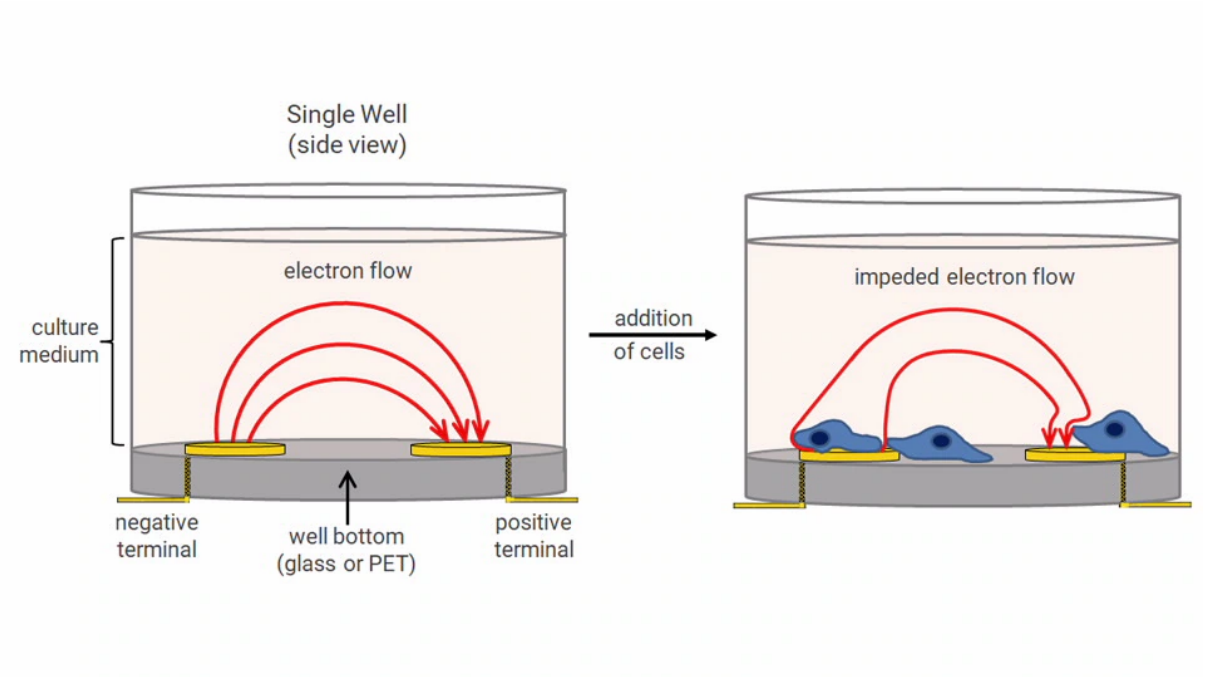

Figure 2.1 Principle of xCELLigence system. If there is only medium in the well, there is no restriction to the flow of current, completing the circuit between the electrodes (left). If there is increase in cell number or change in cellular morphology, the electrons flow will be impeded (right). Image cited from ACEA Biosciences Inc., Agilent (187).

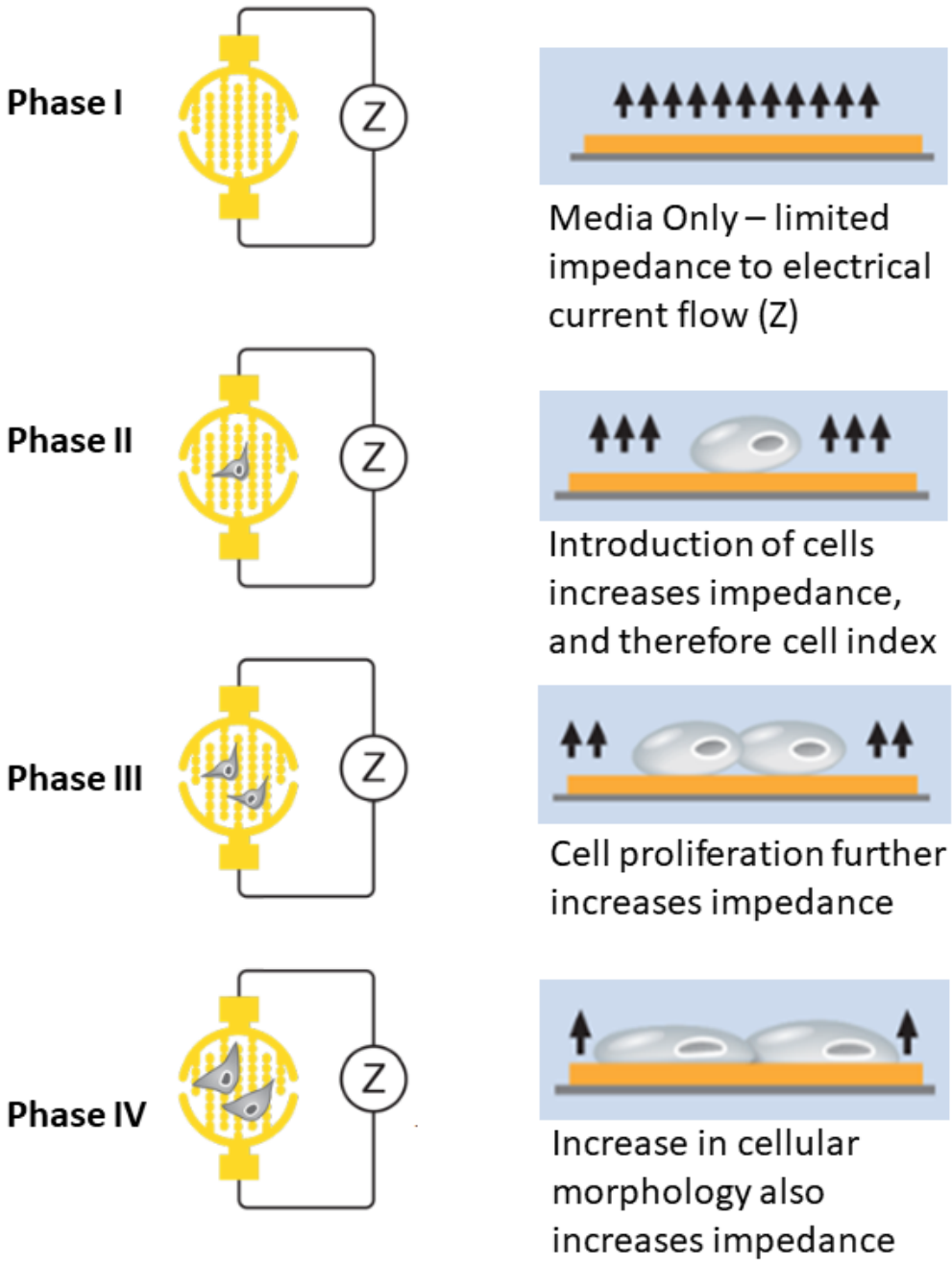

Figure 2.2 An overview of the principles of electrical impedance to detect changes in cellular adhesion, growth and morphology using the xCELLigence technologies. Image cited from ACEA Biosciences Inc., Agilent (187).

Following the manufacture's instruction, prior to cell seeding, 100µl medium was added to each well of a 16-well E-plate and allowed to equilibrate at room temperature for 30 mins. The plate was inserted into the xCELLigence system, housed within the incubator (37°C humidified, 5% CO_2) and the background reading measured. Cells were prepared, suspended in media and cell numbers calculated (see section 2.2). Cells suspension (100 µL) was added to the relevant wells, to a final well volume of 200 µL. On each plate a blank (no cells) well was included through addition of 100 µL of medium. The plate was left at room temperature within the laminar flow cabinet for 45 minutes to allow the cells to settle before re-inserting the plate into the xCELLigence system in the incubator and the experiment initiated. The RTCA system was instructed to record impedance readings at 15–60-minute intervals across the duration of the experiment, with results plotted as cell index values on the xCELLigence software. Following cell attachment (~24 hours), the media was changed, and drug treatments initiated, as appropriate. For AC10 experiments, to recapitulate effects upon adult cardiomyocytes, compounds were added once the plateau growth phase was achieved, approximately 48 hours post-seeding (for $1x10^4$ seeding density) as shown in Figure 2.3. In the case of HCF cells, which remain proliferative within cardiac tissue, compounds were added 24 hours after seeding. In all experiments, compounds were added to each well either in duplicate or quadruplicate wells per treatment, depending upon experimental aims and design. Cells were monitored in real-time throughout the duration of the experiments to observe the time and concentration effects of compound treatment.

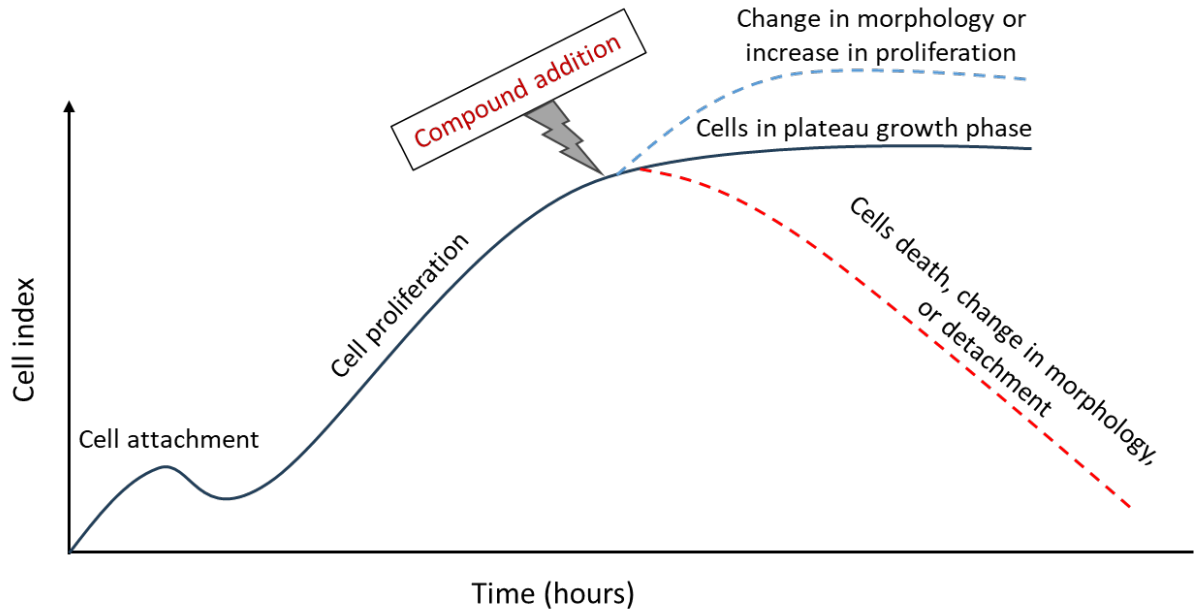

Figure 2.3 Different stages of cell development over time monitored by the xCELLigence RTCA system. The xCELLigence RTCA system records the change in cell index after cell seeding. Initially, cells are attached and settle in, then start to proliferate where cells divided and increase in number. When the cells reach maximum density, they enter the cell plateau phase. The dashed lines on the graph indicate changes in cell status. The red dashed line represents the decline in cell index indicates shrinking of cell size or cell death/detachment due to addition of specific compound. The increase in cell index represent by the blue dashed line indicates cell hypertrophy or increase in cell proliferation due to addition of specific compound.

Data analyses were conducted using the xCELLigence software system, with raw impedance values extracted and transferred to Microsoft excel for analysis. The cell index was normalised to the point of compound addition and the mean normalised cell index values of each treatment condition calculated.

All experiments were performed in triplicate (N) and SEM between replicate were calculated. GraphPad Prism software was used to present data and for statistical analysis (Version 10.4.0, GraphPad Software, Inc.). For comparison, un-paired t-test or One-way analysis of variance (ANOVA) test, and a post-hoc Dunnett's test was used when required. Statistically significant differences were defined as $P<0.05$.

2.6 Assessment of changes in cell morphology using CellMask™ Actin Tracking Stains

Changes in cell morphology were determined fluorescently using green actin tracking staining, following the manufacture's instruction. CellMask™ Actin Tracking Stain (Invitrogen) is a fluorescent dye designed specifically for labelling and visualizing filamentous actin (F-actin) in live or fixed cells, providing clear and detailed visualization of the actin cytoskeleton and its essential roles in maintaining cell shape.

AC10 and HCF cells were seeded into 6-well plate at a density of $2x10^4$ cells/well and the compound added, as per specific experiment conditions and requirements. To prepare cells for staining, cell culture media was removed, cells were washed twice with phosphate-buffered saline (PBS), and the cells fixed in 4% paraformaldehyde (PFA) for 20 minutes at room temperature. After fixation, cells were incubated in 0.1% Triton X-100 (Merk) (v/v in PBS) for 3x5 minutes at room temperature to permeabilize cells for stain entry**.** A stock solution (1000x) of CellMask™ Actin Tracking Stains was prepared by reconstitution of the dye in DMSO, to a final concentration of 1mM. The working solution of the dye was obtained by dilution in PBS, to a final concentration of 1µM. Cell staining was then achieved through addition of 1mL of the dye solution per well and incubation for 15 minutes at room temperature, followed by removal of excess dye by washing 3x5 min in PBS.

Micrograph images were collected by fluorescent microscopy at a magnification of 20x (NikonTE2000 microscope). The surface area of a minimum of 10 cells in 5 random fields per well were determined using ImageJ software (Fiji, Image J 1.52, National Institutes of Health, USA), with the boundary of each individual cell outlined and the cross-sectional area thereafter calculated (μm^2). Using Microsoft excel, the calculated means of each condition were then normalised to vehicle control. All experiments were performed in triplicate (N) and

SEM between replicate were calculated. GraphPad Prism software used to present data and statistical analysis (Version 10.4.0, GraphPad Software, Inc.). For comparison, un-paired t-test or One-way analysis of variance (ANOVA) test, and a post-hoc Dunnett's test was used when required. Statistically significant differences were defined as $P<0.05$.

2.7 Assessment of cellular expression of AT1R using Real-time quantitative polymerase chain reaction (RT-qPCR)

2.7.1 RNA extraction for gene expression analysis

Cells were seeded into 6-well plate at a density of $3x10^5$ cells/well for AC10 $7x10^4$ cells/well for HCF and the compound added, as per specific experiment conditions and requirements. Total RNA was extracted according to the manufacture procedure using RNeasy Mini Kit Qiagen®. Briefly, cells were trypsinized and collected as a cell pellet, as per section 2.1. Then, cells were lysed in Buffer RLT, the lysate transferred to QIAshredder spin column for homogenization and the lysate collected. Ethanol (70%) was added to the lysate and the mixture transferred to a RNeasy spin column and centrifuged, with the flow-through discarded. The column was washed with buffers RW1 and RPE, with subsequent centrifugations, and the RNA finally eluted from the column using RNase-free water. The quality and the quantity of RNA were measured using Nanodrop Spectrophotometer ND-1000 (Nanodrop Technologies), with an 260nm/280nm ratio >2 being considered acceptable for future analyses. Samples were stored at -80°C.

2.7.2 Reverse transcription to cDNA for gene expression analysis

Total RNA (500 ng) was reverse transcribed to cDNA using a High-Capacity cDNA Reverse Transcription kit (Applied Biosystems™), according to the manufacture procedure. Briefly, the 20µl reaction mix was prepared according to (Table 2.1). Samples were incubated under the following conditions using a thermocycler (Applied Biosystem): 25°C for 10 minutes, 37°C for 120 minutes, and 85°C for 5 seconds followed by a 4°C hold. cDNA was 10-fold diluted using Nuclease free H_20 for future experiments in the RT-qPCR and stored at -20°C.

Table 2.1 Master mix preparation

Reagent	Volume per sample (µL)
10X RT buffer	2.0
100mM dNTP	0.8
10X Random Hexamers	2.0
50U/µl Reverse Transcriptase	1.0
500ng total RNA	X µl
Nuclease free H_20	To a final reaction volume of 20µl

2.7.3 Real-time quantitative polymerase chain reaction (RT-qPCR)

SYBR Green was used for RT-qPCR amplifications. Each 10µl reaction contained 9µl of gene master mix (0.4µl of forward and reverse primers, 5µl of SYBR Green and 3.6µl Nuclease free H_20) and 1µl of cDNA. No template controls (NTC) were also included for each primer in duplicate, to confirm a lack of genetic DNA contamination. All reactions were run in triplicate intraexperimentally within a 384-well plate. The plate was centrifuged at 1000g for 20 seconds before being inserted into QuantStudioTM 12K Flex Real-time PCR System (Thermo Fisher Scientific). The following amplification program were used in all RT-qPCR reactions: 50°C for 2 min, 95°C for 10 mins, 40 cycles of 95°C for 15 seconds, and 60°C for 1 minute. For full SYBR gene expression quantification analysis, all experiments were performed in triplicate (N) and SEM between replicates were calculated.

Fluorescence was acquired at the end of each cycle, with post-amplification melting curves determined for each sample by incrementally increasing the temperature from 55-95°C to confirm a single amplicon had been generated for each qRT-PCR reaction and to detect potential impurities and primer-dimers. In addition, standard curves for control were also generated to assess the primer efficiency and stability. 5x dilution series of cDNA template was performed for each target gene including AT1R, ribosomal protein L13a (RPL13A), hypoxanthine-guanine phosphoribosyl transferase 1 (HPRT1), and Beta-actin (β-actin). AT1R, RPL13A, HPRT1, and β-actin. The dose-response curve, based on the mean threshold cycles (Ct) values was generated to allow determination of the detected limit for each gene.

The Ct values and standard deviations for evaluated genes were calculated by QuantStudio 7 software. Relative gene expressions were calculated in which AT1R normalised to stable express gene β-actin (ΔΔCt), then the fold changes of these normalised coefficient Ct values relative to control ($2^{\Delta\Delta ct}$) were calculated. Normalised results were expressed in terms of 'fold change', relative to the experimental control which represented the baseline condition of no treatment or control cell conditions.

GraphPad Prism software used to present data and statistical analysis (Version 10.4.0, GraphPad Software, Inc.). For comparison, un-paired t-test or One-way analysis of variance (ANOVA) test, and a post-hoc Dunnett's test was used when required. Statistically significant differences were defined as $P<0.05$.

Chapter 3. Assessment of the Impact of Angiotensin II and Doxorubicin on Morphology of Cardiac Cells *In Vitro*

3.1 Anthracycline induced cardiotoxicity

Despite clear and evidenced efficacy of anthracyclines against several cancer types, the clinical use of anthracyclines is associated with cardiovascular complications, which often occur several months/years after initial exposure (189). Consequently, the therapeutic success of anthracyclines and improvement of cancer prognosis are tempered by delayed cardiotoxicity. The incidence of cardiovascular morbidity has been reported to range between 4% and 36% and it remains a leading cause of non-cancer-related mortality among breast cancer survivors (190, 191). The incidence of this delayed-cardiotoxicity in adult patients treated with low-cumulative dose anthracycline is reported to be as high as 16.5% of patients when evaluated within 4-5 years of completion of anthracycline therapy (192). Furthermore, the incidence of heart failure after anthracycline therapy has been shown to increase significantly in adult patients receiving higher cumulative doses of anthracycline (8, 20). For example, the incidence of anthracycline cardiotoxicity rises from approximately 5% at a dose of 400 mg/m² to 48% at a dose of 700 mg/m² doxorubicin (20). Importantly, cardiotoxicity is also observed at lower cumulative doses, previously thought unlikely to initiate heart failure, with 150 mg/m² and 300 mg/m² doxorubicin linked to development of progressive heart failure in 0.2% and 1.6% of patients, respectively (20). Therefore, studies are needed to understand the mechanisms of underlying AIC, identify patient-specific risk factors and treatment strategies aiming to improve long-term outcomes and quality of life for cancer survivors.

The mechanisms of anthracycline cardiotoxicity are multifactorial, with several potential mechanisms proposed for effects in cardiomyocytes and CFs (see section 1.4). These changes contribute to an asymptomatic decline in LVEF which chronically progresses to functional cardiotoxicity, including cardiomyopathy and heart failure (193, 194). From the cellular perspective, cardiomyocytes are affected directly by the toxic effect of anthracycline, as exemplified by changes in contractility and cardiac structure (33, 85). CFs, which constitute a large proportion of the cardiac myocardium and play a central role in maintaining structural integrity and physiological functions of the heart are also believed to be involved, especially as they contribute to tissue remodelling and fibrosis/scarring resulting from a progression of

cardiac damage (195-197). This latter effect feeding into heart failure through promotion of stiffness of myocardium resulting in an inability of the heart to contract (198, 199).

A further important relationship also exists between cardiomyocytes and CFs through paracrine signalling and provision of mechanical signals to maintain cardiac functions (200). Cardiomyocytes are known to be affected by factors secreted by CFs, that affect the cardiomyocyte to promote responses such as cellular hypertrophy, programmed cell death and cellular senescence (201). Such responses may also be present with respect to the cardiac effects of anthracyclines, wherein normal physiological are disrupted and cellular crosstalk becomes dysfunctional by the toxic effects of anthracycline directly and indirectly, thus leading to development of cardiac dysfunction (202). Consequently, understanding the crosstalk between CFs and cardiomyocytes is important to understand the mechanism of developing AIC. However, there are limited studies on the role of CFs in developing AIC compared to cardiomyocytes (198).

3.1.1 Perturbation of angiotensin signalling in AIC

Many mechanisms of AIC have been proposed in the literature. However, there is still a deficit in understanding the relationship of short-term acute drug exposure to delayed and late-onset cardiac failure. One potential mechanism is anthracycline-induced cardiac remodelling, involving interaction with the angiotensin-signalling pathway (see section 1.7) and cellular communication between different cellular populations of the heart. This is based on the fact that clinical presentation of AIC is noted as being similar to that observed with other cardiac conditions, such as cardiac hypertrophy and heart failure, and the fact that administration of therapeutics targeting the RAAS pathway, ACEi and ARB, exhibits good efficacy in mitigation of AIC (see section 1.8.3.1) (8, 27, 34, 153). Several proposed hypotheses to explain the clinical cardioprotective effects of ACEi and ARB, ranging reduced afterload, decreased systolic ventricular wall stress and fibrosis (153, 154, 173). Despite these systemic effects, there is also believed to be a direct effect of anthracyclines upon the cellular architecture of cardiac tissue, factors not accounted for in the systemic clinical haemodynamic effects of ACEi and ARB (171, 172). Furthermore, the role of CFs alongside cardiomyocytes in the cardiotoxic response involving potentially angiotensin-signalling is also not yet addressed.

Doxorubicin induces oxidative stress, mitochondrial dysfunction and persistent DNA damage within cardiomyocytes (11, 12). Therefore, a physiological response to anthracycline exposure is postulated to be activation of angiotensin signalling and increased production of

angiotensin II, causing cardiomyocyte hypertrophy (34). From the perspective of CFs, it is known that these become activated and transformed to myofibroblast in response to oxidative stress and inflammatory activation through secretion of TGF-β and other pro-inflammatory cytokines such as IL-6, characterised by expression of α-SMA (93, 203, 204). In addition, activation of RAAS within cardiomyocytes contributes, as angiotensin II also induces the differentiation of CFs to myofibroblast (205, 206). Subsequently, these complex processes of cardiac cell damage and interplay between these two cell types involving activation of RAAS is theorised to worsen cardiac dysfunction and cardiac remodelling, with cardiac tissue deteriorating structurally and functionally, leading to irreversible heart failure (207). Therefore, studies are needed to assess the direct effect of anthracycline on cardiac cells and understand how activation of RAAS, particularly angiotensin II, might influence the cardiac response to anthracycline to elucidate the mechanism of AIC.

3.1.2 Aim and objectives

Aim: Evaluation of response of in vitro cardiac cells, particularly human AC10 cardiomyocyte cell line and HCFs, to clinically relevant exposure of doxorubicin and physiologically relevant concentrations of angiotensin II.

- Evaluation of the growth kinetics of AC10 and HCF using manual counting, MTS assay, and by cell impedance assay using xCELLigence RTCA system.
- Assessment of the sensitivity to AC10 and HCF to clinically relevant concentrations of doxorubicin.
- Evaluation of the sensitivity of AC10 and HCF to physiologically relevant concentrations of angiotensin II.
- Evaluation of time-course and concentration-response relationship of doxorubicin induced hypertrophy in AC10 and HCF using xCELLigence system and fluorescence staining.
- Assessment of morphological changes of AC10 and HCF after exposure to physiologically relevant concentration of angiotensin II using xCELLigence system and fluorescence staining.
- Assessment of the sensitivity of AC10 and HCF to clinically relevant concentrations of doxorubicin in combination with angiotensin II.
- Assessment of the hypertrophic effects of doxorubicin in AC10 and HCF, both independently and in combination with angiotensin II, using xCELLigence system and fluorescence staining.

3.2 Method

3.2.1 Assessment of growth kinetics of AC10 and HCF measured using manual cell counting

The growth curves for both the AC10 and the HCF cells were assessed by monitoring the cell number over time. Cells were seeded at $1x10^5$ cells per T25 flask and the number of cells in a flask determined every 48 hours, as per section 2.2. The cell numbers were used to construct a growth curve, from which cell doubling times were determined.

3.2.2 Optimisation of cell seeding densities of AC10 and HCF for MTS assay experiments

In order to identify the best seeding densities for future cell viability experiments for both AC10 and HCF, cells were seeded into 96-well plates at different seeding densities ($1.25x10^3$-$2x10^4$ cells/well) and allowed to adhere to the plate overnight. Viability was assessed for 24-, 48-, 72-, 96-, and 120 hours by MTS assay, as previously described (section 2.4). These data were utilised to identify cell growth doubling times.

3.2.3 Optimisation of cell seeding densities of AC10 and HCF for xCELLigence experiments

The growth curves for both the AC10 and the HCF cells were assessed in xCELLigence RTCA to identify the best seeding densities for future experiments. Cells were seeded into 16-well E-plate in different seeding densities (AC10: $1.25x10^3$-$2x10^4$ cells/well; HCF: $1.25x10^3$-$2x10^4$ cells/well). The growth of cells was monitored in xCELLigence, as per section 2.5, with media changed every 48 hrs. The growth curves were subsequently utilised to calculate cell doubling times.

3.2.4 Assessment of cell sensitivity of AC10 and HCF to angiotensin II

AC10 and HCF were seeded into four 96-wells plates at a density of $5x10^3$ cells/well and viability assessed following exposure to angiotensin II for 24-, 48-, 72-, and 96-hours using MTS assay, as previously described (section 2.4).

On Day 0, cells were seeded and allowed to adhere to the plate overnight, on Day 1, exposed to subsequent physiological-relevant concentrations of angiotensin II (200-600pM) exposure repeated every 24 hrs to mimic the physiological condition (208). The experimental

endpoint (cellular viability) measured after the incubation period. All studies were repeated a minimum of three times.

3.2.5 Assessment of cell survival following exposure to doxorubicin in AC10 and HCF

Cell viability of AC10 and HCF was assessed following exposure to doxorubicin for 24-, 48-, 72-, and 96-hours using MTS assay, as previously described (section 2.4).

On Day 0, cells were seeded into 96-wells plates at a density of $5x10^3$ cells/well and allowed to adhere to the plate overnight, on Day 1, treated with doxorubicin or vehicle control (DMSO) and the experimental endpoint (cellular viability) measured after the incubation period to generate an IC_{50} value. Final concentrations of doxorubicin ranged from 15.6nM to 2µM. This dose range was selected to include the clinically reported C_{max} for doxorubicin in the clinic (approximately 1.1 µM), thereby ensuring that the in vitro model reflects clinically relevant exposures (209). On day 2, 24h after drug exposure, doxorubicin exposure was ceased, with the media in wells replaced with media containing drug vehicle alone. In all cases the maximal exposure to DMSO did not exceed 0.1%. All studies were repeated a minimum of three times.

3.2.6 Assessment of cells survival following exposure to different concentrations of doxorubicin in the presence of angiotensin II in AC10 and HCF

AC10 and HCF cells were seeded into 96-well plates at a density of $4x10^3$ cells/well and viability assessed following exposure to doxorubicin in the presence of 500pM angiotensin II using the MTS assay, as previously described (section 2.4).

On Day 0, cells were seeded and allowed to adhere to the plate overnight, on day 1, the top half of the plate (rows A-D) treated with doxorubicin in the absence of angiotensin II (instead adding drug vehicle, DMSO) and the bottom half of the plate (E-H) was treated with doxorubicin in the presence of 500pM angiotensin II. In relation to doxorubicin, final concentrations ranged from 15.6nM to 2µM. On day 1, 24h after drug exposure, doxorubicin exposure was ceased, with the media in rows A-D replaced with media alone and media in rows E-H replaced with media containing 500pM angiotensin II. The experimental endpoint (cellular viability) was measured after 24-, 48-, 72-, and 96-hours to generate IC_{50} values. In all cases the maximal exposure to DMSO did not exceed 0.1%. All studies were repeated a minimum of three times and IC50 values determined from three replicates.

3.2.7 Assessment of changes in cell morphology following exposure to angiotensin II in AC10 and HCF, determined by xCELLigence RTCA

In order to evaluate the cell morphology changes of AC10 and HCF following exposure to angiotensin II, AC10 and HCF cells were seeded at a density of (AC10: $1x10^4$ cells/well, HCF: $5x10^3$ cells/well) into a 16-well E-Plate of the xCELLigence RTCA system, as previously described (section 2.5). For AC10, cells were then maintained for up to a 48h period, until the plateau growth phase was reached then were exposed to 300pM angiotensin II. For HCF, after 24 hours of seeding, cells were exposed to 300pM angiotensin II. The effect of angiotensin II on morphology of AC10 and HCF was assessed non-invasively in real-time for a further 48 hours after the initial angiotensin II exposure.

3.2.8 Evaluation of changes in cell morphology following exposure to angiotensin II in AC10 and HCF, determined by measurement of cell size

AC10 and HCF cells were seeded at a density of $2x10^4$ cells per well into a 6-well flat-bottomed cell culture plate and allowed to adhere overnight. Cells were then exposed to 300pM angiotensin II. The effect of angiotensin II on the morphology of AC10 and HCF cells was assessed 48 hours after the initial angiotensin II exposure. Cells were exposed to 1X of CellMask™ Actin Tracking Stains solution for a period of 15 minutes (section 2.6). Micrograph images were collected by fluorescent microscopy at a magnification of 20x (NikonTE2000 microscope). The surface area of a minimum of 100 cells in 5 random fields per well were determined using ImageJ software.

3.2.9 Assessment of changes in cell morphology following exposure to different concentrations of doxorubicin in AC10 and HCF, determined by xCELLigence RTCA

In order to evaluate the cell morphology changes of AC10 and HCF following exposure to doxorubicin, AC10 and HCF cells were seeded at a density of (AC10: $1x10^4$ cells/well, HCF: $5x10^3$ cells/well) into a 16-well E-Plate of the xCELLigence RTCA system, as previously described (section 2.5). For AC10, cells were then maintained for up to a 48h period, until the plateau growth phase was reached then were exposed to 50-500nM doxorubicin or to drug vehicle (DMSO). For HCF, after 24 hours of seeding, cells were exposed to 50-500nM doxorubicin or to drug vehicle (DMSO). After a 24h period, media was replaced with media in

the absence of doxorubicin. The effect of doxorubicin on morphology of AC10 and HCF was assessed non-invasively in real-time for a further 48 h after the initial doxorubicin exposure.

3.2.10 Assessment of changes in cell morphology following exposure to angiotensin II and sub-toxic concentration of doxorubicin in AC10 and HCF, determined by xCELLigence RTCA

AC10 and HCF cells were seeded at a density of (AC10: $1x10^4$ cells/well, HCF: $5x10^3$ cells/well) into a 16-well E-Plate of the xCELLigence RTCA system, as previously described (section 2.5). For AC10, cells were then maintained for up to a 48h period, until the plateau growth phase was reached then were exposed to 50nM doxorubicin presence or absence of 300pM angiotensin II or drug vehicle (DMSO). For HCF, after 24 hours of seeding, cells were exposed to 50nM doxorubicin presence or absence of 300pM angiotensin II or drug vehicle (DMSO). After a 24h period, media was replaced with that containing media in the absence of doxorubicin or replaced with 300pM angiotensin II for respective wells. The effect of doxorubicin on morphology of AC10 and HCF in presence and absence of angiotensin II was assessed non-invasively in real-time for a further 48 h after the initial doxorubicin exposure.

3.2.11 Assessment of changes in cell morphology following exposure to angiotensin II and sub-toxic concentration of doxorubicin in AC10 and HCF, determined by measurement of cell size

The cell morphology changes were evaluated in AC10 and HCF following exposure to doxorubicin in presence and absence of angiotensin II. AC10 and HCF cells were seeded at a density of $2x10^4$ cells per well into a 6-well flat-bottomed cell culture plate and allowed to adhere overnight. Cells were then exposed to 50nM doxorubicin presence or absence of 300pM angiotensin II or drug vehicle (DMSO). After a 24h period, media was replaced with media in the absence of doxorubicin for doxorubicin alone well and replaced with 300pM angiotensin II for doxorubicin in combination with angiotensin II wells. The effect of 50nM doxorubicin presence or absence of 300pM angiotensin II on the morphology of AC10 and HCF cells was assessed 48 hours after the initial doxorubicin exposure. Cells were exposed by CellMask™ Actin Tracking Stain (section 2.6). The surface area of a minimum of 100 cells in 5 random fields per well were determined using ImageJ software.

3.3 Results

3.3.1 Growth kinetics of AC10 and HCF cells measured using manual counting

The normal growth pattern (lag, exponential, plateau phases) of AC10 and HCF cells assessed using manual counting, as shown in Figure 3.1. The exponential doubling time of AC10 and HCF was determined as 27.7±1.7 and 46.6±3.8 hours, respectively.

3.3.2 Validation of MTS assay for determination of cell growth of AC10 and HCF cells

Before starting the experiments using the MTS assay, defining the appropriate cell seeding density in the 96 well plate was an important prerequisite. AC10 and HCF were seeded in different densities in 96-well plate starting from $2X10^4$ cells/well ($6.2x10^4$ cells/cm^2). An MTS assay was performed from day 1-5 the absorbance vs time readings were identified each day (Figure 3.2). The exponential doubling time of AC10 and HCF was determined as 31±7 and 66.5±22.8 hours, respectively. A seeding density of $5x10^3$ cells/well was selected to be optimal for MTS assay in both AC10 and HCF cells.

3.3.3 Validation of xCELLigence for determination of cell growth of AC10 and HCF cells

Defining the appropriate cell seeding density in the 16-well E-plate was an important prerequisite before starting experiments using the xCELLigence system. AC10 cells were seeded in different densities in the 16-well E-plate starting from $2×10^4$ cell/well ($1.02×10^4$ cells/cm^2). The exponential doubling time of AC10 was determined as 34.4±9 hours. To achieve a plateau-phase growth state in AC10 cells, a seeding density of $1x10^4$ cells/well was selected as optimal for xCELLigence assays and compounds were subsequently added 48 hours post-seeding.

For HCF, cells were seeded starting from $2×10^4$ cell/well ($1.02×10^4$ cells/cm^2). The exponential doubling time of HCF was determined as 69±14.2 hours (Figure 3.3). In the case of HCF cells, which remain proliferative within cardiac tissue, $5x10^3$ have been chosen as the best seeding density in xCELLigence and compounds were added 24 hours after seeding.

3.3.4 Comparison of growth kinetics using manual counting, MTS assay, and xCELLigence RTCA

The doubling time of AC10 and HCF were determined using different methodologies to show cells growth rate (Table 3.1). There is agreement in doubling times between different methodology with AC10 showing of 27.7±1.7, 31±7, and 34.4±9 hours using manual cell count, MTS assay, and xCELLigence RTCA, respectively. The doubling time using manual cell count in HCF appears slightly lower than other methods, with HCF showing 46.6±3.8, 66.5±22.8, and 69±14.2 hours using manual cell count, MTS assay, and xCELLigence RTCA, respectively.

One parameter that was different between the methodologies was however the standardisation of seeding densities between the methodologies. To address this, growth kinetics of cells comparatively at an initial density of 4000 cells/cm² was thus appraised (Table 3.2). As reported above, the doubling time in AC10 remains consistent across different methodologies (27.7 vs 31.7 vs 26.2 hours). However, for HCF a slow growth rate is observed MTS assay and xCELLigence methods compares to manual counting method (46.6 vs 70 vs 76 hours).

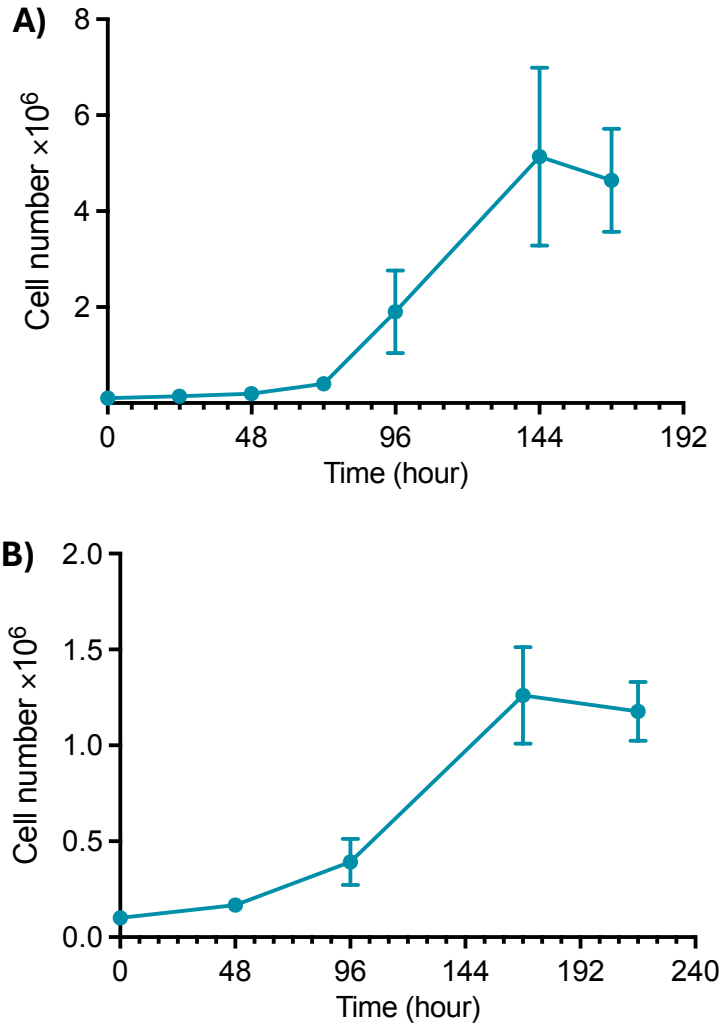

Figure 3.1 Evaluation of the normal growth pattern of AC10 and HCF cells. Manual counting of cells over time. A) Growth characteristics of AC10, doubling time: 27.7±1.7 hours. B) Growth characteristics of HCF, doubling time: 46.6±3.8 hours. Each growth curve was independently repeated three times.

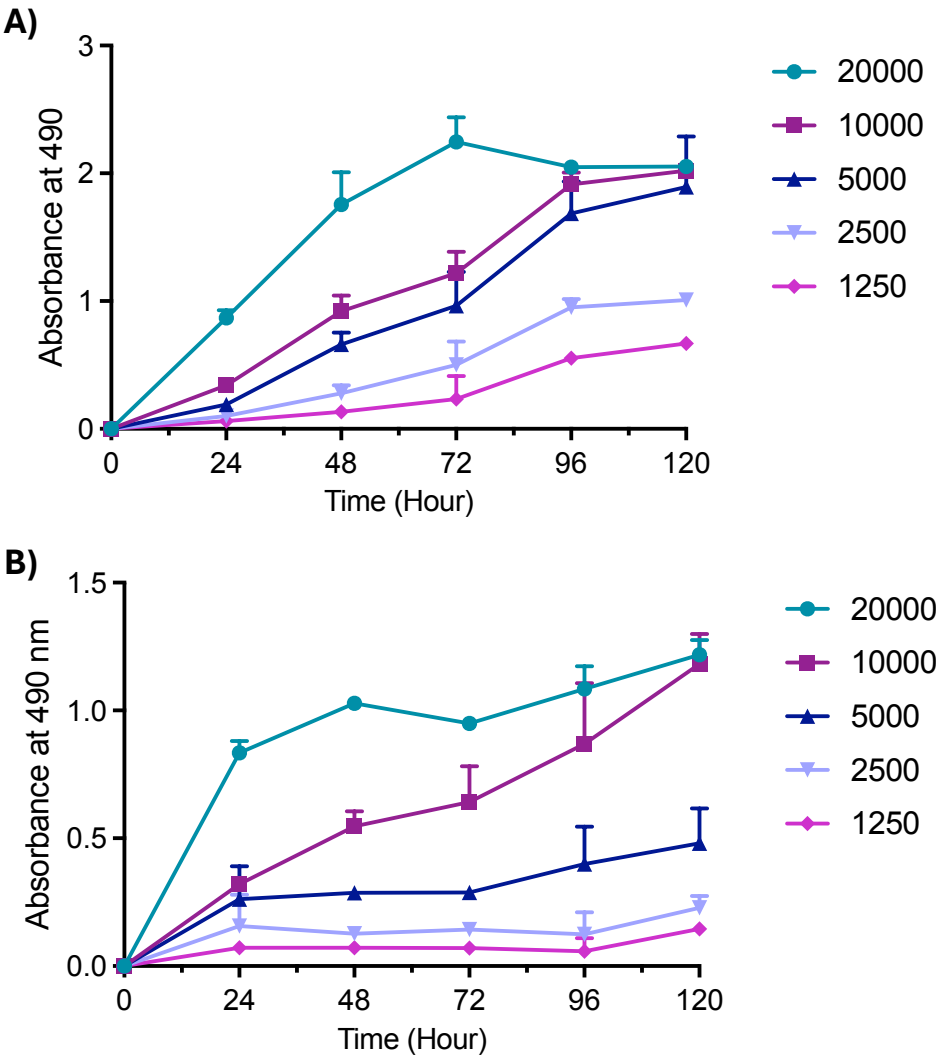

Figure 3.2 Optimization of cell seeding density of AC10 and HCF using an MTS assay. Cells were seeded in different densities and incubated for 5 days. The absorbance at 490 nm of different cell densities was measured every 24 hours. A) AC10, doubling time: 31±7 hours. B) HCF, doubling time: 66.5±22.8 hours.

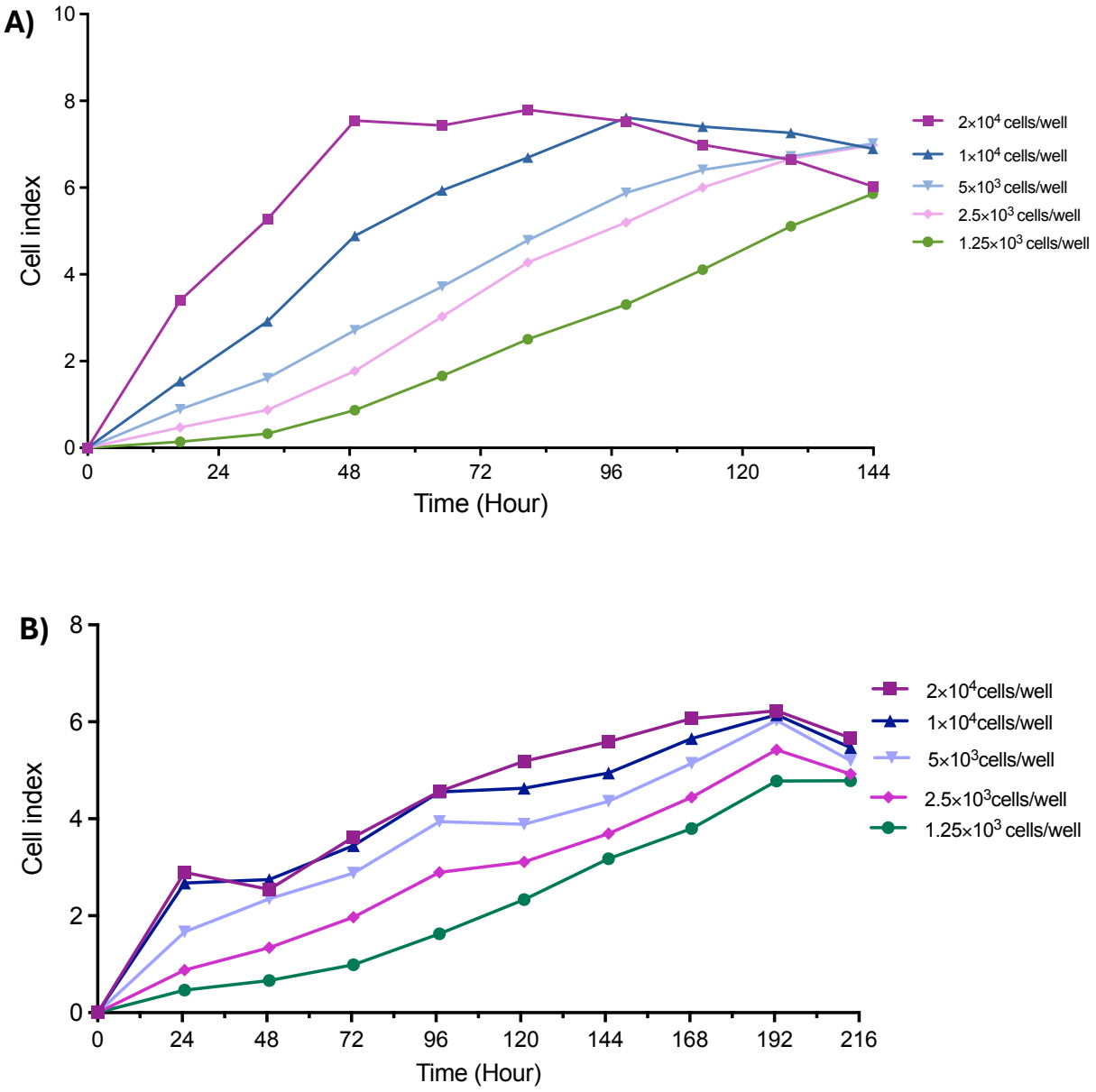

Figure 3.3 Evaluation of the normal growth pattern of AC10 and HCF cells determined by cellular impedance using xCELLigence. Growth curves in xCELLigence show the cell index over time. A) AC10, doubling time: 34.4±9 hours. B) HCF, doubling time: 69±14.2 hours.

Table 3.1 Doubling time by different methodologies.

Cell line	Methodology	Initial seeding density (Cells/cm^2)	Doubling time (Mean ± SEM, hours)
AC10	Haemocytometer manual cell count	4×10^3 cells/cm^2	27.7±1.7
	MTS assay	(3.9–62.5) $\times10^3$ cells/cm^2	31±7
	xCELLigence instrument	(0.64–10.2) $\times10^3$ cells/cm^2	34.4±9
HCF	Haemocytometer manual cell count	4×10^3 cells/cm^2	46.6±3.8
	MTS assay	(3.9–62.5) $\times10^3$ cells/cm^2	66.5±22.8
	xCELLigence instrument	(0.64–10.2) $\times10^3$ cells/cm^2	69±14.2

Table 3.2 Doubling time by different methodologies at initial seeding density 4×10^3 cells/cm^2.

Cell line	Methodology	Initial seeding density (Cells/cm^2)	Doubling time (hour)
AC10	Haemocytometer manual cell count	4×10^3 cells/cm^2	27.7
	MTS assay	4×10^3 cells/cm^2	31.7
	xCELLigence instrument	4×10^3 cells/cm^2	26.2
HCF	Haemocytometer manual cell count	4×10^3 cells/cm^2	46.6
	MTS assay	4×10^3 cells/cm^2	70
	xCELLigence instrument	4×10^3 cells/cm^2	76

3.3.5 Cytotoxic response of AC10 and HCF to doxorubicin

To assess the cytotoxic response of AC10 and HCF to doxorubicin, the viability assessed following exposure to doxorubicin, with concentrations ranging from 15.6nM to 2μM for a 24, 48, 72- and 96-hours continuous period using the MTS assay.

Both AC10 and HCF showed a concentration and time-dependent response to doxorubicin, with cell viability decreasing over time (Figure 3.4 and Figure 3.5). The IC_{50} values were determined as 0.34±0.09, 0.17±0.06, and 0.06±0.01 with AC10 and 1.001±0.12, 0.47±0.06, and 0.27±0.02 for HCF, after 48-, 72-, and 96-hour exposure, respectively (Table 3.3 and Table 3.4).

3.3.6 Exposure to physiological concentration of angiotensin II has no effect the cellular viability of AC10 or HCF

Cell viability of AC10 and HCF after exposure to different physiological range of angiotensin II was evaluated by MTS assay. Angiotensin II from 200 to 600pM has no significant reduction in viability relative to control and angiotensin II within this physiological range has no significant cytotoxic effect over different time points against either AC10 (Figure 3.6) or HCF cells (Figure 3.7).

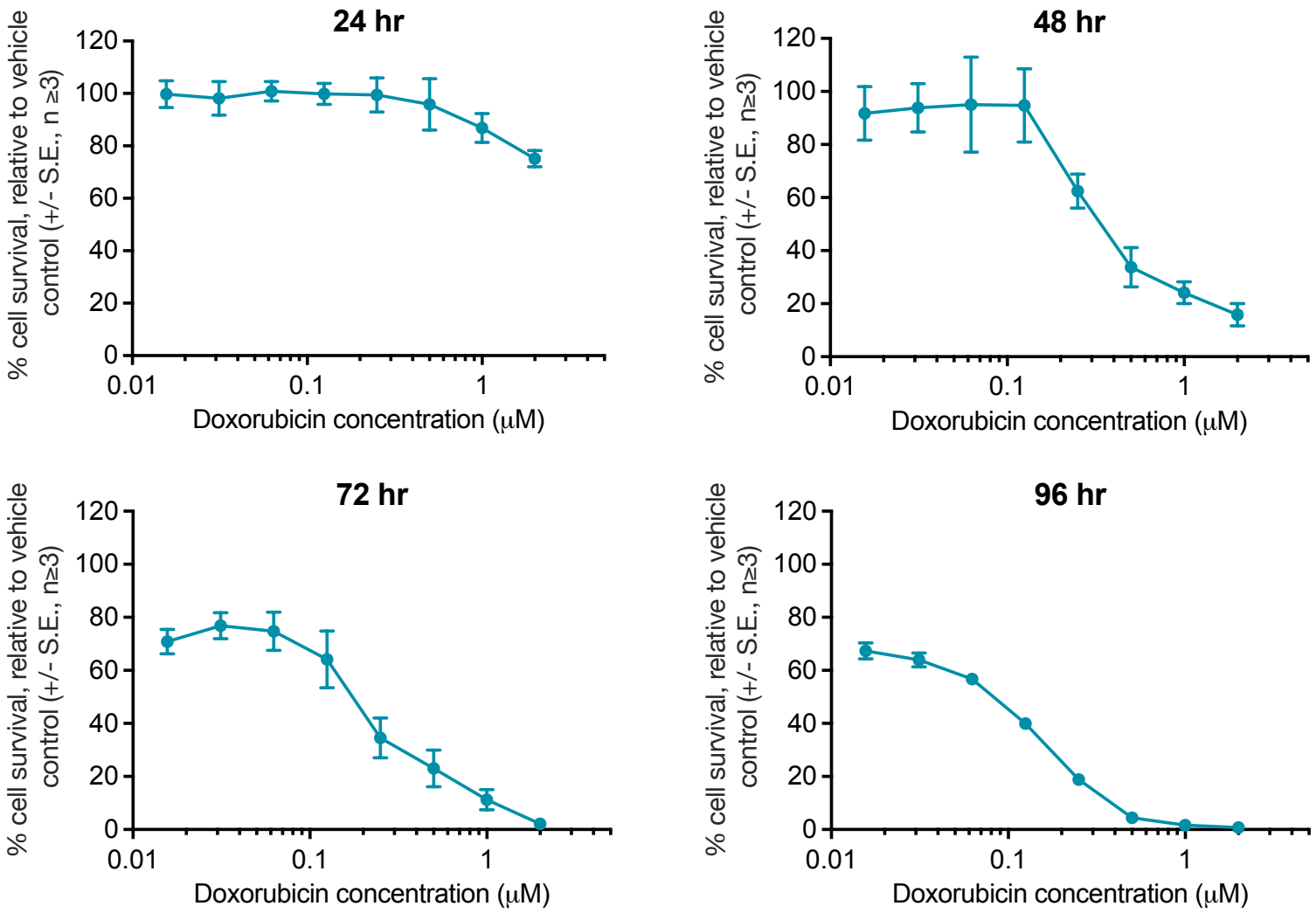

Figure 3.4 Dose response curve of AC10 following expose to different concentrations of doxorubicin expressed as a % of the mean normalised to control. AC10 exposed to different concentrations of doxorubicin ranging from 15.6nM to 2μM for a 24-,48-, 72- and 96-hours continuous period and cell viability assessed using the MTS assay. Data is representative of at least three repeats ±SEM.

Table 3.3 Exposure duration IC_{50} of doxorubicin against human AC10 cardiomyocyte. Data is determined from MTS data and is representative of at least three repeats and presented as IC_{50} ±SEM.

	Cytotoxicity IC_{50} (μM)			
	24 hr	**48 hr**	**72 hr**	**96 hr**
Doxorubicin	>2	0.34±0.09	0.17±0.06	0.06±0.01

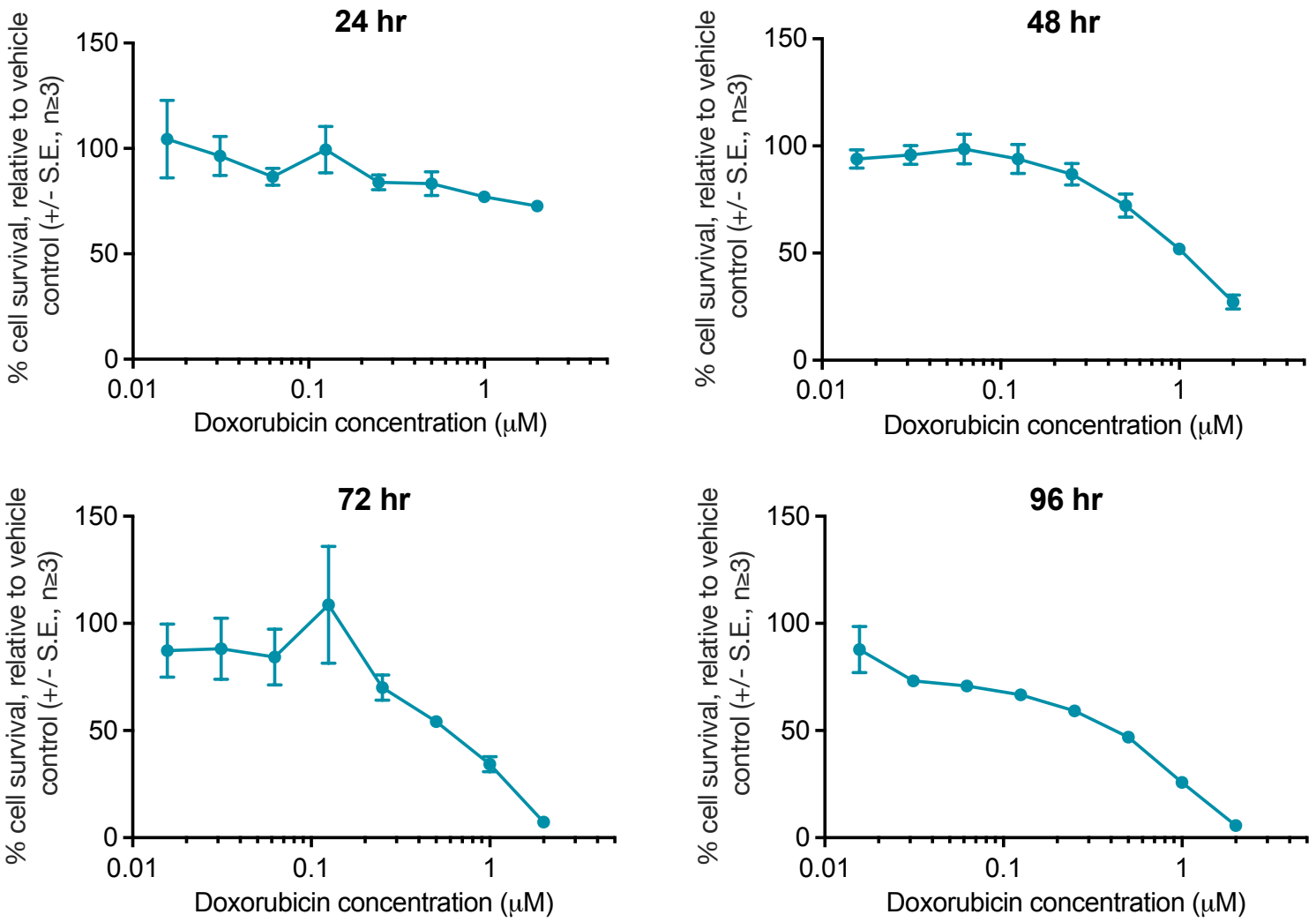

Figure 3.5 Dose response curve of HCF following expose to different concentrations of doxorubicin expressed as a % of the mean normalised to control. HCF exposed to different concentrations of doxorubicin ranging from 15.6nM to 2μM for a 24-,48-, 72- and 96-hours continuous period and cell viability assessed using the MTS assay. Data is representative of at least three repeats ±SEM.

Table 3.4 Exposure duration IC_{50} of doxorubicin against HCFs. Data is determined from MTS data and is representative of at least three repeats and presented as IC_{50} ±SEM.

	Cytotoxicity IC_{50} (μM)			
	24 hr	**48 hr**	**72 hr**	**96 hr**
Doxorubicin	>2	1.001±0.12	0.47±0.06	0.27±0.02

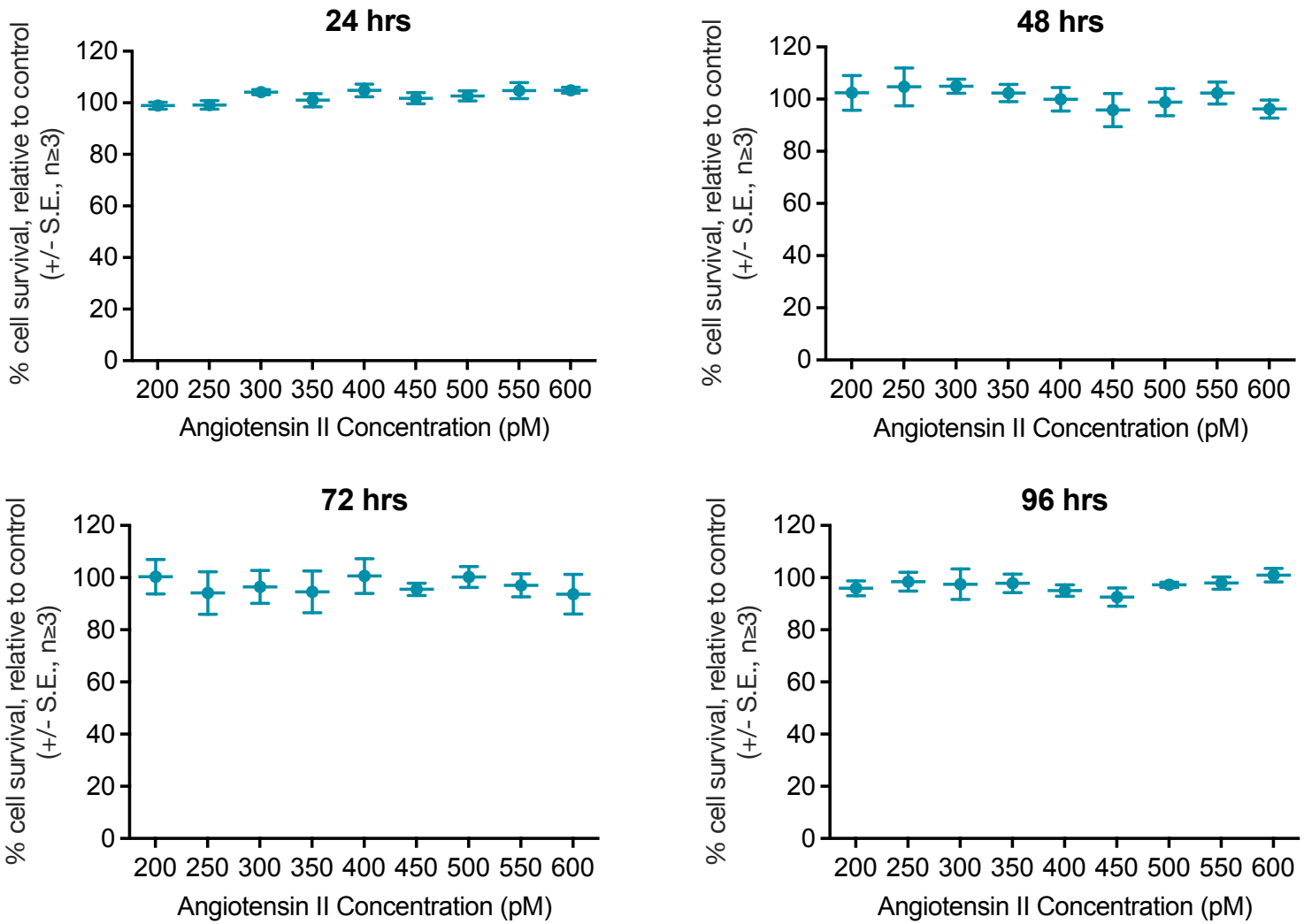

Figure 3.6 Dose response curve of AC10 following expose to different concentrations of angiotensin II ranging from 200 to 600 pM daily expressed as a % of the mean normalised to control. An MTS assay was performed after 24, 48, 72, and 96 hrs to assess cell viability. Data is representative of at least three repeats ±SEM.

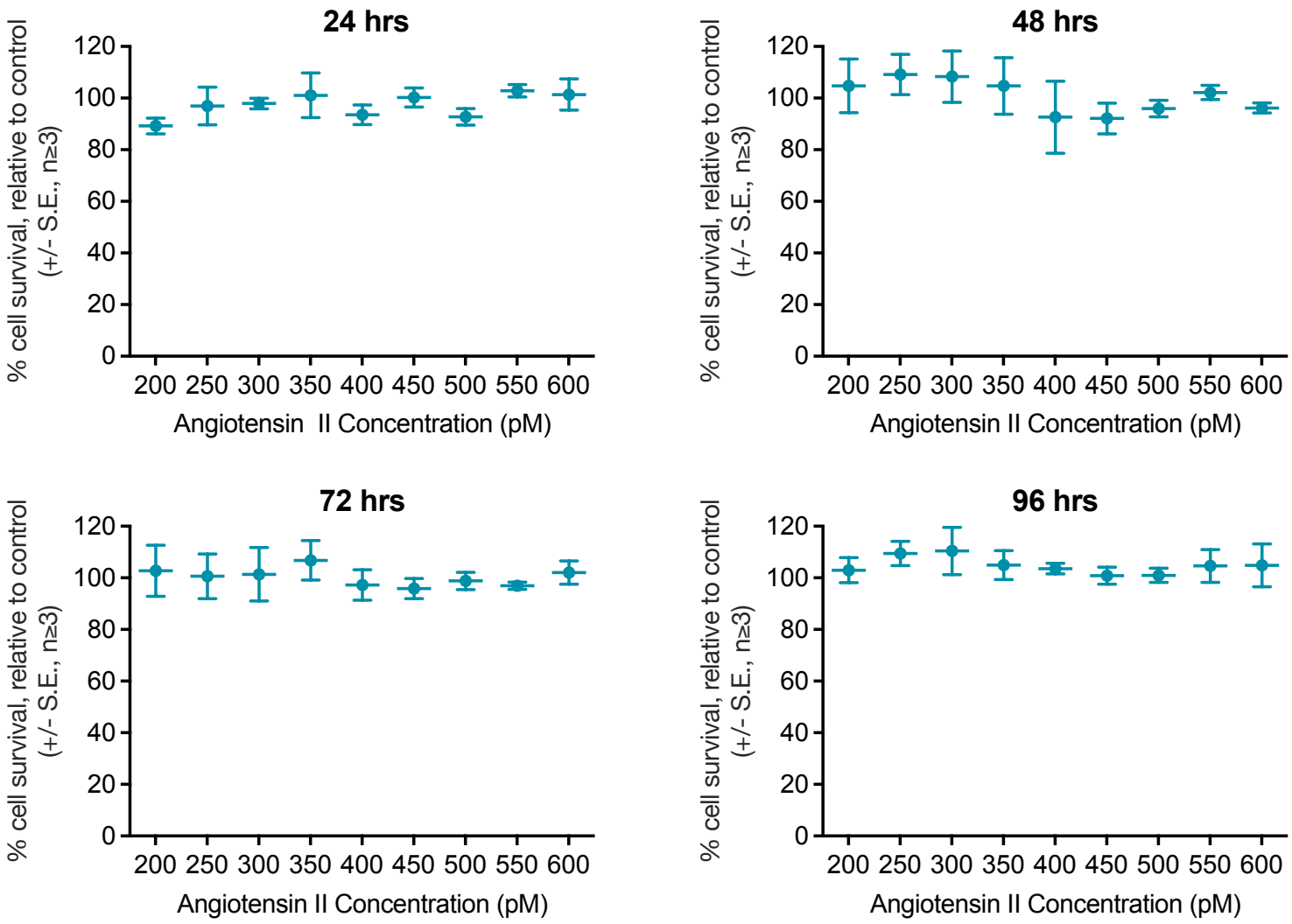

Figure 3.7 Dose response curve of HCF following expose to different concentrations of angiotensin II ranging from 200 to 600pM daily expressed as a % of the mean normalised to control. An MTS assay was performed after 24, 48, 72, and 96 hrs to assess cell viability. Data is representative of at least three repeats ±SEM.

3.3.7 Exposure to physiological concentration of angiotensin II has no effect on the sensitivity of AC10 or HCF to doxorubicin

MTS assay was performed over time points to investigate the cytotoxic response of both AC10 and HCF to various concentrations of doxorubicin ranging from 15.6nM to 2µM in combination with 500pM angiotensin II. Exposure to 500pM angiotensin does not affect the sensitivity of either AC10 cardiomyocytes or HCF to doxorubicin (Figure 3.8 for AC10 and Figure 3.9 for HCF).

Furthermore, angiotensin II within this physiological range did not significantly alter the IC_{50} of doxorubicin over the various time points (Table 3.5 for AC10 and Table 3.6 for HCF). The IC_{50} values for doxorubicin alone versus the combination of doxorubicin and angiotensin II (500pM) in AC10 were 0.34±0.085 vs 0.51±0.16 at 48 hours, 0.17±0.06 vs 0.12±0.055 at 72 hours, and 0.06±0.005 vs 0.065±0.004 at 96 hours and in HCF were 1.005±0.123 vs 0.929±0.113 at 48 hours, 0.466±0.06 vs 0.38±0.038 at 72 hours, and 0.270±0.017 vs 0.252±0.053 at 96 hours, respectively.

3.3.8 Angiotensin II induces morphological changes in AC10

The effects of exposure to angiotensin II on the cell morphology of AC10 were determined by xCELLigence RTCA in real-time. The cell index of cells, which were in the plateau growth phase, increased in cells exposed to 300pM angiotensin II, when normalised to the point of angiotensin II addition and after 48 hours of initial angiotensin II exposure (Figure 3.10A and B). No significant change ($p=0.144$) in cell number or viability was associated with this response, as determined by MTS assay performed 48 hours after angiotensin II exposure (Figure 3.10C). This finding was further validated by analysing changes in cell size using imaging, with a significant increase in cell area of AC10 observed in cells exposed to 300pM angiotensin II compared to control (Figure 3.10D and E). The results confirmed that angiotensin II induces cell hypertrophy in AC10 cardiomyocytes.

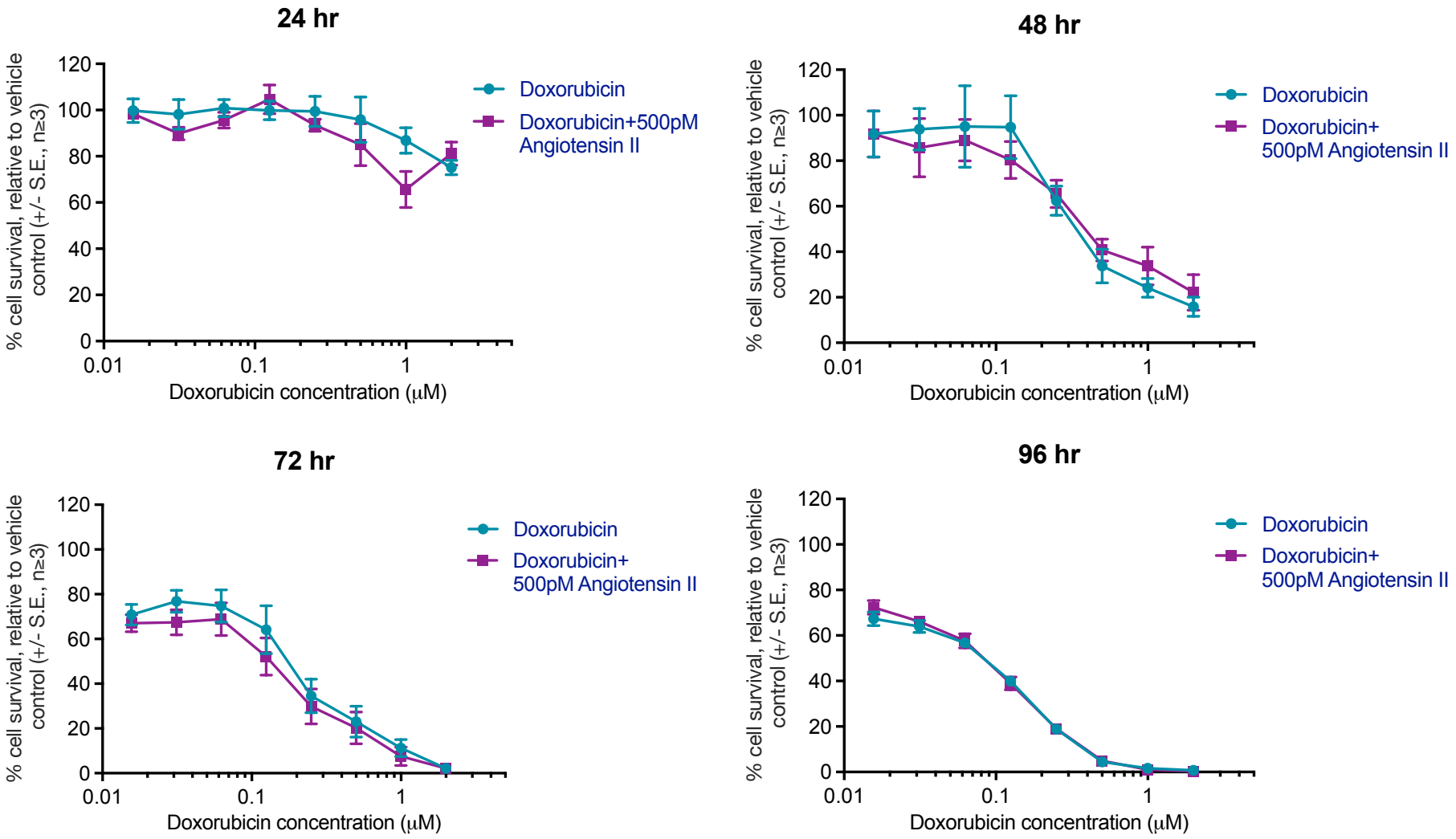

Figure 3.8 Dose-response curve of AC10 after exposure to varying concentrations of doxorubicin, starting from 2 µM with a 1:2 serial dilution + 500pM angiotensin II daily expressed as a % of the mean normalised to vehicle control. An MTS assay was performed after 24 hrs 48 hrs 72 hrs and 96 hrs. Data is representative of at least three repeats ±SEM.

Table 3.5 IC_{50} of human AC10 cardiomyocyte cells in response to exposure to doxorubicin in the presence or absence of 500pM angiotensin II. Data is determined by MTS assay and is representative of at least three repeats, presented as mean IC_{50} ±SEM. Statistical significance was determined by un-paired t-test.

	Cytotoxicity IC_{50} (μM)			
	24 hr	**48 hr**	**72 hr**	**96 hr**
Doxorubicin	>2	0.34±0.09	0.17±0.06	0.06±0.01
Doxorubicin + 500pM Angiotensin II	>2	0.51±0.16	0.12±0.06	0.07±0.00
p-value		0.4379	0.5550	0.4420

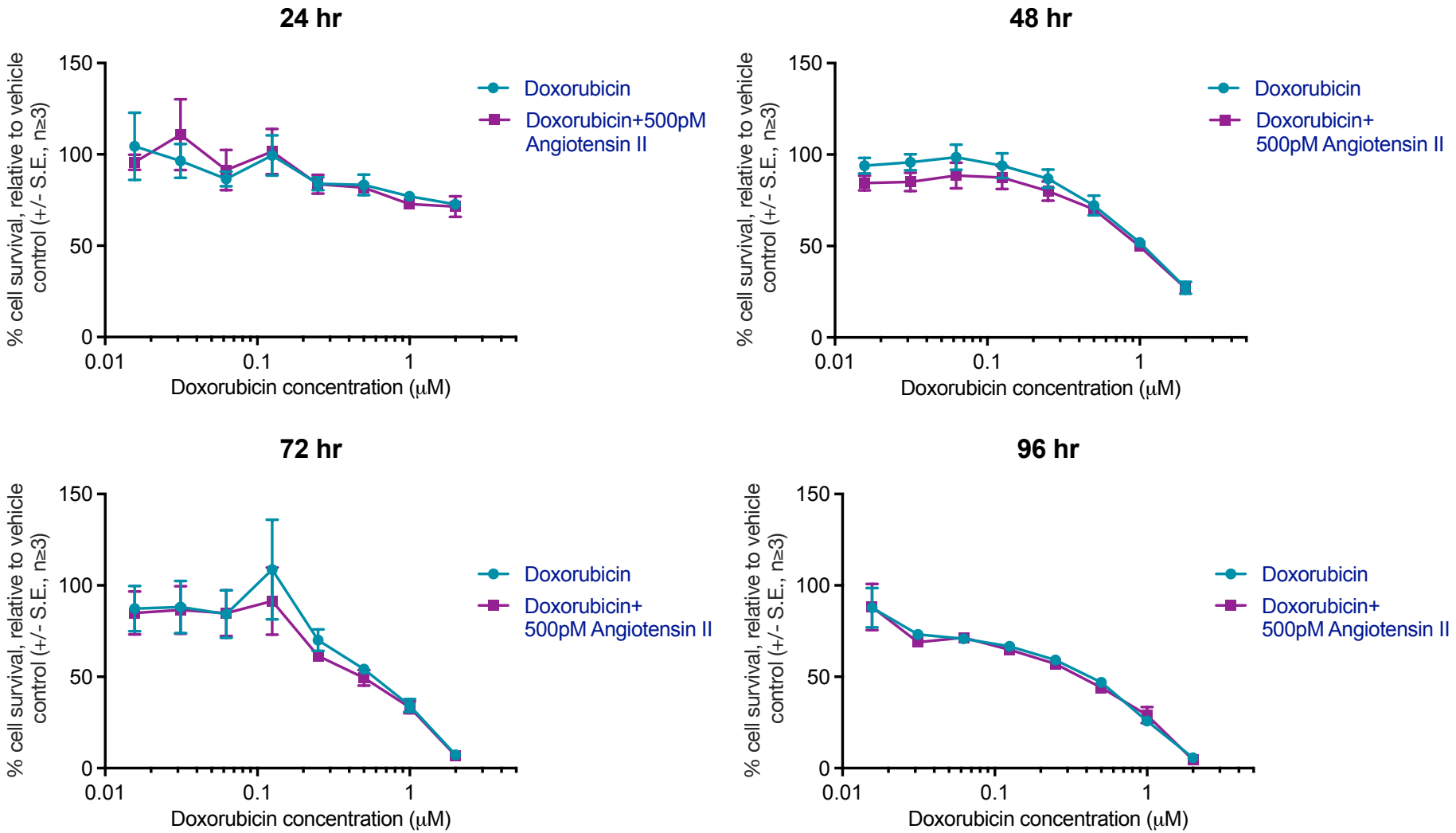

Figure 3.9 Dose-response curve of HCF after exposure to varying concentrations of doxorubicin, starting from 2 µM with a 1:2 serial dilution + 500pM angiotensin II daily expressed as a % of the mean normalised to vehicle control. An MTS assay was performed after 24 hrs 48 hrs 72 hrs and 96 hrs. Data is representative of at least three repeats ±SEM.

Table 3.6 IC_{50} of HCF after exposure to doxorubicin in response to exposure to doxorubicin in the presence or absence of 500pM angiotensin II. Data is determined by MTS assay and is representative of at least three repeats and presented as IC_{50} ±SEM. Statistical significance was determined by un-paired t-test.

	Cytotoxicity IC_{50} (µM)			
	24 hr	**48 hr**	**72 hr**	**96 hr**
Doxorubicin	>2	1.001±0.12	0.47±0.06	0.27±0.02
Doxorubicin + 500pM Angiotensin II	>2	0.93±0.11	0.38±0.04	0.25±0.05
p-value		0.6694	0.2937	0.7712

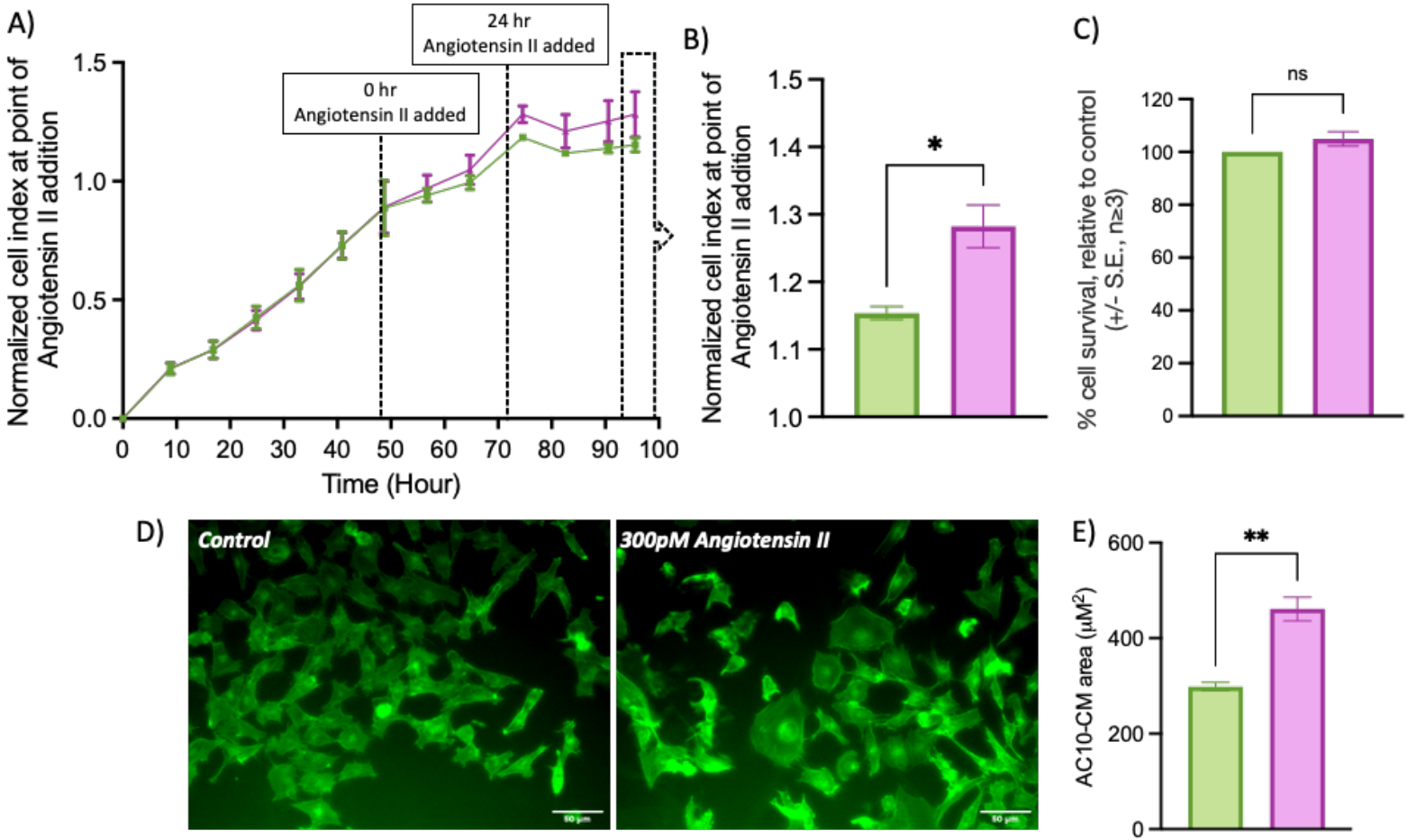

Figure 3.10 Angiotensin II-induced hypertrophy of AC10 cardiomyocytes. (A) Time vs cell index (xCELLigence output). Dashed line indicates the points of angiotensin II additions. (B) Normalised cell index after 48hrs of daily Angiotensin II addition. (C) Viability of the cells at 48 hrs following daily additions of 300PM Angiotensin II was assessed using an MTS assay. (D) Representative images show cell area changes in AC10 exposed to 300pM angiotensin II for 48 hours. E) The quantification graph illustrates mean cell area (µm²) increased in cells exposed to 300pM angiotensin II for 48 hours. Mean cell area (µm²) was calculated using ImageJ. Each data point = mean +/- SE, n ≥ 3. Statistical significance was determined by an un-paired t test (* = $p < 0.05$, ** = $p < 0.01$). (Scale bar: 50 µm) (Magnification:20x). Control, 300pM Angiotensin II.

3.3.9 Doxorubicin induces morphological changes in AC10

RTCA xCELLigence system was used to monitor the morphological and proliferation changes in AC10 which were in the plateau growth phase after exposure to different concentrations of doxorubicin. When cell index normalised to point of doxorubicin addition, a dose-dependent increase in the cell index of cells exposed to 50nM, 100nM, 250nM, 500nM doxorubicin compared to control after 24 hours of initial doxorubicin exposure, indicated that doxorubicin increased the cell size or proliferation rate of AC10. After 48 hours of initial doxorubicin exposure, the increase in cell index only observed in cell index of cells exposed to 50nM and 100nM concentrations of doxorubicin and the cell index of cells exposed to 250nM and 500nM doxorubicin declined compared to control (Figure 3.11 A,B and C).

MTS assay was performed to assess whether the increase of cell index was due to change in proliferation or not in AC10 after 24 and 48 hours. As Figure 3.11D and E shown, the cell viability of AC10 did not change when exposed to 50nM, 100nM, 250nM, 500nM doxorubicin compared to vehicle control after 24 hours ($p=0.84$), indicated that doxorubicin did not change the proliferation of AC10. However, the cell viability not changed with 50nM ($p=0.95$) and 100nM ($p=0.94$) doxorubicin but significantly decreased with 250nM and 500nM doxorubicin at 48 hours. This indicated that doxorubicin induces concentration dependent hypertrophy in AC10 after 24 hours and after 48 hours induces hypertrophy with 50nM and 100nM doxorubicin and decrease in cell viability with 250nM and 500nM doxorubicin.

3.3.10 Morphological changes in response to doxorubicin in AC10 additive to those induced by angiotensin II

To assess whether the combination of doxorubicin and angiotensin II has an additive effect compared to angiotensin II induced hypertrophy in AC10, the morphological changes of AC10 after exposure to 50nM doxorubicin in combination with 300pM angiotensin II were evaluated using RTCA xCELLigence system. When the cell index normalised to the point of doxorubicin addition, the cell index of cells exposed to 50nM doxorubicin, 300pM angiotensin II, or their combination increased compared to cell index of control after 48 hours of initial doxorubicin exposure (Figure 3.12A and B). The cell index of cells exposed to the combination of 50nM doxorubicin and 300pM angiotensin II was not significantly higher than cell index of cells

exposed to angiotensin II (p=0.10), indicated that doxorubicin did not induce additive effect to those induced by angiotensin II in AC10 in xCELLigence.

In addition, to determine whether this increase in cell index was due to an increase in AC10 cell proliferation or not, MTS assay was performed after 48 hours of exposure to 50nM doxorubicin, 300pM angiotensin II, or their combination (Figure 3.12C). The cell viability of AC10 was not significantly affected (p=0.28), indicated that 50nM doxorubicin, 300pM angiotensin II, and the combination of 50nM doxorubicin and 300pM angiotensin II did not change the proliferation of AC10.

This finding was further validated by analysing changes in cell size using imaging, with a significant increase in cell area of AC10 observed in cells exposed to 50nM doxorubicin, 300pM angiotensin II, and the combination of 50nM doxorubicin and 300pM angiotensin II compared to control (Figure 3.12D and E). Furthermore, cell area of AC10 cells exposed to the combination of 50nM doxorubicin and 300pM angiotensin II was higher than cells exposed to 300pM angiotensin II alone (p=0.004). The results confirmed that both 50nM doxorubicin, 300pM angiotensin II induce cell hypertrophy in AC10 cardiomyocytes and that doxorubicin induces additive effect to those induced by angiotensin II in AC10.

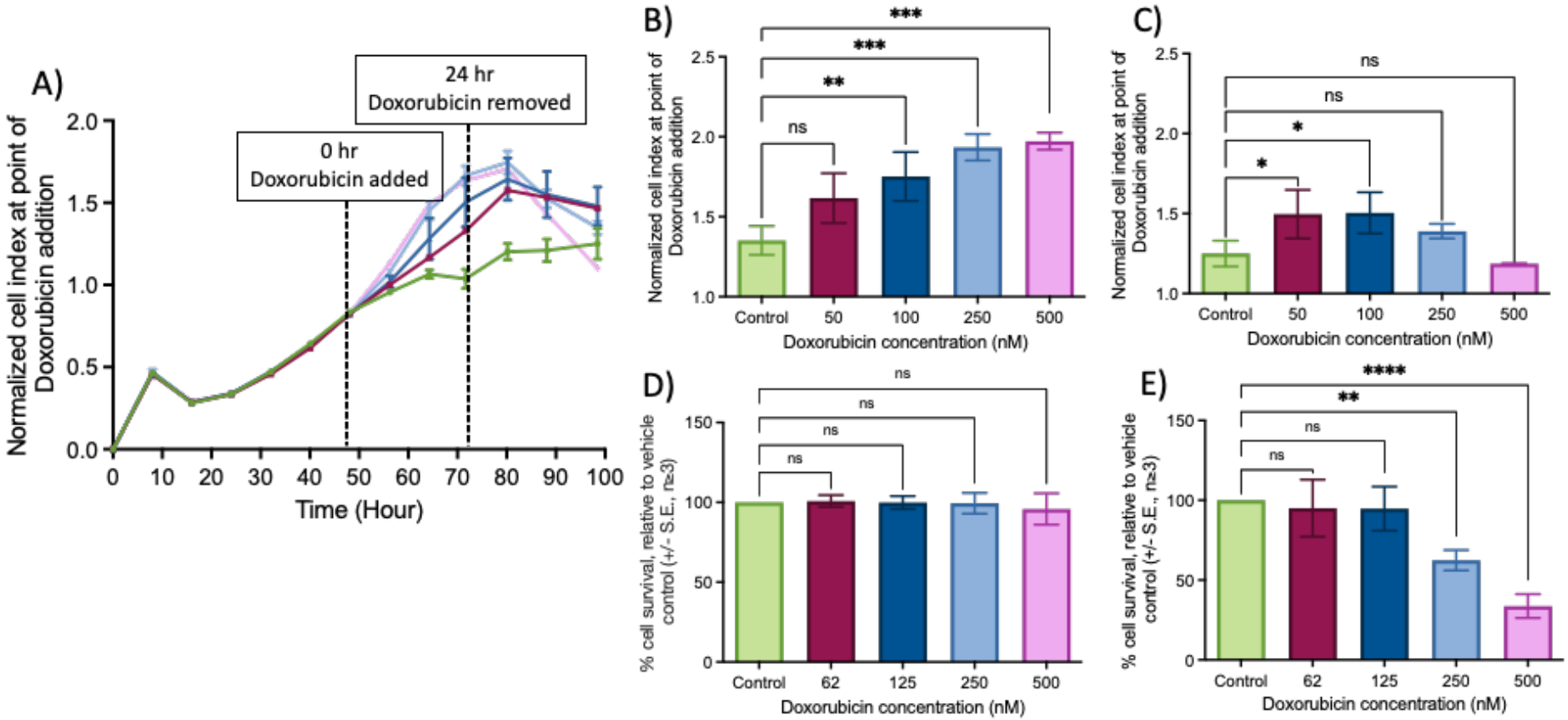

Figure 3.11 Doxorubicin-induced hypertrophy of AC10 cardiomyocytes. (A) Time vs cell index (xCELLigence output). Dashed line indicates the points of Doxorubicin addition and remove. (B) Normalised cell index after 24 hrs of initial Doxorubicin addition. (C) Normalised cell index after 48 hrs of initial Doxorubicin addition. D) Viability of the cells at 24hrs following additions of Doxorubicin was assessed using an MTS assay. E) Viability of the cells at 48hrs following additions of Doxorubicin was assessed using an MTS assay. Each data point = mean +/- SE, n ≥ 3. Statistical significance was determined by a One-way ANOVA with post-hoc Dunnett's multiple comparison test. (* = $p < 0.05$, ** = $p < 0.01$, *** = $p < 0.001$, **** = $p < 0.0001$). Control, 50nM Doxorubicin, 100nM Doxorubicin, 250nM Doxorubicin, 500nM Doxorubicin.

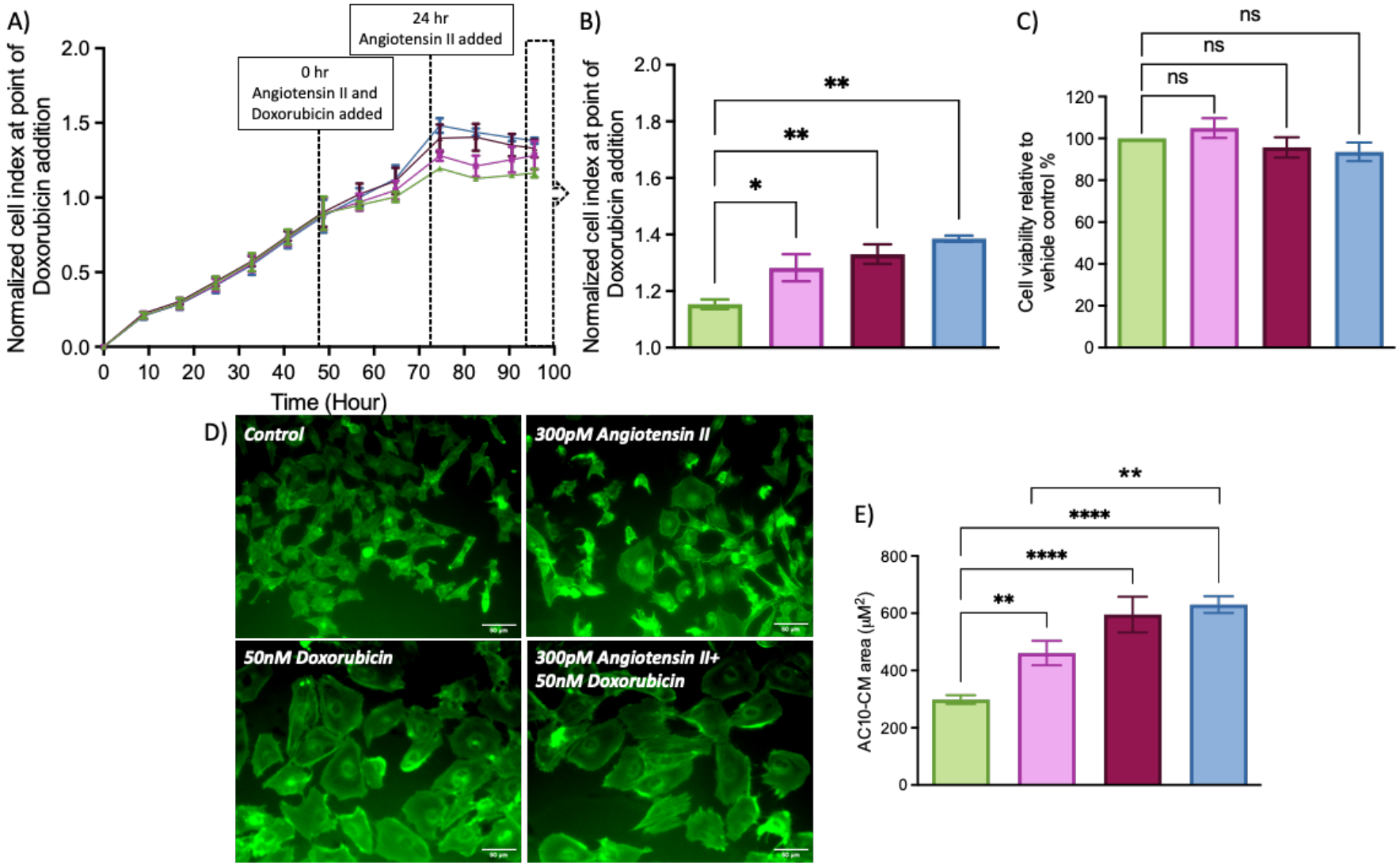

Figure 3.12 Sub-toxic concentration of doxorubicin-induced hypertrophy of AC10 cardiomyocytes. (A) Time vs cell index (xCELLigence output) of AC10 cells following exposure to 300pM angiotensin II or 50nM doxorubicin and their combination for 48 hrs. The cell index normalised to the point of

doxorubicin addition as indicated in the graph. (B) This quantification graph extracted from xCELLigence graph demonstrates the effect of exposure to 300pM angiotensin II or 50nM doxorubicin and their combination on AC10 48 hours after the initial exposure to doxorubicin. The cell index was normalised at point of Doxorubicin and Angiotensin II addition. (C) Confirmation that AC10 maintain viability 48 hrs following additions of 300pM angiotensin II or 50nM doxorubicin and their combination relative to vehicle control, assessed using an MTS assay. (D) Representative images show cell area changes in AC10 exposed to 300pM angiotensin II or 50nM doxorubicin and their combination for 48 hrs. E) The quantification graph illustrates that the mean cell area (µm²) increased in cells exposed to 300pM angiotensin II or 50nM doxorubicin and their combination compared to control. Mean cell area (µm²) was calculated using ImageJ. Each data point = mean +/- SE, n ≥ 3. Statistical significance was determined by a One-way ANOVA with post-hoc Dunnett's multiple comparison test. (* = $p < 0.05$, ** = $p < 0.01$, *** = $p < 0.001$, **** = $p < 0.0001$). (Scale bar: 50 µm) (Magnification:20x). Control, 300pM Angiotensin II, 50nM Doxorubicin, 50nM Doxorubicin+300pM Angiotensin II.

3.3.11 Cellular morphology of HCF remains unchanged after the addition of angiotensin II

The effects of exposure to angiotensin II on the cell morphology of HCF were determined by xCELLigence RTCA in real-time. As shown in Figure 3.13A and B, there was no increase cell index of cells exposed to 300pM angiotensin II compared to the cell index of control, when normalised to the point of angiotensin II addition and after 48 hours of initial angiotensin II exposure ($p=0.99$), indicating that angiotensin II did not affect cell morphology and proliferation of HCF. MTS assay was performed 48 hours after angiotensin II exposure confirmed that exposure to 300pM angiotensin II did not affect the viability of HCF ($p=0.35$) as shown in Figure 3.13C. This finding was further validated by analysing changes in cell size using imaging. As shown in Figure 3.13D and E**,** no change in cell size of HCF was observed in cells exposed to 300pM angiotensin II compared to control ($p=0.61$). The results confirmed that angiotensin II did not induce morphological changes in HCF.

3.3.12 Cellular morphology of HCF remains unchanged after addition of doxorubicin

RTCA xCELLigence system was used to monitor the morphological and proliferation changes in HCF after exposure to different concentrations of doxorubicin. When cell index normalised to point of doxorubicin addition, a dose-dependent decrease in the cell index of cells exposed to 50nM, 100nM, 250nM, 500nM doxorubicin compared to control after 24 and 48 hours of initial doxorubicin exposure, indicated that doxorubicin decrease the cell size or viability of HCF (Figure 3.14A,B and C).

MTS assay was performed to assess whether the decrease of cell index was due to change in cell viability or decrease in cell size in HCF after 24 and 48 hours. As Figure 3.14D and E shown, the cell viability of HCF did not change when exposed to 50nM, 100nM, 250nM, 500nM doxorubicin compared to control after 24 hours ($p=0.19$). However, the cell viability significantly decreased with 500nM doxorubicin at 48 hours. This result indicated that doxorubicin did not induces the morphological changes in HCF.

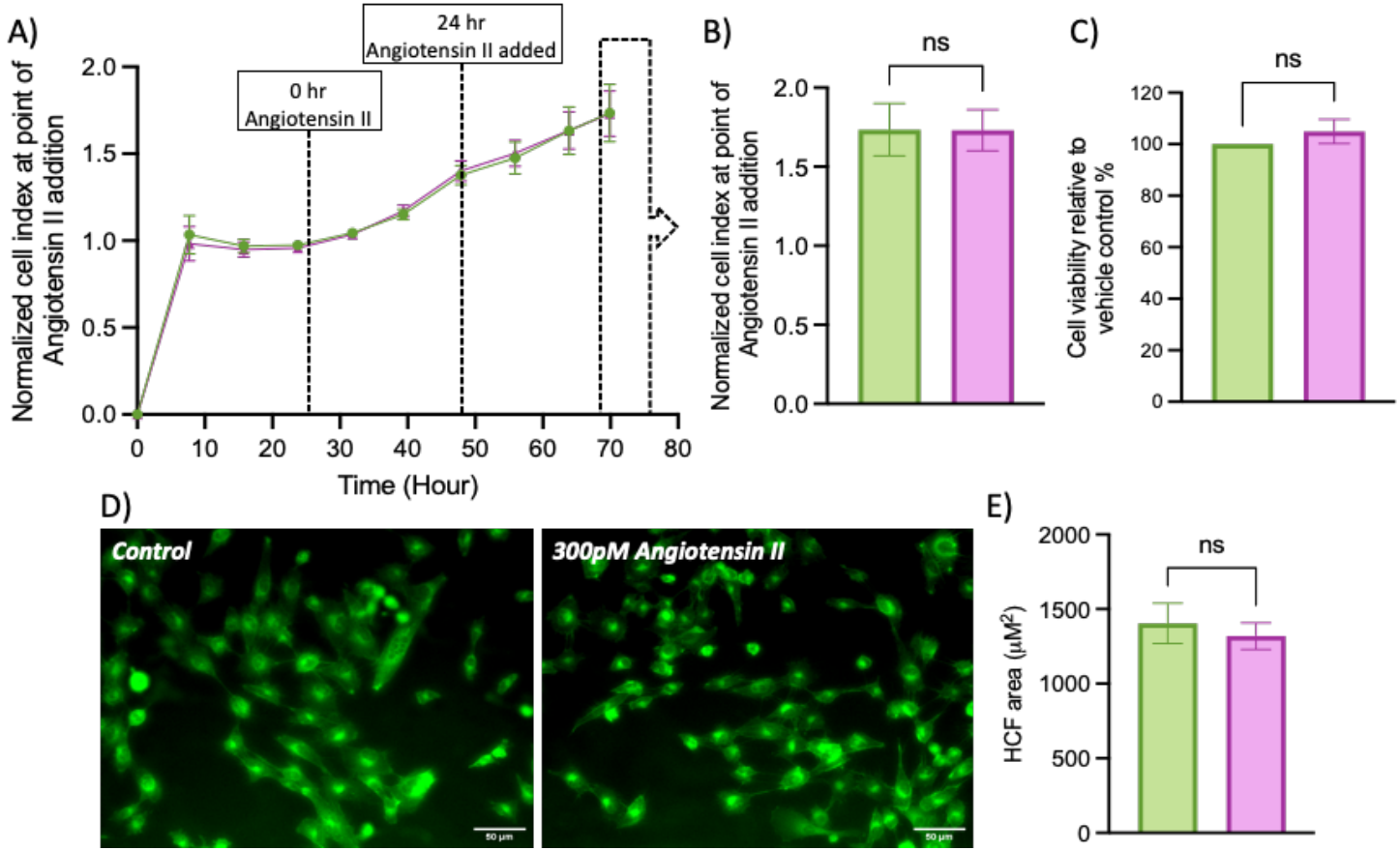

Figure 3.13 No morphological changes in HCF after 48hrs of exposure to Angiotensin II. (A) Time vs cell index (xCELLigence output). Dashed line indicates the points of angiotensin II additions. (B) Normalised cell index after 48hrs of daily Angiotensin II addition. (C) Viability of the cells at 48 hrs following daily additions of 300PM Angiotensin II was assessed using an MTS assay. (D) Representative images show cell area changes in HCF exposed to 300pM angiotensin II for 48 hours. E) The quantification graph illustrates mean cell area (µm²) does not change in cells exposed to 300pM angiotensin II for 48 hours. Mean cell area (µm²) was calculated using ImageJ. Each data point = mean +/- SE, n ≥ 3. Statistical significance was determined by an un-paired t test. (Scale bar: 50 µm) (Magnification:20x). Control, 300pM Angiotensin II.

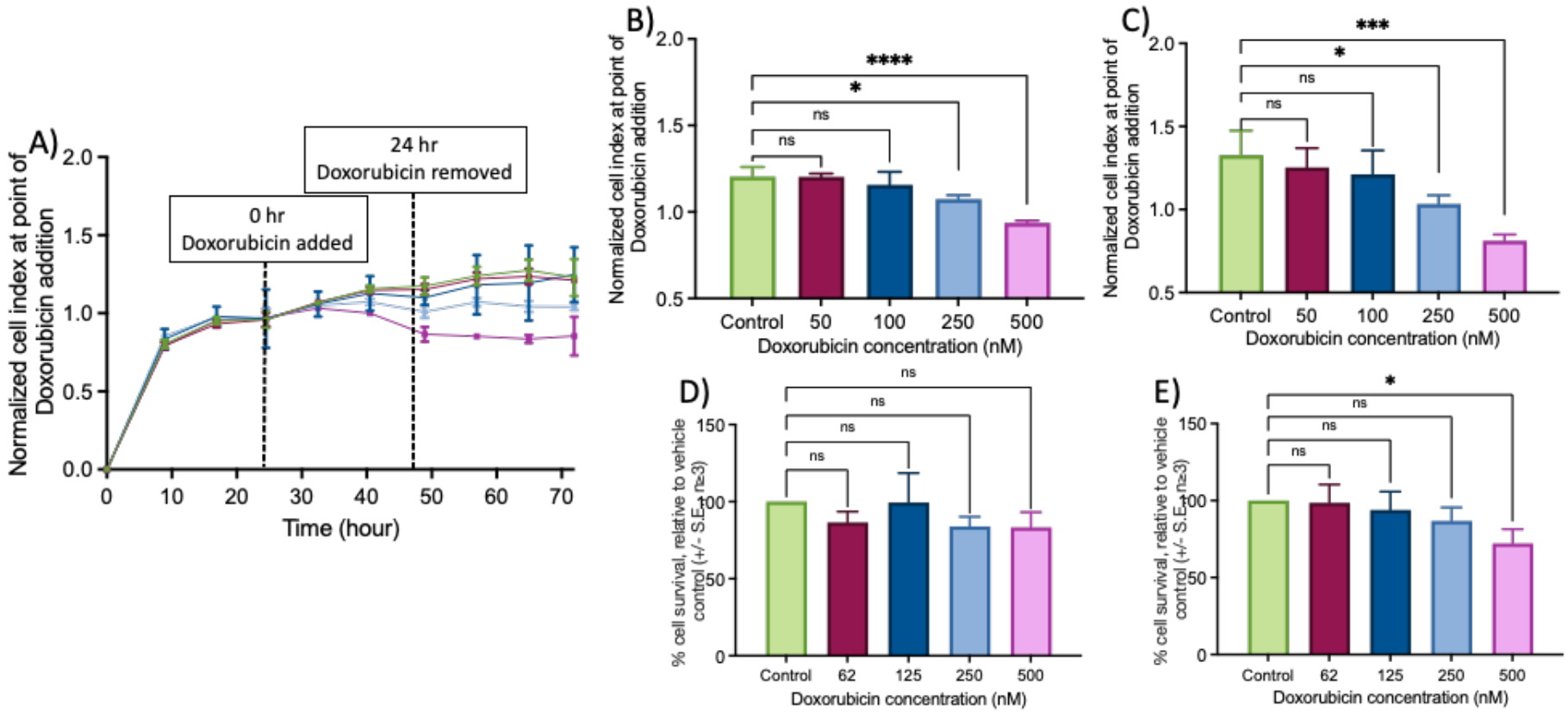

Figure 3.14 No morphological changes after doxorubicin exposure in HCF. (A) Time vs cell index (xCELLigence output). Dashed line indicates the points of Doxorubicin addition and remove. (B) Normalised cell index after 24 hrs of initial Doxorubicin addition. (C) Normalised cell index after 48 hrs of initial Doxorubicin addition. D) Viability of the cells at 24hrs following additions of Doxorubicin was assessed using an MTS assay. E) Viability of the cells at 48hrs following additions of Doxorubicin was assessed using an MTS assay. Each data point = mean +/- SE, n ≥ 3. Statistical significance was determined by a One-way ANOVA with post-hoc Dunnett's multiple comparison test. (* = $p < 0.05$, ** = $p < 0.01$, *** = $p < 0.001$, **** = $p < 0.0001$). Control, 50nM Doxorubicin, 100nM Doxorubicin, 250nM Doxorubicin, 500nM Doxorubicin.

3.3.13 Addition of doxorubicin does not alter the morphological response of HCF to angiotensin II

To assess whether doxorubicin changes the response of HCF to angiotensin II, the morphological changes of HCF after exposure to 50nM doxorubicin in combination with 300pM angiotensin II were evaluated using RTCA xCELLigence system. When the cell index normalised to the point of doxorubicin addition, the cell index of cells exposed to 50nM doxorubicin, 300pM angiotensin II, or their combination did not change compared to cell index of control after 48 hours of initial doxorubicin exposure (p=0.91). There was no difference of the cell index of cell exposed to the combination of 50nM doxorubicin and 300pM angiotensin II compared to cell index of cells exposed to 300pM angiotensin II alone (p=0.58) (Figure 3.15A and B).

In addition, MTS assay was performed after 48 hours of exposure to 50nM doxorubicin, 300pM angiotensin II, or their combination to determine whether the combination of 50nM doxorubicin and 300pM angiotensin II affect cell proliferation or not in HCF. The cell viability of HCF was not significantly affected in different treatment conditions compared to control (p=0.59) (Figure 3.15C).

This finding was further validated by analysing changes in cell size using imaging, without significant difference of cell area of HCF between treatment conditions compared to control (p=0.95) (Figure 3.15D and E). Furthermore, cell area of HCF cells exposed to the combination of 50nM doxorubicin and 300pM angiotensin II was not changed compared to cells exposed to 300pM angiotensin II alone (p=0.56). The results confirmed that both 50nM doxorubicin, 300pM angiotensin II did not change the cell morphology in HCF and that doxorubicin did not change the HCF response to angiotensin II.

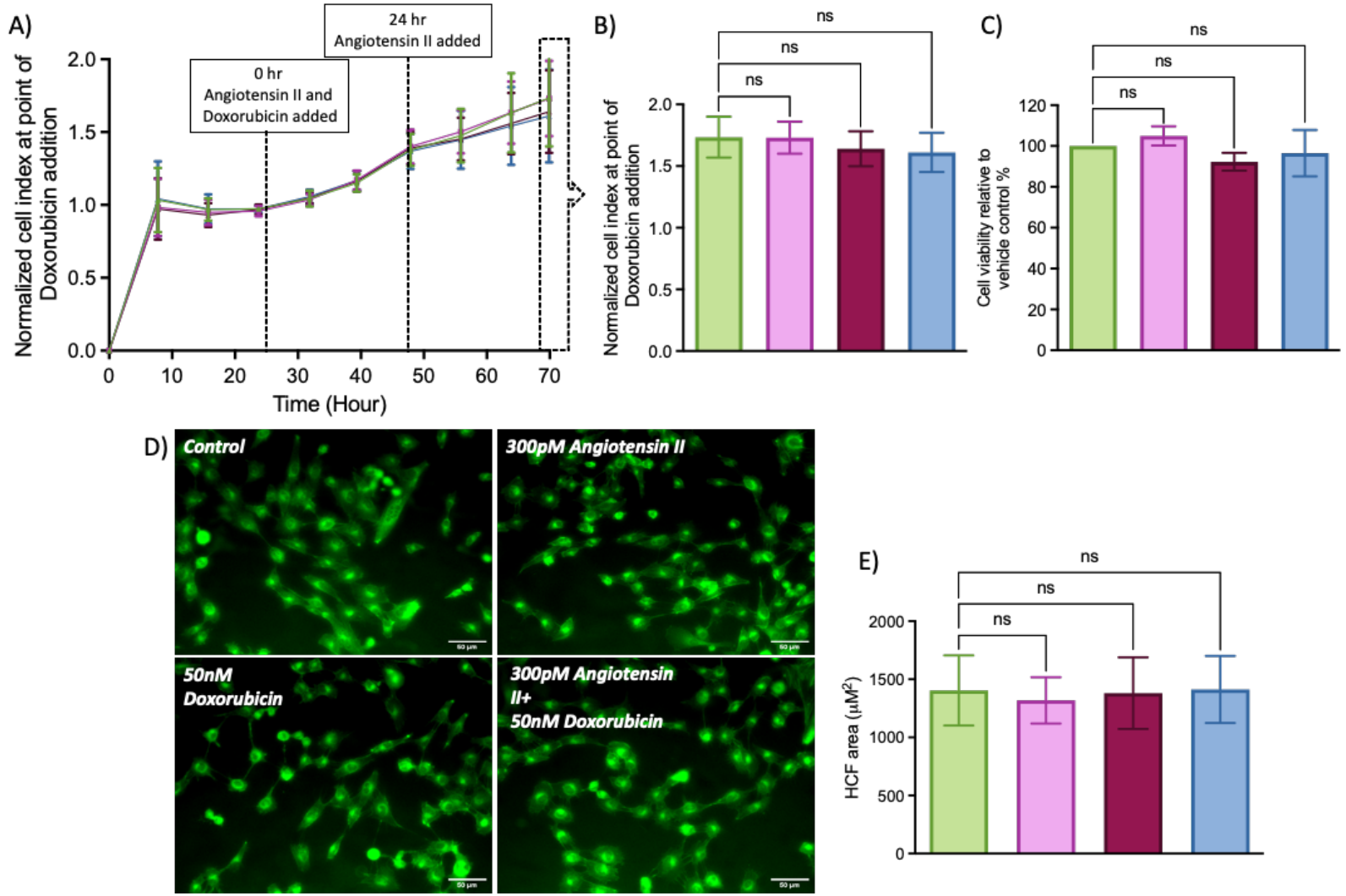

Figure 3.15 No morphological changes in HCF after 48hrs of exposure to Doxorubicin. (A) Time vs cell index (xCELLigence output) of HCF cells following exposure to 300pM angiotensin II or 50nM doxorubicin and their combination for 48 hrs. The cell index normalised to the point of doxorubicin addition

as indicated in the graph. (B) This quantification graph extracted from xCELLigence graph demonstrates the effect of exposure to 300pM angiotensin II or 50nM doxorubicin and their combination on HCF 48 hours after the initial exposure to doxorubicin. The cell index was normalised at point of Doxorubicin and Angiotensin II addition. (C) Confirmation that HCF maintain viability 48 hrs following additions of 300pM angiotensin II or 50nM doxorubicin and their combination relative to vehicle control, assessed using an MTS assay. (D) Representative images show cell area changes in HCF exposed to 300pM angiotensin II or 50nM doxorubicin and their combination for 48 hrs. E) The quantification graph illustrates that no changes in mean cell area (µm² in cells exposed to 300pM angiotensin II or 50nM doxorubicin and their combination compared to control. Mean cell area (µm²) was calculated using ImageJ. Each data point = mean +/- SE, n ≥ 3. Statistical significance was determined by a One-way ANOVA with post-hoc Dunnett's multiple comparison test. (Scale bar: 50 µm) (Magnification:20x). Control, 300pM Angiotensin II, 50nM Doxorubicin, 50nM Doxorubicin+300pM Angiotensin II.

3.4 Discussion

The process of AIC is progressive that begins at cellular level with myocardial injury and continues with LVEF decline and in severe cases congestive heart failure (27). This progressive effect started with structural cardiotoxicity of cardiac cells which alter the cellular structure and involve cardiac remodelling, such as cellular hypertrophy or fibrosis which are often asymptomatic, but in many cases, it progresses to severe cardiac dysfunction, which induces symptomatic functional cardiotoxicity (193). The usefulness of anticancer activity of anthracycline is limited by this long term side effects on the heart which often presents several years after cessation of therapy (189). However, the mechanism of AIC still not understood and there is a deficit in understanding the relationship of short-term acute drug exposure to delayed and late-onset cardiac failure. Furthermore, cardiac cell responses to doxorubicin are also not fully characterised. Thus, using *in vitro* models, this study aims to assess the cardiac cells viability after exposure to clinically relevant concentrations of doxorubicin and identify and link cellular responses to the clinical scenario of AIC.

The immortalised human cardiomyocyte model, AC10 cell line, has been widely used in cardiotoxicity studies (178, 210). It was originally developed by Davidson et al. by fusing human ventricular cardiomyocytes with human fibroblasts that had been depleted of mtDNA (168). This cell line has been characterised and shown to express several cardiac proteins, such as troponins, tropomyosin, and α-actinin, though they remain in a pre-contractile state. They also express gap junction proteins, including connexin-40 and connexin-43, which are essential for electrical signalling between cardiac cells (175, 178). Although AC10 cells are useful for modelling cardiac biology, one reported limitation of the AC10 model of cardiomyocyte in this study is the fact they are proliferative and expression of vimentin, a mesenchymal marker absent in cardiomyocytes, which have a limited capacity to regenerate in the heart (42). In this context, the fibroblast-like features of AC10 cells can be seen as a strength as cardiomyocytes in the heart naturally coexist with fibroblasts, which are involved in cardiac remodelling and ECM production. To recapitulate this clinical situation of quiescence, in this study AC10 were seeded to reach quiescent state before addition of tested drug, by undertaking evaluations whilst in the plateau growth phase. Methodologies and seeding densities were therefore adapted to achieve plateau phase growth 48 hours of

seeding, permitting consistency across studies. Taken together, these characteristics reinforce the suitability of AC10 cells as a human cardiac model for study AIC *in vitro*.

Whilst cardiomyocytes are considered the primary target of anthracycline, CFs contributes to fibrosis and tissue remodelling which results in progression of cardiac damage (196). CFs are the most abundant cells in the myocardium and provide the structural support to cardiomyocytes (211). However, there are limited studies on how CFs contributes to developing AIC (198). The pathogenesis of AIC involves complex interactions between cardiomyocyte damage and CFs activation, with emerging evidence highlighting CFs as key contributors to early myocardial remodelling. CFs exhibit increased glycolytic activity, mitochondrial dysfunction, and differentiated to myofibroblasts within days of doxorubicin exposure, even before detectable cardiac dysfunction (95). The early metabolic dysfunction and differentiation to myofibroblasts were not the only CFs response to anthracycline, proteomic analyses have shown that doxorubicin exposure can alter CFs protein expression profile, particularly those affecting pathways associated with mitochondrial energy metabolism, ECM remodelling, cell cycle regulation and arrest, as well as cell survival (212). A disruption that potentially affect CFs electrophysiology and amplifying fibrotic signalling. In addition, doxorubicin has been shown to upregulate TGF-β, IL-6, and matrix metalloproteinases (MMP-2/MMP-9), which contribute to collagen deposition and increase myocardial stiffness (199). Taken together, these findings demonstrated that CFs are effector cells and involved in the early stages of pathogenesis of AIC. Understanding CFs contributions in AIC require further investigation.

In order to characterise cell response to any agent *in vitro*, an understanding of cell behaviours is therefore required and the methodologies associated with these analyses need to be qualified. The assessment of doubling time allows to understand growth rate of each cell line which is important in the future studies in this project to assess cell health, behaviour, and how these cells respond to different treatment and the cytotoxic drug. The doubling time for AC10 and HCF using manual counting was 27.7±1.7 and 46.6±3.8 hours, respectively. The doubling time for AC10 and HCF using MTS assay was a bit longer than manual counting with 31±7and 66.5±22.8 hours, respectively. The doubling time using xCELLigence system further confirm the previous trend of growth rate with 34.4±9 and 69±14.2 hours for AC10 and HCF, respectively. The short doubling time of AC10 across three methods indicates that AC10 grow relatively faster than HCF. The difference in doubling time between methods may be due to the way of measuring cell viability and proliferation between methods. The manual counting

quantifies the total number of dead and live cells, but it does not assess the changes in cell metabolic activity or behaviour. Due to its limitations in accurately reflecting cell viability, manual counting was not pursued further in this study. In contrast, MTS assay provides more functional measure of cell viability, depending on dehydrogenase enzymes that present in metabolic active cell. The amount of formazan produced by dehydrogenase enzymes is directly proportional to the number of living cells in culture and can be measured spectrophotometrically at 490nm (213). The MTS assay is widely recognised for its accuracy and has been extensively used for cytotoxicity assessment studies, including those assessing cardiotoxicity (214, 215). In addition, xCELLigence RTCA system is continuously measure the cell proliferation, attachment, and behaviour in real time (188). This system measures the electrical impedance which is sensitive to a change in behaviour of cells and change in cell proliferation following exposure to tested compound (188). A reduction in cell index reflects decrease in cell viability or cell size, while an increase indicates the increase proliferation or cell enlargement (187). The combined use of MTS assay, xCELLigence RTCA system, and fluorescence imaging in this study provided a comprehensive approach to assess metabolic activity, change in cell morphology and real-time behavioural responses of cardiomyocytes and CFs. It allowed to assess the response to treatment at specific time points, factors that are particularly relevant in assessment of structural cardiotoxicity.

Doxorubicin is the most commonly used anthracycline analogue with the highest cardiovascular risk (27). Concentration- and time-dependent effects of doxorubicin on AC10 and HCF were assessed, and IC_{50} values were calculated to provide a baseline understanding of the cytotoxic responses of AC10 and HCF to doxorubicin. Acute doxorubicin exposure produced a dose-dependent reduction viability in both AC10 cardiomyocyte and HCF cell models. The IC_{50} of AC10 after 48- and 96-hours exposure to doxorubicin were determined as 340±90 and 60±10nM, respectively, values consistent with the previous studies which determined IC_{50} values of 182.5nM and 40.67nM against AC10 cells *in vitro* (178, 210). With regards toxicity against fibroblasts, the IC_{50} of doxorubicin against HCF after the same periods (48 and 96 hours) were 1010±120 and 270±170nM, respectively. These findings suggest that cardiac cells become more sensitive to doxorubicin with increasing exposure, which is clinically relevant as prolonged exposure time to anthracycline is a risk factor of developing AIC (27). Interestingly, these data also indicate that HCF are less sensitive to doxorubicin than cardiomyocytes. One explanation for the higher sensitivity of AC10 cardiomyocytes than HCF to doxorubicin could be the comparative doubling times and growth characteristics of these

cell types, with HCF demonstrating a much longer doubling time than the cardiomyocyte cell line. From a therapeutic mechanism of anthracyclines perspective this is highly plausible as its mode of action centres around targeting proliferative cells (11-13). Alternatively, cardiomyocytes rely on mitochondria to meet their energy demand for continuous contractile function and have a lower level of antioxidant compared to other cell types (49, 50), making them susceptible to mitochondrial dysfunction induced by ROS formation and oxidative stress, mitochondrial DNA damage, and cell death induced by doxorubicin (33, 48, 216). In contrast, CFs, while also reliant on mitochondrial function, have a lower energy demand, less oxygen consumption, and fewer number of mitochondria than cardiomyocytes (217). These findings suggest that the effect of anthracycline extended beyond the proliferation rate assessment and should consider the pharmacodynamics activities of cells.

A comparison of sensitivity of cardiac cells to doxorubicin *in vitro* against clinically used concentrations implies some interesting differences for consideration. The reported C_{max} for doxorubicin in the clinic is 1.1µM, whereas the cytotoxicity IC_{50} following 48 hours exposure *in vitro* was determined as 0.34±0.09µM and 1.01±0.12µM for AC10 cardiomyocytes and HCF, respectively (209). This indicates that clinical concentrations of doxorubicin are approximately equal to those required to kill 50% of HCF and much higher than the cytotoxicity sensitivity of cardiomyocytes, which would theoretically suggest direct loss of cardiac cells, predominantly cardiomyocytes, when doxorubicin is administered clinically. However, this does not account for pharmacokinetics of doxorubicin which exhibits a rapid distribution phase of 3-5 minutes and a terminal half-life phase of 20 to 30 hours (209, 218). Therefore, it is plausible that the concentration of active doxorubicin reaching cardiac tissue is lower than the reported C_{max}, due to metabolism and distribution throughout the body. Furthermore, the quiescent nature of cardiomyocytes in clinical tissue, as opposed to AC10 cells *in vitro*, will also play a contributory factor and is likely to reflect a higher 'resistance' to doxorubicin clinically. Nevertheless, these data support the concept that doxorubicin, and potentially other anthracyclines, initially may result in direct cytotoxicity and loss of cardiomyocytes and CFs (although less-so than cardiomyocytes) and initial induction of stress upon cardiac tissue and reactive development of a fibrotic response (95, 193, 196). However, in the context of delayed cardiotoxicity and progressive development of clinical heart failure associated with anthracyclines, it is important to appreciate that these 'dead' cells do not directly contribute to this longer-term effect. The cell population responsible for these delayed responses are those that remain after the toxicological insult, those which have experienced sub-lethal

effects and their responses. Therefore, in essence, AIC is believed to develop as a consequence of a minor initial acute cytotoxic episode, with myocardial cellular loss and a responsive fibrotic response, coupled to the major pathophysiological response of the remaining cardiac cells, leading to progressive development of heart failure (27, 193). It is this latter element of AIC and the relative involvement of cardiomyocytes and CFs which requires further investigation, to better understand the condition in terms of both its monitoring and management.

Development of heart failure in the clinic is often associated with haemodynamic changes, such as hypertension, and a direct reactionary response of cardiac tissue, such as cardiac remodelling, changes in contractile force and reduced cardiac output (219). In this context, similarities were observed between development of heart failure and clinical presentation of AIC (8, 27, 153). For instance, both conditions are characterised by progressive myocardial dysfunction and decline in LVEF, ventricular remodelling, and activation of neurohormonal pathways, including RAAS (8, 27, 153). Based on this comparative presentation, several clinical studies have thus applied therapeutic principles for management of heart failure to that of management of AIC (152-161, 164-169). A common evaluated approach is the administration of therapeutics which interfere with or modify the RAAS system, particularly ACEi and ARBs (34). Although in many cases still preliminary, several studies have indicated an ability of ACEi (and ARBs) to reduce the impact of anthracycline effects upon the cardiac system (34). These studies thereby highlighting the putative relationship between angiotensin signalling and AIC.

The therapeutic mechanism of ACEi and ARB is known to involve systemic effects as a consequence on the action of these drugs to reduce blood volume and pressure, which undoubtedly offers a contribution to limiting progressive development of heart failure (see section 1.8.3) (26). However, there is now strong evidence that angiotensin signalling also acts at the local level within cardiac tissue, through direct stimulation and/or activity of cardiac cellular responses such as modulation of contractility and stimulation of hypertrophy (207, 220). In order to address a role for angiotensin signalling in AIC and the underpinning mechanism, qualification of the cellular models used in this project was required. Exposure to physiological concentrations of the effector molecule angiotensin II across a 96-hour period was not associated with either growth promotion or growth inhibition in either AC10 cardiomyocytes or HCF. As expected, although there was no hypo- or hyperplastic response, angiotensin II did cause an increase in cellular size and/or hypertrophy in AC10

cardiomyocytes, confirmed by several methodologies including xCELLigence RTCA, cell viability assessments and cellular imaging. These observations were in alignment with previous studies exemplifying angiotensin-induced cardiac cell hypertrophy (221-223). This relationship is further supported by *in vivo* transgenic murine studies in which cardiomyocytes overexpression of AT1R demonstrated that angiotensin II can directly induce hypertrophy in cardiomyocyte and associated with increased cardiovascular-related morbidity (221).

In contrast to cardiomyocytes, in which the response to angiotensin II is reported in several studies, the direct effect upon CFs remains elusive (198). In this context, an important finding in this study is that angiotensin II does not induce hypertrophy in HCF, with no significant change in proliferation rate detected in HCF following exposure to angiotensin II. This lack of reactionary response of HCF to angiotensin II appears to contradict a study using HCF isolated from ventricles of explanted hearts, in which exposure to angiotensin II reportedly promoted cellular growth *in vitro* (206). However, the reason for this discrepancy is likely to be the concentration of angiotensin II used, with the study herein using physiological relevant concentrations (300-600pM) (208), compared to supraphysiological concentrations 150-300x higher (100nM) (206). In addition, the differential cellular response may also be a consequence of cellular density and/or growth phase at the point of angiotensin II addition, with lower densities being more prone to activation of a proliferative stimulus than higher confluency cells wherein proliferation would be limited by contact inhibition (224). Alternatively, there may also be differences in the cell population, with the commercially sourced HCF used in this study confirmed as a pure population, whereas the cells used in the opposing study are an enriched population of HCF from a cardiac explant and thus may contain a number of other cell types alongside the enriched HCF population. If correct, then the modest hyperplastic response reported in these latter cells may be a consequence of indirect mechanism involving paracrine signalling rather than a direct HCF-mediated response. Despite these apparent discrepancies, importantly neither study identified a hypertrophic response of HCF to angiotensin II, in contrast to that confirmed for cardiomyocytes. This however does not preclude an involvement of CFs in the hypertrophic response of cardiac tissue to angiotensin II, as several studies have now highlighted a cell-communication relationship between cardiomyocytes and CFs in this regard (225-227). For instance, conditioned media from HCFs exposed to angiotensin II has been shown to induce hypertrophy of rat cardiac myocytes, exosomes secreted from HCFs in response to angiotensin II can augment cardiomyocyte hypertrophy, with other studies identifying a role for paracrine signalling from

HCF to cardiomyocytes in the hypertrophic response (226-228). This thereby implies a close relationship between HCF and cardiomyocytes in the hypertrophic response to angiotensin II, with significant implications for extrapolation into other cardiac responses to external agents.

Based on similarities in clinical presentations between heart failure and AIC coupled to the fact that ACEi and ARBs can reduce or prevent the progression or development of heart failure associated with anthracyclines, it has been strongly implied that angiotensin signalling links to the toxicological mechanism of anthracyclines, particularly cellular hypertrophy (34). This is supported by histological studies of hearts from adult patients treated with anthracyclines which have shown the presence of extensive myocyte hypertrophy (54, 229). Interestingly, the effects upon cardiomyocytes following anthracyclines, appears to be similar to that observed with excess angiotensin II, which causes inflammation, oxidative stress and cell death, with prolonged effects presenting as cardiac hypertrophy (62). In order to address this relationship, in this study the morphological responses of AC10 cardiomyocytes to sub-toxic concentrations of doxorubicin, mirroring the clinical situation, was explored. This subsequently revealed a concentration dependent hypertrophic response of cardiomyocytes after 24 hours of exposure to doxorubicin, as detected by xCELLigence and confirmed by no change in cell viability and imaging. A cellular size increase was sustained at 48 hours with sub-toxic concentrations (50 and 100nM), analogous to the response expected for 'surviving' cardiomyocytes. However, at concentrations reflective of cytotoxic concentrations of doxorubicin (250 and 500nM), the initial hypertrophic response of cardiomyocytes was reversed by 48 hours, indicative of cellular loss or damage. With respect to HCF, exposure to doxorubicin at concentrations, below those that induce cardiotoxicity, did not induce morphological changes or hypertrophy in this cell population, an observation in agreement with exposure to angiotensin II. Similarly to cardiomyocytes, exposure of higher concentrations of doxorubicin, falling within the range identified as cytotoxic for this cell type, led to a reduction in xCELLigence cell index and comparative loss of cell viability, reinforcing the initial cytotoxic response of cardiac cells at or around their therapeutic dose. These findings thereby support and confirm a close relationship between angiotensin II-induced hypertrophy of cardiomyocytes and that induced by doxorubicin.

The initiation of cardiomyocyte hypertrophy by both angiotensin II and doxorubicin raised the potential for synergistic or additive effects, which would indicate parallel rather than similar effects and molecular pathways. Co-treatment of doxorubicin alongside physiological concentrations of angiotensin II indicated no such combination of effects in

terms of cytotoxicity, with the presence of angiotensin II not significantly affecting IC_{50} values for doxorubicin in either AC10 cardiomyocytes or HCF. Similarly, no synergistic or additive effects were observed with regards the hypertrophic response of AC10 cardiomyocytes, strongly implying that angiotensin II and doxorubicin induce hypertrophy and cytotoxic effects via the same pathway. This supports the hypothesis that angiotensin II signalling pathway plays a role in doxorubicin induced cardiotoxicity and highlights the potential relevance of drugs targeting RAAS to mitigate anthracycline-associated cardiac damage.

In conclusion, while several clinical studies have supported the use of heart failure therapies such as ACEi and ARBs in reducing the delayed cardiotoxicity associated with anthracycline, the mechanism of AIC and the involvement of RAAS in the pathological process of AIC still not understood. The findings in this chapter provide an insight on the direct cardiac cell's response to angiotensin II and doxorubicin which induce hypertrophy in human cardiomyocyte, but not HCF. This highlights the differential cardiac response to doxorubicin and emphasizing the important to consider each type of cells when assessing the cardiotoxic effect of anthracyclines. Notably, combined treatment did not result in an additive hypertrophic or cytotoxic effect, suggesting that angiotensin II and doxorubicin induce hypertrophy and cytotoxic effects via the same pathway and provide further evidence support the relationship between angiotensin II signalling pathway and AIC.

Chapter 4. Characterisation of an Involvement of the Angiotensin-Signalling Pathway in Cardiac Cellular Response to Doxorubicin

4.1 Introduction

The stimulation of cardiomyocyte hypertrophy by doxorubicin at sub-toxic concentrations (Chapter 3), in a manner comparative to that induced by exposure to the physiological stimulus angiotensin II, offers a new perspective in terms of our appreciation of AIC. Instigation of such a morphological change and stress in those cardiac cells which have not succumbed to the cytotoxic effects of this agent, especially at concentrations reportedly non-toxic to these cells and reflective of the exposures related to pharmacokinetic clearance, offers new perspectives in terms of understanding the progressive and delayed manifestation of this toxicity. This is especially pertinent when relating short-term exposure to anthracyclines relative to symptomatic presentation of cardiac failure several years later.

Angiotensin II exerts its effect by binding primarily to AT1R (see section 1.7) (118, 119). In the cardiovascular system, activation of AT1R is implicated in many physiological and pathological functions, playing a key role in regulating cardiac functions, including contractile force, heart rate, and blood vessel tone (110, 115). AT1R has become a significant target for therapeutic interventions in cardiovascular disease, through direct inhibition of angiotensin II effect by treatment with ARBs (146, 147). Generally, ARBs are well-tolerated and have less side effects compared to other drugs perturbating angiotensin II signalling due to selective inhibition of AT1R (230). While all ARBs share the fundamental mechanism of blocking AT1R, they exhibit notable differences in their pharmacokinetic and pharmacodynamic properties. ARBs have varying binding affinity to AT1R as telmisartan has a prolong receptor blocking and dissociates from the AT1R receptor very slowly after binding (231). ARBs also have different half-life as telmisartan has the longest half-life (~24 hours) providing sustained receptor blockade, whereas losartan has a shorter half-life (~2 hours) and weaker affinity to AT1R (232). Some of ARBs are prodrug such as candesartan cilexetil which require activation to their active form in liver or gastrointestinal tract (232, 233). These differences in pharmacological properties may translate into varying clinical outcomes, suggesting that ARBs should not be considered interchangeable within their class (230).

In terms of the molecular mechanisms, AT1R activation and binding has been linked to different cellular responses including oxidative stress, inflammation, and cell death which all contributes to cardiac remodelling and hypertrophy (114, 115). Of importance for the study of anthracycline-induced hypertrophy, several studies have supported the induction of cardiomyocyte hypertrophy, a hallmark of adverse cardiac remodelling, and fibroblast activation through AT1R (114, 170, 234). Together these pathophysiological and structural changes lead to cardiac stiffening and subsequent reduction in the cardiac ejection fraction, independently of effects upon systemic blood pressure (125).

A further dimension to a potential link between AIC and effects caused by angiotensin II is offered by studies indicating a role for AT1R in stimulation or activation of several toxicological mechanisms in cardiac cells, including generation of ROS, induction of mitochondrial damage, and subsequent oxidative stress (11, 12, 34, 235). Therefore, understanding how angiotensin II signalling pathway, particularly AT1R, might influence the cardiac response to doxorubicin is crucial in elucidating the mechanism of AIC.

4.1.1 Aim and objectives

Aim: Determination of the involvement of the angiotensin-signalling pathway in the mechanism of AIC and doxorubicin-induced hypertrophy of human cardiac cells *in vitro*. This will be achieved by the following objectives:

- Assess the effects of therapeutics which perturb angiotensin signalling (ACEi and ARB) upon sensitivity of cardiac cells, specifically AC10 cardiomyocytes and HCF, to doxorubicin-mediated cytotoxicity.
- Characterisation of the requirement for AT1R-mediated activity in doxorubicin-induced hypertrophy of human cardiac cells *in vitro*, using the human AC10 cardiomyocyte, pre-exposed to the angiotensin receptor blocking therapeutic, telmisartan.
- Investigate the effects of doxorubicin and/or angiotensin II on genetic transcription of AT1R in the human AC10 cardiomyocyte, hiPSC-CMs and HCF.
- Determine the effect of exposure of human AC10 cardiomyocyte, and HCF to doxorubicin upon protein expression of AT1R.

4.2 Material and Method

4.2.1 Evaluation of viability of human AC10 cardiomyocytes and HCF following exposure to ACEi and ARBs, determined by MTS assay

AC10 and HCF cells were seeded into 96-well plates at a density of $5x10^3$ cells/well and viability assessed following exposure to the ACEi Enalapril, Enalaprilat (active form on ACEi enalapril), or the ARBs Telmisartan, Losartan or Candesartan, for a 96h continuous period using the MTS assay, as previously described (section 2.4). In all cases, on Day 0-cells were seeded and allowed to adhere to the plate overnight. On Day -1, treated with relevant concentrations of ACEi, ARB or vehicle control (DMSO), and the experimental endpoint (cellular viability) measured after the incubation period to generate an IC_{50} value. A 2x dilution series of test ACEi or ARB were performed across each individual plate, with final concentrations ranging from 0.08 µM to 10 µM which represent clinical exposures (236-239). All studies were repeated a minimum of three times and IC_{50} values determined from three replicates.

4.2.2 Evaluation of ability of ACEi or ARBs to reduce the cytotoxicity response of human AC10 cardiomyocytes and HCF to doxorubicin, determined by MTS assay

AC10 and HCF cells were seeded into 96-well plates at a density of $5x10^3$ cells/well and viability assessed following exposure to doxorubicin in the presence of the ACEi Enalapril, Enalaprilat (active form on ACEi enalapril), or the ARBs Telmisartan, Losartan or Candesartan, for a 96h continuous period using the MTS assay, as previously described (section 2.4). Cells were seeded on Day -0 and allowed to adhere to the plate overnight. On day 1, the top half of the plate (rows A-D) treated with doxorubicin in the absence of ACEi or ARB (instead adding drug vehicle, DMSO) and the bottom half of the plate (E-H) was treated with doxorubicin in the presence of 5 µM of the ACEi or ARB. In relation to doxorubicin, a 10x dilution series was performed across the plate, with final concentrations ranging from 100 fM-10 µM. On day 2, 24h after drug exposure, doxorubicin exposure was ceased, with the media in rows A-D replaced with media containing drug vehicle alone and the media in rows E-H replaced with media containing 5 µM of the respective ACEi or ARB. The experimental endpoint (cellular viability) was measured on day 4 (96h) to generate an IC_{50} value. In all cases the maximal

exposure to DMSO did not exceed 0.1%. All studies were repeated a minimum of three times and IC_{50} values determined from all replicates.

4.2.3 Evaluation of ARBs efficacy in mitigating doxorubicin-induced hypertrophy in AC10, determined by xCELLigence RTCA

AC10 cells were seeded at a density of $1x10^4$ cells per well into a 16-well E-Plate of the xCELLigence RTCA system, as previously described (Section 2.5). Cells were then maintained for up to a 48h period, until the plateau growth phase was reached. Cells were then exposed to either 5 µM of the ARBs telmisartan, losartan, or candesartan, or to drug vehicle (DMSO). After a 24h period, media was replaced with that containing 50nM doxorubicin in the presence or absence of the respective ARB. After a further 24h, media was replaced with that containing the respective ARB (or DMSO) in the absence of doxorubicin. The effect of pre-exposure to ARB drugs on doxorubicin-induced hypertrophy was assessed non-invasively in real-time for a further 48 h after the initial doxorubicin exposure.

4.2.4 Evaluation of ARB Telmisartan to mitigate doxorubicin-induced hypertrophy in AC10, determined by measurement of cell size

AC10 cells were seeded at a density of $2x10^4$ cells per well into a 6-well flat-bottomed cell culture plate and allowed to adhere overnight. Cells were then exposed to either 5 µM of the ARBs telmisartan or to drug vehicle (DMSO). After a 24h period, media was replaced with that containing 50nM doxorubicin in the presence or absence of telmisartan. After a further 24h, media was replaced with that containing the telmisartan (or DMSO as vehicle control) in the absence of doxorubicin. The effect of pre-exposure to telmisartan on doxorubicin-induced hypertrophy was assessed 48 h after the initial doxorubicin exposure. Cells were exposed to 1X CellMask™ Actin Tracking Stains solution (Invitrogen) for a period of 15 minutes (section 2.6). Micrograph images were collected by fluorescent microscopy at a magnification of 20x (NikonTE2000 microscope). The surface area of a minimum of 100 cells in 5 random fields per well were determined using ImageJ software.

4.2.5 Maintenance of human induced pluripotent stem cell derived cardiomyocytes (hiPSC-CMs)

The cryopreserved hiPSC-CMs obtained from FUJIFILM's iCell Cardiomyocytes was cultured and maintained following the iCell® Cardiomyocytes Application Protocol. Briefly, 24-well culture plate was coated with 0.6mL/well of 5µg/ml fibronectin and incubated overnight. Fibronectin is aspirated immediately before addition of cell suspension. Cells were thawed in a 37°C water bath, followed by transferring them into a pre-warmed plating medium. Cell viability and density were determined using a haemocytometer then plated onto culture vessels. hiPSC-CMs were cultured in a cell culture incubator at 37°C, 5% CO2 and the media changed 48 hours post-plating with a Maintenance Medium. Subsequently, the medium is changed every two days to support optimal growth conditions.

4.2.6 Assessment of cellular expression of AT1R using Real-time quantitative polymerase chain reaction (RT-qPCR)

4.2.6.1 RNA extraction for gene expression analysis in human AC10 cardiomyocytes and HCF

AC10 and HCF were seeded at a density of 3 x 10^5 cells/well and 7 x 10^4 cells/well, respectively into a 6-well flat-bottomed cell culture plate and allowed to adhere overnight. Culture conditions for both AC10 and HCF is described in (section 2.1). After a 24h period, cells were exposed to 50nM, 100nM, 250nM, 500nM of doxorubicin, 300pM angiotensin II or the relative concentration of the drug vehicle (DMSO). After a 24h exposure to doxorubicin, angiotensin II or DMSO, media in all wells was replaced with media containing DMSO drug vehicle alone. Throughout these experiments, the maximal exposure to DMSO did not exceed 0.1%. After a further 4-, 8-, 16-, and 24-hours period, cells were immediately washed with HBSS to remove residual cell debris and total RNA was extracted according to the manufacture procedure using RNeasy Mini Kit Qiagen®, (Qiagen, Netherlands) as described in section 2.7.1.

4.2.6.2 RNA extraction for gene expression analysis in human induced pluripotent stem cell derived cardiomyocytes (hiPSC-CMs)

Total RNA was extracted from hiPSC-CMs following the iCell® Cardiomyocytes Application Protocol. Briefly, 24-well cell culture plates were coated with fibronectin to facilitate cellular

adhesion, hiPSC-CMs were seeded at density of 1.6 x 10^5 cells/well and were maintained according to culture conditions for hiPSC-CMs described in (section 4.2.5). The hiPSC-CMs were exposed to 50nM, 100nM, 250nM, or 500nM of doxorubicin or the relative concentration of the drug vehicle (DMSO). After 24, the culture medium was carefully aspirated and immediately washed with PBS to remove residual cell debris. Total RNA was extracted according to the manufacture procedure using RNeasy Micro Kit Qiagen®, (Qiagen, Netherlands). Briefly, RLT lysis buffer was added directly to the well followed by pipetting to ensure complete disruption. Then, the lysate was transferred to QIAshredder spin column for homogenization, diluted in RNase-free water, and supplemented with Proteinase K (Qiagen). The mixture was incubated at 55°C for 10 minutes on a heated block. After centrifugation, the supernatant was mixed with 0.5 volumes 100% ethanol and passed through RNeasy spin column. The RNA was washed with Buffer RW1, treated with DNase I to remove DNA, and subsequently washed with buffers RW1, RPE, and 80% ethanol. Finally, the RNA was eluted from the column using RNase-free water. The quality and the quantity of RNA were measured using Nanodrop Spectrophotometer ND-1000 (Nanodrop Technologies), with an 260nm/280nm ratio >2 being considered acceptable for future analyses. Samples were stored at -80°C.

4.2.6.3 Reverse transcription to cDNA for gene expression analysis

Total RNA 500 ng was reverse transcribed to cDNA using a High-Capacity cDNA Reverse Transcription kit (Applied Biosystems™) according to the manufacture procedure as mentioned in section 2.7.2.

4.2.6.4 Real-time quantitative polymerase chain reaction (RT-qPCR) analysis of housekeeping comparator gene

Identification of a robust housekeeping comparator gene for expression analyses is paramount for quantification of AT1R expression. In the majority of RT-qPCR studies of gene expression in cardiac cells, Glyceraldehyde-3-phosphate dehydrogenase (GAPDH) is used routinely (240, 241). However, GAPDH has been reported as being a translational suppressor for AT1R expression, invalidating its use for this study (242). Thus, various housekeeping genes were chosen for comparison, including ribosomal protein L13a (RPL13A), hypoxanthine-guanine phosphoribosyl transferase 1 (HPRT1), and Beta-actin (β-actin). These housekeeping

genes were selected for comparative analysis to ensure accurate normalisation in AT1R gene expression studies.

RNA is extracted from AC10 and HCF as described in section 2.7.1 and total RNA 500 ng was reverse transcribed to cDNA as described in section 2.7.2. Expression was determined using RT-qPCR for three housekeeping genes RPL13A, HPRT1, and β-actin (see Table 4.1) for primer sequences). RT-qPCR run as per section 2.7.3. The mean threshold cycles (Ct) valued for genes were calculated by QuantStudio 7 software.

Table 4.1 Primer sequences

Gene	Primer	Sequence (5'-3')
RPL13A	Forward	CCT GGA GGA GAA GAG GAA AGA GA
	Reverse	TTG AGG ACC TCT GTG TAT TTG TCA A
HPRT1	Forward	TTG CTT TCC TTG GTC AGG CA
	Reverse	ATC CAA CAC TTC GTG GGG TC
β-actin	Forward	GAC GAC ATG GAG AAA ATC TG
	Reverse	ATG ATC TGG GTC ATC TTC TC

4.2.6.5 Real-time quantitative polymerase chain reaction (RT-qPCR) analysis of AT1R expression

RT-qPCR was performed to analyse AT1R gene expression (see Table 4.2, AT1R primer sequence) following exposure to 50nM, 100nM, 250nM, 500nM concentrations of doxorubicin, 300pM angiotensin II or drug vehicle (DMSO) in AC10, HCF, and hiPSC-CMs. RT-qPCR run as per section 2.7.3.

Table 4.2 AT1R primer sequence

Gene	Primer	Sequence (5'-3')
AT1R	Forward	GAT GAT TGT CCC AAA GCT GG
	Reverse	TAG GTA ATT GCC AAA GGG CC

4.2.7 Assessment of the changes in the AT1R protein expression using western blot

The AT1R protein expression assessed following exposure to doxorubicin for 4-, 8-,16-, 24-, 48-, 72-, and 96-hours in AC10 and HCF. AC10 and HCF were seeded at a density of 3 x 10^5 cells/well and 7 x 10^4 cells/well, respectively into a 6-well flat-bottomed cell culture plate and

allowed to adhere overnight. Culture conditions for both AC10s and HCFs is described in section 2.1. After a 24h period, cells were exposed to 50nM, 100nM, 250nM, or 500nM of doxorubicin or the relative concentration of the drug vehicle (DMSO). After a 24h exposure to doxorubicin or DMSO, media in all wells was replaced with media containing DMSO drug vehicle alone. Throughout these experiments, the maximal exposure to DMSO did not exceed 0.1%. After a further 4-, 8-, 16-, 24-, 48-, 72-, 96-hours period, cells were immediately washed with HBSS to remove residual cell debris and transferred to microcentrifuge tubes for each drug concentration. Cells were lysed using 175 µL lysis buffer and then sonicated for a total of 30 seconds.

BCA protein assay analysis is a colorimetric method for quantifying total protein concentration in a sample (PierceTM BCA Protein Assay Kit, ThermoFisher). Briefly, 10µL of diluted sample 1:10 added in quadruplicate to a 96- well plate. 10µL of protein standards were also added in quadruplicate to the 96-well plate. 190µL of the working reagent composed of Reagent A and Reagent B in 50:1 ratio was added to each well and mixed thoroughly. The plate incubated at 37°C for 30 minutes. After incubation, the absorbance of each well was measured at 562nm using a Thermoscientific Multiskan GO plate reader. The protein concentration of each sample was calculated and 20µg of protein sample mixed with water and 2x laemelli sample buffer (Containing β-mercaptoethanol), heated at 95°C for 5 minutes to denature proteins, then transferred onto wet ice.

Tris-glycine Sodium Dodecyl Sulphate (SDS)-Polyacrylamide 10% loading and 5% stacking gels was made and placed into electrophoresis rig filled with running buffer. 20µL of protein samples and 5µL of protein ladder (ab116028, Abcam) were loaded in the gel. The electrophoresis process was carried out for approximately 60 minutes, or until the dye had reached the gel's bottom, at an electric potential of 150V.

Using a wet transfer method, the separated proteins are transferred from the gel to a Nitrocellulose blotting membrane (Amersham™ Protran®; cytiva). It Involves sandwiching the gel and membrane between filter papers soaked in transfer buffer as follows: sponge – filter paper – membrane – gel – filter paper – sponge arrangement then placed into tank filled with transfer buffer containing 20% methanol and 300mA current supplied for one hour.

When the transfer finish, the membrane was washed with Tris-Buffered Saline (TBS) and blocked using 5% skimmed milk powder dissolved in TBS and 0.1% Tween®-20 (TBS-T) for 1 hour to prevent non-specific antibody binding then washed 2X10 minutes with TBS-T. To probe for expression of AT1R proteins, the membrane incubated overnight at 4°C on a rotating

mixer with the primary AT1R antibody (Abcam ab124734) diluted 1:250 in 1% skimmed milk powder dissolved in TBS-T. Next day, the membrane washed 2X10 minutes with TBS-T and incubated with the secondary antibody polyclonal swine anti-rabbit immunoglobulins/HRP (Agilent Technologies), optimised to 1:1500 for 1 hour on a rotating mixer at room temperature. The membrane then washed 3X10 minutes with TBS-T before chemiluminescence to detect the antibody binding. The enhanced chemiluminescent detection reagent (ECL) added to the membrane and left for 3 minutes. Excess ECL was removed, and bands were detected using a ChemiDoc MP System (BioRad, UK).

HRP Anti-beta Actin antibody [AC-15] (abcam AB49900) diluted 1:10 in 1% skimmed milk powder dissolved in TBS-T was used as loading control to ensure equal protein loading of the gel. The same membrane used to probe AT1R is striped using acid-stripping buffer and blocked once more with 5% milk dissolved in TBS-T for one hour. The membrane then reprobed with the β-actin and incubated for 1 hour on a rotating mixer at room temperature. The membrane then washed 3X10 minutes with TBS-T then visualized as mentioned above.
The molecular weight of the visible bands on the β-actin and AT1R treated membranes was ascertained using the protein ladder, with predicted molecular weights of 48 kDa and 35 kDa, respectively.

Quantifying Western blot bands was analysed using ImageJ software (Fiji, Image J 1.52, National Institutes of Health, USA) following Quantifications of Western Blots with ImageJ protocol (243). Briefly, pixel intensity values are measured for each protein band. This process is repeated for all lanes within the blot, including loading control bands and background areas. Values are recorded then exported to an Excel spreadsheet for further calculations.

Data normalisation is performed by inverting pixel densities using the formula (255 - X), where X represents the ImageJ-recorded value. The net intensity for each protein band is obtained by subtracting the background intensity from the band intensity. The final protein expression level is calculated as the ratio of the net band intensity to the net loading control intensity for each lane.

Statistical analysis was completed by calculating the fold change between the target protein (AT1R) and the loading control (β-actin). All experiments were performed in triplicate (N) and SEM between replicate were calculated. GraphPad Prism software used to present data and statistical analysis (Version 10.4.0, GraphPad Software, Inc.). For comparison, un-paired t test or One-way analysis of variance (ANOVA) test, and a post-hoc Dunnett's test was used when required.

4.3 Results

4.3.1 ACEi and ARBs do not induce cytotoxicity against AC10 and HCFs in vitro

In order to assess the cell viability of AC10 and HCF after exposure to ACEi or ARB, which will inform later studies, cells were exposed to the ACEi the active metabolite of enalapril, enalaprilat, or the ARBs Telmisartan, Losartan, and Candesartan for 96 hours at a concentration range of 0.08 µM to 10 µM. As shown in Figure 4.1, Figure 4.2, Figure 4.3, and Figure 4.4 for AC10 and Figure 4.5, Figure 4.6, Figure 4.7, and Figure 4.8 for HCF, no significant loss of cell viability was observed with any of the ACEi or ARBs across the range of concentrations tested.

4.3.2 Exposure of AC10 cardiomyocytes and HCF to either ACEi or ARBs does not affect cytotoxicity induced by doxorubicin

To assess whether ACEi or ARBs could reduce or mitigate the cytotoxic response of AC10 or HCF cells to doxorubicin, cells were pre-exposed to ACEi or ARBs prior to exposure for 24 hours to doxorubicin, with cell viability determined by MTS assay after a total 96-hour exposure period. As shown in Table 4.3 and Table 4.4 for AC10 and Table 4.5 and Table 4.6 for HCF, neither ACEi (enalapril and enalaprilat) or any of the tested ARBs (telmisartan, candesartan or losartan) resulted in a significant reduction in the cytotoxic IC_{50} of doxorubicin.

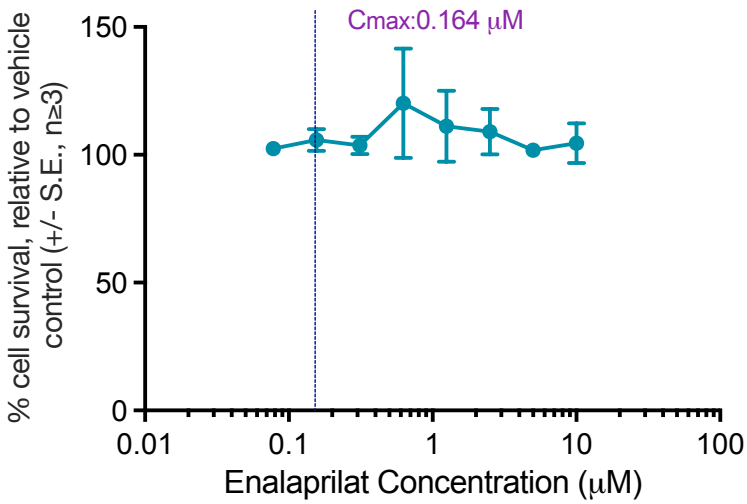

Figure 4.1 ACEi enalaprilat does not induce cytotoxicity in AC10 cells. AC10 exposed to clinically relevant concentrations of the ACEi enalaprilat for 96 hours normalised to DMSO vehicle control, as indicated by MTS cell viability assay. The C_{max} of drug is indicated by a dotted line. Each data point = mean +/- SE, n ≥ 3.

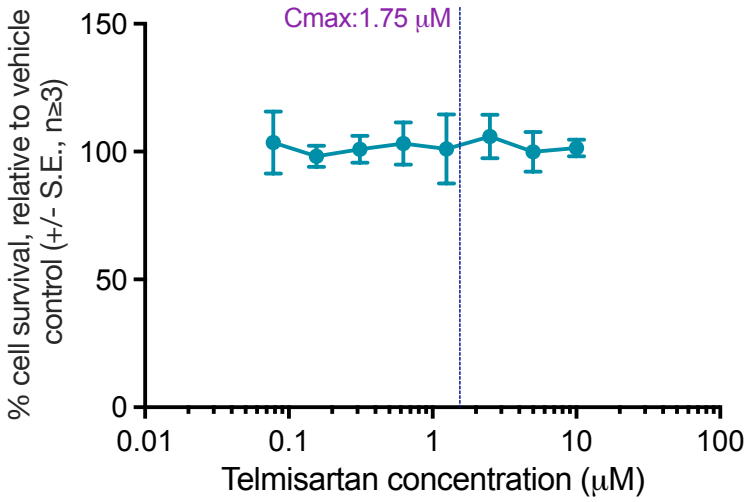

Figure 4.2 ARB Telmisartan does not induce cytotoxicity in AC10 cells. AC10 exposed to clinically relevant concentrations of the ARB Telmisartan for 96 hours normalised to DMSO vehicle control, as indicated by MTS cell viability assay. The C_{max} of drug is indicated by a dotted line. Each data point = mean +/- SE, n ≥ 3.

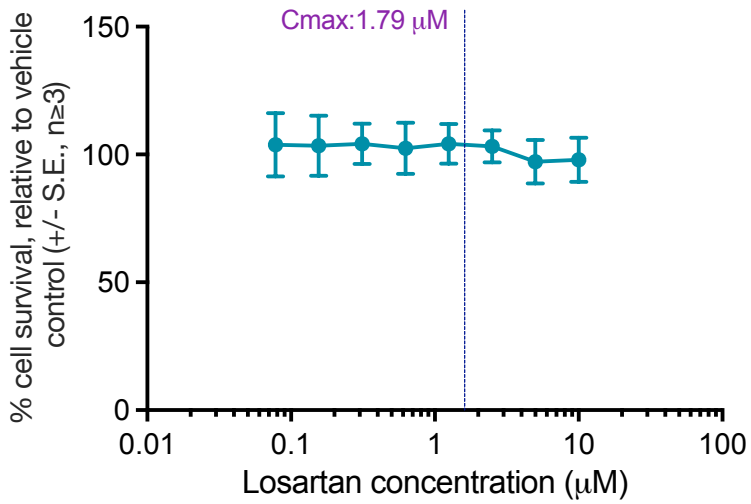

Figure 4.3 ARB Losartan does not induce cytotoxicity in AC10 cells. AC10 exposed to clinically relevant concentrations of the ARB Losartan for 96 hours normalised to DMSO vehicle control, as indicated by MTS cell viability assay. The C_{max} of drug is indicated by a dotted line. Each data point = mean +/- SE, n ≥ 3.

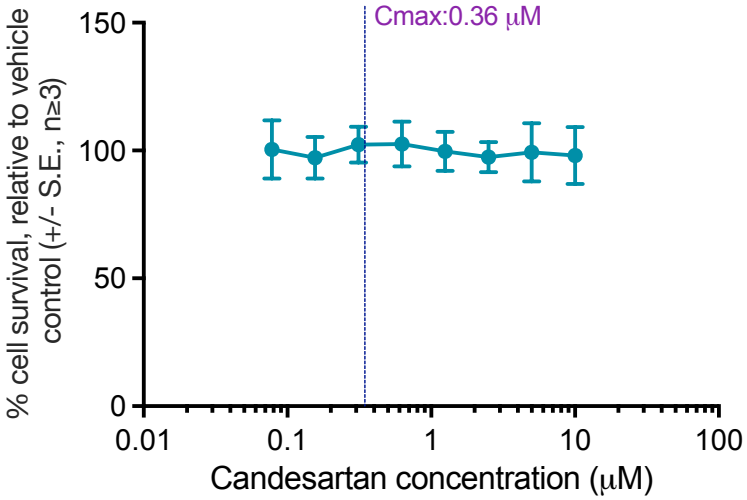

Figure 4.4 ARB Candesartan does not induce cytotoxicity in AC10 cells. AC10 exposed to clinically relevant concentrations of the ARB Candesartan for 96 hours normalised to DMSO vehicle control, as indicated by MTS cell viability assay. The C_{max} of drug is indicated by a dotted line. Each data point = mean +/- SE, n ≥ 3.

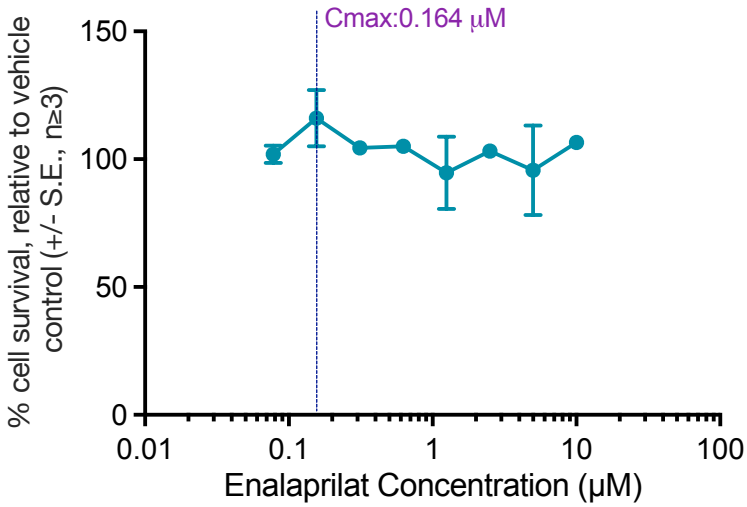

Figure 4.5 ACEi enalaprilat does not induce cytotoxicity in HCF cells. HCF exposed to clinically relevant concentrations of the ACEi enalaprilat for 96 hours normalised to DMSO vehicle control, as indicated by MTS cell viability assay. The C_{max} of drug is indicated by a dotted line. Each data point = mean +/- SE, n ≥ 3.

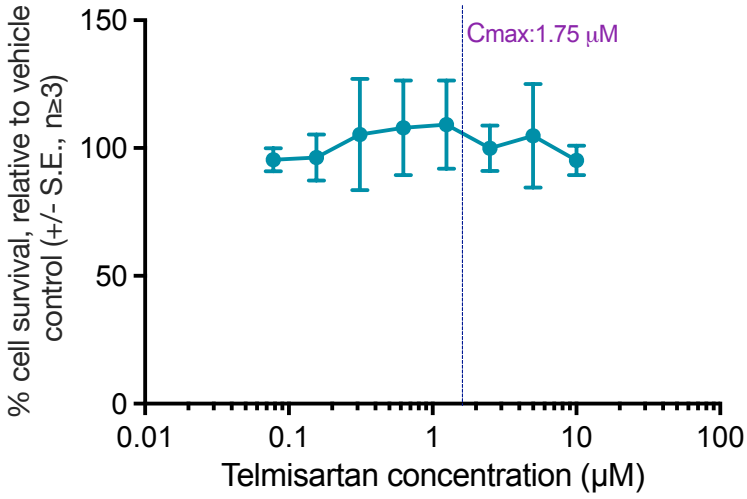

Figure 4.6 ARB Telmisartan does not induce cytotoxicity in HCF cells. HCF exposed to clinically relevant concentrations of the ARB Telmisartan for 96 hours normalised to DMSO vehicle control, as indicated by MTS cell viability assay. The C_{max} of drug is indicated by a dotted line. Each data point = mean +/- SE, n ≥ 3.

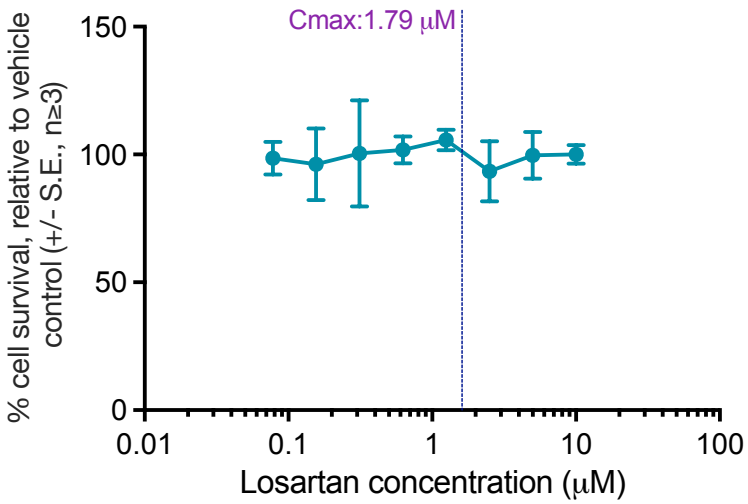

Figure 4.7 ARB Losartan does not induce cytotoxicity in HCF cells. HCF exposed to clinically relevant concentrations of the ARB Losartan for 96 hours normalised to DMSO vehicle control, as indicated by MTS cell viability assay. The C_{max} of drug is indicated by a dotted line. Each data point = mean +/- SE, n ≥ 3.

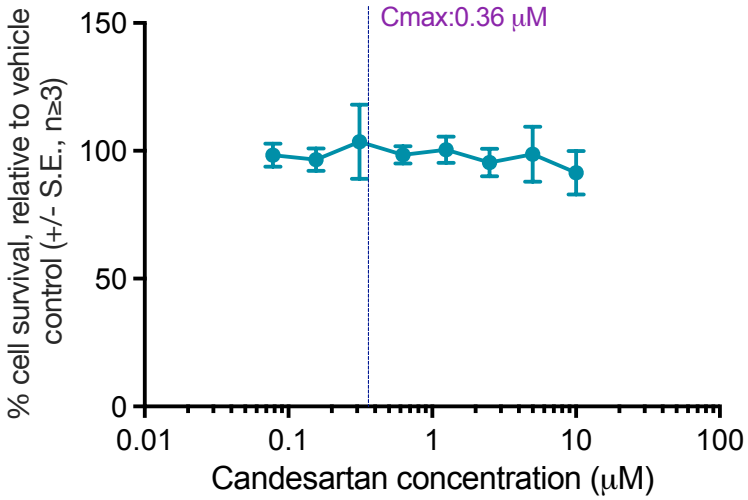

Figure 4.8 ARB Candesartan does not induce cytotoxicity in HCF cells. HCF exposed to clinically relevant concentrations of the ARB Candesartan for 96 hours normalised to DMSO vehicle control, as indicated by MTS cell viability assay. The C_{max} of drug is indicated by a dotted line. Each data point = mean +/- SE, n ≥ 3.

Table 4.3 Change in cytotoxicity IC_{50} of AC10 when exposed to 100 fM-10 µM concentrations of doxorubicin for 96-hours in the presence of 5uM ACEi. Data is determined by MTS assay and is representative of at least three repeats, presented as mean IC_{50} ±SEM. Statistical significance was determined by a One-way ANOVA with post-hoc Dunnett's multiple comparison test.

Doxorubicin	Enalapril	Enalaprilat	IC_{50}±SEM (nM)	p-value
+	-	-	48 ± 12	-
+	+	-	74 ± 19	0.260
+	-	+	56 ± 15	0.709

Table 4.4 Change in cytotoxicity IC_{50} of AC10 when exposed to 100 fM-10 µM concentrations of doxorubicin for 96-hours in the presence of 5uM ARBs. Data is representative of at least three repeats and presented as IC_{50} ±SEM. Statistical significance was determined by a One-way ANOVA with post-hoc Dunnett's multiple comparison test.

Doxorubicin	Telmisartan	Losartan	Candesartan	IC_{50}±SEM (nM)	p-value
+	-	-	-	48 ± 12	-
+	+	-	-	60 ± 2.0	0.4765
+	-	+	-	61 ± 0.9	0.4149
+	-	-	+	82 ± 14	0.1072

Table 4.5 Change in IC_{50} of HCF when exposed 100 fM-10 µM concentrations of doxorubicin for 96-hours in the presence of 5uM ACEi. Data is representative of at least three repeats and presented as IC_{50} ±SEM. Statistical significance was determined by a One-way ANOVA with post-hoc Dunnett's multiple comparison test.

Doxorubicin	Enalapril	Enalaprilat	IC_{50}±SEM (nM)	p-value
+	-	-	795±171	-
+	+	-	1000±281	0.5018
+	-	+	924±661	0.8265

Table 4.6 Change in IC_{50} of HCF when exposed to 100 fM-10 µM concentrations of doxorubicin for 96-hours in the presence of 5uM ARBs. Data is representative of at least three repeats and presented as IC_{50} ±SEM. Statistical significance was determined by a One-way ANOVA with post-hoc Dunnett's multiple comparison test.

Doxorubicin	Telmisartan	Losartan	Candesartan	IC_{50}±SEM (nM)	p-value
+	-	-	-	795±171	-
+	+	-	-	844±232	0.8749
+	-	+	-	795±169	0.9983
+	-	-	+	1068±294	0.4676

4.3.3 Telmisartan attenuates doxorubicin-induced hypertrophy in AC10

The effects of pre-exposure to telmisartan on doxorubicin induced hypertrophy in AC10 were determined by xCELLigence RTCA in real-time. The cell index of cells, which were in the plateau growth phase, increased in cells exposed to 50nM doxorubicin and cells exposed to 50nM doxorubicin in combination with 5µM telmisartan compared to cell index of control, when normalised to the point of telmisartan addition and after 48 hours of initial doxorubicin exposure. However, the cell index of cells pre-exposed to 5 µM telmisartan then exposed to 50nM doxorubicin significantly decreased compared to cell exposed to 50nM doxorubicin alone after 48 hours of initial doxorubicin exposure (Figure 4.9A and B), indicating that telmisartan mitigates the increase in the cell index caused by doxorubicin after 48 hrs of initial doxorubicin exposure.

MTS assay was performed 48 hours after doxorubicin exposure confirmed that neither 50nM doxorubicin or 50nM doxorubicin with 5µM telmisartan affects the viability of AC10 ($p=0.083$) as shown in Figure 4.9C, indicating that doxorubicin alone or telmisartan in combination with doxorubicin are not cytotoxic to AC10.

This finding was further confirmed by analysing changes in cell size using imaging, with a significant increase in cell area of AC10 observed in cells exposed to 50nM doxorubicin for 48 hours compared to control. However, a significant reduction in cell area of AC10 was observed in cells pre-exposed to 5 µM telmisartan then exposed to 50nM doxorubicin after 48 hours compared to cell exposed to doxorubicin alone (Figure 4.10A and B). The results confirmed that doxorubicin causes cell hypertrophy in AC10 cardiomyocytes, but pre-exposure to telmisartan mitigates this hypertrophic effect caused by doxorubicin.

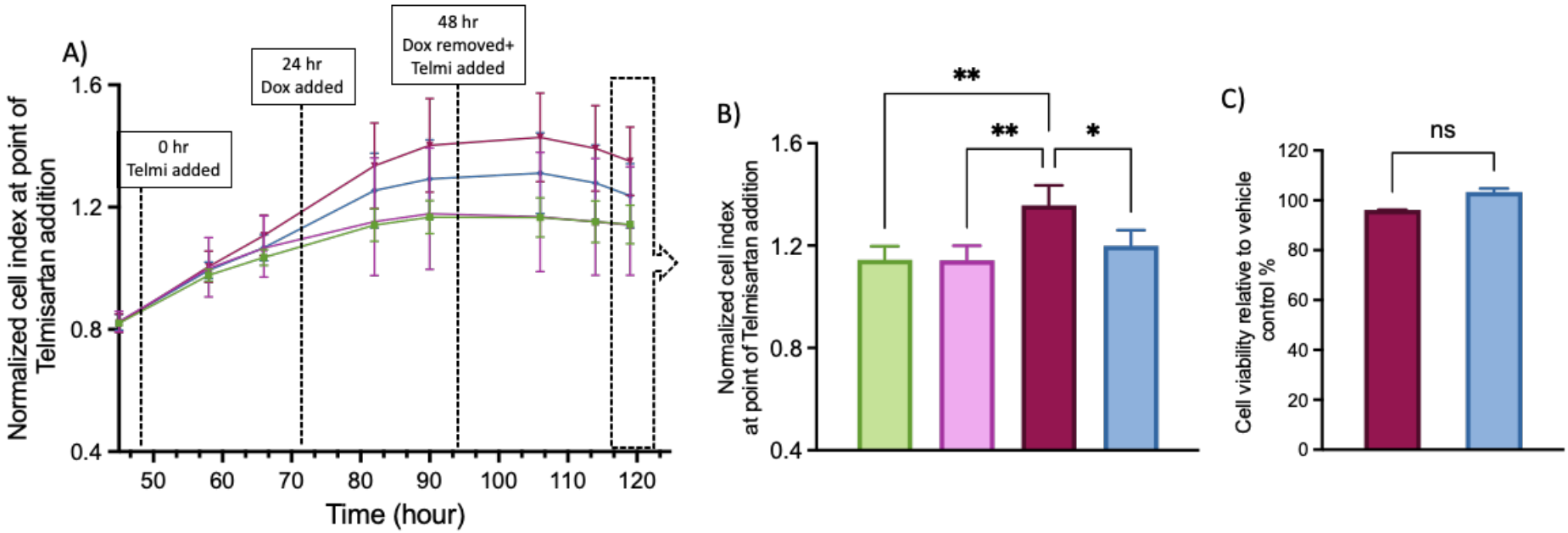

Figure 4.9 The effect of pre-exposure to telmisartan on the increase in cell index in xCELLigence caused by doxorubicin in AC10. (A) Time vs cell index (xCELLigence output) of AC10 cells following exposure to 50nM doxorubicin alone and following pre-exposed to 5µM telmisartan then additions of 50nM doxorubicin for 48 hrs. The cell index normalised to the point of telmisartan addition as indicated in the graph, (B) This quantification graph extracted from xCELLigence graph demonstrates the effect of pre-exposure to telmisartan on AC10 48 hours after the initial exposure to doxorubicin. The cell index was normalised at point of telmisartan addition, and C) Confirmation that AC10 maintain viability 48 hrs following additions of 50nM doxorubicin alone or 50nM doxorubicin+ 5µM telmisartan relative to vehicle control, assessed using an MTS assay. Each data point = mean +/- SE, n ≥ 3. Statistical significance was determined by a One-way ANOVA with post-hoc Dunnett's multiple comparison test. (* = $p < 0.05$, ** = $p < 0.01$). Control, 50nM Doxorubicin, 5µM Telmisartan, and 5µM Telmisartan + 50nM Doxorubicin.

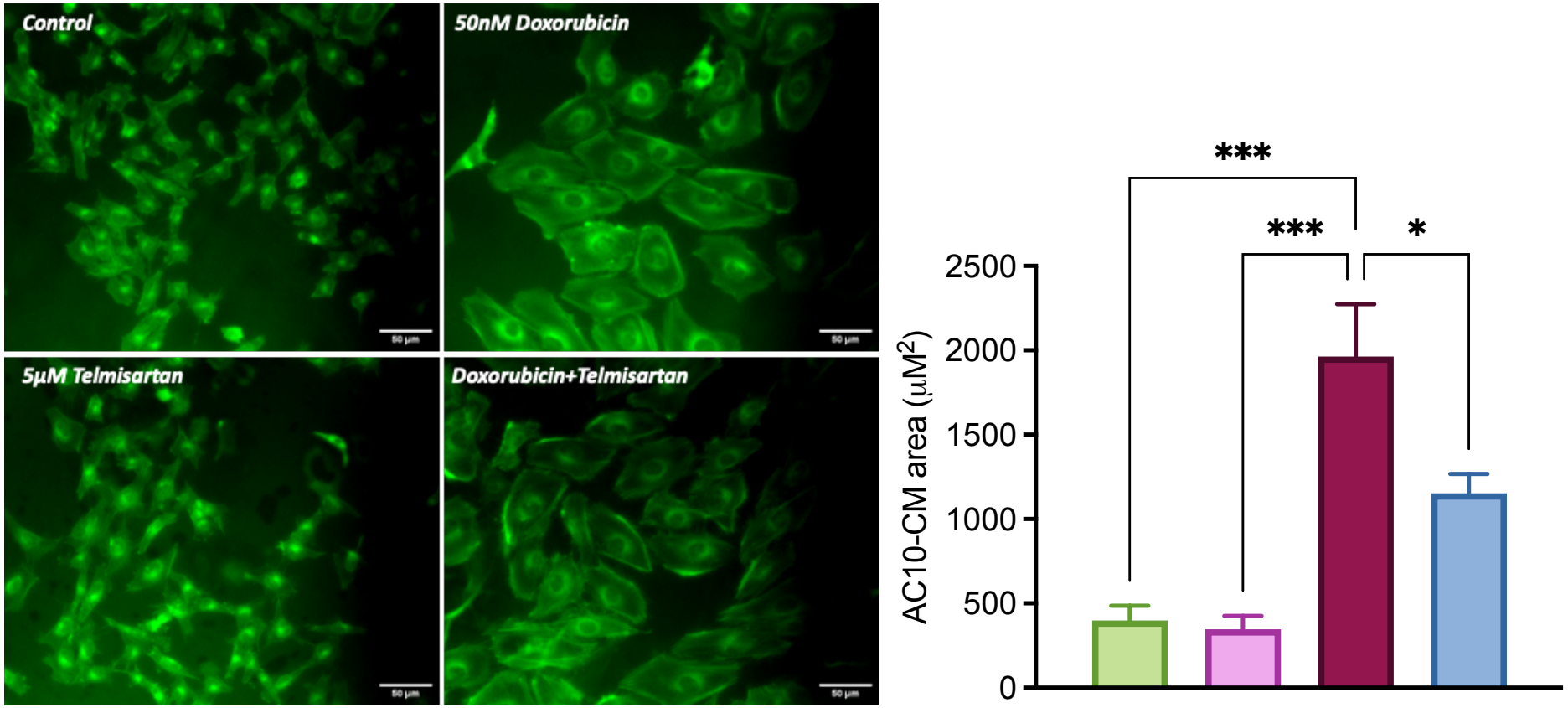

Figure 4.10 Telmisartan attenuates the hypertrophy caused by Doxorubicin in AC10. Representative images show cell area changes in AC10 exposed to 50nM doxorubicin alone or pre-exposed to 5µM telmisartan then exposed to 50nM doxorubicin for 48 hrs. The quantification graph illustrates mean cell area (µm²) increased in cells exposed to 50nM doxorubicin compared to control, but mean cell area (µm²) decreased in cells pre-exposed to 5µM telmisartan then exposed to 50nM doxorubicin compared to cells exposed to 50nM doxorubicin. Cells were stained with a green, fluorescent marker to visualize cell structure. Mean cell area (µm²) was calculated using ImageJ. Each data point = mean +/- SE, n ≥ 3. Statistical significance was determined by a One-way ANOVA with post-hoc Dunnett's multiple comparison test. (* = $p < 0.05$, *** = $p < 0.001$). (Scale bar: 50 µm) (Magnification:20x). Control, 50nM Doxorubicin, 5µM telmisartan, and 5µM telmisartan + 50nM Doxorubicin.

4.3.4 Selective efficacy of telmisartan in mitigation of doxorubicin induced hypertrophy in AC10 compared to other ARBs

In the previous study we observed that telmisartan able to mitigate doxorubicin induced hypertrophy in AC10. In this study, further investigation was done to determine if this effect was unique to telmisartan or if other ARBs, like losartan and candesartan, could also produce similar effect. The effects of pre-exposure to candesartan on doxorubicin induced hypertrophy in AC10 were determined by xCELLigence RTCA in real-time. The cell index of cells, which were in the plateau growth phase, increased in cells exposed to 50nM doxorubicin and cells exposed to 50nM doxorubicin in combination with 5µM candesartan compared to cell index of control, when normalised to the point of candesartan addition and after 48 hours of initial doxorubicin exposure. However, no significant decrease in the cell index of cells pre-exposed to 5 µM candesartan then exposed to 50nM doxorubicin compared to cell exposed to 50nM doxorubicin alone after 48 hours of initial doxorubicin exposure was observed ($p=0.16$) (Figure 4.11A and B), indicating that candesartan did not mitigate doxorubicin induced hypertrophy in AC10. MTS assay was also performed 48 hours after doxorubicin exposure confirmed that exposure to 50nM doxorubicin or 5µM candesartan in combination with 50nM doxorubicin did not affect the viability of AC10 ($p=0.61$) as shown in Figure 4.11C**,** indicating that doxorubicin alone or candesartan in combination with doxorubicin are not cytotoxic to AC10.

As shown in Figure 4.12A and B, the cell index of cells, which were in the plateau growth phase, increased in both cells exposed to 50nM doxorubicin alone and cells exposed to 50nM doxorubicin in combination with 5µM losartan compared to control, when normalised to the point of losartan addition and after 48 hours of initial doxorubicin exposure. However, no significant decrease in the cell index of cells pre-exposed with 5 µM losartan then exposed to 50nM doxorubicin compared to cell exposed to 50nM doxorubicin alone after 48 hours of initial doxorubicin exposure was observed ($p>0.99$). MTS assay was also performed 48 hours after doxorubicin exposure confirmed that exposure to 50nM doxorubicin or 5µM losartan in combination with 50nM doxorubicin did not affect the viability of AC10 ($p=0.86$) as shown in Figure 4.12C, indicating that doxorubicin alone or losartan in combination with doxorubicin are not cytotoxic to AC10.

These findings indicate that pre-exposure to 5µM candesartan and 5µM losartan were unable to mitigate doxorubicin induced hypertrophy in AC10.

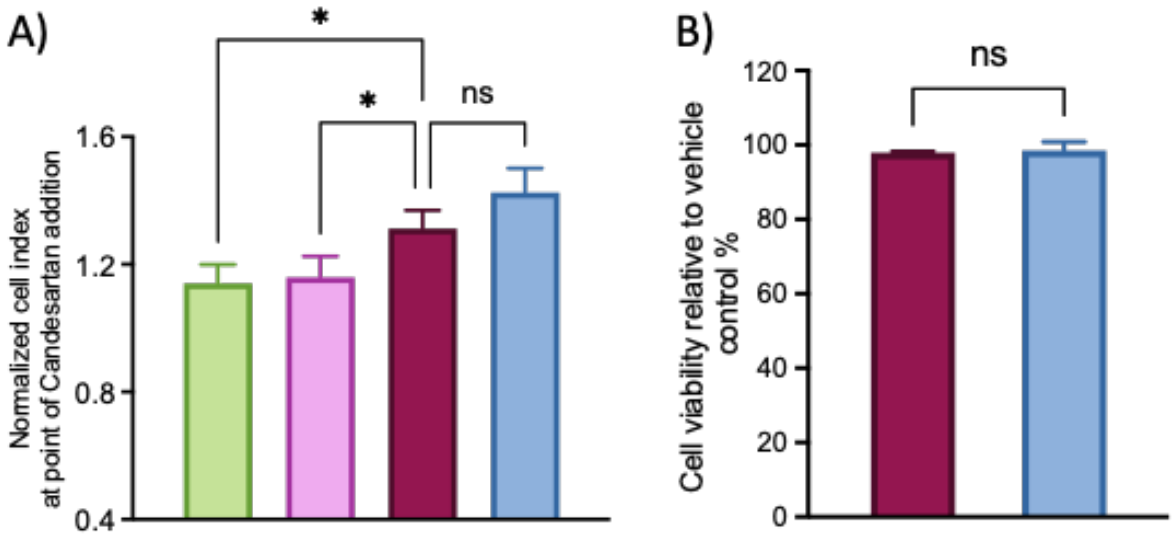

Figure 4.11 Candesartan does not prevent doxorubicin-induced hypertrophy in AC10. (A) Normalised cell index after 48hrs of doxorubicin addition and pre-exposure to Candesartan. (B) Confirmation that AC10 maintain viability 48 hrs following additions of 50nM doxorubicin alone or 50nM doxorubicin+ 5µM candesartan relative to vehicle control, assessed using an MTS assay. Each data point = mean +/- SE, n ≥ 3. Statistical significance was determined by a One-way ANOVA with post-hoc Dunnett's multiple comparison test. (* = $p < 0.05$). Control, 50nM Doxorubicin, 5µM Candesartan, and 5µM Candesartan + 50nM Doxorubicin.

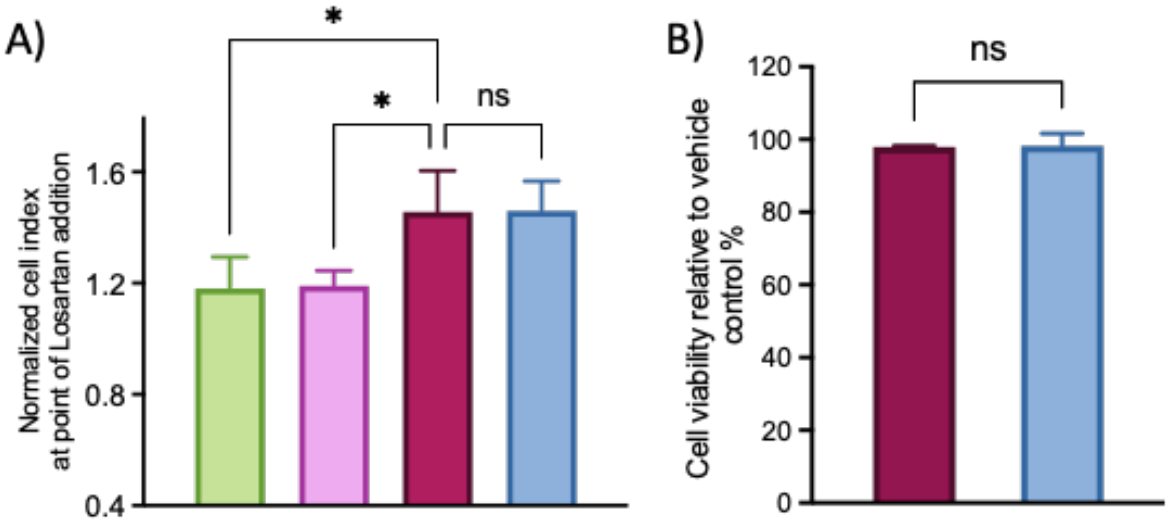

Figure 4.12 Losartan does not prevent Doxorubicin-induced hypertrophy in AC10. (A) Normalised cell index after 48hrs of doxorubicin addition and pre-exposure to Losartan. (B) Confirmation that AC10 maintain viability 48 hrs following additions of 50nM doxorubicin alone or 50nM Doxorubicin+ 5µM Losartan relative to vehicle control, assessed using an MTS assay. Each data point = mean +/- SE, n ≥ 3. Statistical significance was determined by a One-way ANOVA with post-hoc Dunnett's multiple comparison test. (* = $p < 0.05$). Control, 50nM Doxorubicin, 5µM Losartan, and 5µM Losartan + 50nM Doxorubicin.

4.3.5 Confirmation of housekeeping gene to use for standardisation of gene expression analyses in human cardiac cell types

As GAPDH has been reported as being a translational suppressor for AT1R expression, invalidating its use for this study (242), various housekeeping genes were chosen for comparison, including RPL13A, HPRT1, and β-actin. Using cDNA of control sample, melt curve plots of AT1R, RPL13A, HPRT1 and β-actin were generated as shown in Figure 4.13 to assess the specificity of the RT-qPCR amplified products. The melt curve plots show a sharp and single peak, the amplified product appears homogeneous with no presence of non-specific product or primer-dimer, indicating that the target sequence was amplified specifically.

Primer efficiency was assessed using a serial cDNA dilution of the control samples, (AC10: Figure 4.14 and Table 4.7) (HCF: Figure 4.15 and Table 4.8). A standard curve for each reference gene was generated from the qRT-PCR cycle quantification (Cq) values, which were calculated using the QuantStudio 7 software. The correlation coefficients (r^2) and amplification efficiencies were calculated. The standard curves verify the linearity and efficiency of the amplification process, ensuring that the primers function effectively across a range of sample concentrations. Based on the calculations, RPL13A and β-actin were selected as housekeeping genes for future experiment in both AC10 and HCF.

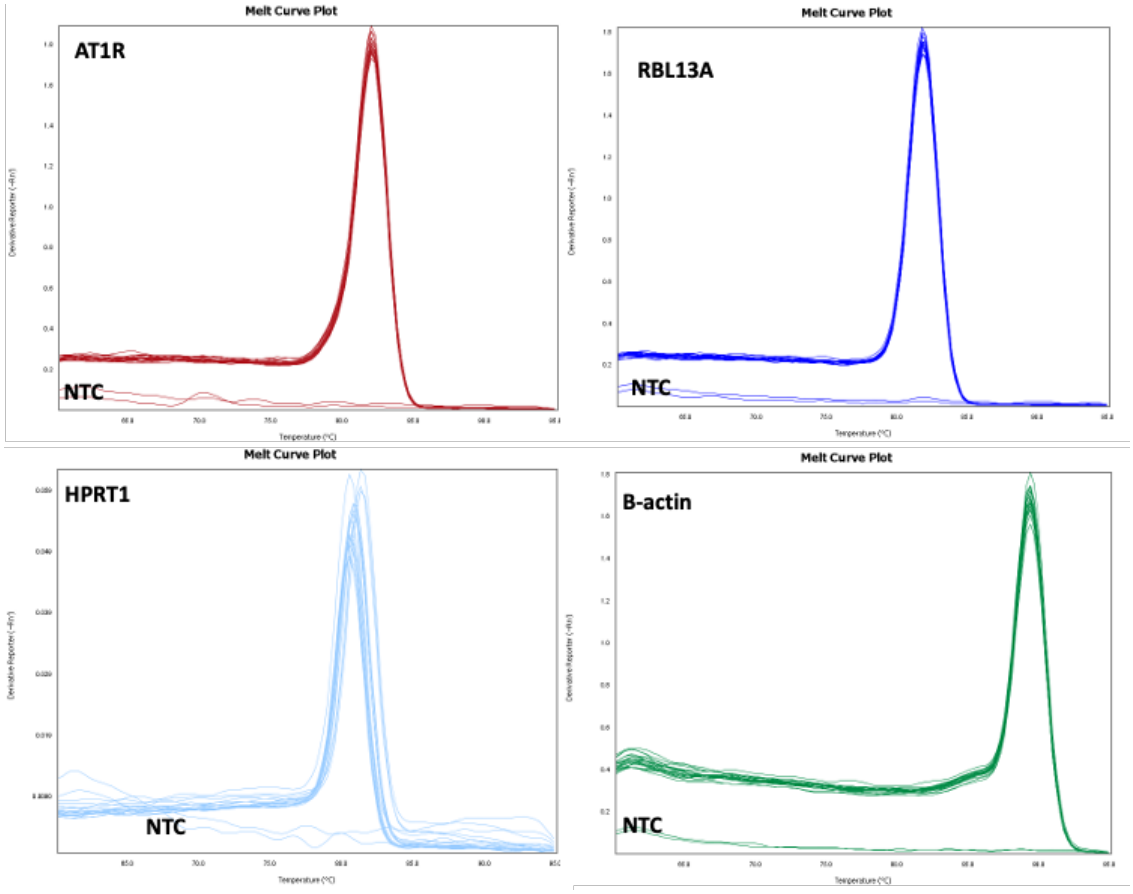

Figure 4.13 Melt curve plots for different genes used in the qPCR experiments. These plots for AT1R, RPL13A, HPRT1, and β-actin are screenshots from QuantStudio 7 software. The lower lines represent the non-target control (NTC).

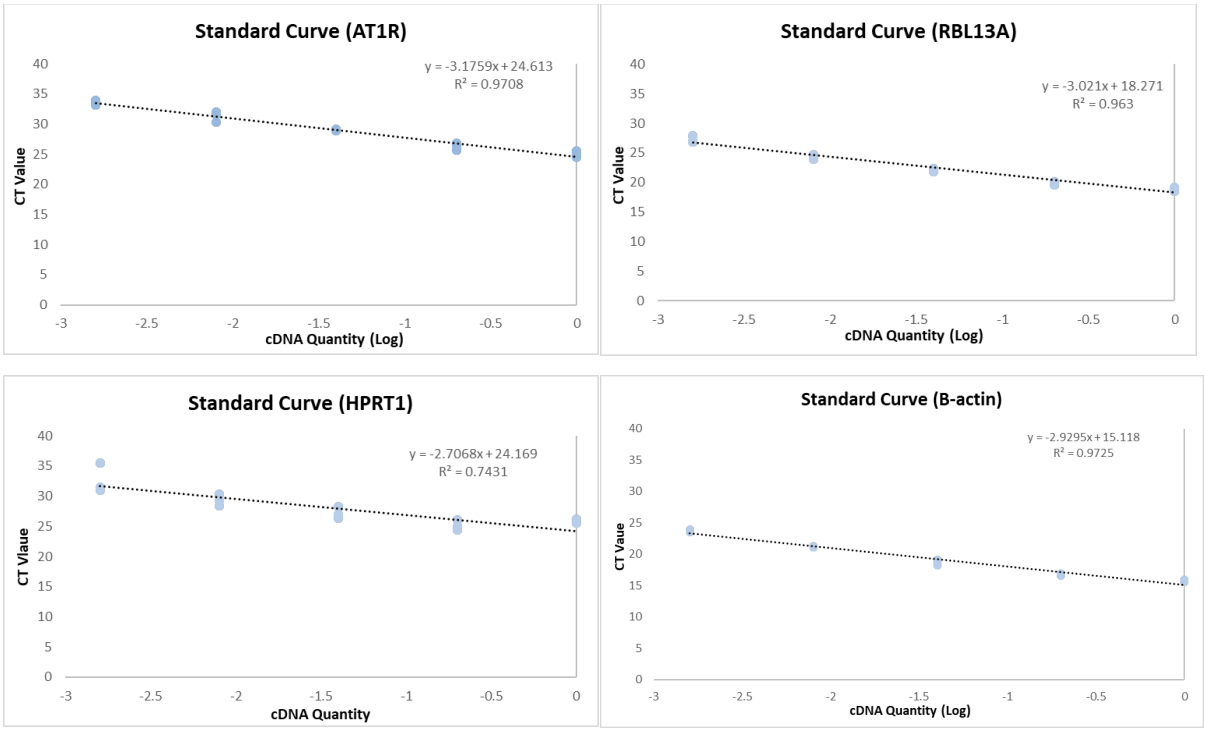

Figure 4.14 Standard curves for different genes generated by serial cDNA dilutions using AC10 control sample.

Table 4.7 Primer efficiency for each gene using cDNA of AC10 control sample.

Gene	Slope	Y-intercept	R^2	Efficiency (%)
AT1R	-3.1759	24.613	0.97	106.47
RPL13A	-3.021	18.271	0.96	114.29
HPRT1	-2.7068	24.169	0.74	134.12
β-actin	-2.9295	15.491	0.97	119.46

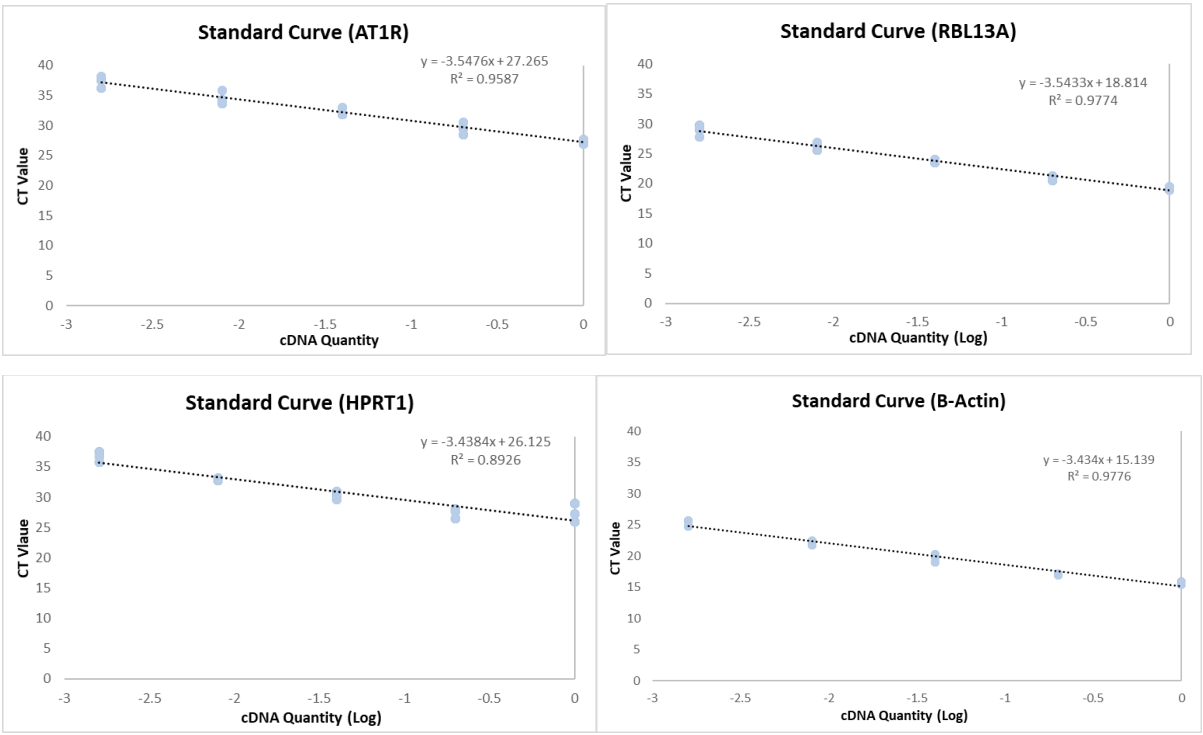

Figure 4.15 Standard curves for different genes generated by serial cDNA dilutions using HCF control sample.

Table 4.8 Primer efficiency for each gene using cDNA of HCF control sample.

Gene	Slope	Y-intercept	R^2	Efficiency (%)
AT1R	-3.5476	27.265	0.96	91.37
RPL13A	-3.5433	18.814	0.98	91.52
HPRT1	-3.4384	26.125	0.89	95.36
β-actin	-3.434	15.139	0.98	95.53

4.3.6 Assessment of housekeeping genes (β-actin and RPL13A) for normalisation of AT1R gene expression over time in human AC10 cardiomyocytes and HCF in vitro

The expression levels of the housekeeping genes β-actin and RPL13A were evaluated over 24-hour period to assess their suitability for the normalisation of AT1R Ct values in future experiments. Mean Ct values of the β-actin, RPL13A, and AT1R were assessed in control sample of AC10 and HCF over a 24-hour time course. As illustrated in Figure 4.16, the AT1R expression was consistent in AC10. However, a reduction in AT1R expression was observed at 16 hours in HCF. Despite this decrease, the AT1R will be normalise to the corresponding time-matched control which would accommodate this change.

For reference genes, the RPL13A was inconsistent across time points in both AC10 and HCF. Therefore, it is unsuitable for use as a reference gene in subsequent experiments. In contrast, the β-actin for control sample is consistent across the timepoints in both AC10 and HCF, confirming that β-actin is stable overtime. This stability confirms the suitability of β-actin as a reference gene and support the reliability of subsequent normalisation for AT1R gene expression analysis in both AC10 and HCF.

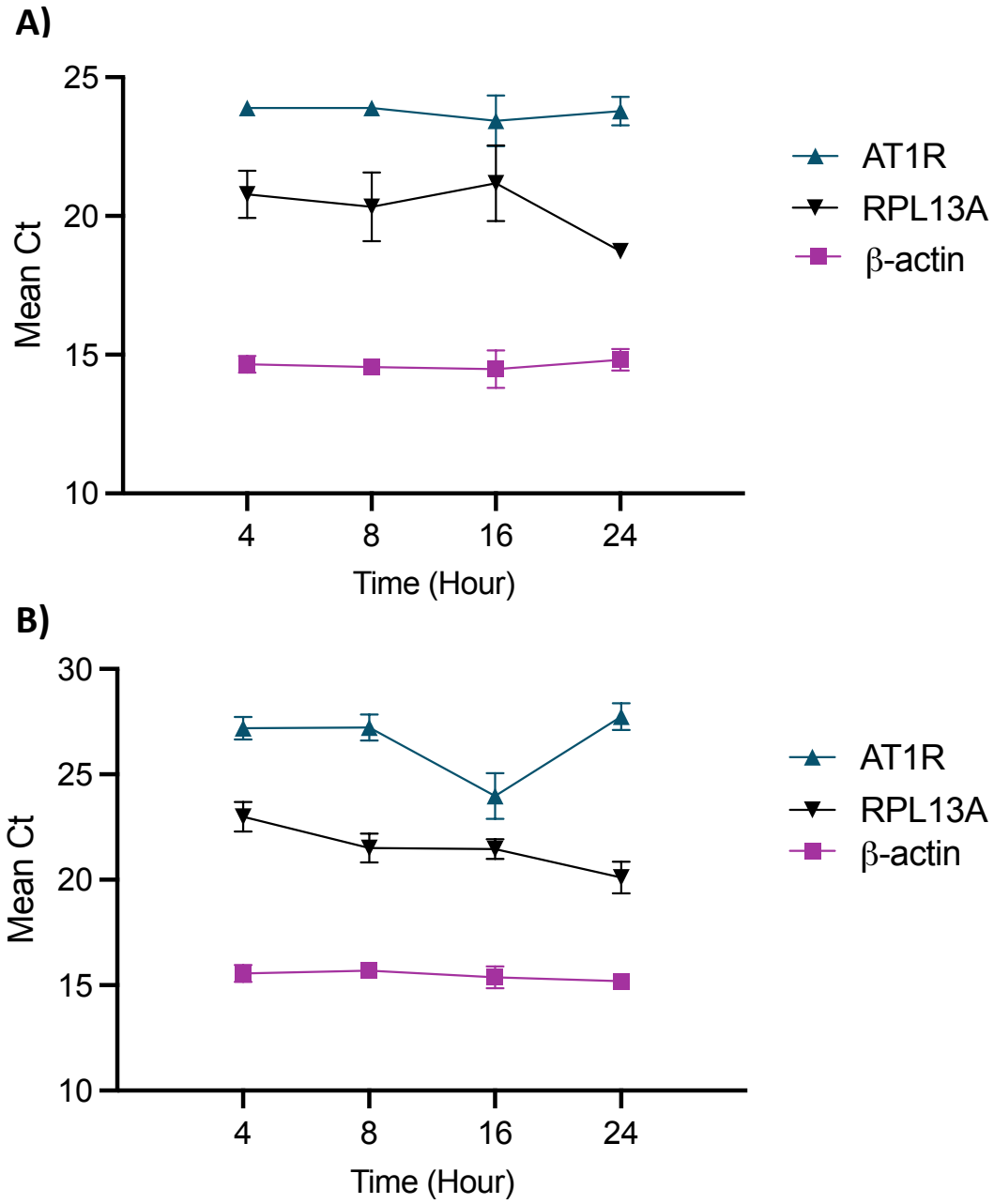

Figure 4.16 Expression levels of β-actin compared to AT1R over timepoints in A) AC10 and B) HCF, calculated using RT-qPCR QuantStudio. The uniform Ct values across time points confirms the stability of β-actin over timepoints. Data are presented as mean ± SEM.

4.3.7 Exposure to Angiotensin II induces AT1R mRNA in human AC10 cardiomyocyte cells but not human cardiac fibroblasts in vitro

The AT1R mRNA level in AC10s was assessed after exposure to physiological relevant concentration of angiotensin II. As Figure 4.17 shown, there is a significant 1.4-fold increase in AT1R mRNA levels compared to control after exposure to 300pM angiotensin II for 24-hours. Similarly, the AT1R mRNA level in HCF was assessed after exposure to physiological relevant concentration of angiotensin II. As Figure 4.18 shown, there is no increase in AT1R mRNA levels compared to control after exposure to 300pM angiotensin II for 24-hours (p= 0.99).

4.3.8 Doxorubicin induces mRNA expression of AT1R in human AC10 cardiomyocytes in vitro

The AT1R mRNA level in AC10 after exposure to different concentrations of doxorubicin was assessed over different time points. As Figure 4.19 shown, doxorubicin demonstrated no significant effect on AT1R mRNA expression compared to the control at 4-hours (p=0.86) or 8-hours (p=0.50) at any tested doxorubicin concentration. However, after 16-hours of high-concentration (500nM) doxorubicin exposure, a significant 1.5-fold increase in AT1R mRNA level relative to control was demonstrated (p=0.034). By 24-hours, a significant 2.2-fold (p=0.0028) and 1.8-fold (p=0.039) increase in AT1R mRNA level relative to control was observed at 250nM and 500nM doxorubicin, respectively.

4.3.9 Doxorubicin induces mRNA expression of AT1R in hiPSC-CMs in vitro

The AT1R mRNA level in hiPSC-CMs after exposure to different concentrations of doxorubicin was assessed at 24 hours. As Figure 4.20 shown, doxorubicin demonstrated a significant 3.2-fold (p=0.021), 3-fold (p=0.040) and 3.5-fold (p=0.0087) increase in AT1R mRNA expression compared to the control at 100nM, 250nM, and 500nM doxorubicin, respectively.

4.3.10 Doxorubicin induces mRNA expression of AT1R in human cardiac fibroblasts in vitro

The AT1R mRNA level in HCF after exposure to different concentrations of doxorubicin was assessed over time points. As Figure 4.21 shown, no significant effect on AT1R mRNA expression compared to the control at 4-hours (p=0.96) or 8-hours (p=0.16) at any tested doxorubicin concentration. However, after 16-hours of high-concentration (500nM)

doxorubicin exposure, a significant 1.7-fold increase in AT1R mRNA level relative to control was demonstrated ($p=0.0062$). By 24-hours, a significant 2.2-fold ($p=0.0025$) and 2-fold ($p=0.016$) increase in AT1R mRNA level relative to control was observed at 250nM and 500nM doxorubicin, respectively.

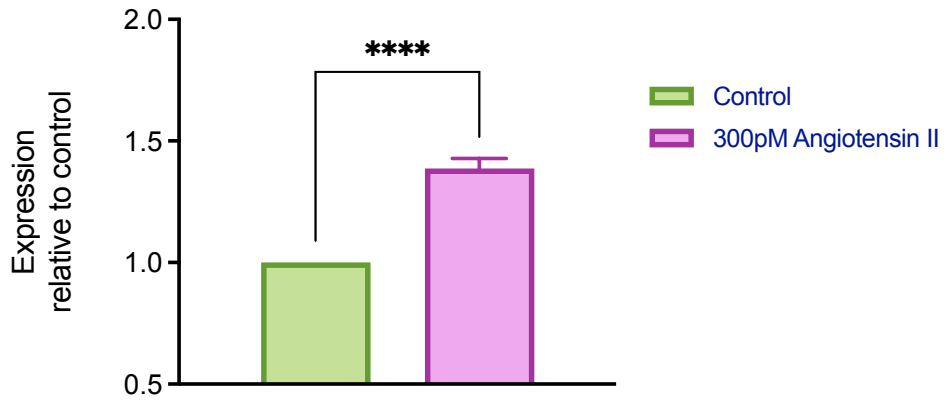

Figure 4.17 Angiotensin II causes a significant change in AT1R in AC10s. Cells were exposed to 300pM Angiotensin II for 24hrs. β-actin was used as a housekeeping gene. Data is representative of three repeats and presented as mean ±SEM. Statistical significance was determined by un-paired t test (**** = $p < 0.0001$).

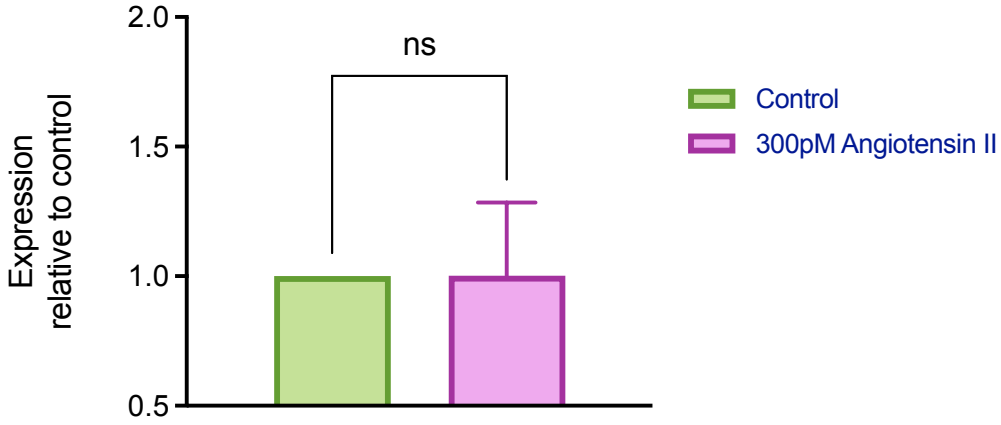

Figure 4.18 Angiotensin II does not cause a change in AT1R expression in HCF. Cells were treated with 300pM Angiotensin II for 24hrs. β-actin was used as a housekeeping gene. Data is representative of three repeats and presented as mean ±SEM.

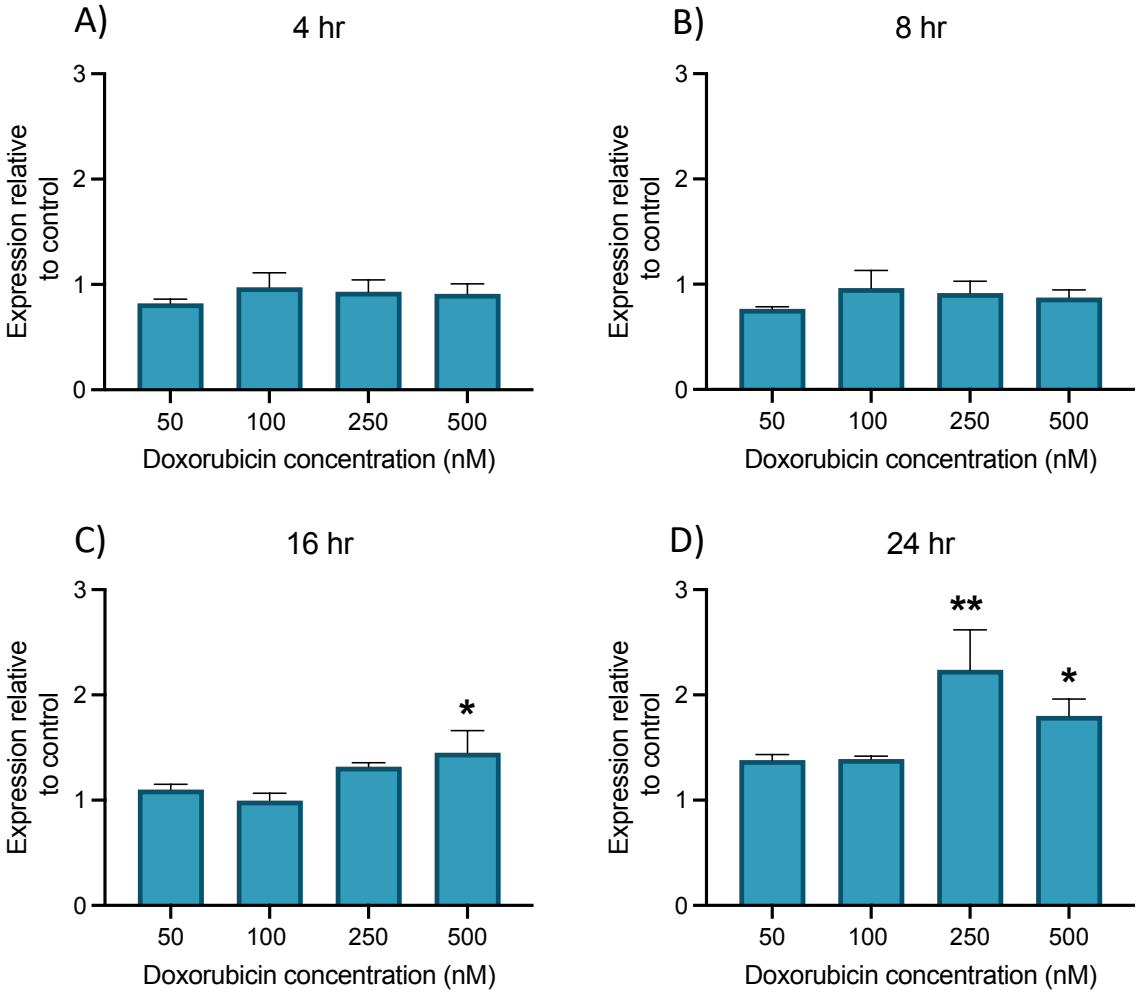

Figure 4.19 The effect of doxorubicin different concentrations on AT1R mRNA expression levels in AC10. Cells were treated with increased concentrations (50nM-500nM) of doxorubicin at different time points (A) 4hrs (B) 8hrs (C) 16hrs (D) 24hrs. β-actin was used as a housekeeping gene. Data is representative of three repeats and presented as mean ±SEM. Statistical significance was determined by a One-way ANOVA with post-hoc Dunnett's multiple comparison test (*=p<0.05, **=p<0.01).

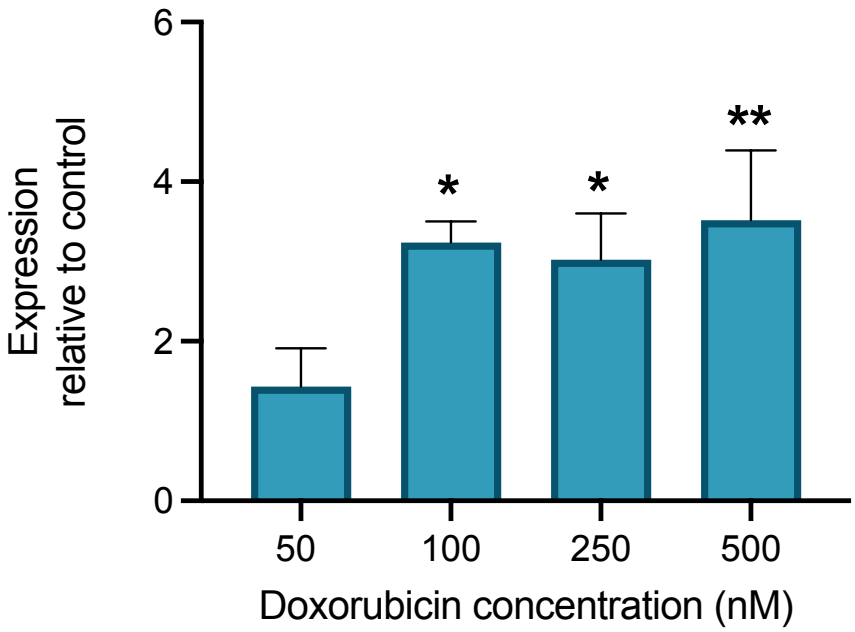

Figure 4.20 Increased concentrations of doxorubicin cause a change in AT1R mRNA expression levels in hiPSC-CM. Cells were treated with increased concentrations (50nM-500nM) of doxorubicin for 24hrs. β-actin was used as a housekeeping gene. Data is representative of three repeats and presented as mean ±SEM. Statistical significance was determined by a One-way ANOVA with post-hoc Dunnett's multiple comparison test (* = $p < 0.05$, ** = $p < 0.01$).

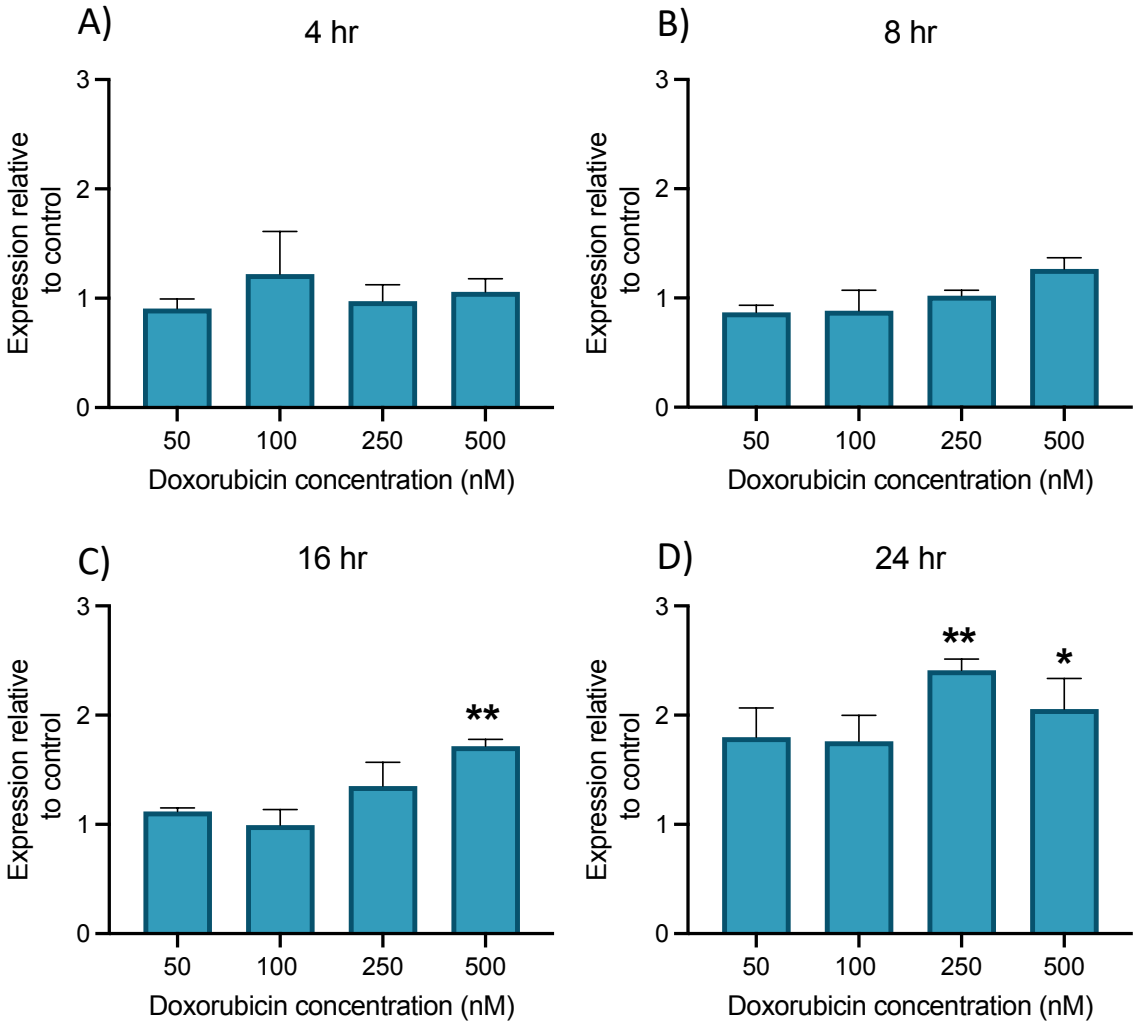

Figure 4.21 The effect of doxorubicin different concentrations on AT1R mRNA expression levels in HCF. Cells were treated with increased concentrations (50nM-500nM) of doxorubicin at different time points (A) 4hrs (B) 8hrs (C) 16hrs (D) 24hrs. β-actin was used as a housekeeping gene. Data is representative of three repeats and presented as mean ±SEM. Statistical significance was determined by a One-way ANOVA with post-hoc Dunnett's multiple comparison test (*=p<0.05, **=p<0.01).

4.3.11 Doxorubicin does not alter protein expression of AT1R at sub-toxic concentrations in human AC10 cardiomyocytes in vitro

The AT1R protein expression in AC10 after exposure to different concentrations of doxorubicin was assessed over different time points. As Figure 4.22 shown, increased concentrations of doxorubicin have no significant effect on AT1R protein expression levels compared to the control of the same time point at 4-hours (p= 0.59), 8-hours (p= 0.69), and 16-hours (p= 0.95) of doxorubicin exposure. Although increased expression of AT1R protein was observed after 24hrs exposure to 50nM, 100nM and 500nM doxorubicin, this was not a significant change relative to control at these timepoints (p=0.33). As Figure 4.23 shown, after 48 hours of doxorubicin exposure, a significant decrease in AT1R protein expression was observed with AC10 treated with 500nM doxorubicin (p=0.02), a concentration > IC_{50} of AC10 at 48 hours 0.34±0.085. At 72 hours of doxorubicin exposure, a significant decrease in AT1R protein expression was observed with AC10 treated with 500nM doxorubicin (p=0.03). After 96 hours of doxorubicin exposure, AT1R protein expression levels were observed to return to pre-treatment levels (p=0.24).

4.3.12 Elevated protein expression of AT1R in HCF after exposure to doxorubicin

The AT1R protein expression in HCF after exposure to different concentrations of doxorubicin was assessed over a 96-hour time course. As Figure 4.24 and Figure 4.25 shown, exposure to doxorubicin had no significant effect on AT1R protein expression levels compared to the control of the same timepoint at 4 hours (p=0.94), 8 hours (p=0.57), 16 hours (p=0.30), 24 hours (p=0.90), 48 hours (p=0.26), 72 hours (p=0.31). However, at 96hours post-exposure to doxorubicin, significant increases in AT1R expression were observed with 250nM and 500nM concentrations of doxorubicin (p=0.005, and 0.008), respectively.

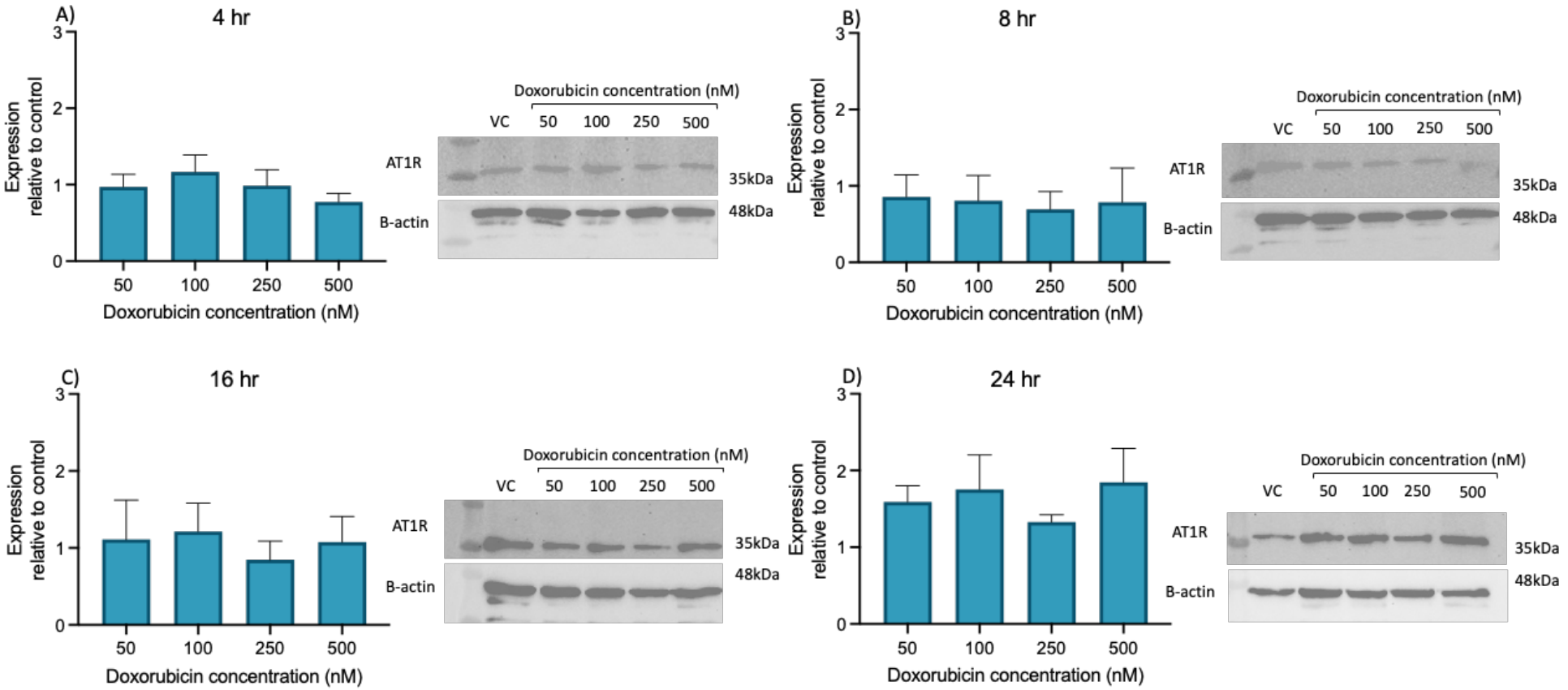

Figure 4.22 The impact of increased concentrations of doxorubicin on AT1R protein expression levels in AC10 over 24-hours. Western blots and densitometric analysis of AT1R protein expression levels relative to the corresponding time-matched control. Cells were treated with increased concentrations (50nM-500nM) of doxorubicin at different time points (A) 4hrs (B) 8hrs (C) 16hrs (D) 24hrs. AT1R protein expression levels were normalised to β-actin. Data is representative of three repeats and presented as mean ±SEM. Statistical significance was determined by a One-way ANOVA with post-hoc Dunnett's multiple comparison test. Uncropped western blot is appended.

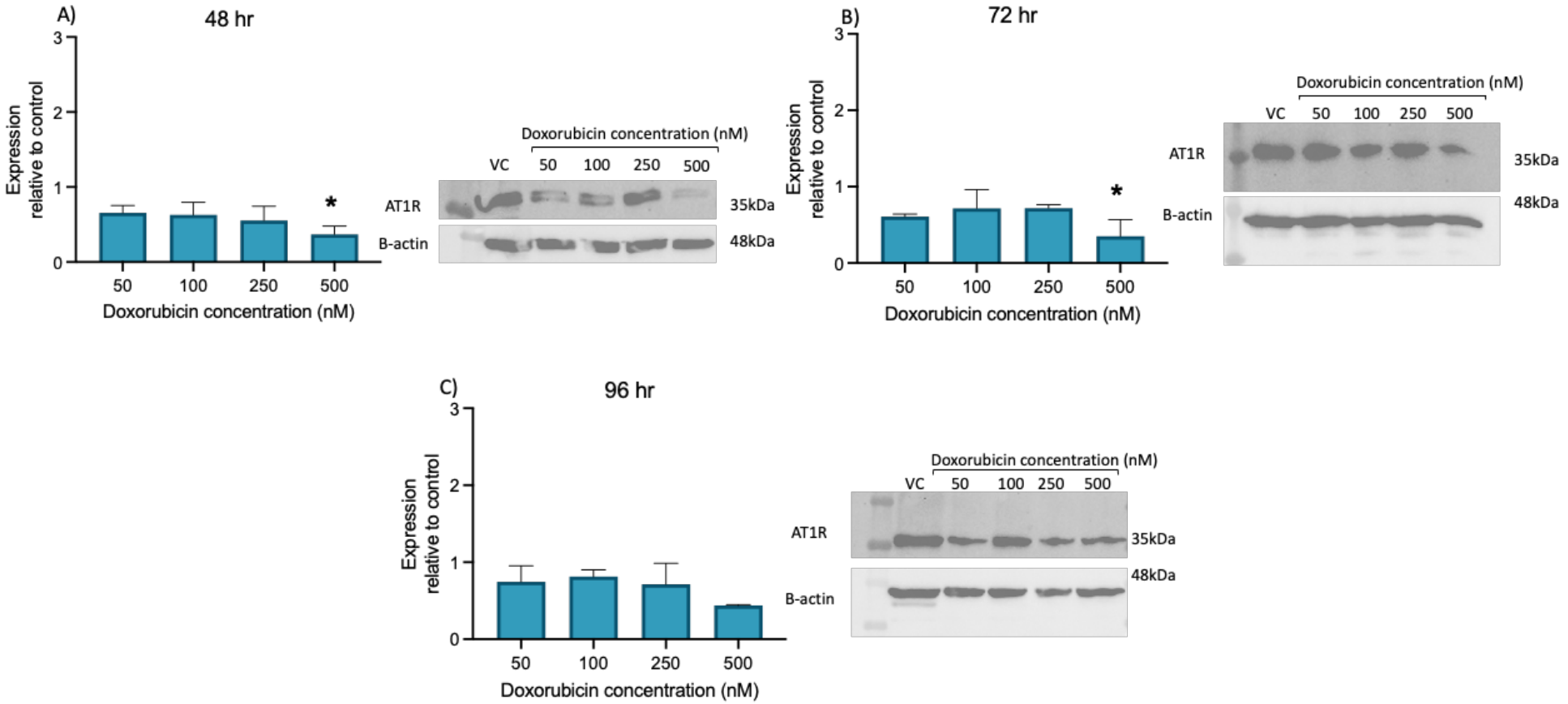

Figure 4.23 The impact of increased concentrations of doxorubicin on AT1R protein expression levels in AC10 at different time points. Western blots and densitometric analysis of AT1R protein expression levels relative to the corresponding time-matched control. Cells were treated with increased concentrations (50nM-500nM) of doxorubicin at different time points (A) 48hrs (B) 72hrs (C) 96hrs. AT1R protein expression levels were normalised to β-actin. Data is representative of three repeats and presented as mean ±SEM. Statistical significance was determined by a One-way ANOVA with post-hoc Dunnett's multiple comparison test (*=p<0.05). Uncropped western blot is appended.

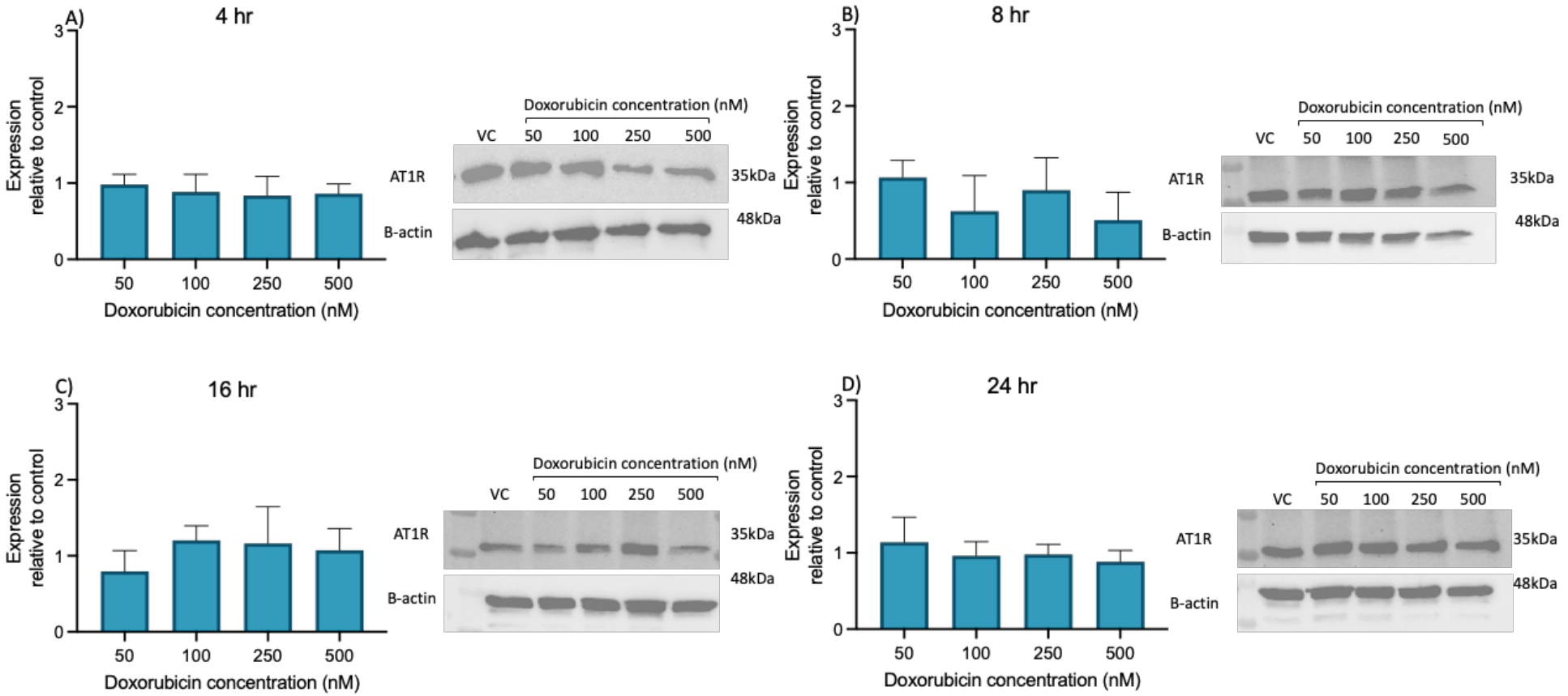

Figure 4.24 The impact of increased concentrations of doxorubicin on AT1R protein expression levels in HCF over 24-hours. Western blots and densitometric analysis of AT1R protein expression levels relative to the corresponding time-matched control. Cells were treated with increased concentrations (50nM-500nM) of doxorubicin at different time points (A) 4hrs (B) 8hrs (C) 16hrs (D) 24hrs. AT1R protein expression levels were normalised to β-actin. Data is representative of three repeats and presented as mean ±SEM. Statistical significance was determined by a One-way ANOVA with post-hoc Dunnett's multiple comparison test (**=p<0.01). Uncropped western blot is appended.

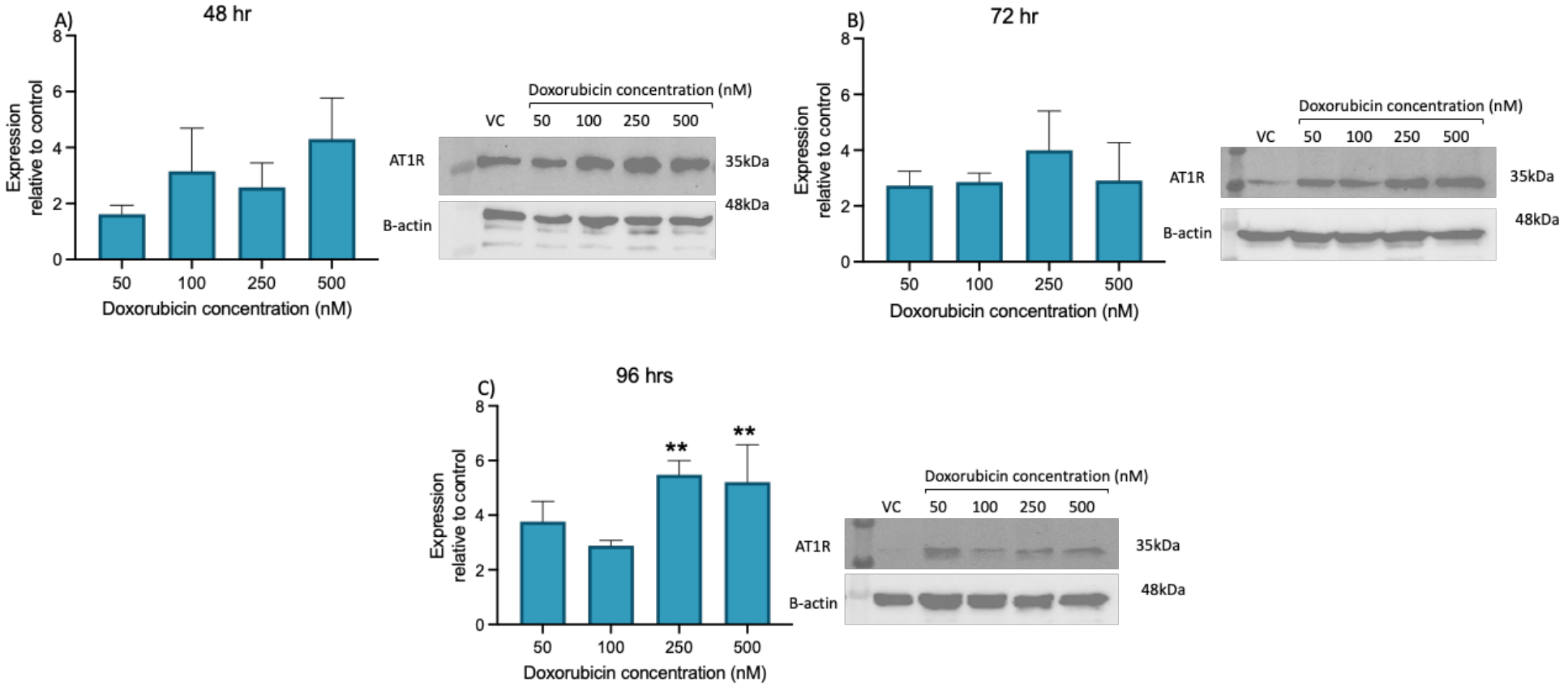

Figure 4.25 The impact of increased concentrations of doxorubicin on AT1R protein expression levels in HCF at different time points. Western blots and densitometric analysis of AT1R protein expression levels relative to the corresponding time-matched control. Cells were treated with increased concentrations (50nM-500nM) of doxorubicin at different time points (A) 48hrs (B) 72hrs (C) 96hrs. AT1R protein expression levels were normalised to β-actin. Data is representative of three repeats and presented as mean ±SEM. Statistical significance was determined by a One-way ANOVA with post-hoc Dunnett's multiple comparison test (**=p<0.01). Uncropped western blot is appended.

4.4 Discussion

Studying the relationship between RAAS, particularly AT1R and cardiotoxicity associated with doxorubicin has gained recent research attention in understanding the underlying mechanism of AIC (34). Recent evidence suggests that doxorubicin interacts with RAAS components and exacerbating cardiotoxic effects and several clinical studies have shown effectiveness of drugs targeting RAAS in preventing AIC (see section 1.8.3.1). This chapter aimed to explore the molecular mechanism of AIC and potential involvement of RAAS, particularly AT1R in mediating cardiotoxicity associated with doxorubicin.

Although the pathogenesis of cardiotoxicity developed after doxorubicin treatment is complex, growing body of evidence suggests that RAAS plays important role in this pathogenesis. The key peptide in the RAAS, angiotensin II, is involved in many cardiovascular disorders and exerts its effects primarily through the activation of the AT1R (235). This activation leads to initiation of downstream angiotensin II signalling pathway and therefore, one of which is promotion of the hypertrophic response in cardiac cells (34). As indicated previously (section 3.3.8), activation of this angiotensin II pathway by angiotensin II leads to cardiomyocyte hypertrophy which contributes to cardiac dysfunction (11, 12, 34, 235). Similarly, exposure to doxorubicin has also been shown to initiate a hypertrophic response in cardiomyocytes (section 3.3.9). This shared effects between anthracycline and angiotensin II emphasized a putative role of activation of the RAAS pathway in developing AIC, a hypothesis supported by many preclinical and clinical studies (34).

As previously shown (Chapter 3), both angiotensin II and doxorubicin can induce hypertrophy in AC10 but not in HCF, highlighting a cell type specific response to angiotensin II. To address this interrelationship between angiotensin signalling and AIC, this study has evaluated the ability of ACEi and ARB, both which affect angiotensin II activities, to affect the cardiac cellular response to the anthracycline doxorubicin. Prior exposure of AC10 and HCF to the ACEi enalapril and its active metabolite enalaprilat was shown to have no effect on cytotoxicity or hypertrophy of any of the cardiac cell types *in vitro*. This is not surprising since ACE is expressed in the lungs within the body where it converts angiotensin I into the active moiety angiotensin II, whereas no such environment is present in the *in vitro* cellular environment (146). It does however indicate a lack of off-target effects for these ACEi within cardiomyocytes and HCF. Similarly, exposure of AC10 or HCF to ARBs, which inhibit activation

of the cell surface receptor for angiotensin II, did not affect the cytotoxicity profile of doxorubicin. In contrast, the ARB telmisartan could retard the hypertrophic response of AC10 cells to doxorubicin, indicating a role for AT1R activation in the cellular hypertrophic response to doxorubicin. Interestingly, although telmisartan mitigated the doxorubicin-mediated hypertrophic response in AC10 cardiomyocytes, this was not observed with other ARBs, including candesartan and losartan. The reason for this difference lies in their distinct pharmacological properties (231). A study into how ARBs block the renin-angiotensin system has shown that telmisartan binds to AT1R for longer periods and dissociates from the receptor more slowly compared to others. Even in the presence of competing ligands, telmisartan remains tightly bound, unlike candesartan which dissociates more readily (231). These differences in receptor binding behaviour could explain why telmisartan was more effective in preventing doxorubicin-induced hypertrophy in AC10 cells. Taken together these results strongly support a role for AT1R in mediating the cardiotoxic response of cardiomyocytes to anthracyclines. The mechanism for this is at this point unclear, a concept which is evaluated within this chapter at both the mRNA and protein level using the previously characterised *in vitro* cellular models.

An important parameter for genetic analyses and quantification is the selection of a robust housekeeping comparator gene for analyses. Previous research identified GAPDH as a translational suppressor of AT1R expression, making it unsuitable as a reference gene in this study (242). Thus, before starting to characterise the response of AT1R in cardiac cells to doxorubicin, this study assessed the suitability of other housekeeping genes for normalisation of AT1R gene analysis studies. Based on RT-qPCR testing and primer efficiency, β-actin has been selected as a reference gene in this study.

In terms of a molecular rationale as an explanation for the hypertrophic response of doxorubicin against human cardiomyocytes but not human CFs, as detailed in Chapter 3, and the mitigation of this hypertrophic response in cardiomyocytes by inhibition of AT1R activity (Figure 4.10), effects of doxorubicin on expression of AT1R was warranted. This study found that angiotensin II at physiological relevant concentrations leads to an upregulation of AT1R mRNA level with 1.4-fold increase compared to control in AC10 cardiomyocytes but not HCF, indicating a differential activation of the angiotensin signalling pathway in these cell types. With reference to doxorubicin, AT1R mRNA levels are upregulated after 16- and 24-hours of exposure in both AC10 and HCF which align with the half-life of doxorubicin, which is between 20 to 30 hours in the human body (209, 218). However, when AC10 exposed to doxorubicin,

the increase in AT1R mRNA levels is not corresponding with increase in protein levels. The highest protein expression levels of AT1R in AC10 was observed at 24 hours exposure then the expression is declined at 48 and 72 hours of exposure, particularly with 500nM concentration. The observed reduction with 500nM concentration of doxorubicin align with previous cytotoxicity studies, indicating that cell viability may affect the AT1R expression and suggesting that cardiac cells become more sensitive to doxorubicin with increasing exposure, leading to reduce protein translational efficiency then reduce AT1R protein expression. A previous study showed a lower AT1R receptor density in damaged ventricular myocardium when compared to healthy tissue, suggesting that cellular death can directly reduce receptor expression (244). Alternatively, the reason for increased AT1R mRNA levels do not result in increase in protein levels may attributed to post-transcriptional regulation mechanisms that may differ in the presence of doxorubicin, including differences in mRNA stability, or protein instability (245). It has been reported that insulin increase protein expression due to AT1R mRNA stability by bind to its 3'-untranslated region (UTR) (245, 246).

However, the highest AT1R protein expression upregulation in HCF was observed at 96 hours with sub- toxic concentrations of doxorubicin, indicating that activation of AT1R in CFs is involved in the cardiac cell response to doxorubicin. Interestingly, the increase in AT1R protein expression closely mirrors the upregulation observed at the mRNA level, suggesting that the induction of AT1R gene expression is efficiently translated into protein in HCF. The findings from cardiomyocytes and CFs support the role of AT1R in the cellular response to doxorubicin.

Consistent with our findings, the AT1R mRNA and protein expression level are upregulated in rat cardiomyocytes after doxorubicin treatment and co-treatment with telmisartan or losartan supress the AT1R upregulation at both mRNA and protein levels (234). In addition, another study revealed that the rat myoblast H9c2 cell line was treated with different doses of doxorubicin for 24 hours demonstrated a dose dependent increase in both AT1R mRNA and protein expression (247). While the upregulation of AT1R in cardiomyocytes align with previous studies, the limitations of previous studies include the models used derived from rat myocardium which does not represent the human cardiomyocyte response to doxorubicin and testing high concentration (above the Cmax) of doxorubicin (178, 218). Previous findings and our results support our hypothesis that angiotensin II signalling, particularly AT1R is involved in AIC and play a crucial role in the cardiac cells response to doxorubicin.

Many *in vitro* cardiomyocyte models are available and were used previously to examine the effect of doxorubicin on cardiac cells. However, the major concern about these studies is the use of animal derived cardiomyocytes which do not represent human clinical situation (185). One of the cardiac cell models that gained recent attention is hiPSC-CM. The hiPSC-CM cell model is physiologically relevant human derived cardiomyocytes, expressing multiple cardiac marker, and can be cultured *in vitro* which make them an ideal model for cardiovascular research, particularly study the mechanism of AIC (184). Despite their advantages, the major limitation of hiPSC-CM including the cost to produce and maintain compared to other models, such as rodent primary cardiomyocytes or commercially available cardiac cell lines (185). Studies utilizing hiPSC-CM as a cardiac model have been shown previously to elucidate mechanisms of AIC including dose dependent cell death, increase in ROS formation, and mitochondrial dysfunction (248). One of the most advanced applications of hiPSC-CMs is patient specific hiPSC-CM, which allow researchers to study genetic variation and assess the interindividual variation in susceptibility of these patients to AIC (249-252). For example, Christidi et al. (2020) found that presence of RARG genetic variation in patient specific hiPSC-CM increases the susceptibility of those patients to AIC and correcting this variant to wild type (WT) can reduce cell death and ROS formation, suggesting that patient specific hiPSC-CM can identify interindividual variation of susceptibility to AIC (252).

In this study the impact of doxorubicin on AT1R mRNA levels in hiPSC-CM was examined. Our findings revealed that doxorubicin increases AT1R mRNA level in a dose dependent manner at 24 hours of exposure with the maximum effect observed at 500nM concentration with 3.5-fold increase in AT1R mRNA relative to control. This finding provides a new insight into the mechanism of AIC, as it demonstrates that human cardiomyocytes respond to doxorubicin by upregulating angiotensin signalling and more representative of the *in vivo* human cardiac environment than previously utilised animal-based models. When compared to AC10 cells, which also demonstrated an upregulation of AT1R mRNA in response to doxorubicin, AC10 cells despite being immortalized, it shared the same effect on AT1R mRNA level with hiPSC-CMs. Due to these similarities, AC10 cells is a reliable model for studying cardiomyocyte responses after doxorubicin exposure, particularly in terms of AT1R regulation, providing an alternative to hiPSC-CMs, cost-effective and time-efficient. However, the higher fold increase of AT1R mRNA in hiPSC-CMs may reflect higher sensitivity of those cells to doxorubicin due to developmental maturity as these cells more closely represent the environment of adult human cardiomyocytes compared to AC10 cells.

In conclusion, the similarity in the cardiac cell response between angiotensin II and doxorubicin raises the possibility that the angiotensin II signalling pathway plays a role in the response of cardiac cells to anthracycline. This is supported by the observation that blocking AT1R using ARBs mitigates the doxorubicin induced hypertrophic response in human cardiomyocytes, suggesting that angiotensin II signalling pathway is involved in the anthracycline cardiotoxicity. Interestingly, both cell types demonstrate mRNA upregulation of AT1R in response to doxorubicin exposure. However, there is a differential response of AT1R protein expression between AC10 cardiomyocytes and HCFs, suggesting a cell-type-specific response to doxorubicin. This differential cellular response underscores the complexity of the cardiac microenvironment and further supports the involvement of angiotensin II signalling pathway in cardiac response to anthracycline. Further studies are warranted to assess whether blocking AT1R is specifically involved in AIC.

Chapter 5. Involvement of Angiotensin II Type 1 Receptor (AT1R) in the Toxicological Response of Cardiac Cells to Anthracycline

5.1 Introduction

5.1.1 Mitigation of AIC by perturbing angiotensin II signalling

The previous studies in this project (Chapter 3 and Chapter 4) clearly show that anthracyclines, specifically doxorubicin, can modulate angiotensin signalling pathways in both cardiomyocytes and CFs. These findings show that sub-toxic concentrations of doxorubicin induce cellular hypertrophy in AC10 cardiomyocytes but not CFs, a cellular change that is inhibited by pharmacological blockade of AT1R. It is also shown that doxorubicin induces both mRNA and protein expression of AT1R in AC10 cardiomyocytes and HCF. This thereby strongly supports a relationship between modulation of angiotensin signalling and toxicological response of cardiac cells to anthracyclines, a concept supported by clinical studies demonstrating administration of ACEi or ARBs can reduce progression of AIC (152-161, 164-169). Further support for a relationship between AIC and the angiotensin signalling pathway is provided from studies of genetically modulated mice in which AT1R expression has been suppressed. These mice exhibit reduced LV-remodelling in response to doxorubicin treatment, compared to WT mice (170). However, despite these studies strongly implying a role for modulation of AT1R signalling in the cardiotoxicological response of the heart to anthracyclines, the central role of this receptor in this response at the cellular (as opposed to systemic) level, the role of the different cardiac cell types, and discrimination of systemic versus local cellular effects is not yet confirmed.

5.1.2 Investigation of the role of a specific gene and/or protein in cellular response by small interfering RNA (siRNA) technologies

A now commonly used approach for modulating gene expression and studying of gene functions in *in vitro* research is Small interfering RNA (siRNA) (253). siRNA technologies degrade the target RNA transcript by inducing post-transcriptional gene silencing (254). Briefly, siRNA enters the cells, forms a RNA-induced silencing complex (RISC), wherein the sense strand is degraded to form a single stranded siRNA (255). This single stranded siRNA,

specifically the antisense strand, leads the RISC to the target mRNA to cleave it resulting in its degradation (256). The result is gene knockdown of the target mRNA in the cell and subsequent suppression of protein synthesis (Figure 5.1) (256).

5.1.2.1 Evidence for a role for AT1R in AIC

Several studies have suggested a significant link between RAAS and AIC in both animal models and clinical studies, involving circumstantial evidence and through use of pharmacological interventions with ACEi and ARBs (34, 257). To indicate a role for AT1R in these responses, murine studies in which expression of AT1R had been genetically knocked down were employed (170). This study revealed that the knockout of AT1R in mice significantly reduced the number of apoptotic cells and mitigated heart LV-remodelling in response to doxorubicin treatment, compared to WT mice. In addition, knockout of AT1R was shown to offer protection against doxorubicin-induced atrial natriuretic peptide (ANP) genetic downregulation, responsible for regulating vascular remodelling (170, 258). However, although together these studies support a role for AT1R, the relationship between doxorubicin and angiotensin signaling pathway within the cardiac system itself and the cells therein is only at this point inferred. To robustly determine whether AT1R is indeed the central conduit for the association between angiotensin signalling and AIC, or whether this receptor is merely a bystander for signalling via another molecular pathway, studies utilsing siRNA against AT1R in cardiac cells is warranted.

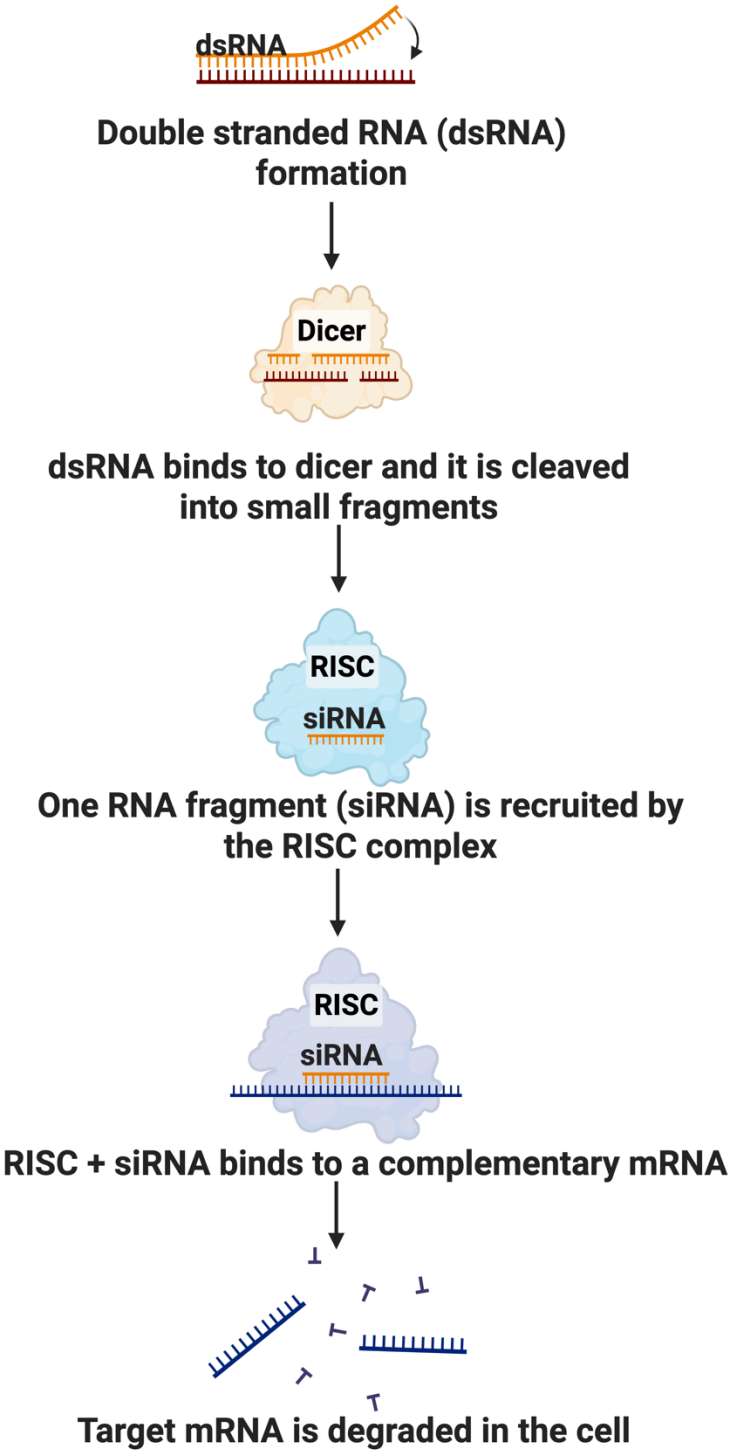

Figure 5.1 Mechanism of siRNA -mediated gene silencing. In the cell cytoplasm, Dicer enzyme cleaves dsRNA into small fragments. The antisense strand siRNA is then incorporated into the RISC complex. Guided by sequence complementarity, the siRNA directs RISC to bind to the target mRNA. This results in degrading of mRNA then suppression of protein synthesis. Adapted from BioRender.

5.1.3 Aim and objectives

Aim: Determination of a central role for AT1R in cardiac cell toxicological response to the anthracycline doxorubicin. This will be achieved by the following objectives:

- Utilisation of siRNA-mediated knockdown of AT1R expression to address the role of the AT1R in the response of cardiac cells to doxorubicin.
- Determination of the potential prophylactic role of targeting AT1R in mitigation of doxorubicin induced cardiomyocyte hypertrophy, through siRNA-mediated knockdown of AT1R.
- Evaluation of the role of AT1R in doxorubicin-induced cardiac cell toxicity, through siRNA-mediated knockdown of AT1R and challenge with doxorubicin

5.2 Material and method

5.2.1 Optimization of siRNA transfection efficiency in AC10 and HCF cells using siGLO Red indicator

AC10 and HCF cells were seeded into 6-well flat-bottomed cell culture plate at a density of $3x10^5$ cells/well and $7x10^4$ cells/well, respectively and allowed to adhere overnight. After a 24 hours period, media was replaced with transfection mixtures of 20nM, 30nM, and 40nM of siGLO Red transfection indicator (Dharmacon Inc., Lafayette, CO) prepared as follow: each concentration of siGLO Red mixed with 250 µL of serum-free medium (Opti-MEM I reduced serum media) and different volumes 5 µL, 7.5 µL, and 10 µL of TransIT-X2 transfection reagent (Mirus, MSC Medical Supply Co. Ltd, Dublin, Ireland). The transfection mixtures incubated at room temperature for 20 minutes to allow complex formation. The prepared transfection mixtures then added to the respective wells. Cells were incubated with the transfection mixture for 24 hours. After the 24-hour incubation period, micrograph images were collected by fluorescent microscopy at a magnification of 10x (NikonTE2000 microscope). This method was designed to identify the optimal transfection efficiency in AC10 and HCF cells by varying the concentration of the transfection indicator and the volume of the transfection reagent.

5.2.2 Confirmation of siRNA-mediated knockdown of AT1R in AC10 and HCF cells

AC10 and HCF cells were seeded into 6-well plates at a density of $3x10^5$ cells/well and $7x10^4$ cells/well, respectively. Cells were seeded on Day 0 and allowed to adhere to the plate overnight. On day 1, the transfection mixtures prepared (as per section 5.2.1) and cells exposed to either fresh media, 7.5 µL of TransIT-X2 transfection reagent alone as mock transfection, transfection mixture of 20nM non-target siRNA (ON-TARGETplus Non-targeting Control siRNAs; Dharmacon), or to transfection mixture of 20nM and 40nM concentration of AT1R siRNA (On-target plus SMARTpool; Dharmacon). After 24 and 48 hrs, cell lysate was collected for downstream analysis to identify the optimal AT1R siRNA concentration and time for transfection using RT-qPCR.

5.2.3 Verification of doxorubicin-induced AT1R mRNA expression via AT1R knockdown in AC10 and HCF

To confirm that the upregulation of AT1R mRNA level observed following doxorubicin exposure is a direct effect, siRNA-mediated knockdown of AT1R was performed. AC10 and HCF cells were seeded into 6-well plates at a density of $3x10^5$ cells/well and $7x10^4$ cells/well, respectively. Cells were seeded on Day 0 and allowed to adhere to the plate overnight. On day 1, the transfection mixtures prepared as above and cells exposed to fresh media, 7.5 µL of TransIT-X2 transfection reagent alone as mock transfection, transfection mixture of 20nM non-target siRNA, or to transfection mixture of 20nM AT1R siRNA. After further 24 hours period, media was replaced with that containing doxorubicin or to drug vehicle (DMSO). After a further 24h, cell lysate was collected for downstream analysis.

5.2.4 Evaluation of ability of AT1R knockdown to reduce the cytotoxicity response of human AC10 cardiomyocytes and HCF to doxorubicin, determined by MTS assay

AC10 and HCF cells were seeded into 96-well plates at a density of $5x10^3$ cells/well and viability assessed following exposure to doxorubicin after knockdown of AT1R for a 24-,48-, and 72-hours continuous period using the MTS assay, as previously described in section 2.4. Cells were seeded on Day 0 and allowed to adhere to the plate overnight. On day 1, the top rows of the plate (rows A-C) exposed to transfection mixture of non-target siRNA. Rows D-E exposed to fresh media and the bottom rows of the plate (F-H) was exposed to transfection mixture of AT1R siRNA. On day 2, media was replaced with that containing doxorubicin or to drug vehicle (DMSO). In relation to doxorubicin, a 5x dilution series was performed across the plate, with final concentrations ranging from 64pM-5 µM. The experimental endpoint (cellular viability) was measured 24-,48-, and 72-hours after initial doxorubicin exposure to generate an IC_{50} value. In all cases the maximal exposure to DMSO did not exceed 0.1%. All studies were repeated a minimum of three times and IC_{50} values determined from all replicates.

5.2.5 Assessment of AT1R knockdown on mitigation of doxorubicin-induced hypertrophy in AC10

AC10 cells were seeded at a density of $2x10^4$ cells per well into a 6-well Plate and allowed to adhere overnight. Cells were then transfected as above and exposed to either 7.5 µL of TransIT-X2 transfection reagent alone as mock transfection, 20nM non-target siRNA, 20nM

AT1R siRNA, or to media alone. After a 24 hours period, media was replaced with that containing 50nM doxorubicin or to drug vehicle (DMSO). After a further 24 hours, media was replaced in the absence of doxorubicin. The effect of transfection to doxorubicin-induced hypertrophy was assessed 48 h after the initial doxorubicin exposure. Cells were exposed to 1X CellMask™ Actin Tracking Stains solution (Invitrogen) for a period of 15 minutes as described in section 2.6. Micrograph images were collected by fluorescent microscopy at a magnification of 20x (NikonTE2000 microscope). The surface area of a minimum of 10 cells in 5 random fields per well were determined using ImageJ software.

5.3 Results

5.3.1 Optimization of transfection reagents and methodology for AC10 cells

Prior to conducting studies of siRNA-mediated knockdown of AT1R expression, the methodology firstly requires optimisation. Transfection efficiency was assessed in AC10 cells using different concentrations of siGLO red indicator (20, 30, 40 nM) and different volumes of transfection reagent (5, 7.5, 10 µL). As shown in Figure 5.2, the intensive red fluorescence signal of siGLO red transfection indicator was observed with 7.5 µL and 10 µL of the transfection reagent. Based on these results, 7.5 µL and 10 µL were selected as the optimal concentrations for subsequent transfection experiments in AC10.

5.3.2 Demonstration of lack of effect of transfection methodology upon expression of AT1R in AC10 cells

To confirm a lack of an effect of siRNA transfection methodology upon baseline expression of AT1R in AC10, cells were mock transfected or transfected with non-target siRNA and the AT1R mRNA expression levels determined using RT-qPCR. As shown in Figure 5.3, AT1R mRNA expression levels were neither affected by mock transfection relative to untreated controls ($p=0.20$) or use of a non-target siRNA relative to mock transfected cells ($p=0.064$), respectively.

5.3.3 Optimization of siRNA concentration for knockdown of AT1R in AC10 cells

To determine the optimal conditions for knockdown of AT1R in AC10 cells, 20nM and 40nM concentrations of AT1R siRNA for 24 and 48 hours were evaluated. As illustrated in Figure 5.4 (A: 24 hours, B: 48 hours), a significant knockdown efficiency of AT1R mRNA expression levels was observed with both 20nM and 40nM AT1R siRNA within 24 hours but a reduction in the knockdown efficiency of AT1R mRNA expression levels was observed at 48 hours. Thus, 20nM AT1R siRNA with a 24-hour post-transfection incubation was selected as the ideal concentration and time for subsequent transfection experiments.

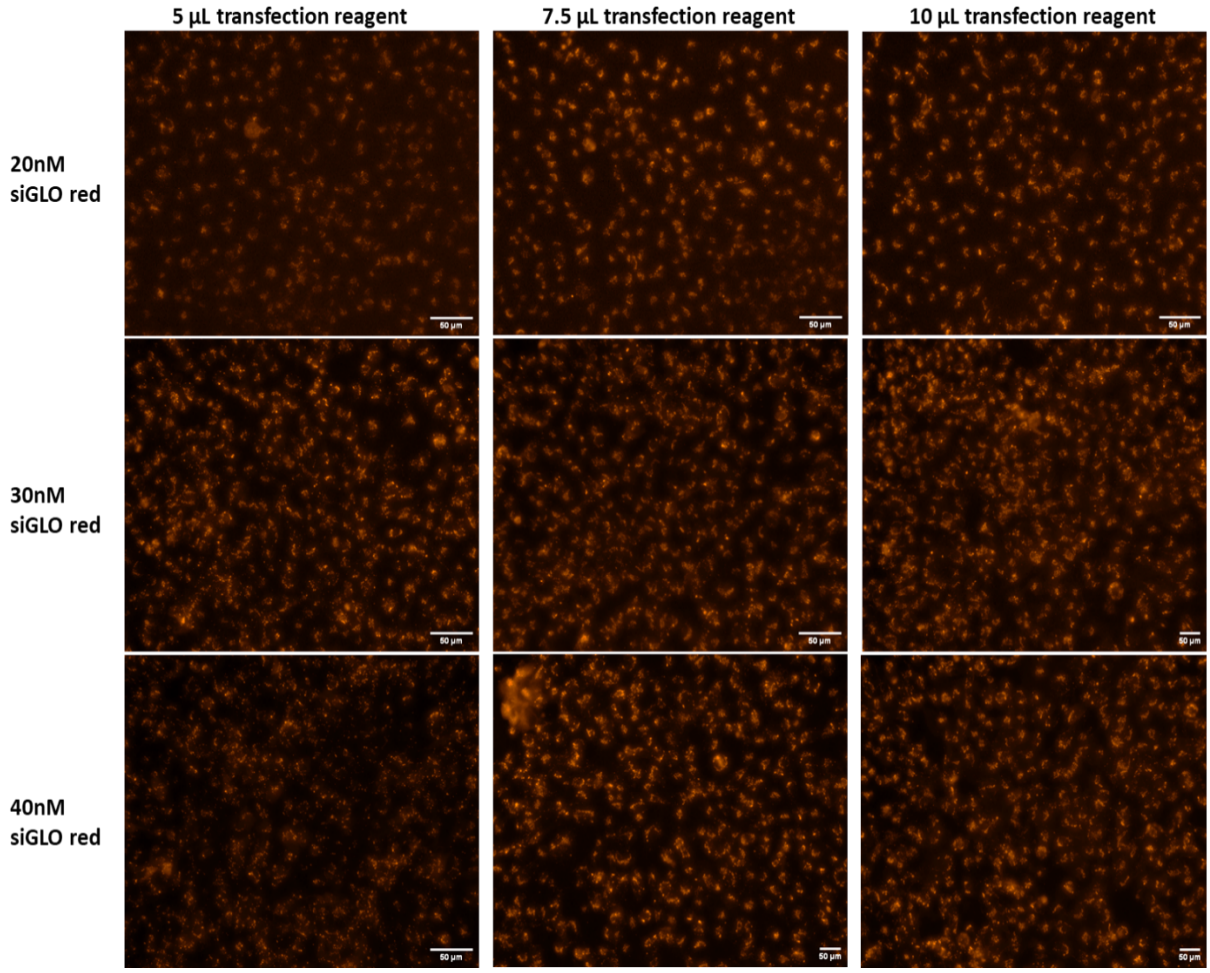

Figure 5.2 Photo micrographs of different concentrations of siGLO red transfection indicator+ transfection reagent (5 µL, 7.5 µL and 10 µL) to identify the optimal concentration for transfection in AC10 cardiomyocytes. (Magnification: 10x).

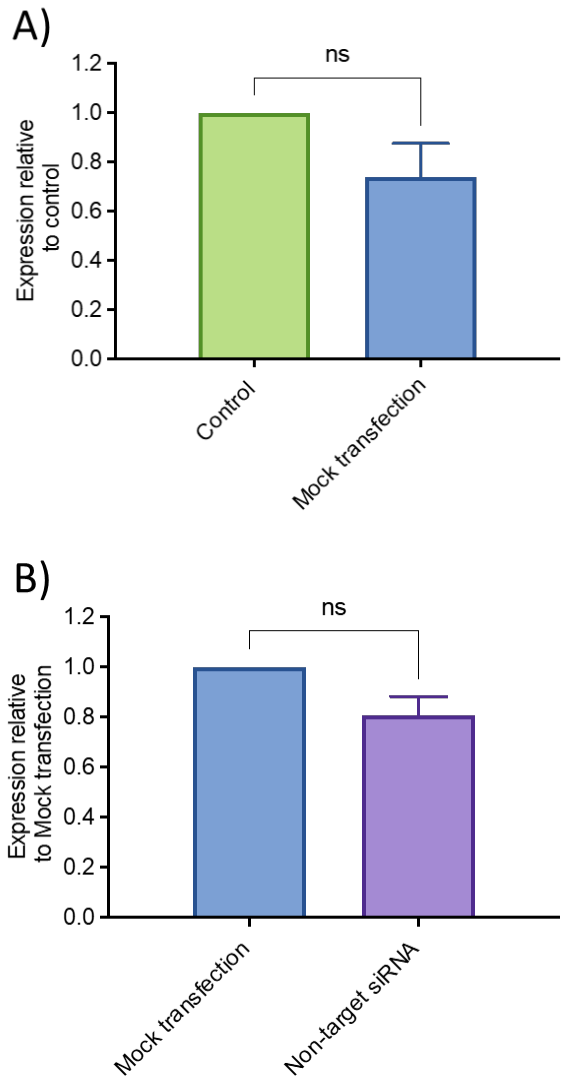

Figure 5.3 Transfection of mock or non-targeting siRNA does not alter baseline AT1R mRNA expression in AC10. A) AT1R mRNA expression level at 24 hrs following mock transfection compared to AT1R mRNA expression level of control. B) AT1R mRNA expression level at 24 hrs following non-target siRNA compared to AT1R mRNA expression level of mock transfection. Each data point = mean +/- SE, n ≥ 3. Un-paired t test was used for comparison.

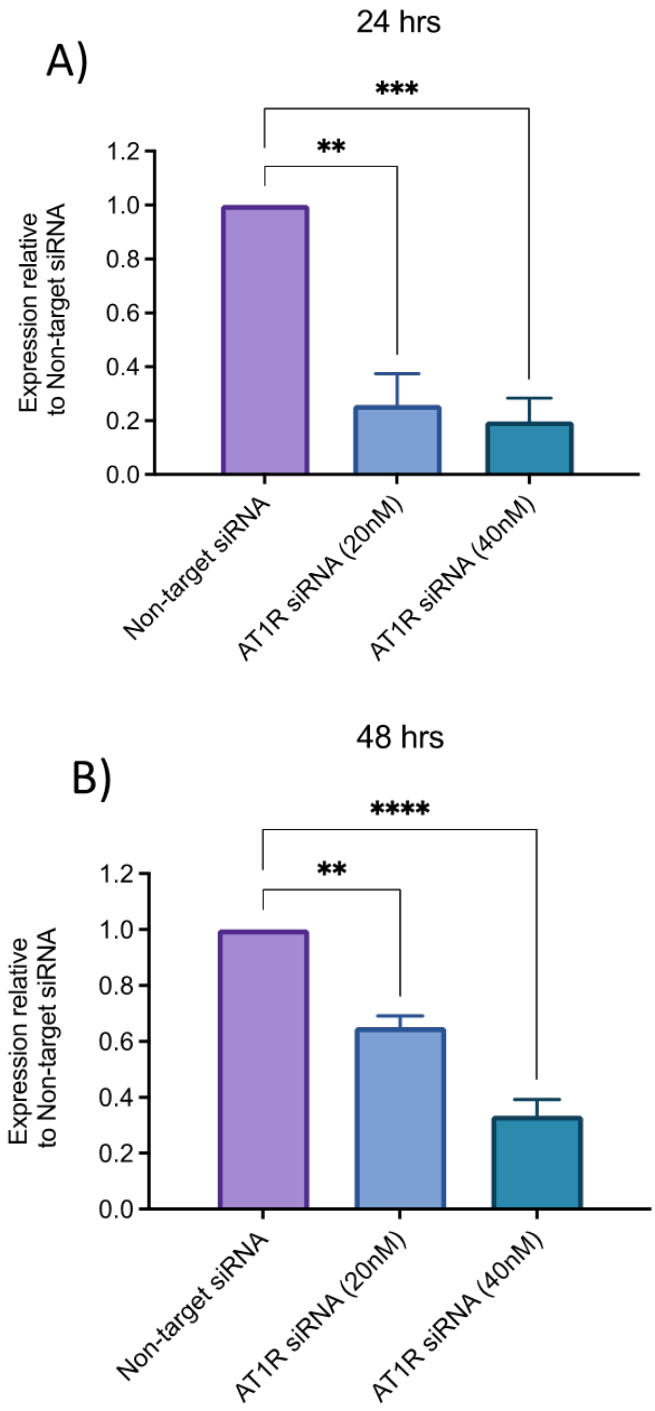

Figure 5.4 Optimal AT1R siRNA concentration for gene knockdown in AC10 cardiomyocytes. A) AT1R mRNA expression level of cells transfected with 20nM and 40nM siRNA directed against AT1R compared to AT1R mRNA expression level of cells transfected with non-target siRNA at 24 hrs and B) AT1R mRNA expression level of cells transfected with 20nM and 40nM siRNA directed against AT1R compared to AT1R mRNA expression level of cells transfected with non-target siRNA at 48hr. Each data point = mean +/- SE, n ≥ 3. Statistical significance was determined by a One-way ANOVA with post-hoc Dunnett's multiple comparison test. (** = $p < 0.01$, *** = $p < 0.001$, **** = $p < 0.0001$).

5.3.4 Transfection methodology does not affect induction of AT1R expression by doxorubicin in AC10 cells

To confirm that the methodology used to introduce siRNA into AC10 cells does not modify their response to doxorubicin, expression analyses were conducted using RT-qPCR. As illustrated in Figure 5.5A, no difference in induction of AT1R mRNA expression levels were observed between mock transfected cells and non-transfected compared to cells exposed to 100nM doxorubicin ($p=0.42$). Similarly, Figure 5.5B shows that introduction of siRNA also did not affect the cellular AT1R response to doxorubicin, with no differential responses observed between cells transfected with non-targeting siRNA and mock transfection to 100nM doxorubicin ($p=0.063$).

5.3.5 siRNA-mediated knockdown of AT1R prevents induction of AT1R expression by doxorubicin in AC10 cells

A significant reduction was detected in AT1R mRNA expression levels in AC10 cells transfected with the optimised 20nM AT1R siRNA, compared to cells transfected with non-target siRNA, qualifying this approach for evaluation of the role of AT1R in cellular responses (Figure 5.5C).

The knockdown of AT1R by siRNA would be expected to mitigate any subsequent cellular response involving upregulation of AT1R genetic (and thus protein) expression, such as in response to doxorubicin. To confirm this direct relationship, AC10 cells were transfected with AT1R siRNA and exposed to doxorubicin. As expected, cells transfected with non-target siRNA demonstrated an upregulation of AT1R expression in response to 100nM doxorubicin, whereas cells transfected with AT1R siRNA showed no significant change in AT1R expression with this anthracycline (Figure 5.5D).

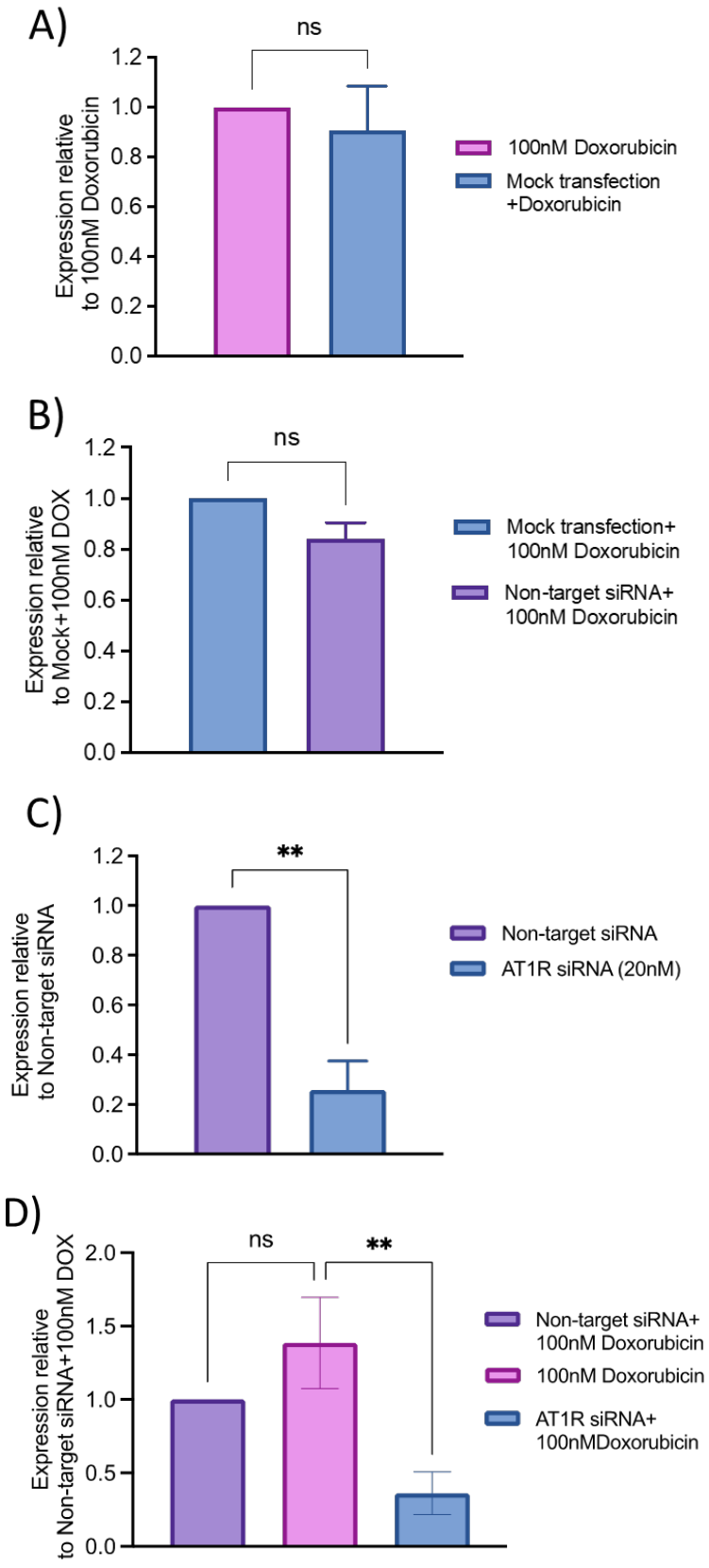

Figure 5.5 AT1R siRNA prevents doxorubicin-induced upregulation of AT1R mRNA expression in AC10. A) AT1R mRNA expression level of cells transfected with mock transfection and then exposed to 100nM doxorubicin compared to AT1R mRNA expression level of cells exposed to 100nM doxorubicin alone at 24 hrs, B) AT1R mRNA expression level of cells transfected with non-target and then exposed to 100nM doxorubicin compared to

AT1R mRNA expression level of cells transfected with mock transfection and then exposed to 100nM doxorubicin, C) AT1R mRNA expression level of cells transfected with 20nM siRNA directed against AT1R compared to AT1R mRNA expression level of cells transfected with non-target siRNA at 24 hrs, and D) AT1R mRNA expression level of cells transfected with 20nM siRNA directed against AT1R and then exposed to 100nM doxorubicin compared to AT1R mRNA expression level of cells transfected with non-target siRNA and then exposed to 100nM doxorubicin and cells exposed to 100nM doxorubicin alone at 24 hrs. Each data point = mean +/- SE, n ≥ 3. Un-paired t test was used for comparison or One-way ANOVA with post-hoc Dunnett's multiple comparison test. (** = $p < 0.01$).

5.3.6 Knockdown of AT1R expression in AC10 cardiomyocytes does not affect sensitivity to doxorubicin cytotoxicity

To assess the cytotoxic response of AC10 to increased concentrations of doxorubicin after knockdown of AT1R, cells were transfected with siRNA directed against AT1R or with non-target siRNA and then exposed to doxorubicin. The viability assessed following exposure to doxorubicin for a 24-,48-, and 72-hours continuous period was determined using the MTS assay. As illustrated in Table 5.1, no significant difference in the cytotoxic IC_{50} of doxorubicin was observed with cells transfected with siRNA directed against AT1R relative to cells transfected with non-target siRNA. This lack of differential response was observed both in terms of concentration or an exposure duration perspective.

5.3.7 Knockdown of AT1R mitigates doxorubicin-induced hypertrophy in AC10 cardiomyocytes

To investigate the role of AT1R in mediating doxorubicin induced hypertrophy in AC10, the effect of siRNA-mediated knockdown of AT1R on the cell area of AC10 in presence and absence of doxorubicin was evaluated after 48 hours of doxorubicin exposure. No difference in cell area of mock transfected cells compared to cell area of non-transfected cells was detected (p=0.998) (Figure 5.6A and B). Similarly, no significant difference in cell area was observed in mock transfected cells compared to non-transfected cells (p=0.998) or cells transfected with non-target siRNA compared to mock-transfected cells when exposed to 50nM doxorubicin, with equivalent hypertrophic responses detected (p=0.999) (Figure 5.6C and D). Together this supports a lack of effect of the transfection process upon cellular morphology.

A lack of an effect for AT1R upon cell morphology (Figure 5.6E and F) was demonstrated by the lack of differential in cell area of cells transfected with non-target siRNA compared to those transfected with AT1R siRNA (p=0.997).

The absence of AT1R, as a result of siRNA knockdown, did however prevent the hypertrophic response of AC10 cells following exposure to doxorubicin. Whereas exposure of AC10 cells transfected with non-target siRNA to 50nM doxorubicin led to an increase in cellular hypertrophy, as previously indicated in section 3.3.10, AC10 cells transfected with AT1R siRNA showed no such hypertrophic response (Figure 5.6E and F), with a significant

statistical difference determined (p=0.0002). Together this implies that AT1R is required for mediation of the hypertrophic response of AC10 cells to doxorubicin.

Table 5.1 No change in IC_{50} values for doxorubicin (64 pM–5 µM) in AC10 cardiomyocytes following transfection with non-targeting or AT1R-siRNA. Data is representative of at least three repeats and presented as IC_{50} ±SEM. Statistical significance was determined by a One-way ANOVA with post-hoc Dunnett's multiple comparison test.

	Cytotoxicity IC_{50} (µM)		
	24 hr	**48 hr**	**72 hr**
Doxorubicin only	>5	0.28±0.07	0.10±0.04
Non-target siRNA transfection+ Doxorubicin	>5	0.36±0.10	0.16±0.05
AT1R siRNA+ Doxorubicin	>5	0.45±0.12	0.17±0.06
P-value	0.42	0.82	0.54

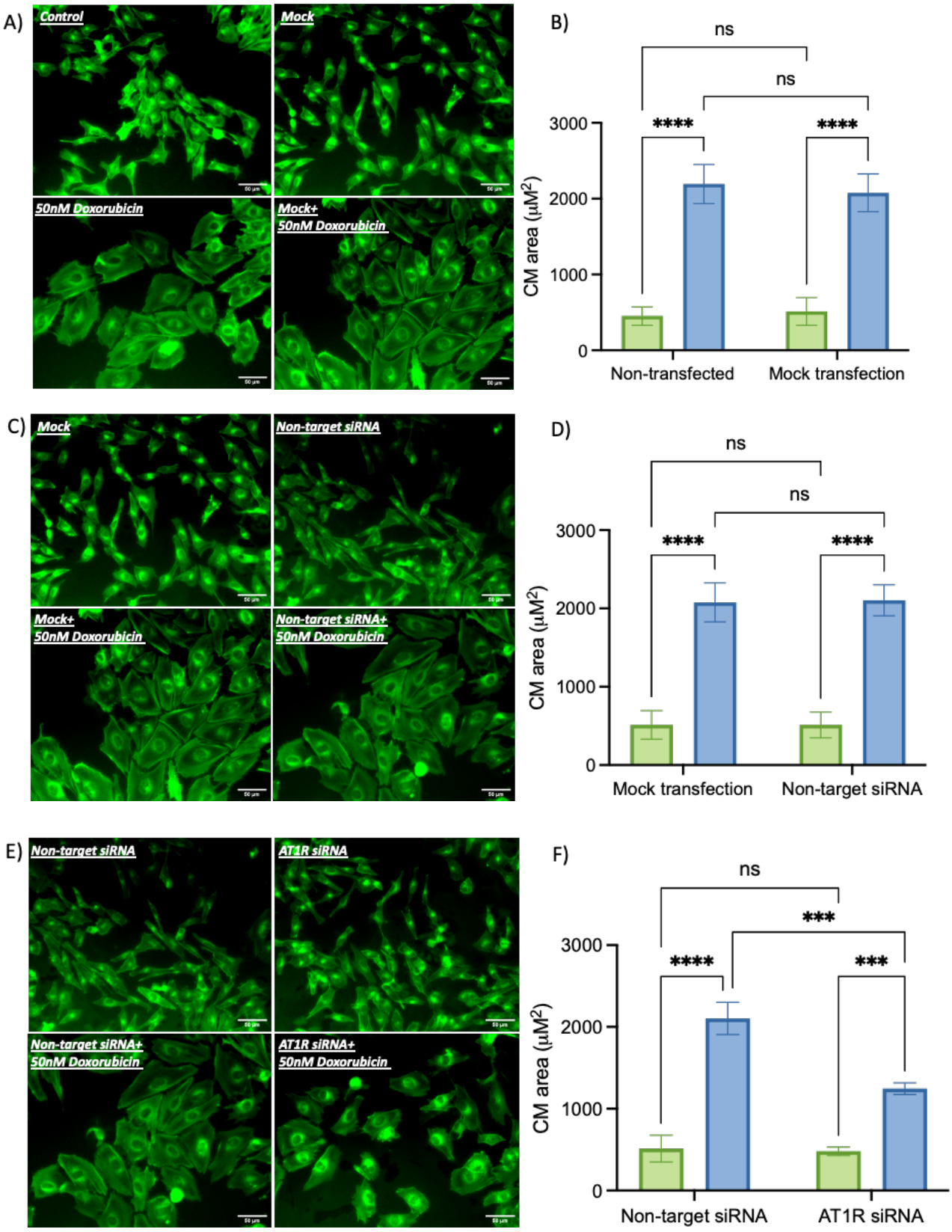

Figure 5.6 Hypertrophy caused by doxorubicin is mitigated following AT1R silencing in AC10. A) Representative images (left) show cell area changes in AC10 in non-transfected cells and mock transfected cells in presence and absence of 50nM doxorubicin. B) The quantification graph (right) illustrates mean cell area (µm²) increased in cells exposed to 50nM doxorubicin compared to control in non-transfected cells and mock transfected cells, C) Representative images (left) show cell area changes in AC10 transfected with either mock or non-targeting

siRNA in presence and absence of 50nM doxorubicin. D) The quantification graph (right) illustrates mean cell area (µm²) increased in cells exposed to 50nM doxorubicin compared to control in mock transfected cells and in cell transfected with non-target siRNA, and E) Representative images (left) show cell area changes in AC10 transfected with either non-targeting siRNA or 20nM AT1R siRNA in presence and absence of 50nM doxorubicin. F) The quantification graph (right) illustrates mean cell area (µm²) increased in cells exposed to 50nM doxorubicin compared to control in cell transfected with non-target siRNA and in cell transfected with AT1R siRNA. However, mean cell area (µm²) decreased in cells transfected with AT1R siRNA and then exposed to 50nM doxorubicin compared to cell transfected with non-target siRNA and then exposed to 50nM doxorubicin. Cells were stained with a green, fluorescent marker to visualize cell structure. Mean cell area (µm²) was calculated using ImageJ. Each data point = mean +/- SE, n ≥ 3. Statistical significance was assessed using two-way ANOVA. (*** = $p < 0.001$, **** = $p < 0.0001$). (Scale bar: 50 µm) (Magnification:20x). ■ Control and ■ 50nM Doxorubicin.

5.3.8 Optimization of transfection reagents and methodology for HCF cells

Prior to conducting studies of siRNA-mediated knockdown of AT1R expression, the methodology firstly requires optimisation. Transfection efficiency was assessed in HCF cells using different concentrations of siGLO red indicator (20, 30, 40 nM) and different volumes of transfection reagent (5, 7.5, 10 µL). As shown in Figure 5.7, the intensive red fluorescence signal of siGLO red transfection indicator was observed with 7.5 µL and 10 µL of the transfection reagent. Based on these results, 7.5 µL and 10 µL were selected as the optimal concentrations for subsequent transfection experiments in HCF.

5.3.9 Demonstration of lack of effect of transfection methodology upon expression of AT1R in HCF cells

To confirm a lack of an effect of siRNA transfection methodology upon baseline expression of AT1R in HCF, cells were mock transfected or transfected with non-target siRNA and the AT1R mRNA expression levels determined using RT-qPCR. As shown in Figure 5.8, the AT1R mRNA expression levels were neither affected by mock transfection relative to untreated controls ($p=0.99$) or use of a non-target siRNA relative to mock transfected cells ($p=0.55$), respectively.

5.3.10 Optimization of siRNA concentration for knockdown of AT1R in HCF cells

To determine the optimal conditions for knockdown of AT1R in HCF, 20nM and 40nM concentrations of AT1R siRNA for 24 and 48 hours were evaluated. As illustrated in Figure 5.9 (A: 24 hours, B: 48 hours), a significant knockdown efficiency of AT1R mRNA expression levels was observed with both 20nM and 40nM AT1R siRNA within 24 hours and 48 hours. Thus, 20nM AT1R siRNA with a 24-hour post-transfection incubation was selected as the ideal concentration and time for subsequent transfection experiments.

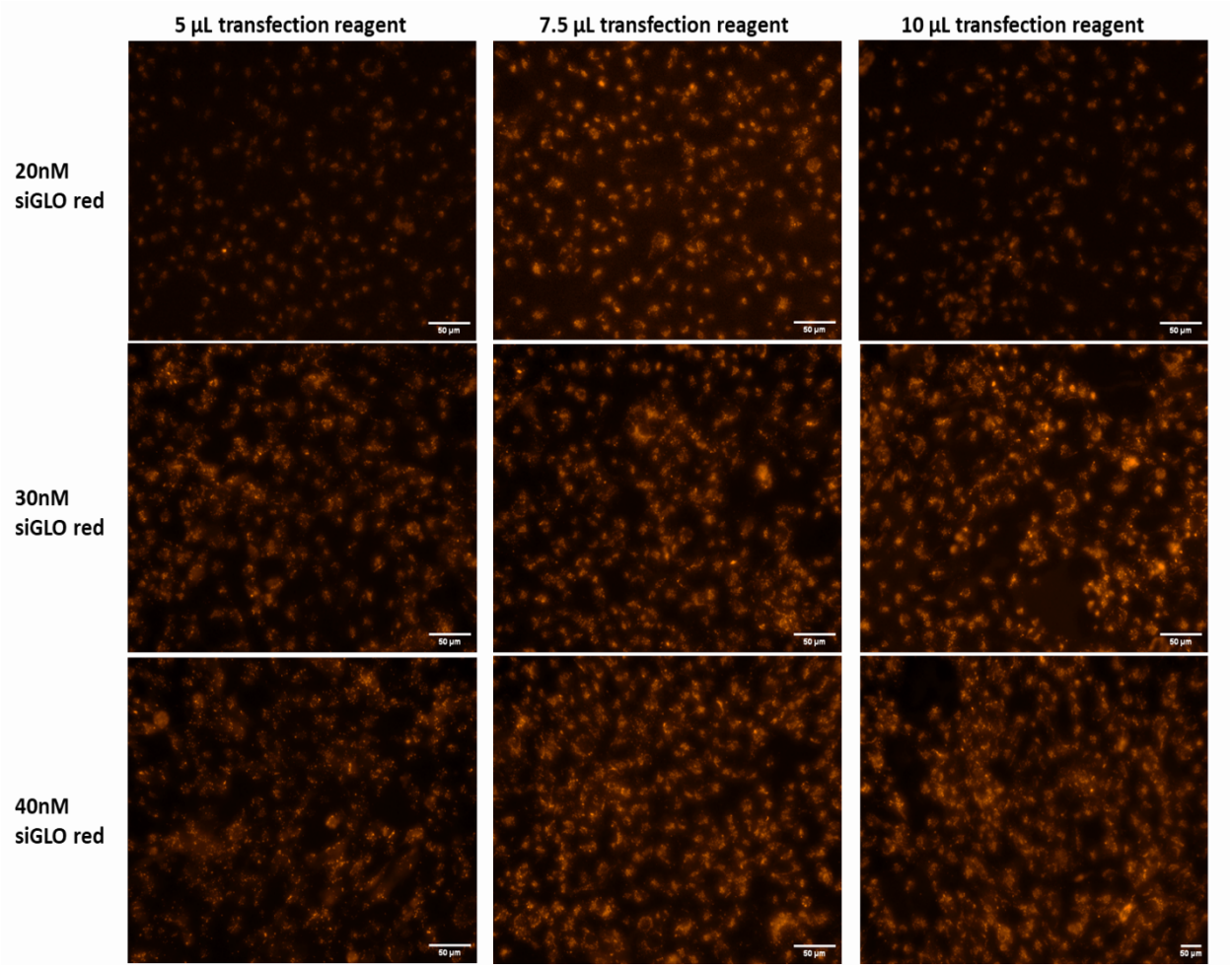

Figure 5.7 Photo micrographs of different concentrations of siGLO red transfection indicator+ transfection reagent (5 µL, 7.5 µL and 10 µL) to identify the optimal concentration for transfection in HCF. (Magnification: 10x).

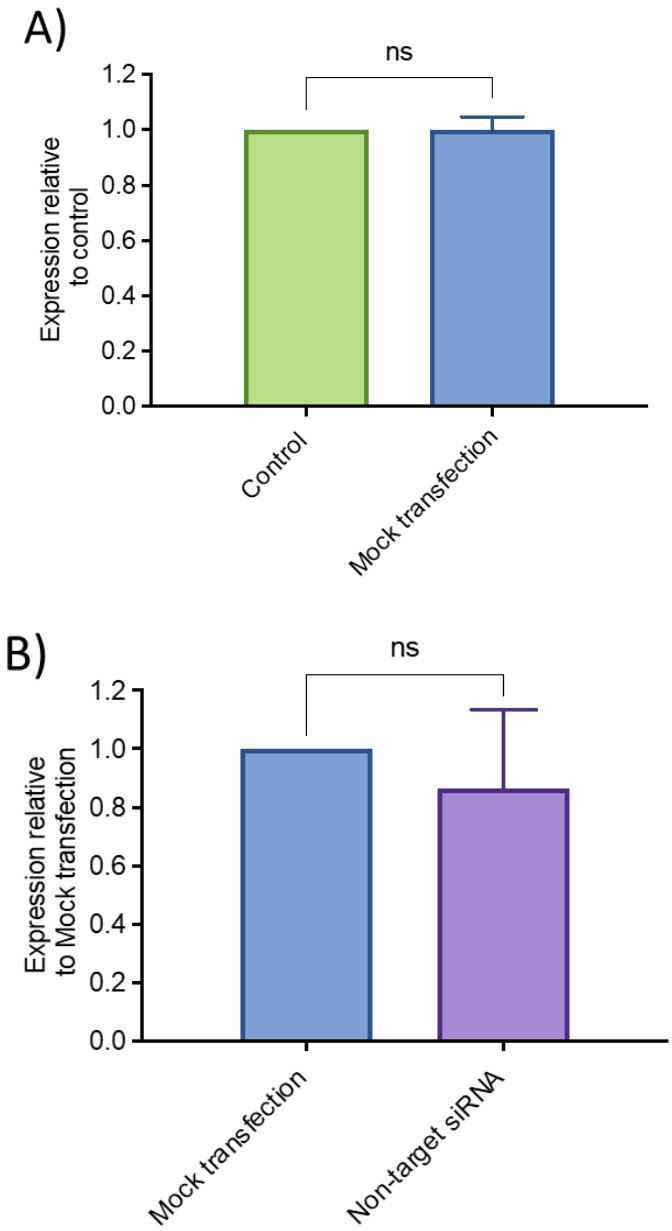

Figure 5.8 Transfection of mock or non-targeting siRNA does not alter baseline AT1R mRNA expression in HCF. A) AT1R mRNA expression level at 24 hrs following mock transfection compared to AT1R mRNA expression level of control. B) AT1R mRNA expression level at 24 hrs following non-target siRNA compared to AT1R mRNA expression level of mock transfection. Each data point = mean +/- SE, n ≥ 3. Un-paired t test was used for comparison.

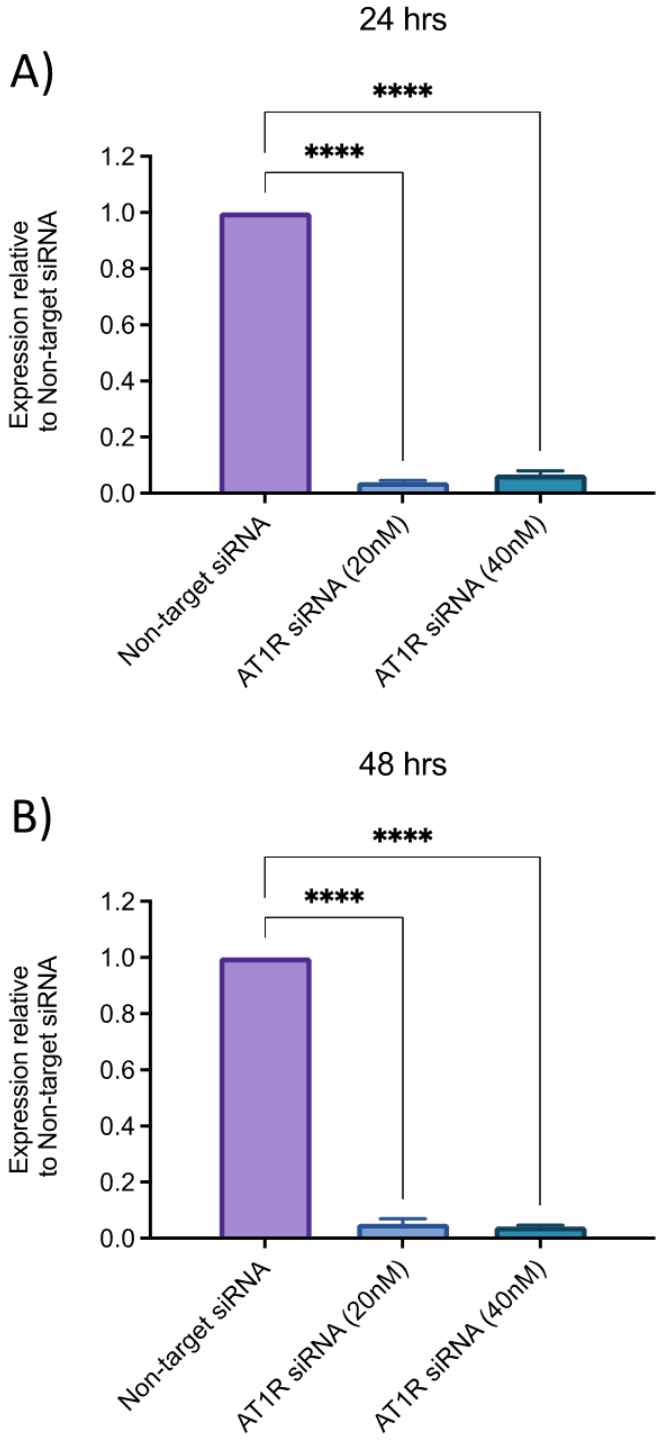

Figure 5.9 Optimal AT1R siRNA concentration for gene knockdown in HCF. A) AT1R mRNA expression level of cells transfected with 20nM and 40nM siRNA directed against AT1R compared to AT1R mRNA expression level of cells transfected with non-target siRNA at 24 hrs and B) AT1R mRNA expression level of cells transfected with 20nM and 40nM siRNA directed against AT1R compared to AT1R mRNA expression level of cells transfected with non-target siRNA at 48hr. Each data point = mean +/- SE, n ≥ 3. Statistical significance was determined by a One-way ANOVA with post-hoc Dunnett's multiple comparison test. (**** = $p < 0.0001$).

5.3.11 Transfection methodology does not affect induction of AT1R expression by doxorubicin in HCF

To investigate the role of the AT1R in the cytotoxic response of HCF to doxorubicin, siRNA-mediated knockdown of AT1R mRNA expression was conducted using RT-qPCR. As illustrated in Figure 5.10A, no difference in AT1R mRNA expression levels were observed between mock transfected and non-transfected HCFs exposed to 500nM doxorubicin ($p=0.27$), with both showing similar levels of AT1R mRNA induction. Similarly, a lack of difference in doxorubicin-induced levels of AT1R mRNA were observed between cells transfected with non-targeting siRNA relative to mock transfected cells ($p=0.13$; Figure 5.10B).

5.3.12 siRNA-mediated knockdown of AT1R prevents induction of AT1R expression by doxorubicin in HCF

A significant reduction was detected in AT1R mRNA expression level in HCF cells transfected with the optimised 20nM AT1R siRNA, compared to cell transfected with non-target siRNA, qualifying this approach for evaluation of the role of AT1R in cellular responses (Figure 5.10C).

The knockdown of AT1R by siRNA would be expected to mitigate any subsequent cellular response involving upregulation of AT1R genetic (and thus protein) expression, such as in response to doxorubicin. To confirm this direct relationship, HCF cells were transfected with AT1R siRNA and exposed to doxorubicin. As expected, cells transfected with non-target siRNA demonstrated an upregulation of AT1R expression in response to 500nM doxorubicin, whereas cells transfected with AT1R siRNA showed no significant change in AT1R expression with this anthracycline (Figure 5.10D).

5.3.13 Knockdown of AT1R expression in HCF does not affect sensitivity to doxorubicin cytotoxicity

To assess the cytotoxic response of HCF to increased concentrations of doxorubicin after knockdown of AT1R, cells were transfected with siRNA directed against AT1R or with non-target siRNA and then exposed to doxorubicin. The viability assessed following exposure to doxorubicin for a 24-,48-, and 72-hours continuous period was determined using the MTS assay. As shown in Table 5.2, no significant difference in the cytotoxic IC_{50} of doxorubicin was observed with cells transfected with siRNA directed against AT1R compared to cells

transfected with non-target siRNA, both in terms of concentration or an exposure duration perspective.

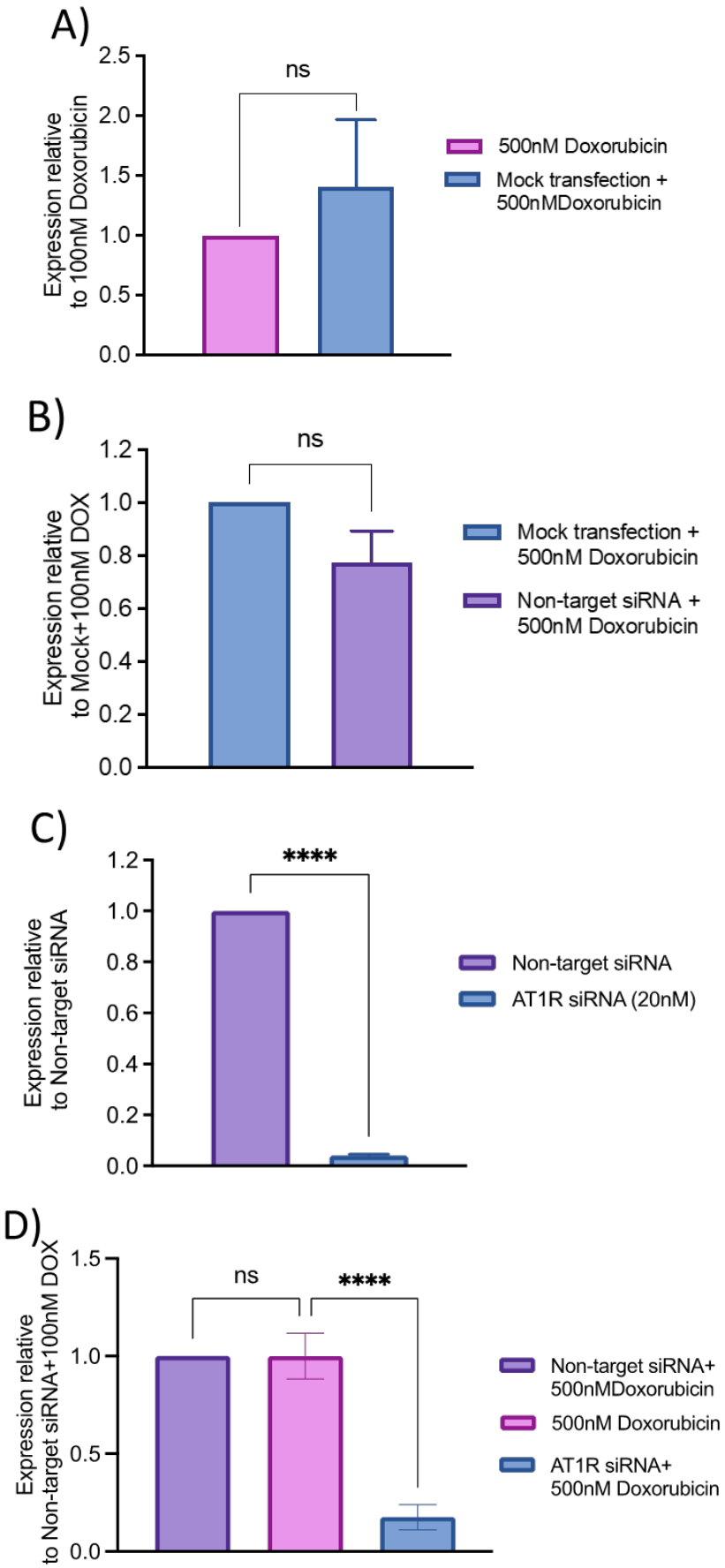

Figure 5.10 AT1R siRNA prevents doxorubicin-induced upregulation of AT1R mRNA expression in HCF. A) AT1R mRNA expression level of cells transfected with mock transfection

and then exposed to 500nM doxorubicin compared to AT1R mRNA expression level of cells exposed to 500nM doxorubicin alone at 24 hrs, B) AT1R mRNA expression level of cells transfected with non-target and then exposed to 500nM doxorubicin compared to AT1R mRNA expression level of cells transfected with mock transfection and then exposed to 500nM doxorubicin, C) AT1R mRNA expression level of cells transfected with 20nM siRNA directed against AT1R compared to AT1R mRNA expression level of cells transfected with non-target siRNA at 24 hrs, and D) AT1R mRNA expression level of cells transfected with 20nM siRNA directed against AT1R and then exposed to 500nM doxorubicin compared to AT1R mRNA expression level of cells transfected with non-target siRNA and then exposed to 500nM doxorubicin and cells exposed to 500nM doxorubicin alone at 24 hrs. Each data point = mean +/- SE, $n \geq 3$. Un-paired t test was used for comparison or One-way ANOVA with post-hoc Dunnett's multiple comparison test. (**** = $p < 0.0001$).

Table 5.2 No change in IC_{50} values for doxorubicin (64 pM–5 µM) in HCF following transfection with non-targeting or AT1R-siRNA. Data is representative of at least three repeats and presented as IC50 ±SEM. Statistical significance was determined by a One-way ANOVA with post-hoc Dunnett's multiple comparison test.

	Cytotoxicity IC_{50} (µM)		
	24 hours	**48 hours**	**72 hours**
Doxorubicin only	>5	0.49±0.22	0.10±0.03
Non-target siRNA+ Doxorubicin	>5	0.40±0.21	0.15±0.09
AT1R siRNA+ Doxorubicin	>5	0.54±0.35	0.18±0.10
P-value	0.41	0.90	0.76

5.4 Discussion

While the precise mechanisms underlying AIC remain unknown, growing evidence suggests the involvement of RAAS in AIC pathogenesis (34). Several clinical studies have evaluated the effect of ARBs, such as telmisartan, in mitigation of AIC (see section 1.8.3.1). In this study it has been shown that doxorubicin induces cardiomyocyte hypertrophy (Chapter 3), with this response being mitigated by exposure to telmisartan. Doxorubicin has also been shown to induce AT1R expression in both AC10 cardiomyocytes and HCFs (Chapter 4). However, it is still unclear whether this hypertrophic cardiomyocyte response and increase in AT1R expression are contributing factors in the toxicological response to doxorubicin or are bystanders independent of AIC pathogenesis. Clarification of this is achieved by removal or elimination of AT1R from the cellular environment, as is achieved by siRNA methodologies.

The use of siRNA as a research tool has gained significant recognition in both basic science and drug development due to its ability to regulate gene expression (259). siRNA can be designed to target a specific gene of interest, thereby minimising off-target effects and offering a valuable approach for therapeutic applications. In this study, siRNA was utilised to knock down the expression of AT1R in both AC10 cardiomyocyte and HCF, allowing for a direct investigation into its role in AIC. In contrast to ACEi and ARBs studies which only assess an involvement for an active angiotensin signalling pathway, gene-silencing offers a more precise evaluation of AT1R involvement, providing mechanistic insights into the involvement of AT1R in the pathogenesis of AIC.

Optimisation of AT1R knockdown identified 7.5 µL of transfection reagent combined with 20nM of AT1R siRNA, with a 24-hour transfection period, for both AC10 and HCF cells. The transfection process was not shown to affect either cellular morphology or response of cells to doxorubicin. Furthermore, AT1R knockdown did not affect cellular cytotoxicity responses to doxorubicin, with IC_{50} values remaining unchanged between AT1R positive and negative cells in both AC10 and HCF cells. This implies that AT1R is not necessary or involved in doxorubicin-mediated cytotoxic response. From a clinical perspective, this observation aligns with findings from the PRADA clinical trial which showed that inhibition of AT1R by ARB candesartan did not prevent early markers of cardiotoxicity such as elevations in cardiac troponin I and T, a sensitive biomarkers of cardiomyocyte injury (166, 260). Therefore, this result reinforces the concept that AT1R may contribute to structural cardiotoxicity such as

hypertrophy and remodelling which appears to occur independently of doxorubicin- cytotoxic response (261).

Despite AT1R having no observable role in doxorubicin-induced cytotoxicity, it was shown to play a central role in the adaptive response of cardiac cells to sub-toxic concentrations of doxorubicin. Such an involvement is highly pertinent for AIC as it is the cells which remain after the initial cytotoxic response and thus contribute to the functional aspects of the cardiac myocardium which are of importance for potential development of cardiac failure often associated with anthracyclines. In this study it was specifically demonstrated that knockdown of AT1R in AC10 human cardiomyocytes mitigated doxorubicin induced hypertrophy, confirming the central function of AT1R in mediating the hypertrophic response of cardiomyocytes to anthracyclines. This reaffirms the actions of telmisartan, which blocked activity of AT1R and subsequently also prevented cellular hypertrophy. This finding supports the hypothesis that doxorubicin induces hypertrophy via AT1R-dependent mechanisms and strengthens the central hypothesis of this study that doxorubicin requires the AT1R for its cardiotoxic actions and blocking of angiotensin II signalling can preserve cardiac function during doxorubicin-based chemotherapy treatment. This also has clinical implications particularly in explaining the interpatient variability in cardiotoxicity risk. The present study demonstrated that doxorubicin upregulates the expression of AT1R, which is now understood to be a critical mediator of its cardiotoxic effects. Therefore, in patients with elevated circulating angiotensin II levels such as those with hypertension, heart failure, or chronic kidney disease, the upregulation of AT1R expression induced by doxorubicin may lead to enhanced receptor availability on cardiomyocytes. Consequently, the presence of more AT1R may amplify the cellular response to angiotensin II and promote greater hypertrophic responses and adverse cardiac remodelling, which may accelerate the progression to heart failure.

AT1R is the most prevalent type of angiotensin II receptor in the cardiovascular system and primary responsible for mediating the well-known effects of angiotensin II, vasoconstriction, hypertension, and the regulation of salt and water balance (115). Activation of AT1R can trigger different cellular response include oxidative stress, hypertrophy, fibrogenesis, inflammation, and cell death which all contributes to cardiac damage (34, 235). Systemic knockdown of AT1R activity or expression have previously been shown to reduce the cardiotoxicity potential of anthracyclines (170, 257, 262). Knockdown of AT1R in mice led to a decrease in the number of apoptotic cells within cardiac tissue, attenuation of ANP levels, and

mitigation of heart LV-remodelling in response to doxorubicin treatment (170). The observations from knockdown of AT1R in cardiomyocytes and HCFs has advanced this observation and has now exemplified the central requirement of AT1R within cardiac cell as opposed to other organs of the body in the context of AIC. While previous studies have implicated the RAAS in systemic cardiovascular pathologies, the present study builds upon this by demonstrating that AT1R expression within cardiac cells is directly modulated by doxorubicin exposure, and that its silencing can mitigate key structural responses such as hypertrophy. This highlights a direct, cell-intrinsic requirement for AT1R in mediating doxorubicin responses, specifically in cardiomyocytes and CFs, thus advancing our understanding beyond broader systemic models.

Although angiotensin II signalling is primarily modulated through AT1R, other receptors are also know to bind angiotensin II such as AT2R (118). In contrast to the effect mediated by AT1R, AT2R activation promotes vasodilatation, prevents cellular proliferation and counterbalances AT1R with an antihypertrophic response (118). Despite the beneficial cardiovascular effects of AT2R receptor, the protective effects against AIC observed in this study by telmisartan or AT1R knockdown do not support a role for AT2R in this context. Given that AT1R blocking was able to mitigate doxorubicin-induced hypertrophy and reduce AT1R overexpression in cardiac cells, it is clear that the protective effects in this study are mediated through AT1R inhibition.

In conclusion, this chapter provides evidence that the presence of AT1R is essential for the cardiomyocyte adaptive toxicological response of sub-toxic doxorubicin but is not involved in the cytotoxicity of doxorubicin against either cardiomyocytes or CFs. Moreover, this reinforces the fact that blocking of AT1R in cardiomyocyte can protect against the longer-term effects of doxorubicin, including cardiac hypertrophy and upregulation of AT1R expression, which exacerbate cardiac damage and contribute to the progressive nature of cardiac failure.

Chapter 6. General Discussion

Anthracyclines are a class of chemotherapeutic agents extensively utilised in the treatment of a broad range of haematological malignancies and solid tumours, including breast, gastric, and lung cancers (10). While their clinical efficacy is well established, with significant evidence for treatment success and improvements in cancer survivorship, their use is strongly associated with significant adverse effects upon the cardiovascular system (8, 9). Patients who have received anthracycline-based therapy presented in the clinic often years later, with clinical symptoms consistent with heart failure (14). To address this significant issue, a number of cardioprotective strategies have been explored. Among these, heart failure therapy such as ACEi and ARBs have been evaluated in many clinical trials for management of AIC (see section 1.8.3.1). This was based on the fact that clinical presentation of AIC is noted as being similar to that observed with heart failure (144, 145). Clinical studies thereby highlighting the putative relationship between angiotensin signalling and AIC. Emerging evidence suggests that doxorubicin contributes to adverse cardiac remodelling and dysfunction by modulating RAAS signalling pathways but the mechanism of this cardiotoxicity still elusive (34). The aim of this study was to investigate the mechanism of AIC by assessing the morphological changes associated with doxorubicin exposure in different cardiac cells and exploring the role of angiotensin II signaling pathway, particularly AT1R, in mediating this cardiotoxicity. The current study conducted *in vitro* which allows for a direct evaluation of cell responses to doxorubicin and investigation of cellular mechanisms underlying doxorubicin-induced cardiotoxicity without the confounding effects of systemic interactions.

Angiotensin II, a well-known effector in the RAAS, exerts its effects primarily through the AT1R, playing a critical role in cardiac remodelling by promoting cardiomyocyte hypertrophy and fibroblast-mediated interstitial fibrosis (206, 263). In order to address the role for angiotensin signalling in AIC and the underpinning mechanism, qualification of the cellular models used in this project was required. Exposure to physiological concentration of angiotensin II induce hypertrophy in AC10 human cardiomyocyte. This aligns with the large body of evidence that shows the important role of angiotensin II in mediating cardiomyocyte hypertrophy and mediating pathogenesis of many cardiovascular diseases (221-223). The activation of AT1R and cardiotoxic effect of anthracycline share common effects including the induction of oxidative stress and generation of ROS, which lead to cardiomyocyte cell death

and/or cell stress (33, 34, 48, 235). These similarities support a mechanistic link between AIC and dysregulation of the angiotensin signalling pathway.

Interestingly, sub-toxic concentrations of doxorubicin have been shown in this study to induce hypertrophy in AC10 human cardiomyocytes. This morphological enlargement after exposure to doxorubicin may indicate the early response of cardiomyocytes to doxorubicin that contributes to cardiotoxicity, potentially to maintain contractile function in response to cellular stress (264). However, sustained hypertrophic response has been implicated in the progression toward decrease LVEF then heart failure (265). The similarity in response between angiotensin II and doxorubicin further support the relationship between angiotensin II signalling and AIC. Both angiotensin II and doxorubicin have been shown to independently induce hypertrophy in AC10 human cardiomyocytes. To further investigate the interplay between angiotensin II and doxorubicin, this study assessed the combined effects of angiotensin II and doxorubicin on cell viability, cellular impedance, and morphological changes in AC10 human cardiomyocytes. Interestingly, these findings indicate that the combination of angiotensin II and doxorubicin does not exacerbate the cytotoxic effects observed with doxorubicin alone in terms of cell viability and morphology, implying that angiotensin II and doxorubicin induce hypertrophy and cytotoxic effects via the same pathway which support the relationship between angiotensin II signalling and AIC.

To address this interrelationship between angiotensin signalling and AIC, this study evaluated the ability of ACEi and ARB, both which affect angiotensin II activities, to affect the cardiac cellular response to the anthracycline doxorubicin. ACEi and ARBs are both used clinically for treatment of hypertension, reduction of LV hypertrophy, and heart failure (26, 266). The mechanism of action for both ACEi and ARBs is inhibition of angiotensin II signalling pathway (113). This attenuation of angiotensin II signalling leads to reduction of cardiac hypertrophy, hypertension, and myocardial injury. Inhibition of angiotensin II signalling by ACEi and ARB have been shown to confer cardioprotective effects in preclinical models of AIC, reportedly through protection against hemodynamic and morphologic changes induced by anthracyclines (34). In addition, the cardioprotective effect of ACEi and ARBs has extended to mitigation of AIC in cancer patients treated with anthracycline as reported by several clinical trials as discussed in (see section 1.8.3.1) (15, 267). These findings underscore the need for further studies to evaluate the mechanism of AIC and its relationship with angiotensin II signalling, not least because systemic effects are difficult to untangle from cellular effects at this scale. In this context, neither the ACEi enalapril nor enalaprilat (the active form of

enalapril) mitigated the toxicological responses of doxorubicin against AC10 cells or HCFs in vitro in this study. This is not surprising since ACE is expressed in non-cardiac tissues within the body where it systemically converts angiotensin I into the active moiety angiotensin II, with no such environment (or by default ACE) present in the *in vitro* cellular environment (146). Conversely, pre-treatment of AC10 cardiomyocytes with the ARB telmisartan mitigated the hypertrophic effect induced by doxorubicin, evidenced by a reduction in the cell index increase exhibited in the xCELLigence assay. This support the hypothesis that doxorubicin-induced hypertrophy is mediated through the AT1R-dependent angiotensin II signalling pathway. Unlike telmisartan, pre-exposure of AC10 to ARBs losartan and candesartan, which inhibit activation of the cell surface receptor for angiotensin II, did not mitigate doxorubicin induced hypertrophy. This difference in the effect between telmisartan and other ARBs can be explained by the pharmacokinetics/dynamic properties of these ARBs. Telmisartan is reported to exhibit prolonged receptor blocking and dissociates from the AT1R receptor very slowly after binding, significantly different from other ARBs (231). This study may help explain the differences between the ARBs in their efficacy in preventing doxorubicin induced hypertrophy in AC10, suggesting that prolonged receptor blocking of these drugs play a role in their protective effect.

To further investigate the underlying mechanism of AIC, its relationship with angiotensin II signalling, and to ascertain that the protective effect of telmisartan was through AT1R, the mechanism of anthracycline induced hypertrophy was further explored by assessing AT1R expression at both mRNA and protein levels in AC10 human cardiomyocytes after exposure to doxorubicin. Previous studies have shown an upregulation of AT1R expression at protein and mRNA levels after doxorubicin exposure in the rat myoblast H9c2 cell line. This result was however hindered by the use of immature cardiac cell lines derived from rat myocardium and suprapharmacological or high toxic concentrations of doxorubicin (234, 247). By using of AC10 human cardiomyocytes, doxorubicin was shown to induce AT1R mRNA expression, suggesting that doxorubicin exacerbates the angiotensin signalling pathway within cardiomyocytes and consequently induce cellular hypertrophy. To increase the clinical relevance of these findings, AT1R mRNA expression was subsequently determined in hiPSC-CMs, which provide a more physiologically relevant human cardiac model compared to immortalized cell lines like AC10, as they better recapitulate the electrophysiological and contractile properties of adult human cardiomyocytes. The confirmation of doxorubicin-

induced AT1R mRNA upregulation in hiPSC-CMs strengthens the use of AC10 human cardiomyocyte cell line as a model of cardiomyocyte in such mechanistic studies.

The role of AT1R in anthracycline cardiotoxicity is supported by observations from Huang et al. (2018) who found that AT1R upregulation was required for doxorubicin-induced cardiotoxicity by mitochondrial ROS-mediated mitogen-activated protein kinase (MAPK) signalling pathways and heat shock factors (HSF2) activation, providing a mechanistic link between oxidative stress, AT1R signalling, and anthracycline cardiotoxicity (247). This is supported also by *in vivo* studies on rats similarly found that pre-treatment with ARBs telmisartan and losartan can reduce the morphological and biochemical changes associated with doxorubicin treatment and mitigate AT1R upregulation in rats (234, 257). Taken together, the results from the study herein indicate that doxorubicin induces cardiotoxicity is largely caused via the AT1R-mediated angiotensin II signalling pathway and blocking of this receptor able to mitigate cardiovascular side effect associated with doxorubicin.

Another observation is provided from Toko et al study who previously showed that treatment with doxorubicin led to decreased heart function and histological anomalies like myofibrillar loss, an increase in apoptotic cells, and cytoplasmic vacuolization in WT mice (170). However, AT1R knockout mice (AT1KO) and the WT mice given an AT1R antagonist (Olmesartan) did not experience these negative effects (170). In this study, the knockdown of AT1R in AC10 human cardiomyocytes has investigated and showed that it did indeed mitigate doxorubicin induced hypertrophy and prevent AT1R upregulation at mRNA level in AC10 human cardiomyocytes, confirming that AT1R upregulation is required for hypertrophic response after exposure to doxorubicin. This finding supports the hypothesis that doxorubicin induces hypertrophy via AT1R-dependent mechanisms and further support the involvement of RAAS in AIC. This also has important clinical implications, particularly in explaining inter-patient variability in cardiotoxicity risk. The present study demonstrated that doxorubicin upregulates the expression of AT1R, which has now been shown to be essential for mediating the hypertrophic response to anthracycline treatment. In patients with elevated circulating angiotensin II levels such as those with hypertension, heart failure, or chronic kidney disease, this upregulation of AT1R would provide more receptors for angiotensin II to activate, potentially amplifying AT1R signalling. This interaction may contribute to heightened cardiotoxic susceptibility in these patient populations (32).

The heart composes of different cells, CFs considered the most abundant cells in the myocardium which provide support to contracting cardiomyocytes and maintaining ECM

composition through regulation of MMP (211). However, there are limited studies on the role of CFs in developing AIC compared to cardiomyocytes (198). A study on neonatal rat heart cells showed that fibroblast and endothelial cell is more sensitive to doxorubicin than cardiomyocytes, with toxicity assessed via metabolic inhibition, morphological changes, and functional impairments. (268). These findings suggest that AIC extends beyond cardiomyocytes, involving a complex interplay between multiple cardiac cell types. To assess the doxorubicin effect on non-myocytes cell types, CFs were included in this study. This study has demonstrated that neither physiological relevant concentrations of angiotensin II nor sub-toxic concentrations of doxorubicin affect the morphology of CFs. The difference in response between cardiomyocytes and CFs is likely due to their distinct cellular functions and the specific receptors and signalling pathways present in each cell type. Cardiomyocytes exhibit morphological enlargement to increase contractile force, while fibroblasts proliferate and produce ECM components in response to stress signals like angiotensin II and doxorubicin (264). In addition, mitochondria play a crucial role in mediating the differential response of cardiomyocytes and CFs to angiotensin II and doxorubicin. Cardiomyocytes are highly rich in mitochondria for energy production due to their continuous contractile function and have a lower level of antioxidant, making them susceptible to mitochondrial dysfunction induced by ROS formation and oxidative stress (216). Doxorubicin is known to accumulate in cardiomyocyte mitochondria, leading to increased ROS generation, mitochondrial DNA damage, and cell death (33, 48). In contrast, CFs, while also reliant on mitochondrial function, have a lower energy demand, less oxygen consumption, and fewer number of mitochondria than cardiomyocytes (217). These reasons explain the doxorubicin-induced hypertrophy in cardiomyocytes but not CFs and the lower IC_{50} observed in AC10 cells compared to HCF which reflects a greater sensitivity of cardiomyocytes to doxorubicin. This however does not preclude an involvement of HCF in the hypertrophic response of cardiac tissue to angiotensin II, as several studies have now highlighted a cell-communication relationship between cardiomyocytes and HCF in this regard. Co-culture of CFs and cardiomyocyte would allow for more physiological environment and a complete assessment of the effect of doxorubicin and the role of angiotensin II signaling pathway on both cells. Studies highlight the contribution of fibroblast-mediated paracrine signalling in exacerbating cardiomyocyte injury. For example, angiotensin II has been shown to stimulate the release of exosomes, nanoparticles that mediate cell communication, from CFs and CF-derived exosomes can induce the AT1R and augment the hypertrophy in cardiomyocyte (228). Many studies have assessed the effect of

angiotensin II on stimulation of rat cardiac myocytes or H9c2 cell line hypertrophy using conditioned media collected from cultured CFs or co-culture of both cell types in the same well and found that angiotensin II mediates cardiomyocyte hypertrophy through activation paracrine signalling pathway from CFs (225-227). In the context of doxorubicin exposure, it has been demonstrated that CFs affect cardiomyocyte apoptosis through paracrine mechanism. These studies demonstrate the critical role paracrine signalling plays in heart function and support the importance of CFs which also could be target of cardiotoxicity caused by anthracycline.

Interestingly, findings from this study have demonstrated doxorubicin induced AT1R upregulation in HCF at both the mRNA and protein level, with AT1R silencing preventing this upregulation, suggesting that non-myocyte also targeted by doxorubicin and confirming the role of angiotensin II signalling in doxorubicin induced cardiotoxicity. Previous studies have demonstrated that AT1R activation in fibroblasts initiates intracellular signalling cascades that lead to myofibroblast differentiation. This process is marked by enhanced α-SMA expression, upregulated pro-fibrotic signalling such as TGF-β, and induced endothelin-1 (ET-1) production (269). AT1R protein expression in HCF after doxorubicin exposure is increased and correlates with the increase in mRNA levels, suggesting efficient translation to protein. However, in this study AT1R mRNA levels did not change after angiotensin II exposure in HCF, suggesting that fibroblasts may regulate AT1R expression differently from cardiomyocytes. Angiotensin II might induce downstream pro-fibrotic signalling such as TGF-β activation without necessarily increasing AT1R mRNA levels as evidence showed that RAAS and TGF-β are promoting cardiac remodelling by acting as part of a signalling network (270). This finding highlights the important of RAAS activation in AIC, the broader impact of doxorubicin-induced cardiac injury beyond cardiomyocytes, and the importance to consider paracrine signalling in this toxicity. Further studies on other cell types in the heart such as endothelial cells are warranted to provide full assessment on the direct effect of doxorubicin on AT1R.

6.1 Conclusion

The current study provides evidence that RAAS is involved in the pathogenesis of AIC, demonstrating that doxorubicin directly affects cardiomyocytes and CFs through AT1R-dependent mechanisms. Angiotensin II and doxorubicin can independently induce hypertrophy in cardiomyocytes accompanied by upregulation in AT1R expression at mRNA level. Moreover, silencing of AT1R by siRNA mitigates this hypertrophy, confirming that AT1R

upregulation is required for hypertrophic response after exposure to doxorubicin and disturbing of angiotensin II signalling pathway can reduce the toxic effect of doxorubicin. Furthermore, this study demonstrated that toxic effect of anthracycline extends beyond cardiomyocytes, involving CFs. Doxorubicin-induced AT1R upregulation in fibroblasts and silencing of AT1R in CFs by AT1R siRNA prevented doxorubicin-induced AT1R upregulation. These findings provide a deep understanding of the important of RAAS in the pathogenesis of AIC and support the use of drugs that disturbing angiotensin II signalling in mitigation of adverse cardiac effect after anthracycline therapy.

6.2 Limitations and future directions

An important future direction would involve the use of patient-specific hiPSC-CMs. While this study utilised commercially available hiPSC-CMs and AC10 cells to model the cardiac response, patient-specific hiPSC-CMs would offer a more personalised relevant system. This approach would allow for the assessment of inter-individual variability in AT1R expression and doxorubicin sensitivity, potentially identifying factors that predispose certain individuals to AIC. Moreover, studying AT1R regulation in patient-specific hiPSC-CMs could help in the development of predictive biomarkers or targeted therapeutic interventions. Ultimately, integrating patient-specific hiPSC-CMs models into future studies would strengthen the translational potential of this work.

In addition, there is a need to examine the role of other relevant cell types, such as endothelial cells which are known to contribute to cardiac injury, inflammation, and repair processes. Furthermore, the current experiments were conducted in monolayer cultures, either cardiomyocytes or CFs. Co-culture systems combining cardiomyocytes and fibroblasts could provide a more realistic model of the myocardial environment, especially when studying the role of paracrine signalling in mediating hypertrophy of cardiac cells after angiotensin II and doxorubicin exposure. These models could offer deeper insight into how different cell populations respond collectively to doxorubicin exposure.

Finally, this study demonstrated that doxorubicin exposure leads to a significant increase in AT1R mRNA levels in both AC10 cardiomyocytes and CFs. Importantly, knockdown of AT1R attenuated this upregulation, suggesting a direct involvement of the AT1R in mediating the cardiotoxic effects of doxorubicin. However, to fully establish the mechanistic link between doxorubicin and AT1R induction, further studies are required to explore the intracellular pathways responsible for this response. Understanding how doxorubicin drives

AT1R expression at the molecular level would clarify how angiotensin signalling activated in cardiac cells.

References

1. Sarkar S, Horn G, Moulton K, Oza A, Byler S, Kokolus S, et al. Cancer development, progression, and therapy: an epigenetic overview. International Journal of Molecular Sciences. 2013;14(10):21087-113.

2. Bray F, Laversanne M, Sung H, Ferlay J, Siegel RL, Soerjomataram I, et al. Global cancer statistics 2022: GLOBOCAN estimates of incidence and mortality worldwide for 36 cancers in 185 countries. CA: A Cancer Journal for Clinicians. 2024;74(3):229-63.

3. Cancer Research UK. Worldwide cancer statistics [cited 2024 November]. Available from: https://www.cancerresearchuk.org/health-professional/cancer-statistics/worldwide-cancer#heading-Zero.

4. Arruebo M, Vilaboa N, Sáez-Gutierrez B, Lambea J, Tres A, Valladares M, et al. Assessment of the evolution of cancer treatment therapies. Cancers (Basel). 2011;3(3):3279-330.

5. Rudd SG. Targeting pan-essential pathways in cancer with cytotoxic chemotherapy: challenges and opportunities. Cancer Chemotherapy and Pharmacology. 2023;92(4):241-51.

6. Mollaei M, Hassan ZM, Khorshidi F, Langroudi L. Chemotherapeutic drugs: Cell death- and resistance-related signaling pathways. Are they really as smart as the tumor cells? Translational Oncology. 2021;14(5):101056.

7. Bansal N, Adams MJ, Ganatra S, Colan SD, Aggarwal S, Steiner R, et al. Strategies to prevent anthracycline-induced cardiotoxicity in cancer survivors. Cardio-Oncology. 2019;5:1-22.

8. Von Hoff DD, Layard MW, Basa P, Davis HL, Jr., Von Hoff AL, Rozencweig M, et al. Risk factors for doxorubicin-induced congestive heart failure. Annals of Internal Medicine. 1979;91(5):710-7.

9. Qiu Y, Jiang P, Huang Y. Anthracycline-induced cardiotoxicity: mechanisms, monitoring, and prevention. Frontiers in Cardiovascular Medicine. 2023;10:1242596.

10. Hortobágyi GN. Anthracyclines in the treatment of cancer. An overview. Drugs. 1997;54 Suppl 4:1-7.

11. Tewey KM, Rowe TC, Yang L, Halligan BD, Liu LF. Adriamycin-induced DNA damage mediated by mammalian DNA topoisomerase II. Science. 1984;226(4673):466-8.

12. Trouet A, Deprez-De Campeneere D. Daunorubicin-DNA and doxorubicin-DNA. A review of experimental and clinical data. Cancer Chemotherapy and Pharmacology. 1979;2(1):77-9.

13. Delgado JL, Hsieh CM, Chan NL, Hiasa H. Topoisomerases as anticancer targets. The Biochemical Journal. 2018;475(2):373-98.

14. Von Hoff DD, Rozencweig M, Layard M, Slavik M, Muggia FM. Daunomycin-induced cardiotoxicity in children and adults. A review of 110 cases. The American Journal of Medicine. 1977;62(2):200-8.

15. Cardinale D, Colombo A, Bacchiani G, Tedeschi I, Meroni CA, Veglia F, et al. Early detection of anthracycline cardiotoxicity and improvement with heart failure therapy. Circulation. 2015;131(22):1981-8.

16. Tan VZZ, Chan NM, Ang WL, Mya SN, Chan MY, Chen CK. Cardiotoxicity After Anthracycline Chemotherapy for Childhood Cancer in a Multiethnic Asian Population. Frontiers in Pediatrics. 2021;9:639603.

17. Alafifi S, Wahdan S, Elsherbiny D, Azab SS. Doxorubicin-induced testicular toxicity: possible underlying mechanisms and promising pharmacological treatments in experimental models. Archives of Pharmaceutical Sciences Ain Shams University. 2022;6(2):196-207.

18. Lefrak EA, Pitha J, Rosenheim S, Gottlieb JA. A clinicopathologic analysis of adriamycin cardiotoxicity. Cancer. 1973;32(2):302-14.

19. Kremer LC, van Dalen EC, Offringa M, Ottenkamp J, Voûte PA. Anthracycline-induced clinical heart failure in a cohort of 607 children: long-term follow-up study. Journal of Clinical Oncology. 2001;19(1):191-6.

20. Swain SM, Whaley FS, Ewer MS. Congestive heart failure in patients treated with doxorubicin: a retrospective analysis of three trials. Cancer. 2003;97(11):2869-79.

21. Lipshultz SE, Lipsitz SR, Sallan SE, Dalton VM, Mone SM, Gelber RD, et al. Chronic progressive cardiac dysfunction years after doxorubicin therapy for childhood acute lymphoblastic leukemia. Journal of Clinical Oncology. 2005;23(12):2629-36.

22. De Angelis A, Urbanek K, Cappetta D, Piegari E, Ciuffreda LP, Rivellino A, et al. Doxorubicin cardiotoxicity and target cells: a broader perspective. Cardio-oncology. 2016;2(1):2.

23. Rivankar S. An overview of doxorubicin formulations in cancer therapy. Journal of Cancer Research and Therapeutics. 2014;10(4):853-8.

24. Mitry MA, Edwards JG. Doxorubicin induced heart failure: Phenotype and molecular mechanisms. International Journal of Cardiology Cardiovascular Risk and Prevention. 2016;10:17-24.

25. Nair N, Gongora E. Heart failure in chemotherapy-related cardiomyopathy: Can exercise make a difference? BBA Clinical. 2016;6:69-75.

26. McDonagh TA, Metra M, Adamo M, Gardner RS, Baumbach A, Böhm M, et al. 2023 Focused Update of the 2021 ESC Guidelines for the diagnosis and treatment of acute and chronic heart failure: Developed by the task force for the diagnosis and treatment of acute and chronic heart failure of the European Society of Cardiology (ESC) With the special contribution of the Heart Failure Association (HFA) of the ESC. European Heart Journal. 2023;44(37):3627-39.

27. Volkova M, Russell R, 3rd. Anthracycline cardiotoxicity: prevalence, pathogenesis and treatment. Current Cardiology Reviews. 2011;7(4):214-20.

28. Cho H, Lee S, Sim SH, Park IH, Lee KS, Kwak MH, et al. Cumulative incidence of chemotherapy-induced cardiotoxicity during a 2-year follow-up period in breast cancer patients. Breast Cancer Research and Treatment. 2020;182(2):333-43.

29. Grenier MA, Lipshultz SE. Epidemiology of anthracycline cardiotoxicity in children and adults. Seminars in Oncology. 1998;25(4 Suppl 10):72-85.

30. Lipshultz SE, Lipsitz SR, Mone SM, Goorin AM, Sallan SE, Sanders SP, et al. Female sex and higher drug dose as risk factors for late cardiotoxic effects of doxorubicin therapy for childhood cancer. The New England Journal of Medicine 1995;332(26):1738-43.

31. Glen C, Morrow A, Roditi G, Hopkins T, Macpherson I, Stewart P, et al. Cardiovascular sequelae of trastuzumab and anthracycline in long-term survivors of breast cancer. Heart. 2024;110(9):650-6.

32. Philip LJ, Findlay SG, Gill JH. Baseline blood pressure and development of cardiotoxicity in patients treated with anthracyclines: A systematic review. International Journal of Cardiology Cardiovascular Risk and Prevention. 2022;15:200153.

33. Li H, Wang M, Huang Y. Anthracycline-induced cardiotoxicity: An overview from cellular structural perspective. Biomedicine & Pharmacotherapy. 2024;179:117312.

34. Sobczuk P, Czerwińska M, Kleibert M, Cudnoch-Jędrzejewska A. Anthracycline-induced cardiotoxicity and renin-angiotensin-aldosterone system-from molecular mechanisms to therapeutic applications. Heart Failure Reviews. 2022;27(1):295-319.

35. Capranico G, Tinelli S, Austin CA, Fisher ML, Zunino F. Different patterns of gene expression of topoisomerase II isoforms in differentiated tissues during murine development. Biochimica et Biophysica Acta (BBA)-Gene Structure and Expression. 1992;1132(1):43-8.

36. Zhang S, Liu X, Bawa-Khalfe T, Lu LS, Lyu YL, Liu LF, et al. Identification of the molecular basis of doxorubicin-induced cardiotoxicity. Nature Medicine. 2012;18(11):1639-42.

37. Li W, Zhang Y, Wei Y, Ling G, Zhang Y, Li Y, et al. New insights into mitochondrial quality control in anthracycline-induced cardiotoxicity: molecular mechanisms, therapeutic targets, and natural products. International Journal of Biological Sciences. 2025;21(2):507-23.

38. Geisberg CA, Sawyer DB. Mechanisms of anthracycline cardiotoxicity and strategies to decrease cardiac damage. Current Hypertension Reports. 2010;12(6):404-10.

39. Maejima Y, Adachi S, Ito H, Hirao K, Isobe M. Induction of premature senescence in cardiomyocytes by doxorubicin as a novel mechanism of myocardial damage. Aging Cell. 2008;7(2):125-36.

40. Doroshow JH, Davies KJ. Redox cycling of anthracyclines by cardiac mitochondria. II. Formation of superoxide anion, hydrogen peroxide, and hydroxyl radical. The Journal of Biological Chemistry. 1986;261(7):3068-74.

41. Seara FAC, Kasai-Brunswick TH, Nascimento JHM, Campos-de-Carvalho AC. Anthracycline-induced cardiotoxicity and cell senescence: new therapeutic option? Cellular and Molecular Life of Sciences. 2022;79(11):568.

42. Bergmann O, Zdunek S, Felker A, Salehpour M, Alkass K, Bernard S, et al. Dynamics of Cell Generation and Turnover in the Human Heart. Cell. 2015;161(7):1566-75.

43. Cui N, Wu F, Lu WJ, Bai R, Ke B, Liu T, et al. Doxorubicin-induced cardiotoxicity is maturation dependent due to the shift from topoisomerase IIα to IIβ in human stem cell derived cardiomyocytes. Journal of Cellular and Molecular Medicine. 2019;23(7):4627-39.

44. Hanna AD, Lam A, Tham S, Dulhunty AF, Beard NA. Adverse effects of doxorubicin and its metabolic product on cardiac RyR2 and SERCA2A. Molecular Pharmacology. 2014;86(4):438-49.

45. Xie S, Sun Y, Zhao X, Xiao Y, Zhou F, Lin L, et al. An update of the molecular mechanisms underlying anthracycline induced cardiotoxicity. Frontiers in Pharmacology. 2024;15:1406247.

46. Tokarska-Schlattner M, Dolder M, Gerber I, Speer O, Wallimann T, Schlattner U. Reduced creatine-stimulated respiration in doxorubicin challenged mitochondria: Particular sensitivity of the heart. Biochimica et Biophysica Acta (BBA) - Bioenergetics. 2007;1767(11):1276-84.

47. Thorn CF, Oshiro C, Marsh S, Hernandez-Boussard T, McLeod H, Klein TE, et al. Doxorubicin pathways: pharmacodynamics and adverse effects. Pharmacogenet Genomics. 2011;21(7):440-6.

48. Huang J, Wu R, Chen L, Yang Z, Yan D, Li M. Understanding Anthracycline Cardiotoxicity From Mitochondrial Aspect. Frontiers in Pharmacology. 2022;13:811406.

49. Woodcock EA, Matkovich SJ. Cardiomyocytes structure, function and associated pathologies. The International Journal of Biochemistry & Cell Biology. 2005;37(9):1746-51.

50. Renu K, V.G A, P.B TP, Arunachalam S. Molecular mechanism of doxorubicin-induced cardiomyopathy – An update. European Journal of Pharmacology. 2018;818:241-53.

51. Ichikawa Y, Ghanefar M, Bayeva M, Wu R, Khechaduri A, Naga Prasad SV, et al. Cardiotoxicity of doxorubicin is mediated through mitochondrial iron accumulation. The Journal Clinical Investigation. 2014;124(2):617-30.

52. Marcillat O, Zhang Y, Davies KJ. Oxidative and non-oxidative mechanisms in the inactivation of cardiac mitochondrial electron transport chain components by doxorubicin. The Biochemical Journal. 1989;259(1):181-9.

53. Reichwagen A, Ziepert M, Kreuz M, Gödtel-Armbrust U, Rixecker T, Poeschel V, et al. Association of NADPH oxidase polymorphisms with anthracycline-induced cardiotoxicity in

the RICOVER-60 trial of patients with aggressive CD20(+) B-cell lymphoma. Pharmacogenomics. 2015;16(4):361-72.

54. Cascales A, Pastor-Quirante F, Sánchez-Vega B, Luengo-Gil G, Corral J, Ortuño-Pacheco G, et al. Association of anthracycline-related cardiac histological lesions with NADPH oxidase functional polymorphisms. Oncologist. 2013;18(4):446-53.

55. Cappetta D, Rossi F, Piegari E, Quaini F, Berrino L, Urbanek K, et al. Doxorubicin targets multiple players: A new view of an old problem. Pharmacological Research. 2018;127:4-14.

56. Burgoyne JR, Mongue-Din H, Eaton P, Shah AM. Redox signaling in cardiac physiology and pathology. Circulation Research. 2012;111(8):1091-106.

57. Carrasco R, Castillo RL, Gormaz JG, Carrillo M, Thavendiranathan P. Role of Oxidative Stress in the Mechanisms of Anthracycline-Induced Cardiotoxicity: Effects of Preventive Strategies. Oxidative Medicine and Cellular Longevity. 2021;2021:8863789.

58. Ayala A, Muñoz MF, Argüelles S. Lipid peroxidation: production, metabolism, and signaling mechanisms of malondialdehyde and 4-hydroxy-2-nonenal. Oxidative Medicine and Cellular Longevity. 2014;2014:360438.

59. Koleini N, Nickel BE, Edel AL, Fandrich RR, Ravandi A, Kardami E. Oxidized phospholipids in Doxorubicin-induced cardiotoxicity. Chemico-Biological Interactions. 2019;303:35-9.

60. Ge W, Yuan M, Ceylan AF, Wang X, Ren J. Mitochondrial aldehyde dehydrogenase protects against doxorubicin cardiotoxicity through a transient receptor potential channel vanilloid 1-mediated mechanism. Biochimica et Biophysica Acta (BBA)-Molecular Basis of Disease. 2016;1862(4):622-34.

61. Rahmatollahi M, Baram SM, Rahimian R, Saeedi Saravi SS, Dehpour AR. Peroxisome proliferator-activated receptor-α inhibition protects against doxorubicin-induced cardiotoxicity in mice. Cardiovascular toxicology. 2016;16:244-50.

62. Zablocki D, Sadoshima J. Angiotensin II and oxidative stress in the failing heart. Antioxidants and Redox Signaling. 2013;19(10):1095-109.

63. Šimůnek T, Štěrba M, Popelová O, Adamcová M, Hrdina R, Geršl V. Anthracycline-induced cardiotoxicity: overview of studies examining the roles of oxidative stress and free cellular iron. Pharmacological reports. 2009;61(1):154-71.

64. Gammella E, Maccarinelli F, Buratti P, Recalcati S, Cairo G. The role of iron in anthracycline cardiotoxicity. Frontiers in Pharmacology. 2014;5:25.

65. Li N, Jiang W, Wang W, Xiong R, Wu X, Geng Q. Ferroptosis and its emerging roles in cardiovascular diseases. Pharmacological Research. 2021;166:105466.

66. Gkouvatsos K, Papanikolaou G, Pantopoulos K. Regulation of iron transport and the role of transferrin. Biochimica et Biophysica Acta (BBA) - General Subjects. 2012;1820(3):188-202.

67. Ichikawa Y, Bayeva M, Ghanefar M, Potini V, Sun L, Mutharasan RK, et al. Disruption of ATP-binding cassette B8 in mice leads to cardiomyopathy through a decrease in mitochondrial iron export. Proceedings of the National Academy of Sciences U S A. 2012;109(11):4152-7.

68. Minotti G, Menna P, Salvatorelli E, Cairo G, Gianni L. Anthracyclines: molecular advances and pharmacologic developments in antitumor activity and cardiotoxicity. Pharmacological Reviews. 2004;56(2):185-229.

69. Xu X, Persson HL, Richardson DR. Molecular pharmacology of the interaction of anthracyclines with iron. Molecular Pharmacology. 2005;68(2):261-71.

70. Booth LK, Redgrave RE, Folaranmi O, Gill JH, Richardson GD. Anthracycline-induced cardiotoxicity and senescence. Frontiers in Aging. 2022;3:1058435.

71. Campisi J, d'Adda di Fagagna F. Cellular senescence: when bad things happen to good cells. Nature Reviews Molecular Cell Biology. 2007;8(9):729-40.

72. Chularojmontri L, Gerdprasert O, Wattanapitayakul SK. Pummelo protects Doxorubicin-induced cardiac cell death by reducing oxidative stress, modifying glutathione transferase expression, and preventing cellular senescence. Evidence-Based Complementary and Alternative Medicine. 2013;2013:254835.

73. Mitry MA, Laurent D, Keith BL, Sira E, Eisenberg CA, Eisenberg LM, et al. Accelerated cardiomyocyte senescence contributes to late-onset doxorubicin-induced cardiotoxicity. American Journal of Physiology Cell Physiology. 2020;318(2):C380-c91.

74. Jackson JG, Pereira-Smith OM. p53 is preferentially recruited to the promoters of growth arrest genes p21 and GADD45 during replicative senescence of normal human fibroblasts. Cancer research. 2006;66(17):8356-60.

75. Anderson R, Lagnado A, Maggiorani D, Walaszczyk A, Dookun E, Chapman J, et al. Length-independent telomere damage drives post-mitotic cardiomyocyte senescence. The EMBO Journal. 2019;38(5):e100492.

76. Chen MS, Lee RT, Garbern JC. Senescence mechanisms and targets in the heart. Cardiovascular Research. 2022;118(5):1173-87.

77. Demaria M, O'Leary MN, Chang J, Shao L, Liu S, Alimirah F, et al. Cellular Senescence Promotes Adverse Effects of Chemotherapy and Cancer Relapse. Cancer Discovery. 2017;7(2):165-76.

78. Männer J. When Does the Human Embryonic Heart Start Beating? A Review of Contemporary and Historical Sources of Knowledge about the Onset of Blood Circulation in Man. Journal of Cardiovascular Development and Disease. 2022;9(6).

79. Talman V, Kivelä R. Cardiomyocyte-Endothelial Cell Interactions in Cardiac Remodeling and Regeneration. Frontiers in Cardiovascular Medicine. 2018;5:101.

80. Moorman AF, Christoffels VM. Cardiac chamber formation: development, genes, and evolution. Physiological Reviews. 2003;83(4):1223-67.

81. Litviňuková M, Talavera-López C, Maatz H, Reichart D, Worth CL, Lindberg EL, et al. Cells of the adult human heart. Nature. 2020;588(7838):466-72.

82. Ripa R, George T, Shumway KR, Sattar Y. Physiology, cardiac muscle. StatPearls [Internet]: StatPearls Publishing; 2023.

83. Yutzey KE. Cardiomyocyte Proliferation. Circulation Research. 2017;120(4):627-9.

84. Zheng K, Hao Y, Xia C, Cheng S, Yu J, Chen Z, et al. Effects and mechanisms of the myocardial microenvironment on cardiomyocyte proliferation and regeneration. Frontiers in Cell and Developmental Biology. 2024;12:1429020.

85. Bazgir F, Nau J, Nakhaei-Rad S, Amin E, Wolf MJ, Saucerman JJ, et al. The Microenvironment of the Pathogenesis of Cardiac Hypertrophy. Cells. 2023;12(13).

86. Ceauşu Z, Socea B, Costache M, Predescu D, Şerban D, Smarandache CG, et al. Fibroblast involvement in cardiac remodeling and repair under ischemic conditions. Experimental and Therapeutic Medicine. 2021;21(3):269.

87. Humeres C, Frangogiannis NG. Fibroblasts in the Infarcted, Remodeling, and Failing Heart. JACC: Basic to Translational Science. 2019;4(3):449-67.

88. Bers DM. Cardiac excitation-contraction coupling. Nature. 2002;415(6868):198-205.

89. Grant AO. Cardiac Ion Channels. Circulation: Arrhythmia and Electrophysiology. 2009;2(2):185-94.

90. Bartos DC, Grandi E, Ripplinger CM. Ion Channels in the Heart. Comprehensive Physiology. 2015;5(3):1423-64.

91. Yue L, Xie J, Nattel S. Molecular determinants of cardiac fibroblast electrical function and therapeutic implications for atrial fibrillation. Cardiovascular Research. 2011;89(4):744-53.

92. Camelliti P, Borg TK, Kohl P. Structural and functional characterisation of cardiac fibroblasts. Cardiovascular Research. 2005;65(1):40-51.

93. Hall C, Gehmlich K, Denning C, Pavlovic D. Complex Relationship Between Cardiac Fibroblasts and Cardiomyocytes in Health and Disease. Journal of the American Heart Association. 2021;10(5):e019338.

94. Xuan Y, Chen C, Wen Z, Wang DW. The Roles of Cardiac Fibroblasts and Endothelial Cells in Myocarditis. Frontiers in Cardiovascular Medicine. 2022;9:882027.

95. Telesca M, Donniacuo M, Bellocchio G, Riemma MA, Mele E, Dell'Aversana C, et al. Initial Phase of Anthracycline Cardiotoxicity Involves Cardiac Fibroblasts Activation and Metabolic Switch. Cancers (Basel). 2023;16(1).

96. Brutsaert DL. Cardiac endothelial-myocardial signaling: its role in cardiac growth, contractile performance, and rhythmicity. Physiological Reviews. 2003;83(1):59-115.

97. Lipshultz SE, Adams MJ, Colan SD, Constine LS, Herman EH, Hsu DT, et al. Long-term cardiovascular toxicity in children, adolescents, and young adults who receive cancer therapy: pathophysiology, course, monitoring, management, prevention, and research directions: a scientific statement from the American Heart Association. Circulation. 2013;128(17):1927-95.

98. Su H, Cantrell AC, Zeng H, Zhu SH, Chen JX. Emerging Role of Pericytes and Their Secretome in the Heart. Cells. 2021;10(3).

99. Nees S, Weiss DR, Juchem G. Focus on cardiac pericytes. Pflugers Arch. 2013;465(6):779-87.

100. Witman N, Sahara M. Cardiac Progenitor Cells in Basic Biology and Regenerative Medicine. Stem Cells International. 2018;2018:8283648.

101. Urbanek K, Torella D, Sheikh F, De Angelis A, Nurzynska D, Silvestri F, et al. Myocardial regeneration by activation of multipotent cardiac stem cells in ischemic heart failure. Proceeding of the Natlional Academy Sciences of the U S A. 2005;102(24):8692-7.

102. Lewis-McDougall FC, Ruchaya PJ, Domenjo-Vila E, Shin Teoh T, Prata L, Cottle BJ, et al. Aged-senescent cells contribute to impaired heart regeneration. Aging Cell. 2019;18(3):e12931.

103. Cardinale D, Iacopo F, Cipolla CM. Cardiotoxicity of Anthracyclines. Frontiers of Cardiovascular Medicine. 2020;7:26.

104. Fountoulaki K, Dagres N, Iliodromitis EK. Cellular Communications in the Heart. Cardiac Failure Review 2015;1(2):64–8. 2015.

105. Jongsma HJ, Wilders R. Gap Junctions in Cardiovascular Disease. Circulation Research. 2000;86(12):1193-7.

106. Lo CW. Role of gap junctions in cardiac conduction and development: insights from the connexin knockout mice. Circulation Research. 2000;87(5):346-8.

107. Zhang S, Fan Y, Zheng B, Wang Y, Miao C, Su Y, et al. Bilirubin Improves Gap Junction to Alleviate Doxorubicin-Induced Cardiotoxicity by Regulating AMPK-Axl-SOCS3-Cx43 Axis. Frontiers in Pharmacology. 2022;13:828890.

108. Segers VFM, De Keulenaer GW. Autocrine Signaling in Cardiac Remodeling: A Rich Source of Therapeutic Targets. Journal of the American Heart Association. 2021;10(3):e019169.

109. Ziolo MT, Kohr MJ, Wang H. Nitric oxide signaling and the regulation of myocardial function. Journal of Molecular and Cellular Cardiology. 2008;45(5):625-32.

110. Li Y, Li B, Chen WD, Wang YD. Role of G-protein coupled receptors in cardiovascular diseases. Frontiers in Cardiovascular Medicine. 2023;10:1130312.

111. Wheeler-Jones CP. Cell signalling in the cardiovascular system: an overview. Heart. 2005;91(10):1366-74.

112. George AJ, Thomas WG, Hannan RD. The renin-angiotensin system and cancer: old dog, new tricks. Nature Reviews Cancer. 2010;10(11):745-59.

113. Fountain JH, Kaur J, Lappin SL. Physiology, Renin Angiotensin System. StatPearls. Treasure Island (FL): StatPearls Publishing
Copyright © 2024, StatPearls Publishing LLC.; 2024.

114. Dasgupta C, Zhang L. Angiotensin II receptors and drug discovery in cardiovascular disease. Drug Discovery Today. 2011;16(1-2):22-34.

115. Baker KM, Booz GW, Dostal DE. Cardiac actions of angiotensin II: Role of an intracardiac renin-angiotensin system. Annual review of physiology. 1992;54:227-41.

116. Fountain JH, Kaur J, Lappin SL. Physiology, renin angiotensin system. 2017.

117. Patel S, Rauf A, Khan H, Abu-Izneid T. Renin-angiotensin-aldosterone (RAAS): The ubiquitous system for homeostasis and pathologies. Biomedicine & Pharmacotherapy. 2017;94:317-25.

118. Iwai N, Inagami T. Identification of two subtypes in the rat type I angiotensin II receptor. FEBS Lett. 1992;298(2-3):257-60.

119. Hebert PR, Foody JM, Hennekens CH. The renin-angiotensin system: the role of inhibitors, blockers, and genetic polymorphisms in the treatment and prevention of heart failure. Current vascular pharmacology. 2003;1(1):33-9.

120. De Mello WC, Danser AHJ. Angiotensin II and the Heart. Hypertension. 2000;35(6):1183-8.

121. Nádasy GL, Balla A, Dörnyei G, Hunyady L, Szekeres M. Direct Vascular Effects of Angiotensin II (A Systematic Short Review). International Journal of Molecular Sciences. 2025;26(1):113.

122. Blaustein MP, Zhang J, Chen L, Hamilton BP. How does salt retention raise blood pressure? American Journal of Physiology, Regulatory, Integrative and Comparative Physiology. 2006;290(3):R514-23.

123. Hunyady L, Catt KJ. Pleiotropic AT1 receptor signaling pathways mediating physiological and pathogenic actions of angiotensin II. Molecular Endocrinology. 2006;20(5):953-70.

124. Allen AM, Zhuo J, Mendelsohn FA. Localization and function of angiotensin AT1 receptors. American Journal of Hypertension. 2000;13(1 Pt 2):31s-8s.

125. Ainscough JFX, Drinkhill MJ, Sedo A, Turner NA, Brooke DA, Balmforth AJ, et al. Angiotensin II type-1 receptor activation in the adult heart causes blood pressure-independent hypertrophy and cardiac dysfunction. Cardiovascular Research. 2008;81(3):592-600.

126. Ozono R, Wang ZQ, Moore AF, Inagami T, Siragy HM, Carey RM. Expression of the subtype 2 angiotensin (AT2) receptor protein in rat kidney. Hypertension. 1997;30(5):1238-46.

127. Hutchinson HG, Hein L, Fujinaga M, Pratt RE. Modulation of vascular development and injury by angiotensin II. Cardiovascular Research. 1999;41(3):689-700.

128. Wharton J, Morgan K, Rutherford RA, Catravas JD, Chester A, Whitehead BF, et al. Differential distribution of angiotensin AT2 receptors in the normal and failing human heart. The Journal of Pharmacology and Experimental Therapeutics. 1998;284(1):323-36.

129. Fatima N, Patel SN, Hussain T. Angiotensin II Type 2 Receptor: A Target for Protection Against Hypertension, Metabolic Dysfunction, and Organ Remodeling. Hypertension. 2021;77(6):1845-56.

130. Patel VB, Zhong JC, Grant MB, Oudit GY. Role of the ACE2/Angiotensin 1-7 Axis of the Renin-Angiotensin System in Heart Failure. Circulation Research. 2016;118(8):1313-26.

131. Zhong J, Basu R, Guo D, Chow FL, Byrns S, Schuster M, et al. Angiotensin-converting enzyme 2 suppresses pathological hypertrophy, myocardial fibrosis, and cardiac dysfunction. Circulation. 2010;122(7):717-28, 18 p following 28.

132. Hamming I, Cooper ME, Haagmans BL, Hooper NM, Korstanje R, Osterhaus AD, et al. The emerging role of ACE2 in physiology and disease. The Journal of Pathology. 2007;212(1):1-11.

133. Patel VB, Clarke N, Wang Z, Fan D, Parajuli N, Basu R, et al. Angiotensin II induced proteolytic cleavage of myocardial ACE2 is mediated by TACE/ADAM-17: a positive feedback mechanism in the RAS. Journal of Molecular and Cellular Cardiology. 2014;66:167-76.

134. Patel VB, Zhong JC, Fan D, Basu R, Morton JS, Parajuli N, et al. Angiotensin-converting enzyme 2 is a critical determinant of angiotensin II-induced loss of vascular smooth muscle cells and adverse vascular remodeling. Hypertension. 2014;64(1):157-64.

135. Wang J, He W, Guo L, Zhang Y, Li H, Han S, et al. The ACE2-Ang (1-7)-Mas receptor axis attenuates cardiac remodeling and fibrosis in post-myocardial infarction. Molecular Medicine Reports. 2017;16(2):1973-81.

136. Martyniak A, Tomasik PJ. A New Perspective on the Renin-Angiotensin System. Diagnostics (Basel). 2022;13(1).

137. Vejpongsa P, Yeh ET. Prevention of anthracycline-induced cardiotoxicity: challenges and opportunities. Journal of the American College Cardiology. 2014;64(9):938-45.

138. Zheng H, Zhan H. Preventing Anthracycline-Associated Heart Failure: What Is the Role of Dexrazoxane?: JACC: CardioOncology Controversies in Cardio-Oncology. JACC CardioOncol. 2024;6(2):318-21.

139. Krone R, Merchant A, Mitchell JD. Cardioprotection Using Doxorubicin: The Role of Dexrazoxane. In: Rauf A, editor. Drug Development and Safety. Rijeka: IntechOpen; 2024.

140. Farzam K, Jan A. Beta blockers. 2018.

141. He D, Hu J, Li Y, Zeng X. Preventive use of beta-blockers for anthracycline-induced cardiotoxicity: A network meta-analysis. Frontiers in Cardiovascular Medicine. 2022;9:968534.

142. Spallarossa P, Garibaldi S, Altieri P, Fabbi P, Manca V, Nasti S, et al. Carvedilol prevents doxorubicin-induced free radical release and apoptosis in cardiomyocytes in vitro. Journal of Molecular and Cellular Cardiology. 2004;37(4):837-46.

143. Arozal W, Watanabe K, Veeraveedu PT, Ma M, Thandavarayan RA, Sukumaran V, et al. Protective effect of carvedilol on daunorubicin-induced cardiotoxicity and nephrotoxicity in rats. Toxicology. 2010;274(1-3):18-26.

144. Camilli M, Cipolla CM, Dent S, Minotti G, Cardinale DM. Anthracycline Cardiotoxicity in Adult Cancer Patients: JACC: CardioOncology State-of-the-Art Review. JACC: CardioOncology. 2024;6(5):655-77.

145. López-Sendón J, Álvarez-Ortega C, Zamora Auñon P, Buño Soto A, Lyon AR, Farmakis D, et al. Classification, prevalence, and outcomes of anticancer therapy-induced cardiotoxicity: the CARDIOTOX registry. European Heart Journal. 2020;41(18):1720-9.

146. Electronic Medicines Compendium. Enalapril Summary of product characteristics [cited 2024 November]. Available from: https://www.medicines.org.uk/emc/product/561/smpc#gref.

147. Electronic Medicines Compendium. Telmisartan Summary of product characteristics [cited 2024 November]. Available from: https://www.medicines.org.uk/emc/product/3165/smpc

148. Yancy CW, Jessup M, Bozkurt B, Butler J, Casey DE, Jr., Colvin MM, et al. 2017 ACC/AHA/HFSA Focused Update of the 2013 ACCF/AHA Guideline for the Management of Heart Failure: A Report of the American College of Cardiology/American Heart Association Task Force on Clinical Practice Guidelines and the Heart Failure Society of America. Circulation. 2017;136(6):e137-e61.

149. Williams B, Mancia G, Spiering W, Agabiti Rosei E, Azizi M, Burnier M, et al. 2018 ESC/ESH Guidelines for the management of arterial hypertension: The Task Force for the management of arterial hypertension of the European Society of Cardiology and the European Society of Hypertension: The Task Force for the management of arterial hypertension of the European Society of Cardiology and the European Society of Hypertension. J Hypertens. 2018;36(10):1953-2041.

150. Li K, Chen X. Protective effects of captopril and enalapril on myocardial ischemia and reperfusion damage of rat. Journal of Molecular and Cellular Cardiology. 1987;19(9):909-15.

151. Bauer IH, Reams GP, Wu Z, Lau-Sieckman A. Effects of losartan on the renin-angiotensin-aldosterone axis in essential hypertension. Journal of Human Hypertension. 1995;9(4):237-43.

152. Cardinale D, Colombo A, Sandri MT, Lamantia G, Colombo N, Civelli M, et al. Prevention of high-dose chemotherapy-induced cardiotoxicity in high-risk patients by angiotensin-converting enzyme inhibition. Circulation. 2006;114(23):2474-81.

153. Cardinale D, Colombo A, Lamantia G, Colombo N, Civelli M, De Giacomi G, et al. Anthracycline-induced cardiomyopathy: clinical relevance and response to pharmacologic therapy. Journal of the American College of Cardiology. 2010;55(3):213-20.

154. Bosch X, Rovira M, Sitges M, Domènech A, Ortiz-Pérez JT, de Caralt TM, et al. Enalapril and carvedilol for preventing chemotherapy-induced left ventricular systolic dysfunction in patients with malignant hemopathies: the OVERCOME trial (preventiOn of left Ventricular dysfunction with Enalapril and caRvedilol in patients submitted to intensive ChemOtherapy for the treatment of Malignant hEmopathies). Journal of the American College of Cardiology. 2013;61(23):2355-62.

155. Janbabai G, Nabati M, Faghihinia M, Azizi S, Borhani S, Yazdani J. Effect of Enalapril on Preventing Anthracycline-Induced Cardiomyopathy. Cardiovascular Toxicology. 2017;17(2):130-9.

156. Cardinale D, Ciceri F, Latini R, Franzosi MG, Sandri MT, Civelli M, et al. Anthracycline-induced cardiotoxicity: A multicenter randomised trial comparing two strategies for guiding prevention with enalapril: The International CardioOncology Society-one trial. European Journal of Cancer. 2018;94:126-37.

157. Gupta V, Kumar Singh S, Agrawal V, Bali Singh T. Role of ACE inhibitors in anthracycline-induced cardiotoxicity: A randomized, double-blind, placebo-controlled trial. Pediatric Blood and Cancer. 2018;65(11):e27308.

158. Słowik A, Jagielski P, Potocki P, Streb J, Ochenduszko S, Wysocki P, et al. Anthracycline-induced cardiotoxicity prevention with angiotensin-converting enzyme inhibitor ramipril in women with low-risk breast cancer: results of a prospective randomized study. Kardiologia Polska. 2020;78(2):131-7.

159. Wihandono A, Azhar Y, Abdurahman M, Hidayat S. The Role of Lisinopril and Bisoprolol to Prevent Anthracycline Induced Cardiotoxicity in Locally Advanced Breast Cancer Patients. Asian Pacific Journal of Cancer Prevention. 2021;22(9):2847-53.

160. Livi L, Barletta G, Martella F, Saieva C, Desideri I, Bacci C, et al. Cardioprotective Strategy for Patients With Nonmetastatic Breast Cancer Who Are Receiving an Anthracycline-Based Chemotherapy: A Randomized Clinical Trial. JAMA Oncology. 2021;7(10):1544-9.

161. Austin D, Maier RH, Akhter N, Sayari M, Ogundimu E, Maddox JM, et al. Preventing Cardiac Damage in Patients Treated for Breast Cancer and Lymphoma: The PROACT Clinical Trial. JACC: CardioOncology. 2024;6(5):684-96.

162. Ponikowski P, Voors AA, Anker SD, Bueno H, Cleland JGF, Coats AJS, et al. 2016 ESC Guidelines for the diagnosis and treatment of acute and chronic heart failure: The Task Force for the diagnosis and treatment of acute and chronic heart failure of the European Society of Cardiology (ESC)Developed with the special contribution of the Heart Failure Association (HFA) of the ESC. European Heart Journal. 2016;37(27):2129-200.

163. Maier RH, Plummer C, Kasim AS, Akhter N, Ogundimu E, Maddox J, et al. Preventing cardiotoxicity in patients with breast cancer and lymphoma: protocol for a multicentre randomised controlled trial (PROACT). BMJ Open. 2022;12(12):e066252.

164. Nakamae H, Tsumura K, Terada Y, Nakane T, Nakamae M, Ohta K, et al. Notable effects of angiotensin II receptor blocker, valsartan, on acute cardiotoxic changes after standard chemotherapy with cyclophosphamide, doxorubicin, vincristine, and prednisolone. Cancer. 2005;104(11):2492-8.

165. Cadeddu C, Piras A, Mantovani G, Deidda M, Dessì M, Madeddu C, et al. Protective effects of the angiotensin II receptor blocker telmisartan on epirubicin-induced inflammation, oxidative stress, and early ventricular impairment. American Heart Journal. 2010;160(3):487.e1-7.

166. Gulati G, Heck SL, Ree AH, Hoffmann P, Schulz-Menger J, Fagerland MW, et al. Prevention of cardiac dysfunction during adjuvant breast cancer therapy (PRADA): a 2 × 2 factorial, randomized, placebo-controlled, double-blind clinical trial of candesartan and metoprolol. European Heart Journal. 2016;37(21):1671-80.

167. Heck SL, Mecinaj A, Ree AH, Hoffmann P, Schulz-Menger J, Fagerland MW, et al. Prevention of Cardiac Dysfunction During Adjuvant Breast Cancer Therapy (PRADA): Extended Follow-Up of a 2×2 Factorial, Randomized, Placebo-Controlled, Double-Blind Clinical Trial of Candesartan and Metoprolol. Circulation. 2021;143(25):2431-40.

168. Lee M, Chung WB, Lee JE, Park CS, Park WC, Song BJ, et al. Candesartan and carvedilol for primary prevention of subclinical cardiotoxicity in breast cancer patients without a cardiovascular risk treated with doxorubicin. Cancer Medicine. 2021;10(12):3964-73.

169. Henriksen PA, Hall P, MacPherson IR, Joshi SS, Singh T, Maclean M, et al. Multicenter, Prospective, Randomized Controlled Trial of High-Sensitivity Cardiac Troponin I–Guided Combination Angiotensin Receptor Blockade and Beta-Blocker Therapy to Prevent Anthracycline Cardiotoxicity: The Cardiac CARE Trial. Circulation. 2023;148(21):1680-90.

170. Toko H, Oka T, Zou Y, Sakamoto M, Mizukami M, Sano M, et al. Angiotensin II type 1a receptor mediates doxorubicin-induced cardiomyopathy. Hypertension Research. 2002;25(4):597-603.

171. Yusoff NSN, Mustapha Z, Sharif SET, Govindasamy C, Sirajudeen KNS. Effect of Antihypertensive Drug Treatment on Oxidative Stress Markers in Heart of Spontaneously Hypertensive Rat Models. Journal Environmental Pathololgy, Toxicology, and Oncology. 2017;36(1):43-53.

172. Hiona A, Lee AS, Nagendran J, Xie X, Connolly AJ, Robbins RC, et al. Pretreatment with angiotensin-converting enzyme inhibitor improves doxorubicin-induced cardiomyopathy via preservation of mitochondrial function. The Journal of Thoracic and Cardiovascular Surgery 2011;142(2):396-403.e3.

173. Dong H, Yao L, Wang M, Wang M, Li X, Sun X, et al. Can ACEI/ARB prevent the cardiotoxicity caused by chemotherapy in early-stage breast cancer?-a meta-analysis of randomized controlled trials. Translational Cancer Research. 2020;9(11):7034-43.

174. Kimes BW, Brandt BL. Properties of a clonal muscle cell line from rat heart. Experimental Cell Research. 1976;98(2):367-81.

175. Davidson MM, Nesti C, Palenzuela L, Walker WF, Hernandez E, Protas L, et al. Novel cell lines derived from adult human ventricular cardiomyocytes. Journal of Molecular and Cellular Cardiology. 2005;39(1):133-47.

176. Claycomb WC, Lanson NA, Jr., Stallworth BS, Egeland DB, Delcarpio JB, Bahinski A, et al. HL-1 cells: a cardiac muscle cell line that contracts and retains phenotypic characteristics of the adult cardiomyocyte. Proceeding National Academy of Scieinces of the U S A. 1998;95(6):2979-84.

177. Ginis I, Luo Y, Miura T, Thies S, Brandenberger R, Gerecht-Nir S, et al. Differences between human and mouse embryonic stem cells. Developmental Biology. 2004;269(2):360-80.

178. ROCKLEY K. In Vitro evaluation of Anthracycline-Induced Cardiotoxicity and Mitigation by Perturbation of Angiotensin Signalling: Durham University; 2018.

179. Kim HD. Expression of intermediate filament desmin and vimentin in the human fetal heart. The Anatomical Record. 1996;246(2):271-8.

180. Lin Y, Marin-Argany M, Dick CJ, Redhage KR, Blancas-Mejia LM, Bulur P, et al. Mesenchymal stromal cells protect human cardiomyocytes from amyloid fibril damage. Cytotherapy. 2017;19(12):1426-37.

181. Elgenaidi IS, Spiers JP. Hypoxia modulates protein phosphatase 2A through HIF-1α dependent and independent mechanisms in human aortic smooth muscle cells and ventricular cardiomyocytes. British Journal of Pharmacology. 2019;176(11):1745-63.

182. Rockley K, Gill J. Characterisation of Novel Molecular Mechanisms Involved in Anthracycline-Induced Cardiotoxicity. Journal of Pharmacological and Toxicological Methods. 2017;88:202.

183. Gintant G, Burridge P, Gepstein L, Harding S, Herron T, Hong C, et al. Use of Human Induced Pluripotent Stem Cell–Derived Cardiomyocytes in Preclinical Cancer Drug Cardiotoxicity Testing: A Scientific Statement From the American Heart Association. Circulation Research. 2019;125(10):e75-e92.

184. Asnani A, Moslehi JJ, Adhikari BB, Baik AH, Beyer AM, de Boer RA, et al. Preclinical Models of Cancer Therapy–Associated Cardiovascular Toxicity: A Scientific Statement From the American Heart Association. Circulation Research. 2021;129(1):e21-e34.

185. Paik DT, Chandy M, Wu JC. Patient and Disease-Specific Induced Pluripotent Stem Cells for Discovery of Personalized Cardiovascular Drugs and Therapeutics. Pharmacological Reviews. 2020;72(1):320-42.

186. Promega. CellTiter 96® AQueous One Solution Cell Proliferation Assay (MTS) [cited 2025 April]. Available from: https://www.promega.co.uk/products/cell-health-assays/cell-viability-and-cytotoxicity-assays/celltiter-96-aqueous-one-solution-cell-proliferation-assay-_mts_/?catNum=G3580.

187. Agilent. xCELLigence RTCA DP [cited 2025 April]. Available from: https://www.agilent.com/en/product/cell-analysis/real-time-cell-analysis/rtca-analyzers/xcelligence-rtca-dp-cell-invasion-migration-741226.

188. Ke N, Wang X, Xu X, Abassi YA. The xCELLigence system for real-time and label-free monitoring of cell viability. Methods in Molecular Biology. 2011;740:33-43.

189. De Angelis A, Urbanek K, Cappetta D, Piegari E, Ciuffreda LP, Rivellino A, et al. Doxorubicin cardiotoxicity and target cells: a broader perspective. Cardiooncology. 2016;2(1):2.

190. Khouri MG, Douglas PS, Mackey JR, Martin M, Scott JM, Scherrer-Crosbie M, et al. Cancer Therapy–Induced Cardiac Toxicity in Early Breast Cancer. Circulation. 2012;126(23):2749-63.

191. Valiyaveettil D, Joseph D, Malik M. Cardiotoxicity in breast cancer treatment: Causes and mitigation. Cancer Treatment and Research Communications. 2023;37:100760.

192. Mata Caballero R, Serrano Antolín JM, Jiménez Hernández RM, Talavera Calle P, Curcio Ruigómez A, Del Castillo Arrojo S, et al. Incidence of long-term cardiotoxicity and evolution of the systolic function in patients with breast cancer treated with anthracyclines. Cardiology Journal. 2022;29(2):228-34.

193. Raj S, Franco VI, Lipshultz SE. Anthracycline-induced cardiotoxicity: a review of pathophysiology, diagnosis, and treatment. Current Treatment Options in Cardiovascular Medicine. 2014;16(6):315.

194. Renu K, V GA, P BT, Arunachalam S. Molecular mechanism of doxorubicin-induced cardiomyopathy - An update. European Journal of Pharmacology. 2018;818:241-53.

195. Pellman J, Zhang J, Sheikh F. Myocyte-fibroblast communication in cardiac fibrosis and arrhythmias: Mechanisms and model systems. J Mol Cell Cardiol. 2016;94:22-31.

196. Cohn JN, Ferrari R, Sharpe N. Cardiac remodeling--concepts and clinical implications: a consensus paper from an international forum on cardiac remodeling. Behalf of an International Forum on Cardiac Remodeling. Journal of the American College of Cardiology. 2000;35(3):569-82.

197. Souders CA, Bowers SL, Baudino TA. Cardiac fibroblast: the renaissance cell. Circulation Research. 2009;105(12):1164-76.

198. Patricelli C, Lehmann P, Oxford JT, Pu X. Doxorubicin-Induced Modulation of TGF-β Signaling Cascade in Mouse Fibroblasts: Insights into Cardiotoxicity Mechanisms. Research Square. 2023.

199. Narikawa M, Umemura M, Tanaka R, Hikichi M, Nagasako A, Fujita T, et al. Doxorubicin induces trans-differentiation and MMP1 expression in cardiac fibroblasts via cell death-independent pathways. PLoS One. 2019;14(9):e0221940.

200. Zhang P, Su J, Mende U. Cross talk between cardiac myocytes and fibroblasts: from multiscale investigative approaches to mechanisms and functional consequences. American Journal of Physiology Heart and Circulatory Physiology. 2012;303(12):H1385-96.

201. Luan Y, Zhu X, Jiao Y, Liu H, Huang Z, Pei J, et al. Cardiac cell senescence: molecular mechanisms, key proteins and therapeutic targets. Cell Death Discovery. 2024;10(1):78.

202. Packard RRS. Cardiac fibrosis in oncologic therapies. Current Opinion in Physiology. 2022;29.

203. Kong P, Christia P, Frangogiannis NG. The pathogenesis of cardiac fibrosis. Cellular and Molecular Life Sciences. 2014;71(4):549-74.

204. Frangogiannis N. Transforming growth factor-β in tissue fibrosis. Journal of Experimental Medicine. 2020;217(3):e20190103.

205. Wang L-P, Fan S-J, Li S-M, Wang X-J, Gao J-L, Yang X-H. Protective role of ACE2-Ang-(1–7)-Mas in myocardial fibrosis by downregulating K Ca 3.1 channel via ERK1/2 pathway. Pflügers Archiv-European Journal of Physiology. 2016;468:2041-51.

206. Kawano H, Do YS, Kawano Y, Starnes V, Barr M, Law RE, et al. Angiotensin II has multiple profibrotic effects in human cardiac fibroblasts. Circulation. 2000;101(10):1130-7.

207. Xu J, Carretero OA, Liao TD, Peng H, Shesely EG, Xu J, et al. Local angiotensin II aggravates cardiac remodeling in hypertension. American Journal of Physiology Heart and Circulatory Physiology. 2010;299(5):H1328-38.

208. Basu R, Poglitsch M, Yogasundaram H, Thomas J, Rowe BH, Oudit GY. Roles of Angiotensin Peptides and Recombinant Human ACE2 in Heart Failure. Journal of the American College of Cardiology. 2017;69(7):805-19.

209. Barpe DR, Rosa DD, Froehlich PE. Pharmacokinetic evaluation of doxorubicin plasma levels in normal and overweight patients with breast cancer and simulation of dose adjustment by different indexes of body mass. European Journal of Pharmaceutical Sciences. 2010;41(3):458-63.

210. Findlay SG. Mitigation of Anthracycline Cardiotoxicity & Cardiovascular Risk Profiling of Cancer Patients: Newcastle University; 2024.

211. Zhou P, Pu WT. Recounting Cardiac Cellular Composition. Circulation Research. 2016;118(3):368-70.

212. Bagchi A, Holdiness R, Dhar A, Stolarz A, Bagchi R. Proteomics Approach to Identify Anthracycline-induced Cardiotoxicity Mechanisms in Human Cardiac Fibroblasts. Physiology. 2024;39(S1):2606.

213. Barltrop JA, Owen TC, Cory AH, Cory JG. 5-(3-carboxymethoxyphenyl)-2-(4,5-dimethylthiazolyl)-3-(4-sulfophenyl)tetrazolium, inner salt (MTS) and related analogs of 3-(4,5-dimethylthiazolyl)-2,5-diphenyltetrazolium bromide (MTT) reducing to purple water-soluble formazans As cell-viability indicators. Bioorganic & Medicinal Chemistry Letters. 1991;1(11):611-4.

214. El Khoury R, Ramirez SP, Loyola CD, Joddar B. Demonstration of doxorubicin's cardiotoxicity and screening using a 3D bioprinted spheroidal droplet-based system. RSC advances. 2023;13(12):8338-51.

215. Malich G, Markovic B, Winder C. The sensitivity and specificity of the MTS tetrazolium assay for detecting the in vitro cytotoxicity of 20 chemicals using human cell lines. Toxicology. 1997;124(3):179-92.

216. Li X, Lin Y, Wang S, Zhou S, Ju J, Wang X, et al. Extracellular Superoxide Dismutase Is Associated With Left Ventricular Geometry and Heart Failure in Patients With Cardiovascular Disease. Journal of American Heart Association. 2020;9(15):e016862.

217. Zhao J, Gao JL, Zhu JX, Zhu HB, Peng X, Jiang M, et al. The different response of cardiomyocytes and cardiac fibroblasts to mitochondria inhibition and the underlying role of STAT3. Basic Research in Cardiology. 2019;114(2):12.

218. Rawat PS, Jaiswal A, Khurana A, Bhatti JS, Navik U. Doxorubicin-induced cardiotoxicity: An update on the molecular mechanism and novel therapeutic strategies for effective management. Biomedecine & Pharmacotherapy. 2021;139:111708.

219. Verbrugge FH, Guazzi M, Testani JM, Borlaug BA. Altered Hemodynamics and End-Organ Damage in Heart Failure. Circulation. 2020;142(10):998-1012.

220. Dostal DE, Baker KM. The Cardiac Renin-Angiotensin System. Circulation Research. 1999;85(7):643-50.

221. Paradis P, Dali-Youcef N, Paradis FW, Thibault G, Nemer M. Overexpression of angiotensin II type I receptor in cardiomyocytes induces cardiac hypertrophy and remodeling. Proceeding of the Natlional Academy of Sciences of the U S A. 2000;97(2):931-6.

222. Watkins SJ, Borthwick GM, Oakenfull R, Robson A, Arthur HM. Angiotensin II-induced cardiomyocyte hypertrophy in vitro is TAK1-dependent and Smad2/3-independent. Hypertension Research. 2012;35(4):393-8.

223. Consegal M, Valls-Lacalle L, Rodríguez-Sinovas A. Angiotensin II-induced cardiomyocyte hypertrophy: A complex response dependent on intertwined pathways. Revista portuguesa de cardiologia. 2021;40(3):201-3.

224. Eagle H, Levine EM. Growth regulatory effects of cellular interaction. Nature. 1967;213(5081):1102-6.

225. Duangrat R, Parichatikanond W, Morales NP, Pinthong D, Mangmool S. Sustained AT1R stimulation induces upregulation of growth factors in human cardiac fibroblasts via Gαq/TGF-β/ERK signaling that influences myocyte hypertrophy. European Journal of Pharmacology. 2022;937:175384.

226. Gray MO, Long CS, Kalinyak JE, Li HT, Karliner JS. Angiotensin II stimulates cardiac myocyte hypertrophy via paracrine release of TGF-beta 1 and endothelin-1 from fibroblasts. Cardiovascular Research. 1998;40(2):352-63.

227. Lee AA, Dillmann WH, McCulloch AD, Villarreal FJ. Angiotensin II stimulates the autocrine production of transforming growth factor-β1 in adult rat cardiac fibroblasts. Journal of Molecular and Cellular Cardiology. 1995;27(10):2347-57.

228. Lyu L, Wang H, Li B, Qin Q, Qi L, Nagarkatti M, et al. A critical role of cardiac fibroblast-derived exosomes in activating renin angiotensin system in cardiomyocytes. Journal of Molecular and Cellular Cardiology. 2015;89(Pt B):268-79.

229. Segura AM, Radovancevic R, Demirozu ZT, Frazier OH, Buja LM. Anthracycline treatment and ventricular remodeling in left ventricular assist device patients. Texas Heart Institute Journal. 2015;42(2):124-30.

230. Gallo G, Volpe M, Rubattu S. Angiotensin Receptor Blockers in the Management of Hypertension: A Real-World Perspective and Current Recommendations. Vascular Health and Risk Management. 2022;18:507-15.

231. Maillard MP, Perregaux C, Centeno C, Stangier J, Wienen W, Brunner HR, et al. In vitro and in vivo characterization of the activity of telmisartan: an insurmountable angiotensin II receptor antagonist. The Journal of Pharmacology and Experimental Therapeutics. 2002;302(3):1089-95.

232. Abraham HM, White CM, White WB. The comparative efficacy and safety of the angiotensin receptor blockers in the management of hypertension and other cardiovascular diseases. Drug Safety. 2015;38(1):33-54.

233. Taylor AA, Siragy H, Nesbitt S. Angiotensin receptor blockers: pharmacology, efficacy, and safety. The Journal of Clinical Hypertension (Greenwich). 2011;13(9):677-86.

234. Zong W-n, Yang X-h, Chen X-m, Huang H-j, Zheng H-j, Qin X-y, et al. Regulation of angiotensin-(1–7) and angiotensin II type 1 receptor by telmisartan and losartan in adriamycin-induced rat heart failure. Acta Pharmacologica Sinica. 2011;32(11):1345-50.

235. Santos RAS, Oudit GY, Verano-Braga T, Canta G, Steckelings UM, Bader M. The renin-angiotensin system: going beyond the classical paradigms. American Journal of Physiology Heart and Circulatory Physiology. 2019;316(5):H958-h70.

236. Arafat T, Awad R, Hamad M, Azzam R, Al-Nasan A, Jehanli A, et al. Pharmacokinetics and pharmacodynamics profiles of enalapril maleate in healthy volunteers following determination of enalapril and enalaprilat by two specific enzyme immunoassays. Journal of clinical pharmacy and therapeutics. 2005;30(4):319-28.

237. Zhang P, Zhang Y, Chen X, Li R, Yin J, Zhong D. Pharmacokinetics of telmisartan in healthy Chinese subjects after oral administration of two dosage levels. Arzneimittelforschung. 2006;56(8):569-73.

238. Patel R, Palmer JL, Joshi S, Di Ció Gimena A, Esquivel F. Pharmacokinetic and bioequivalence studies of a newly developed branded generic of candesartan cilexetil tablets in healthy volunteers. Clinical Pharmacology in Drug Development. 2017;6(5):492-8.

239. Bienert A, Brzeziński R, Szałek E, Grześkowiak E, Dyderski S, Drobnik L, et al. Bioequivalence study of two losartan formulations administered orally in healthy male volunteers. Arzneimittelforschung. 2006;56(11):723-8.

240. Julian GS, Oliveira RW, Tufik S, Chagas JR. Analysis of the stability of housekeeping gene expression in the left cardiac ventricle of rats submitted to chronic intermittent hypoxia. Journal Brasilero de Pneumologia. 2016;42(3):211-4.

241. Tan SC, Carr CA, Yeoh KK, Schofield CJ, Davies KE, Clarke K. Identification of valid housekeeping genes for quantitative RT-PCR analysis of cardiosphere-derived cells preconditioned under hypoxia or with prolyl-4-hydroxylase inhibitors. Molecular Biology Reports. 2012;39(4):4857-67.

242. Backlund M, Paukku K, Daviet L, De Boer RA, Valo E, Hautaniemi S, et al. Posttranscriptional regulation of angiotensin II type 1 receptor expression by glyceraldehyde 3-phosphate dehydrogenase. Nucleic Acids Research. 2009;37(7):2346-58.

243. H D. Quantifications of Western Blots with ImageJ: York University; [Available from: https://www.yorku.ca/yisheng/Internal/Protocols/ImageJ.pdf.

244. Haywood GA, Gullestad L, Katsuya T, Hutchinson HG, Pratt RE, Horiuchi M, et al. AT1 and AT2 angiotensin receptor gene expression in human heart failure. Circulation. 1997;95(5):1201-6.

245. Nickenig G, Röling J, Strehlow K, Schnabel P, Böhm M. Insulin induces upregulation of vascular AT1 receptor gene expression by posttranscriptional mechanisms. Circulation. 1998;98(22):2453-60.

246. Paukku K, Backlund M, De Boer RA, Kalkkinen N, Kontula KK, Lehtonen JYA. Regulation of AT1R expression through HuR by insulin. Nucleic Acids Research. 2012;40(12):5250-61.

247. Huang CY, Chen JY, Kuo CH, Pai PY, Ho TJ, Chen TS, et al. Mitochondrial ROS-induced ERK1/2 activation and HSF2-mediated AT1R upregulation are required for doxorubicin-induced cardiotoxicity. Journal of Cellular Physiology. 2018;233(1):463-75.

248. Maillet A, Tan K, Chai X, Sadananda SN, Mehta A, Ooi J, et al. Modeling Doxorubicin-Induced Cardiotoxicity in Human Pluripotent Stem Cell Derived-Cardiomyocytes. Scientific Reports. 2016;6(1):25333.

249. Haupt LP, Rebs S, Maurer W, Hübscher D, Tiburcy M, Pabel S, et al. Doxorubicin induces cardiotoxicity in a pluripotent stem cell model of aggressive B cell lymphoma cancer patients. Basic Research in Cardiology. 2022;117(1):13.

250. Magdy T, Jiang Z, Jouni M, Fonoudi H, Lyra-Leite D, Jung G, et al. RARG variant predictive of doxorubicin-induced cardiotoxicity identifies a cardioprotective therapy. Cell Stem Cell. 2021;28(12):2076-89.e7.

251. Pang L, Cai C, Aggarwal P, Wang D, Vijay V, Bagam P, et al. Predicting oncology drug-induced cardiotoxicity with donor-specific iPSC-CMs—a proof-of-concept study with doxorubicin. Toxicological Sciences. 2024;200(1):79-94.

252. Christidi E, Huang H, Shafaattalab S, Maillet A, Lin E, Huang K, et al. Variation in RARG increases susceptibility to doxorubicin-induced cardiotoxicity in patient specific induced pluripotent stem cell-derived cardiomyocytes. Scientific Reports. 2020;10(1):10363.

253. Roberts TC, Ezzat K, El Andaloussi S, Weinberg MS. Synthetic SiRNA Delivery: Progress and Prospects. Methods in Molecular Biology. 2016;1364:291-310.

254. Bernstein E, Caudy AA, Hammond SM, Hannon GJ. Role for a bidentate ribonuclease in the initiation step of RNA interference. Nature. 2001;409(6818):363-6.

255. Rand TA, Petersen S, Du F, Wang X. Argonaute2 cleaves the anti-guide strand of siRNA during RISC activation. Cell. 2005;123(4):621-9.

256. Liu J, Carmell MA, Rivas FV, Marsden CG, Thomson JM, Song JJ, et al. Argonaute2 is the catalytic engine of mammalian RNAi. Science. 2004;305(5689):1437-41.

257. Iqbal M, Dubey K, Anwer T, Ashish A, Pillai KK. Protective effects of telmisartan against acute doxorubicin-induced cardiotoxicity in rats. Pharmacological Reports. 2008;60(3):382-90.

258. Song W, Wang H, Wu Q. Atrial natriuretic peptide in cardiovascular biology and disease (NPPA). Gene. 2015;569(1):1-6.

259. Liu F, Wang C, Gao Y, Li X, Tian F, Zhang Y, et al. Current Transport Systems and Clinical Applications for Small Interfering RNA (siRNA) Drugs. Molecular Diagnosis Therapy. 2018;22(5):551-69.

260. Cardinale D, Sandri MT, Colombo A, Colombo N, Boeri M, Lamantia G, et al. Prognostic Value of Troponin I in Cardiac Risk Stratification of Cancer Patients Undergoing High-Dose Chemotherapy. Circulation. 2004;109(22):2749-54.

261. Schieffer B, Wirger A, Meybrunn M, Seitz S, Holtz J, Riede UN, et al. Comparative effects of chronic angiotensin-converting enzyme inhibition and angiotensin II type 1 receptor blockade on cardiac remodeling after myocardial infarction in the rat. Circulation. 1994;89(5):2273-82.

262. Zong WN, Yang XH, Chen XM, Huang HJ, Zheng HJ, Qin XY, et al. Regulation of angiotensin-(1-7) and angiotensin II type 1 receptor by telmisartan and losartan in adriamycin-induced rat heart failure. Acta Pharmacologica Sinica. 2011;32(11):1345-50.

263. Schnee JM, Hsueh WA. Angiotensin II, adhesion, and cardiac fibrosis. Cardiovascular Research. 2000;46(2):264-8.

264. Michalak M, Agellon LB. Stress Coping Strategies in the Heart: An Integrated View. Frontiers in Cardiovascular Medicine. 2018;5:168.

265. Coelho-Filho OR, Shah RV, Mitchell R, Neilan TG, Moreno H, Jr., Simonson B, et al. Quantification of cardiomyocyte hypertrophy by cardiac magnetic resonance: implications for early cardiac remodeling. Circulation. 2013;128(11):1225-33.

266. McEvoy JW, McCarthy CP, Bruno RM, Brouwers S, Canavan MD, Ceconi C, et al. 2024 ESC Guidelines for the management of elevated blood pressure and hypertension: Developed by the task force on the management of elevated blood pressure and hypertension of the European Society of Cardiology (ESC) and endorsed by the European Society of Endocrinology (ESE) and the European Stroke Organisation (ESO). European Heart Journal. 2024;45(38):3912-4018.

267. Vaduganathan M, Hirji SA, Qamar A, Bajaj N, Gupta A, Zaha V, et al. Efficacy of Neurohormonal Therapies in Preventing Cardiotoxicity in Patients with Cancer Undergoing Chemotherapy. JACC: CardioOncology. 2019;1(1):54-65.

268. Wenzel DG, Cosma GN. A model system for measuring comparative toxicities of cardiotoxic drugs for cultured rat heart myocytes, endothelial cells and fibroblasts. II. Doxorubicin, 5-fluorouracil and cyclophosphamide. Toxicology. 1984;33(2):117-28.

269. Duangrat R, Parichatikanond W, Mangmool S. Dual Blockade of TGF-β Receptor and Endothelin Receptor Synergistically Inhibits Angiotensin II-Induced Myofibroblast Differentiation: Role of AT(1)R/G(αq)-Mediated TGF-β1 and ET-1 Signaling. International Journal of Molecular Sciences. 2023;24(8).

270. Rosenkranz S. TGF-β1 and angiotensin networking in cardiac remodeling. Cardiovascular Research. 2004;63(3):423-32.

Appendices

Appendix A: xCELLigence output

A) Angiotensin II-induced hypertrophy of AC10 cardiomyocytes (xCELLigence output)

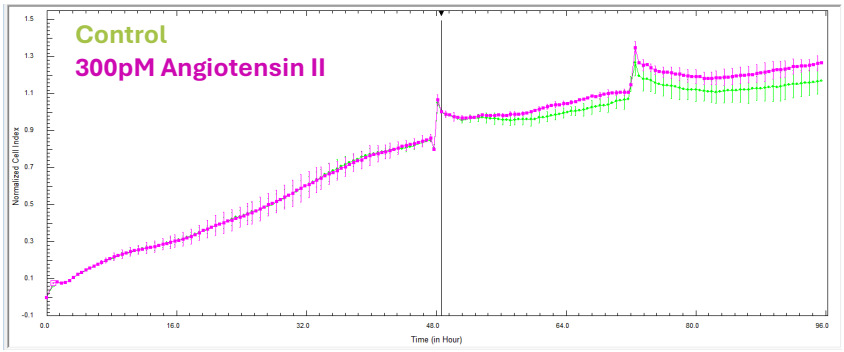

B) AC10 cardiomyocytes exposed to different concentrations of Doxorubicin (xCELLigence output)

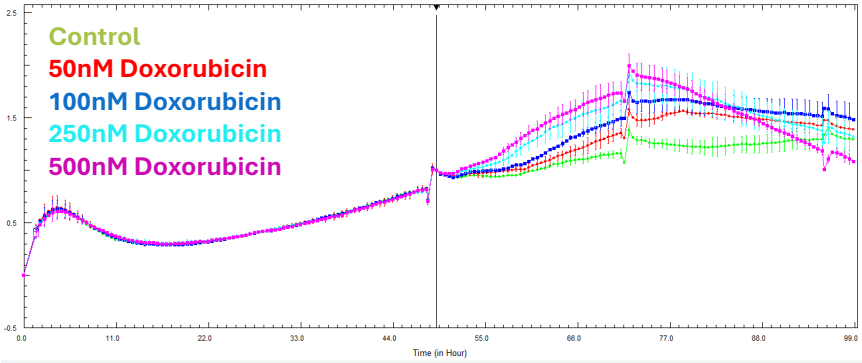

C) Doxorubicin-induced hypertrophy of AC10- cardiomyocytes (xCELLigence output)

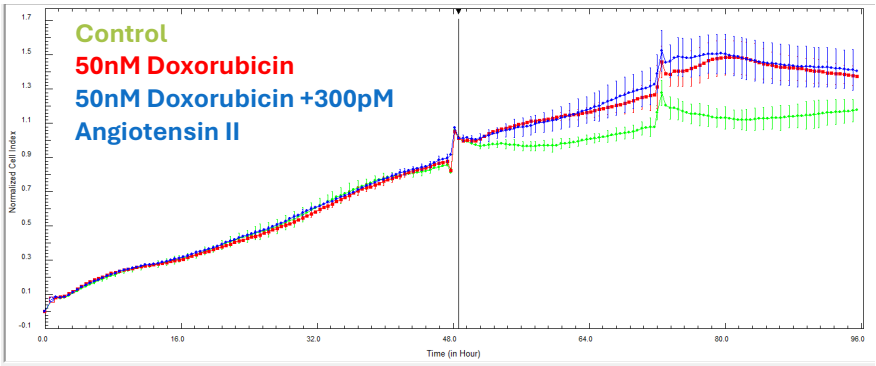

D) HCF exposed to different concentrations of Doxorubicin (xCELLigence output)

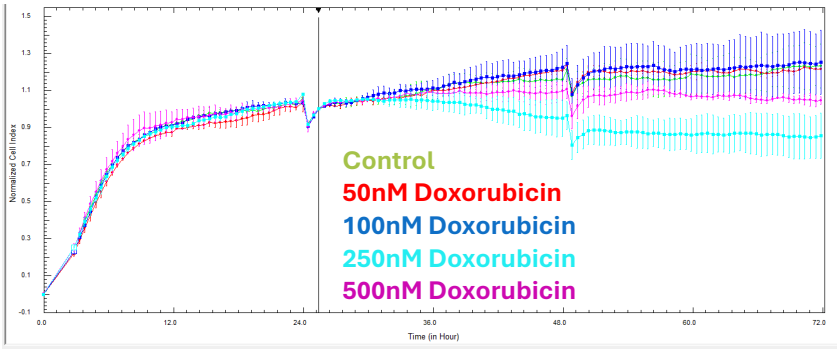

E) No morphological changes in HCF after 48hrs of exposure to Angiotensin II (xCELLigence output)

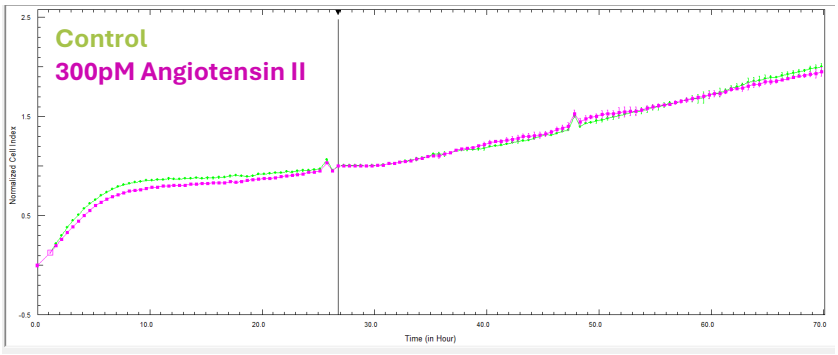

F) No morphological changes in HCF after 48hrs of exposure to Doxorubicin (xCELLigence output)

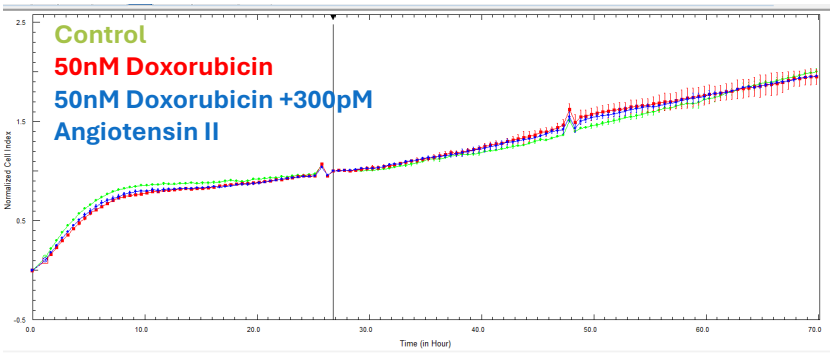

G) Mitigation of doxorubicin-induced hypertrophy of AC10 cardiomyocytes (xCELLigence output) using Telmisartan

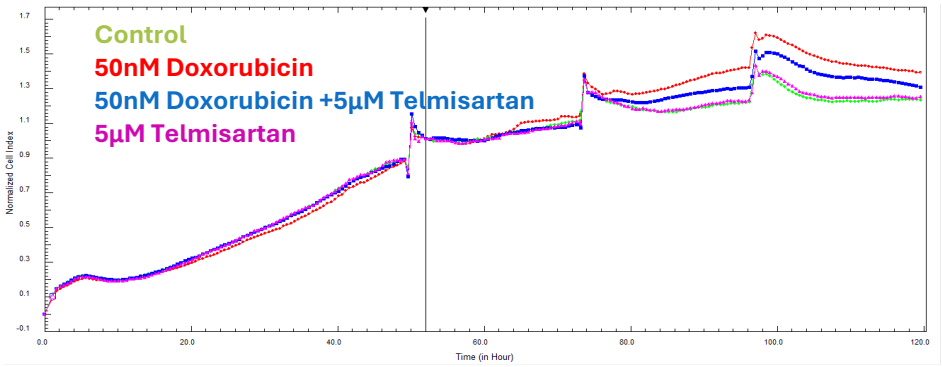

Appendix B: Western Blots

A) Uncropped western blot for AC10 cells when exposed to different concentrations of doxorubicin for 4 hours.

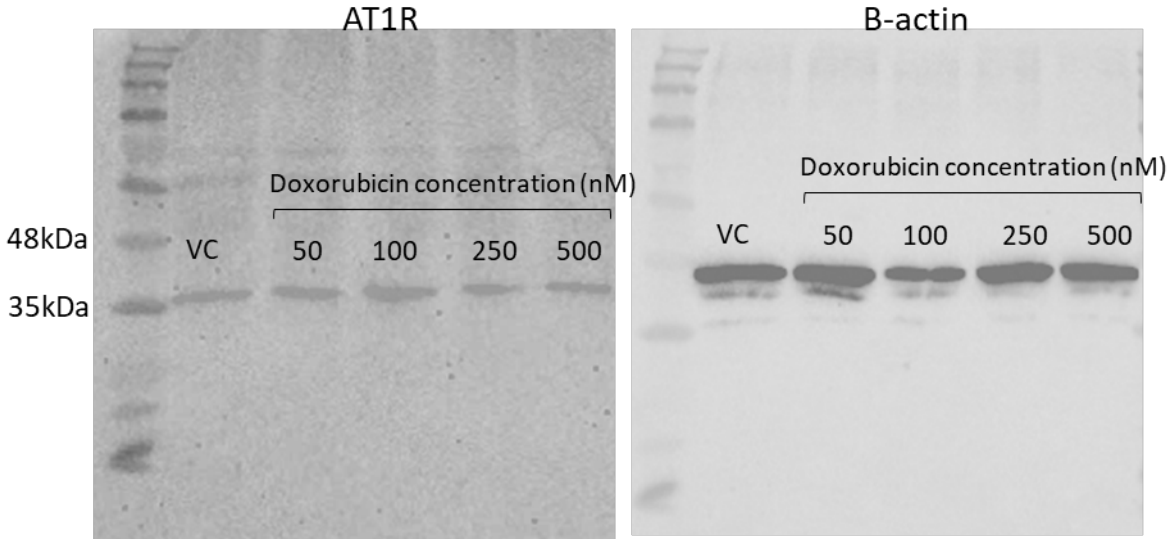

B) Uncropped western blot for AC10 cells when exposed to different concentrations of doxorubicin for 8 hours.

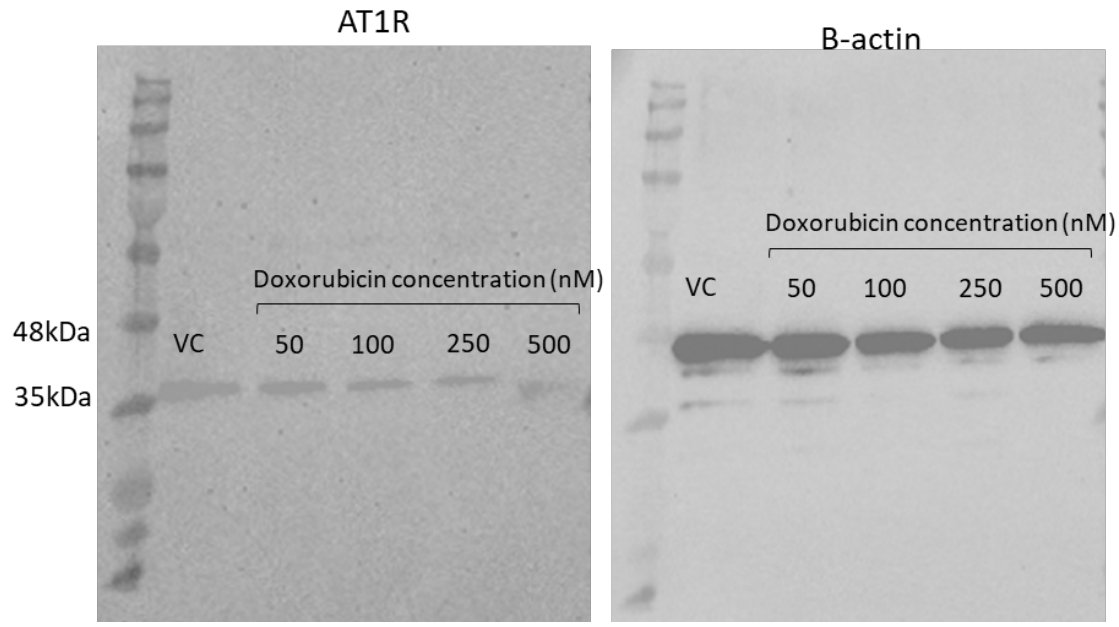

C) Uncropped western blot for AC10 cells when exposed to different concentrations of doxorubicin for 16 hours.

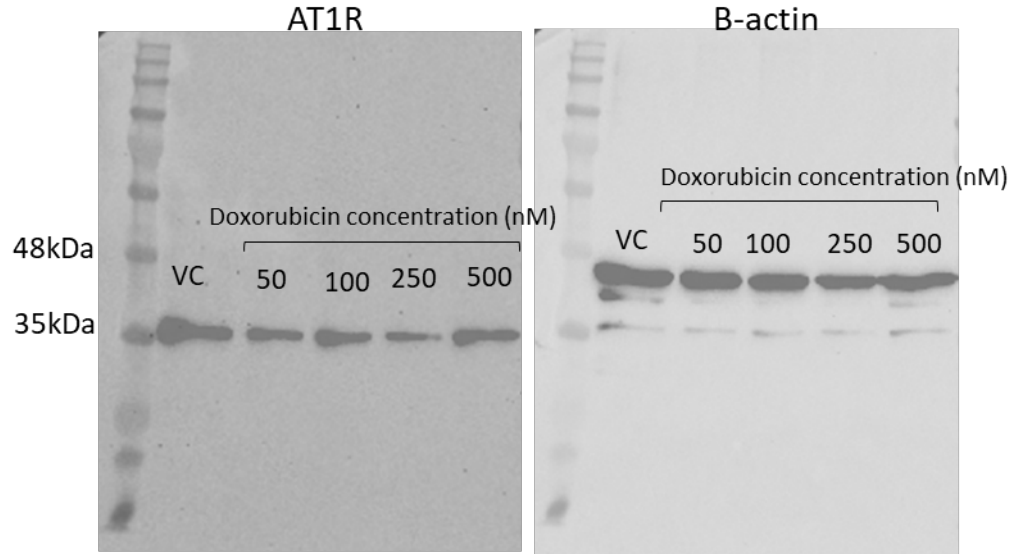

D) Uncropped western blot for AC10 cells when exposed to different concentrations of doxorubicin for 24 hours.

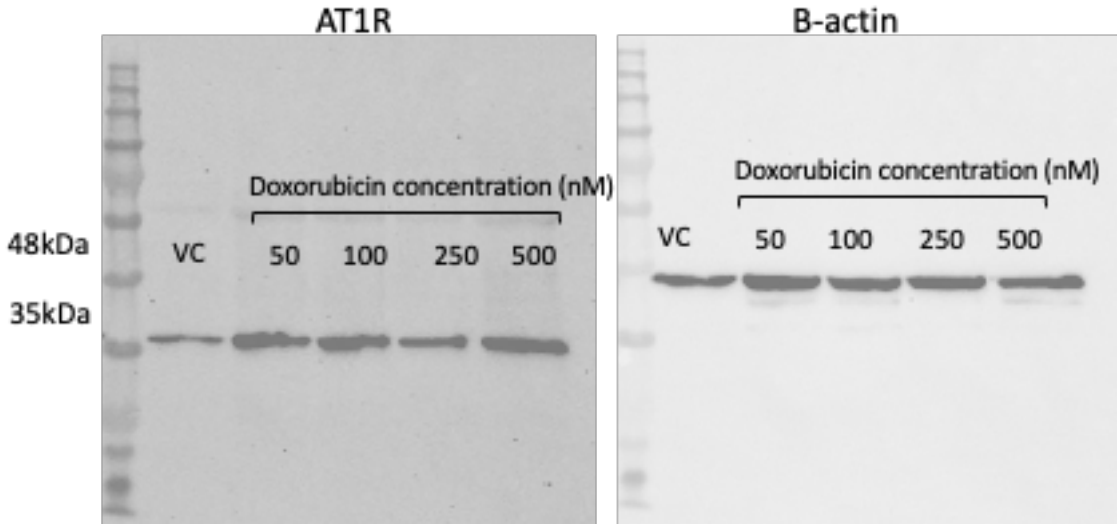

E) Uncropped western blot for AC10 cells when exposed to different concentrations of doxorubicin for 48 hours.

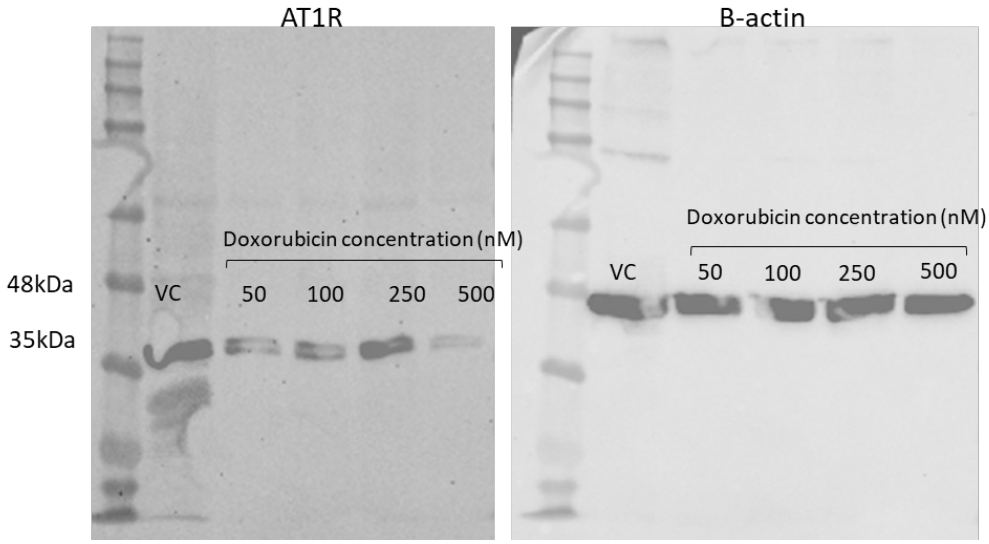

F) Uncropped western blot for AC10 cells when exposed to different concentrations of doxorubicin for 72 hours.

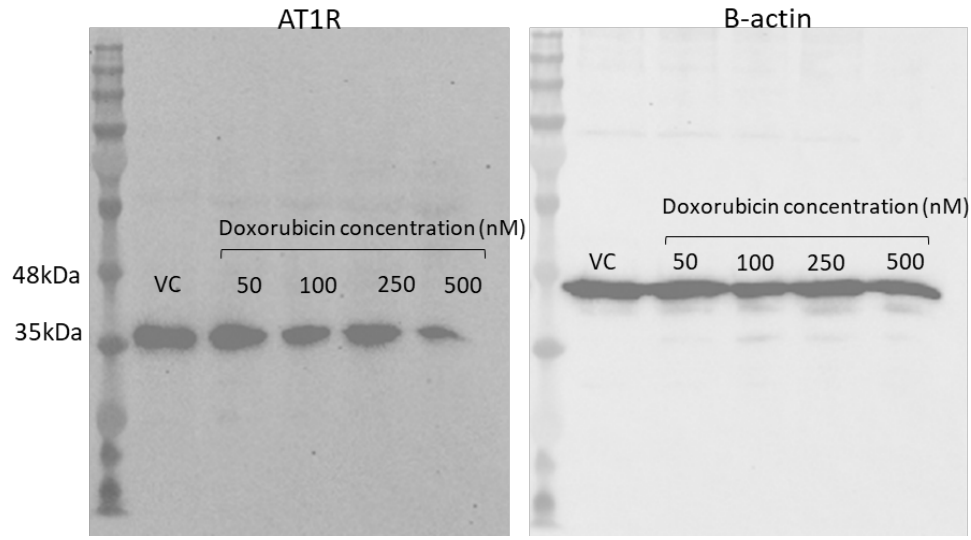

G) Uncropped western blot for AC10 cells when exposed to different concentrations of doxorubicin for 96 hours.

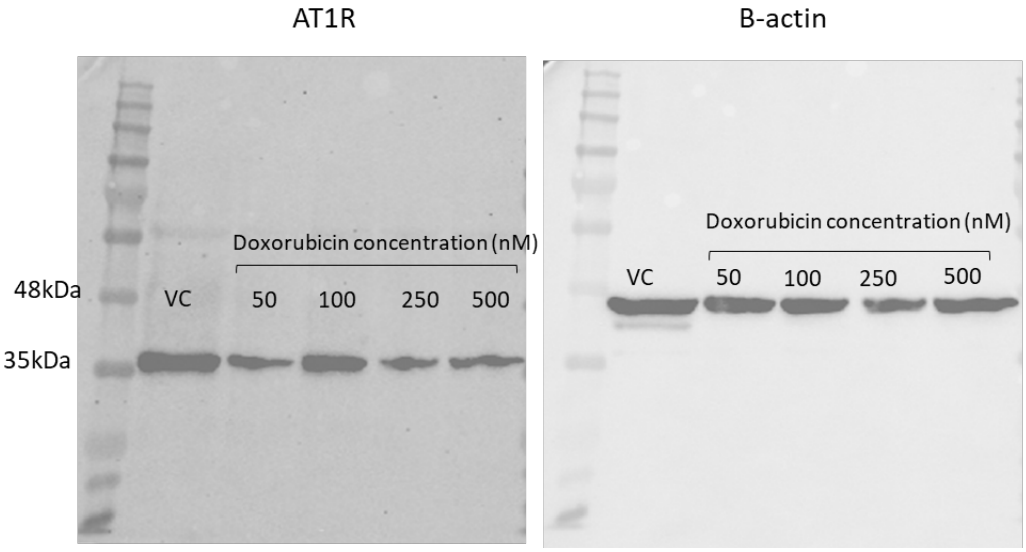

H) Uncropped western blot for HCF cells when exposed to different concentrations of doxorubicin for 4 hours.

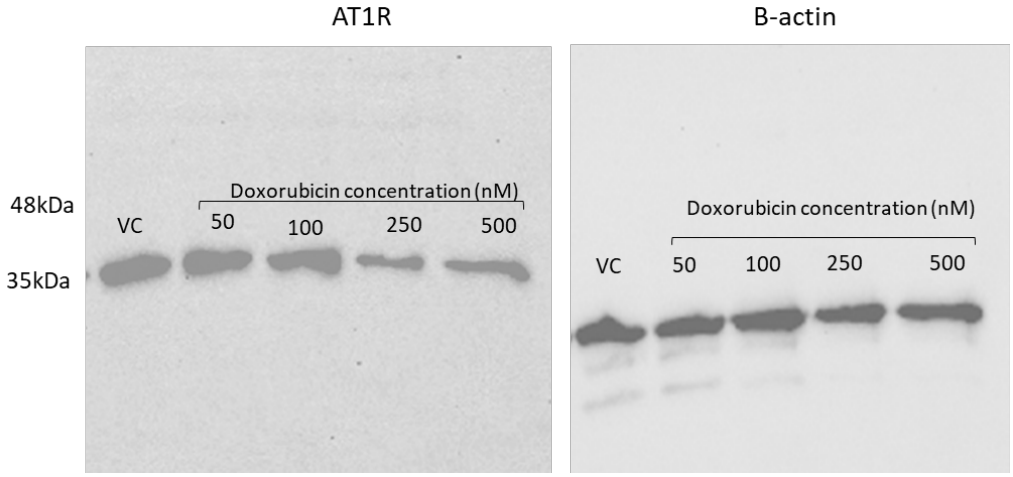

I) Uncropped western blot for HCF cells when exposed to different concentrations of doxorubicin for 8 hours.

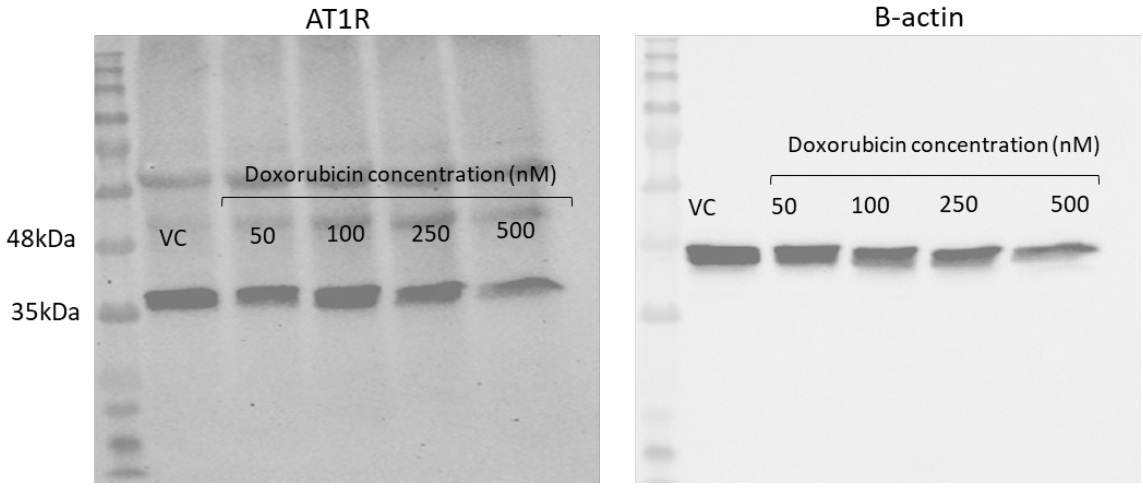

J) Uncropped western blot for HCF cells when exposed to different concentrations of doxorubicin for 16 hours.

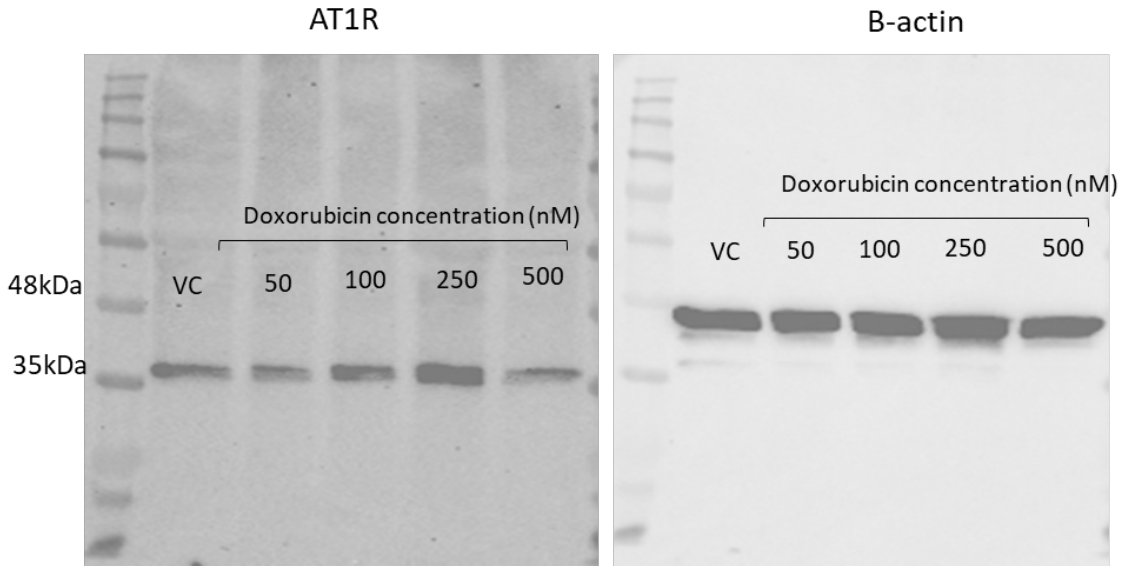

K) Uncropped western blot for HCF cells when exposed to different concentrations of doxorubicin for 24 hours.

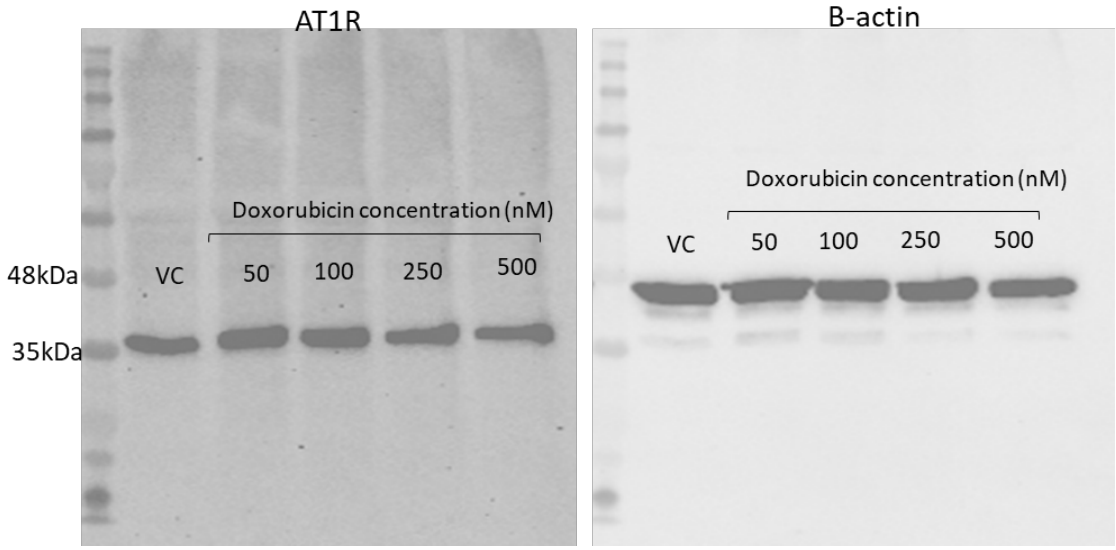

L) Uncropped western blot for HCF cells when exposed to different concentrations of doxorubicin for 48 hours.

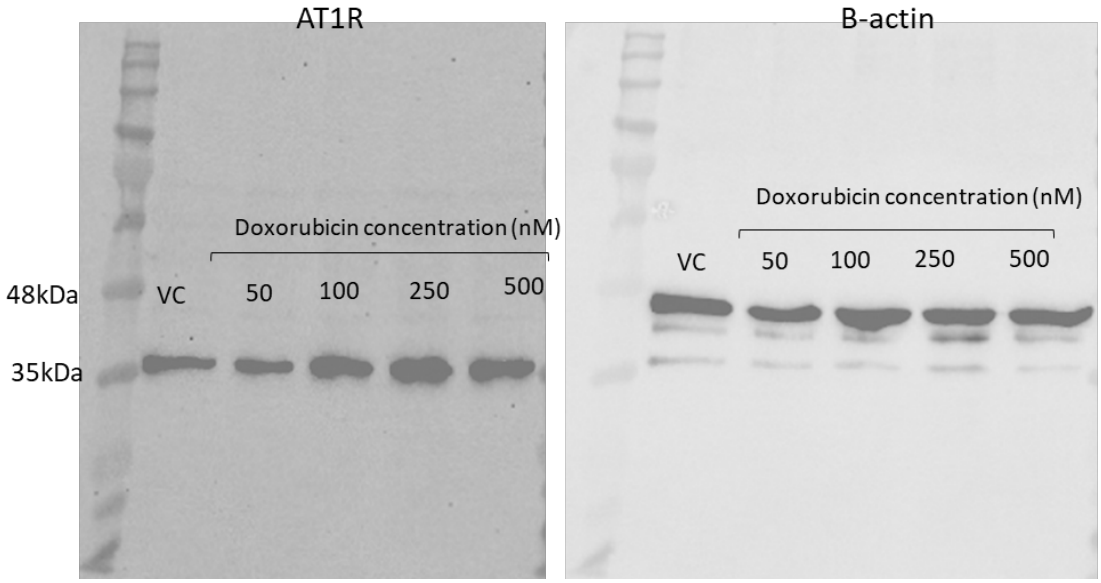

M) Uncropped western blot for HCF cells when exposed to different concentrations of doxorubicin for 72 hours.

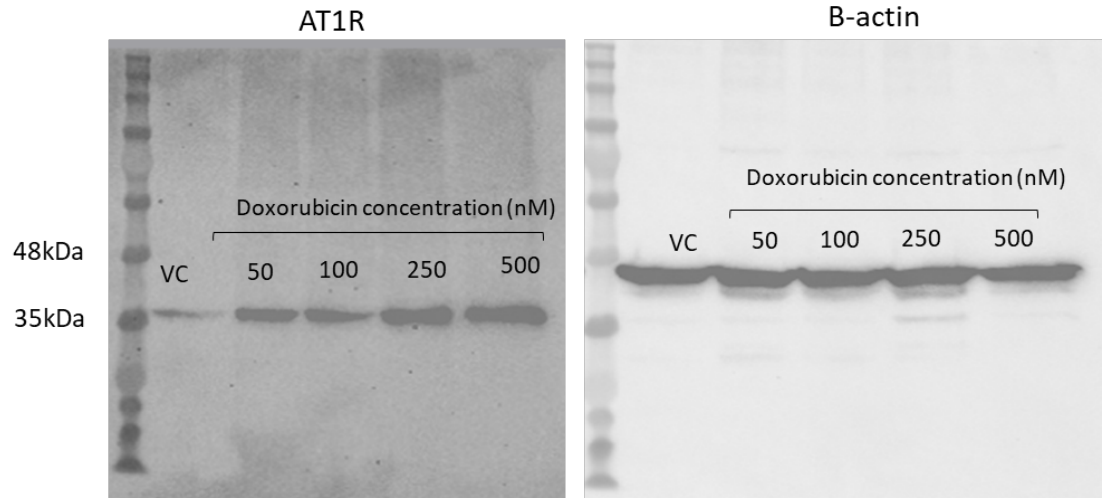

N) Uncropped western blot for HCF cells when exposed to different concentrations of doxorubicin for 96 hours.

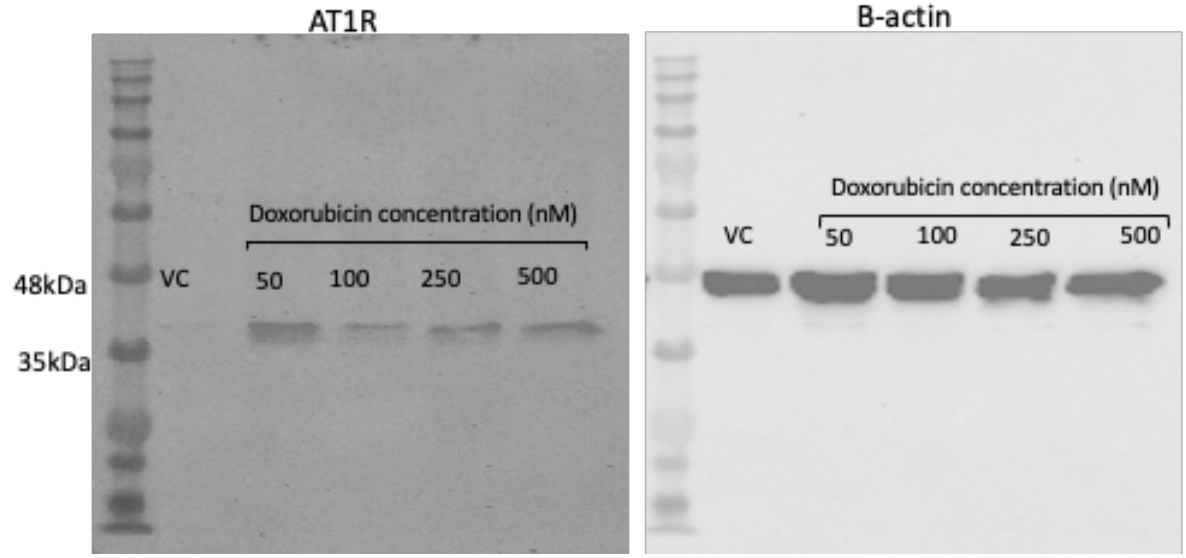

Appendix C: Compositions of solution and gel for western blot

Table A. Lysis buffer composition

Chemical	Stock	Volume
Tris HCl pH 7.5	1 M	1 mL
EGTA	0.5 M	100 µL
EDTA	0.5 M	100 µL
Sodium Chloride	5 M	660 µL
Triton x100	10%	2 mL
DTT	1 M	20 µL
Mini protease inhibitor tablet (Roche, Germany)	1 tablet per 50ml of lysis buffer	
dH_2O	-	15.98 mL

Table B. Tris-glycine Sodium Dodecyl Sulphate (SDS)-Polyacrylamide 10% loading gel

Chemical	Stock	Volume
dH_2O		1.67ml
Buffer A (1.5M Tris-HCl with 10% SDS)		5ml
Acrylamide	30%	3.33ml
APS	10%	100µl
TEMED		10µl

Table C. Tris-glycine Sodium Dodecyl Sulphate (SDS)-Polyacrylamide 5% stacking gels

Chemical	Stock	Volume
dH_2O		1.45ml
Buffer B (0.5M Tris-HCl with 10% SDS)		2.5ml
Acrylamide	30%	1mL
APS	10%	50µl
TEMED		5µl

Table D. Composition of running buffer

Chemical	Concentration
Glycine	7.1% (w/v)
Tris	1.5% (w/v)
SDS	0.5% (w/v)
dH_2O	To volume

Table E. Composition of transfer buffer

Chemical	Concentration
Glycine	11.26% (w/v)
Tris	3% (w/v)
dH_2O	To volume

Table F. Composition of Tris-buffered saline with Tween-20 (TBS-T)

Chemical	Concentration
NaCl	14.62% (w/v)
Tris	1.21% (w/v)
dH_2O	To volume
Adjust pH to 7.5 with 6M HCl	
Tween-20	0.1% (v/v)

Table G. Composition of Acid Stripping Buffer

Chemical	Concentration
Glycine	1.5% (w/v)
SDS	0.1% (w/v)
Tween-20	1% (v/v)
dH_2O	To volume
Adjust pH to 2.2 with concentrated HCl	

Appendix D: Conference Abstracts

A) 22nd International Congress of the European Society of Toxicology In Vitro: Prague, Czech Republic, 3rd – 6th June 2024

Primary author: ***"Interplay between cardiomyocytes and cardiac fibroblasts in cardiotoxicity caused by anthracyclines, involvement of the angiotensin-signalling pathway"***

Delayed cardiotoxicity is a major clinical issue with anthracyclines and cancer treatment, with the effectiveness of these therapeutics limited by life-threatening heart failure. In recent studies, drugs interfering with the angiotensin-signalling system have shown promise in the reduction of anthracycline-induced cardiotoxicity (AIC) in the clinic. Unfortunately, the mechanisms underpinning mitigation of AIC by these drugs remains unclear. We have previously shown both angiotensin II stimulation and exposure to sub-therapeutic concentrations of the anthracycline doxorubicin induce cellular hypertrophy in human cardiomyocyte cells, an effect associated with a significant upregulation of expression of the angiotensin receptor (AT1R). In contrast, our recent studies have demonstrated that no such morphological changes are observed in primary human cardiac fibroblasts (HCF). However, despite no observable structural change to HCF, exposure to doxorubicin did cause a time and concentration-dependent increase in AT1R expression. This suggests a potential interplay between these two cell types of the myocardium in AIC, involving crosstalk of the angiotensin-signalling pathway. From a therapeutic perspective, the hypertrophic response of cardiomyocytes was mitigated by pre-exposure to the angiotensin-receptor blocking drug telmisartan, offering an explanation for the cardioprotective effects of blocking angiotensin-signalling in AIC. In addition, AC10 sensitivity to Doxorubicin was mitigated by knockdown of AT1R using small interfering RNA. Together these findings support an involvement for angiotensin signalling in drug-induced hypertrophy and subsequent cardiotoxicity, with scope for interaction of this pathway for mitigation of chronic cardiotoxicity in the clinic.

Interplay between cardiomyocytes and cardiac fibroblasts in cardiotoxicity caused by anthracyclines, involvement of the angiotensin-signalling pathway

Ray Alsuhaibani[1,2], Laura booth[1,2],Gavin Richardson[3], Jason Gill[1,2]

[1] Transitional and Clinical Research Institute, Faculty of Medical Sciences, Newcastle University, UK

[2] School of Pharmacy, Faculty of Medical Sciences, Newcastle University, UK

[3] Biosciences Institute, Newcastle University, UK

E-mail: r.alsuhaibani2@newcastle.ac.uk

Introduction

The effects of anthracyclines, such as doxorubicin, on the cardiovascular system are one of the major toxicological challenges of cancer treatment. Despite clinical efficacy, these therapeutics are associated with significant drug-induced cardiotoxicity, resulting in delayed, irreversible and life-threatening heart failure. Consequently, a greater understanding of the molecular mechanisms responsible for these toxicities and identification of strategies to mitigate these effects are of the upmost importance. Recently, clinical studies have demonstrated administration of drugs targeting the angiotensin system have potential to mitigate anthracycline-induced cardiotoxicity. However, the mechanisms responsible for these effects are as yet unknown. Understanding of the molecular pathways involved in these effects at the cellular level will significantly improve our understanding of anthracycline-induced cardiotoxicity and its management.

Study Aims

- Characterise the effects of sub-toxic concentrations of doxorubicin upon human cardiomyocytes (AC10 cells) and human cardiac fibroblasts (HCF)
- Determine degree of morphological change in AC10 and HCF cells in response to doxorubicin, in presence and absence of angiotensin II
- Evaluate expression of angiotensin II receptor (AT1R) in both AC10 and HCF, in response to doxorubicin
- Assess effects of AT1R knockdown upon cellular responses to doxorubicin

Results

1. Doxorubicin induces cellular hypertrophy in AC10-Cardiomyocytes

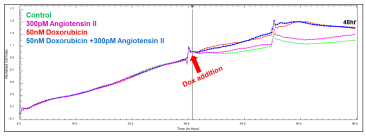

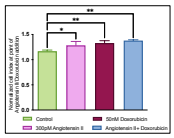

- AC10 cardiomyocytes in the plateau growth phase were exposed to 300pM angiotensin II, 50nM Doxorubicin, and their combination for 48 hours, with the responses monitored non-invasively and in real-time by xCELLigence cell analysis.
- **Doxorubicin and Angiotensin II both induced significant increases in cell index.**

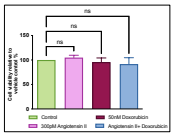

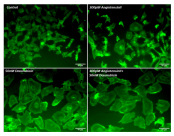

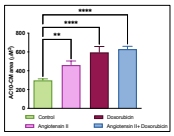

- Cellular viability determined by MTS assay.
- **No significant change in cell survival or viability was identified**
- Cell morphology determined fluorescently (x20 magnification) using Green actin tracking staining and cell surface area calculated by ImageJ software.
- **Doxorubicin and Angiotensin II both resulted in increased cell size**

2. Doxorubicin Does Not Induce Morphological Change of Cardiac Fibroblasts

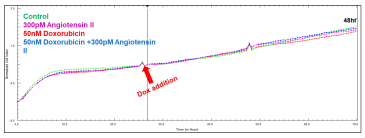

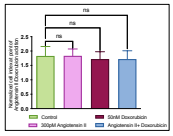

- Human cardiac fibroblasts (HCF) were exposed to 300pM angiotensin II, 50nM Doxorubicin, and their combination for 48 hours, with the responses monitored non-invasively and in real-time by xCELLigence cell analysis.
- **Doxorubicin and Angiotensin II did not induce significant increases in cell index**

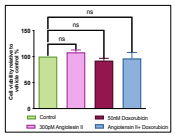

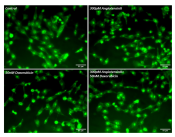

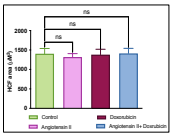

- Cellular viability determined by MTS assay.
- **No significant change in cell survival or viability was identified**
- Cell morphology determined fluorescently (x20 magnification) using Green actin tracking staining and cell surface area calculated by ImageJ software.
- **Doxorubicin and Angiotensin II do not cause change in cell size of human cardiac fibroblasts**

3. Doxorubicin induced expression of angiotensin receptor (AT1R) in AC10-cardiomyocytes.

- AC10 cardiomyocytes were exposed for 4-24 hours to clinically relevant sub-toxic concentrations of Doxorubicin (0-500nM), genetic expression of AT1R determined by quantitative RT-PCR.
- **At 24 hours post-exposure to 100nM doxorubicin, a significant 1.5-fold increase in AT1R gene expression was observed**

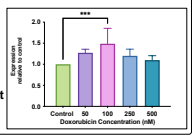

4. Doxorubicin induced expression of angiotensin receptor (AT1R) in human cardiac fibroblasts.

- Human cardiac fibroblasts were exposed for 4-24 hours to clinically relevant sub-toxic concentrations of Doxorubicin (0-500nM) and genetic expression of AT1R determined by quantitative RT-PCR.
- **At 24 hours post-exposure to 500nM doxorubicin, a significant 2-fold increase in AT1R expression was observed.**

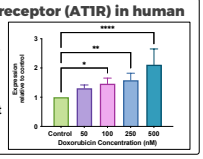

5. Knockdown of angiotensin receptor (AT1R) mitigate cellular hypertrophy and downregulate the expression of AT1R in AC10-cardiomyocytes.

Table 1: IC_{50} of AC10-CM exposed to Doxorubicin alone and in combination with AT1R siRNA (μM)

	48 hours	72 hours
Doxorubicin only	0.251±0.115	0.096±0.038
Non-target siRNA+ Doxorubicin	0.292±0.206	0.159±0.052
AT1R siRNA+ Doxorubicin	0.427±0.257	0.173±0.058

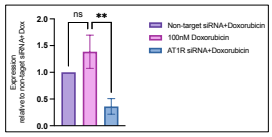

- Cellular viability determined by MTS assay.
- **No significant change in cell survival or viability was identified**
- AC10 cardiomyocytes were knockdown using siRNA technique for 24 hours then exposed to 100nM Doxorubicin for 24 hours, genetic expression of AT1R determined by quantitative RT-PCR.
- **At 24 hours post-transfection to 100nM doxorubicin, a significant decrease in AT1R gene expression was observed**

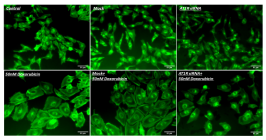

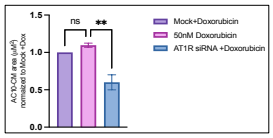

- Cell morphology determined fluorescently (x20 magnification) using Green actin tracking staining and cell surface area calculated by ImageJ software.
- **At 48 hours post-exposure to 40nM doxorubicin, a significant decrease in AC10 cell size was observed.**

6. Knockdown of angiotensin receptor (AT1R) downregulate the expression of AT1R in human cardiac fibroblast .

Table 2: IC_{50} of HCF exposed to Doxorubicin alone and in combination with AT1R siRNA (μM)

	48 hours	72 hours
Doxorubicin only	0.687±0.341	0.096±0.031
Non-target siRNA+ Doxorubicin	0.432±0.373	0.148±0.088
AT1R siRNA+ Doxorubicin	0.688±0.609	0.181±0.103

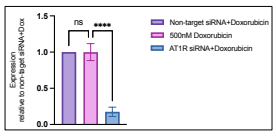

- Cellular viability determined by MTS assay.
- **No significant change in cell survival or viability was identified**
- HCF were knockdown using siRNA technique for 24 hours then exposed to 500nM Doxorubicin for 24 hours, genetic expression of AT1R determined by quantitative RT-PCR.
- **24 hours post-transfection, a significant decrease in AT1R gene expression was observed**

Conclusion

- Angiotensin II and doxorubicin induce cellular hypertrophy of AC10 human cardiomyocytes, but not human cardiac fibroblasts.
- Expression of angiotensin type-1 receptor (AT1R) is induced by doxorubicin in both cardiomyocytes and cardiac fibroblasts.
- Activation of the angiotensin signaling pathway is implicated in cellular hypertrophy of cardiomyocytes.

➢ **A potential interplay exists between cardiomyocytes and cardiac fibroblasts of the myocardium in anthracycline-induced cardiotoxicity, involving crosstalk of the angiotensin signalling pathway.**

Qassim University جامعة القصيم

Newcastle University

B) British Toxicology Society Annual Congress: Birmingham, April 17th – 19th 2023
Primary author: "*Identification of the molecular mechanisms of anthracycline-induced cardiotoxicity and its relationship with renin-angiotensin system in different types of human cardiac cell lines*".
Awarded a student bursary to attend the BTS annual symposium.

Delayed cardiotoxicity is a major clinical issue with anthracyclines and cancer treatment, with the effectiveness of these therapeutics limited by life-threatening heart failure. In recent studies, drugs interfering with the angiotensin-signalling system have shown promise in the reduction of anthracycline-induced cardiotoxicity (AIC) in the clinic. Unfortunately, the mechanisms underpinning mitigation of AIC by these drugs remains unclear. We have previously shown both angiotensin II stimulation and exposure to sub-therapeutic concentrations of the anthracycline doxorubicin induce cellular hypertrophy in human cardiomyocyte cells, an effect associated with a significant upregulation of expression of the angiotensin receptor (AT1R). In contrast, our recent studies have demonstrated that no such morphological changes are observed in primary human cardiac fibroblasts (HCF). However, despite no observable structural change to HCF, exposure to doxorubicin did cause a time and concentration-dependent increase in AT1R expression. This suggests a potential interplay between these two cell types of the myocardium in AIC, involving crosstalk of the angiotensin-signalling pathway. From a therapeutic perspective, the hypertrophic response of cardiomyocytes was mitigated by pre-exposure to the angiotensin-receptor blocking drug telmisartan, offering an explanation for the cardioprotective effects of blocking angiotensin-signalling in AIC. In addition, the upregulation of expression of the AT1R was mitigated by knockdown of AT1R using small interfering RNA. Together these findings support an involvement for angiotensin signalling in drug-induced hypertrophy and subsequent cardiotoxicity, with scope for interaction of this pathway for mitigation of chronic cardiotoxicity in the clinic.

Identification of the molecular mechanisms of anthracycline-induced cardiotoxicity and relationship to angiotensin signalling

Ray Alsuhaibani[1,2], Gavin Richardson[3], Jason Gill[1,2]

[1] Transitional and Clinical Research Institute, Faculty of Medical Sciences, Newcastle University, UK
[2] School of Pharmacy, Faculty of Medical Sciences, Newcastle University, UK
[3] Biosciences Institute, Newcastle University, UK
E-mail: r.alsuhaibani2@newcastle.ac.uk

Introduction

The effects of anthracyclines, such as doxorubicin, on the cardiovascular system are one of the major toxicological challenges of cancer treatment. Despite clinical efficacy, these therapeutics are associated with significant drug-induced cardiotoxicity, resulting in delayed, irreversible and life-threatening heart failure. Consequently, a greater understanding of the molecular mechanisms responsible for these toxicities and identification of strategies to mitigate these effects are of the upmost importance. Recently, clinical studies have demonstrated administration of drugs targeting the angiotensin system have potential to mitigate anthracycline-induced cardiotoxicity. However, the mechanisms responsible for these effects are as yet unknown. Understanding of the molecular pathways involved in these effects at the cellular level will significantly improve our understanding of anthracycline-induced cardiotoxicity and its management.

Study Aims

- Characterise the effects of sub-toxic concentrations of doxorubicin upon human cardiomyocytes (AC10 cells) and human cardiac fibroblasts (HCF)
- Determine degree of morphological change in AC10 and HCF cells in response to doxorubicin, in presence and absence of angiotensin II
- Evaluate expression of angiotensin II receptor (AT1R) in both AC10 and HCF, in response to doxorubicin
- Assess effects of AT1R blockade upon cellular responses to doxorubicin

Results

1. Doxorubicin induces cellular hypertrophy in AC10-Cardiomyocytes

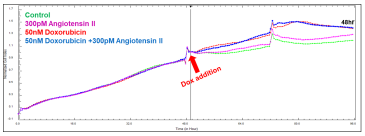

- AC10 cardiomyocytes in the plateau growth phase were exposed to 300pM angiotensin II, 50nM Doxorubicin, and their combination for 48 hours, with the responses monitored non-invasively and in real-time by xCELLigence cell analysis.
- **Doxorubicin and Angiotensin II both induced significant increases in cell index.**

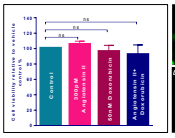

- Cellular viability determined by MTS assay.
- **No significant change in cell survival or viability was identified**

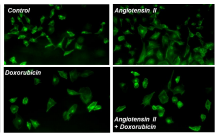

- Cell morphology determined fluorescently (x20 magnification) using Green actin tracking staining and cell surface area calculated by ImageJ software.
- **Doxorubicin and Angiotensin II both resulted in increased cell size**

2. Doxorubicin Does Not Induce Morphological Change of Cardiac Fibroblasts

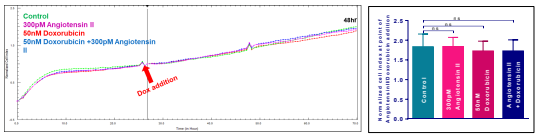

- Human cardiac fibroblasts (HCF) were exposed to 300pM angiotensin II, 50nM Doxorubicin, and their combination for 48 hours, with the responses monitored non-invasively and in real-time by xCELLigence cell analysis.
- **Doxorubicin and Angiotensin II did not induce significant increases in cell index**

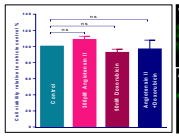

- Cellular viability determined by MTS assay.
- **No significant change in cell survival or viability was identified**

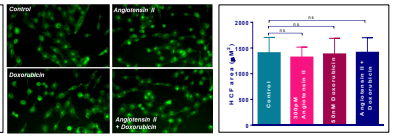

- Cell morphology determined fluorescently (x20 magnification) using Green actin tracking staining and cell surface area calculated by ImageJ software.
- **Doxorubicin and Angiotensin II do not cause change in cell size of human cardiac fibroblasts**

3. Doxorubicin induced expression of angiotensin receptor (AT1R) in AC10-cardiomyocytes.

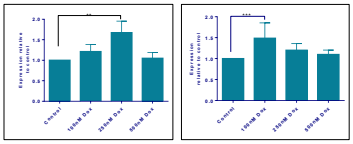

- AC10 cardiomyocytes were exposed for 4-24 hours to clinically relevant sub-toxic concentrations of Doxorubicin (0-500nM) and genetic expression of AT1R determined by quantitative RT-PCR.
- **At 16 hours post-exposure to 250nM doxorubicin, a significant 1.7-fold increase in AT1R expression was observed.**
- **At 24 hours post-exposure to 100nM doxorubicin, a significant 1.5-fold increase in AT1R expression was observed.**

4. Doxorubicin induced expression of angiotensin receptor (AT1R) in human cardiac fibroblasts.

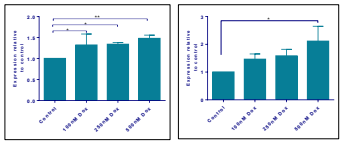

- Human cardiac fibroblasts were exposed for 4-24 hours to clinically relevant sub-toxic concentrations of Doxorubicin (0-500nM) and genetic expression of AT1R determined by quantitative RT-PCR.
- **At 16 hours post-exposure to 500 doxorubicin, a significant 1.5-fold increase in AT1R expression was observed.**
- **At 24 hours post-exposure to 500nM doxorubicin, a significant 2-fold increase in AT1R expression was observed.**

5. Angiotensin induces expression of angiotensin receptor (AT1R) in human cardiac fibroblasts but not AC10-cardiomyocytes.

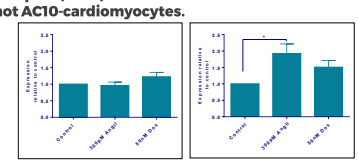

- AC10 cardiomyocytes and Human cardiac fibroblasts were exposed for 24 hours to either Angiotensin II (300pm) or Doxorubicin (50nM) and genetic expression of AT1R determined by quantitative RT-PCR.
- **A significant 2-fold increase in AT1R expression was observed in response to Angiotensin in HCF, but not cardiomyocytes**

6. Blockade of the Angiotensin Receptor Mitigates Doxorubicin-induced Hypertrophy of AC10 cardiomyocytes

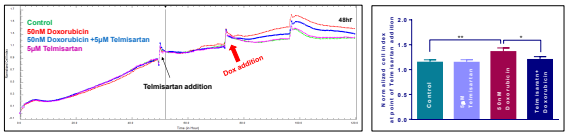

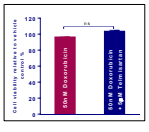

- AC10 cardiomyocytes in the plateau growth phase were pre-exposed to the Angiotensin Receptor Blocker (ARB) drug, telmisartan (5μM), for 24 hours, with the responses monitored non-invasively and in real-time by xCELLigence cell analysis.
- **AT1R blockade attenuates the hypertrophic effect of doxorubicin.**
- **No significant change in cell survival or viability was identified**

Conclusion

- Angiotensin II and doxorubicin induce cellular hypertrophy of AC10 human cardiomyocytes, but not human cardiac fibroblasts.
- Expression of angiotensin type-1 receptor (AT1R) is induced by doxorubicin in both cardiomyocytes and cardiac fibroblasts.
- Expression of angiotensin type-1 receptor (AT1R) is induced by angiotensin II only in human cardiac fibroblasts, not cardiomyocytes.
- Activation of the angiotensin signaling pathway is implicated in cellular hypertrophy of cardiomyocytes.

➢ **A potential interplay exists between cardiomyocytes and cardiac fibroblasts of the myocardium in anthracycline-induced cardiotoxicity, involving crosstalk of the angiotensin signalling pathway.**

Qassim University جامعة القصيم

Newcastle University

C) British Toxicology Society Annual Congress: Gateshead, April 4th – 6th 2022
Primary author: *"Interplay of the angiotensin signalling pathway in anthracycline-induced cardiotoxicity of different cell types of the myocardium".*

Cardiotoxicity is a major complication of anthracycline chemotherapy, used in the management of many cancer types, impacting the quality of life and patient survivorship. Consequently, greater understanding of the molecular mechanisms responsible for these toxicities, and identification of therapeutic strategies to mitigate cardiotoxicity are important. Recently, drugs interfering with the angiotensin-signalling system have shown promise in the reduction of anthracycline-induced cardiotoxicity. The aim of this study was to examine the role of angiotensin II in mediating anthracycline-induced cardiotoxicity, in both human adult cardiomyocytes (AC10 cell line) and human primary cardiac fibroblasts. Whereas angiotensin II and the anthracycline doxorubicin induced cellular hypertrophy in cardiomyocytes, no such morphological change was observed in cardiac fibroblasts. The hypertrophic response in cardiomyocytes was mitigated by pre-exposure to clinically-utilised angiotensin receptor blocker (ARB) drugs; implicating these effects were mediated through the angiotensin receptor. In terms of the cardiac fibroblasts, although no morphological changes were observed, a significant difference in cellular viability was observed between cells treated with doxorubicin alone and cells treated with doxorubicin in combination with angiotensin II. These differential cellular response of cardiomyocytes and cardiac fibroblasts to anthracyclines and angiotensin II implicates a potential interplay between these two cell types of the myocardium in anthracycline-induced cardiotoxicity, with potential for mitigation of this toxicity through interference of the angiotensin-signalling pathway in the clinic.

Interplay of the Angiotensin-Signalling Pathway in Anthracycline-Induced Cardiotoxicity of Different Cell Types of the Myocardium

Alsuhaibani R[1,2], Booth L[1], Richardson G[1], Gill JH[1,2]

Transitional and Clinical Research Institute, Faculty of Medical Sciences, Newcastle University, UK

Cardiotoxicity is a major complication of many anticancer therapies, particularly anthracyclines, impacting the quality of life and overall survival of patients. Consequently, greater understanding of the molecular mechanisms responsible for these toxicities, and identification of therapeutic strategies to mitigate and overcome these toxicities are significantly important. Recently, clinical studies have demonstrated that administration of drugs that act upon the angiotensin system may reduce the cardiotoxicity of anthracyclines. However, despite showing promise, the molecular mechanisms responsible for toxicity mitigation are currently unknown.

Aims

- To determine the role of angiotensin II in mediating anthracycline induced cardiotoxicity
- To evaluate differential responses of human cardiomyocytes (AC10 cell line) and human cardiac fibroblasts (HCF) to anthracyclines in the presence/absence of angiotensin II

Methods

- Changes in cellular morphology and survival of AC10 and HCF following exposure to clinically relevant concentrations of angiotensin II, the anthracycline doxorubicin, and a panel of angiotensin receptor blockers, were monitored *in vitro* in real-time by cellular impedance (xCELLigence system) **(Figure 1)**

- Cellular viability in response to these agents was determined in parallel by the MTS tetrazolium-salt assay.

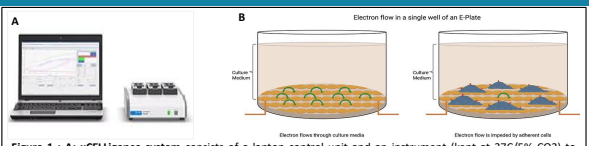

Figure 1 : A: xCELLigence system consists of a laptop control unit and an instrument (kept at 37C/5% CO2) to monitor cell behaviour. Cells were seeded in specialized 16-well plates. **B: Principle of xCELLigence system.** The electrons flow will be impeded if there is increase in cell number or change in cellular morphology.

Results

Figure 2: Angiotensin II induces morphological change and hypertrophy in AC10 cardiomyocytes but not human cardiac fibroblasts

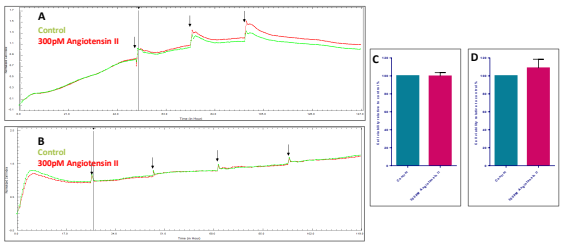

AC10 cardiomyocytes (**A**) and HCF (**B**) were exposed to 300pM angiotensin II for 96 hour, with cellular responses determined by xCELLigence assay. Changes in cellular impedance were not associated with a changes in viable cell number, as determined in parallel by MTS assay, for AC10 (**C**) or HCF (**D**).

► ***Angiotensin II induces hypertrophy of cardiomyocytes, but not cardiac fibroblasts.***

Figure 3: Doxorubicin induces morphological change and hypertrophy in AC10 cardiomyocytes but not human cardiac fibroblasts

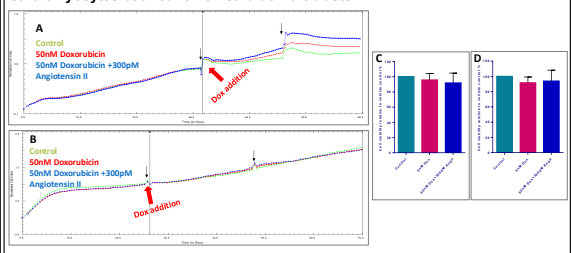

AC10 cardiomyocytes (**A**) and HCF **(B)** were exposed to doxorubicin (50nM) in presence or absence of angiotensin II (300pM), with changes in cellular impedance determined by xCELLigence assay. Changes in cellular impedance were not associated with changes in viable cell number, as determined in parallel by MTS assay, for either AC10 (**C**) or HCF (**D**).

► ***Doxorubicin induces hypertrophy of cardiomyocytes, but not cardiac fibroblasts.***

► ***Angiotensin II further increases doxorubicin-induced hypertrophy of cardiomyocytes***

Figure 4: Blockade of the Angiotensin Receptor mitigates doxorubicin-induced hypertrophy of AC10 cardiomyocytes

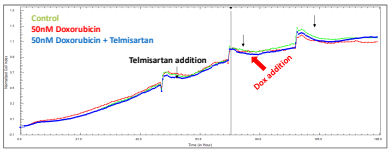

Pre-exposure to the Angiotensin Receptor Blocker (ARB) drug, telmisartan (5μM), for 24 hours attenuates the hypertrophic effect of doxorubicin against AC10 cardiomyocytes, determined by xCELLigence assay.

► ***Hypertrophic response of doxorubicin against AC10 cardiomyocytes involves signalling through the angiotensin receptor.***

Figure 5: Angiotensin II mitigates cytotoxicity of doxorubicin against human cardiac fibroblasts but not AC10 cardiomyocytes

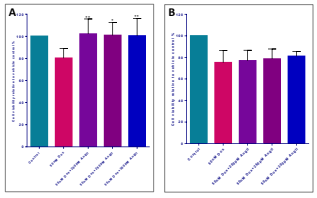

HCF (**A**) and AC10 (**B**) were exposed to 50nM doxorubicin in presence of angiotensin II (0-300pM) for 96 hour, with cellular viability determined by MTS assay. *p<0.05 **p<0.01, relative to doxorubicin alone

► ***Angiotensin II produces a protective effect against doxorubicin in cardiac fibroblasts but not in AC10 cardiomyocytes.***

Figure 6: Blockade of Angiotensin Receptor reduces toxicity of doxorubicin against AC10 cardiomyocytes but not human cardiac fibroblasts

	Doxorubicin IC_{50} (nM)	
Drug Treatment	**HCF**	**AC10**
Doxorubicin Alone	240 ±	23 ±
Doxorubicin+ Telmisartan	200 ±	114 ±
Doxorubicin+ Losartan	210 ±	60 ±
Doxorubicin+ Candesartan	240 ±	19 ±

Pre-exposure to Angiotensin Receptor Blocker (ARB) drugs (5μM) does not affect cytotoxicity of doxorubicin against human cardiac fibroblasts. **(A)**:Telmisartan, **(B)**: Losartan, **(C)**:Candesartan. (n=3)

► ***Doxorubicin toxicity against human fibroblasts does not involve activation of the angiotensin receptor***

► ***Doxorubicin toxicity against AC10 cardiomyocytes involves the angiotensin receptor***

Conclusion

- Angiotensin II and doxorubicin induce cellular hypertrophy of AC10 human cardiomyocytes, but do not cause these effects in human cardiac fibroblasts.
- Activation of the angiotensin signaling pathway is implicated in both cellular hypertrophy and cytotoxicity of cardiomyocytes.
- Doxorubicin-induced activation of the angiotensin signaling pathway is not involved in the cytotoxic action of doxorubicin against human cardiac fibroblasts.
- In contrast to cardiomyocytes, exposure to angiotensin reduces doxorubicin-induced cytotoxicity against human cardiac fibroblasts

► ***Differential and potentially opposing responses to angiotensin and the anthracycline doxorubicin are demonstrated by both human cardiac fibroblasts and human cardiomyocytes, with significant implications for clinical mitigation and management of this toxicity through interference with the angiotensin signaling pathway.***